

Synthesis, Analysis, and Pharmacological Profile of Designer Piperazine Drugs

by

Mohammed Almaghrabi

A dissertation submitted to the Graduate Faculty of
Auburn University
in partial fulfillment of the
requirements for the Degree of
Doctor of Philosophy

Auburn, Alabama
August 7, 2021

Keywords: Piperazines, Designer drugs, Synthesis, Analysis, GC-MS, Pharmacology

Copyright 2021 by Mohammed Almaghrabi

Approved by

Muralikrishnan Dhanasekaran, Chair, Professor of Pharmacology

C. Randall Clark, Co-Chair, Professor of Medicinal Chemistry

Jack DeRuiter, Chair, Professor of Medicinal Chemistry

Timothy Moore, Professor of pharmacology

Abstract

New or novel Psychoactive substances (NPS) or designer drugs are often uncontrolled synthetic chemicals that are analogs to classic controlled substances and have been a public health threat in the last two decades. The rapid expansion in manufacturing and trafficking of NPS is an alarmingly significant challenge to global health. It has led to drastic abuse, especially among young people. Due to relatively limited information regarding the analytical characteristics, pharmacokinetic, pharmacodynamic, and toxicological profile, there is a need for pertinent research on these substances immediately. Many research areas are associated with NPS phenomena, such as forensic analysis, neuropharmacology, epidemiology, toxicology, and prevention science. The first step to face this issue is the identification and detection of these kinds of substances. Forensic analysis of illicit drugs is a significant path to help in resolving this issue. One of the reasons that facilitate the spread of NPS is the simplicity of designing these kinds of substances. In addition, the availability of chemical precursors can produce uncountable regioisomers related to controlled substances. Designer piperazine drugs are a novel class of NPS that has been introduced in the market of illicit drugs in 2000 and known as party pills. The most used recreational drugs in the piperazine class are benzylpiperazine (BZP) and 3-trifluoromethylphenylpiperazine (3-TFMPP). These compounds are usually used in combination to mimic the psychostimulant effects of amphetamine and MDMA, but ten-fold less potent. In the current study, several piperazine derivatives have been designed and synthesized based on the structural elemental of BZP and 3-TFMPP. In addition to creating an analytical profile of each compound using the gas chromatography, mass spectrometry, and infrared spectroscopy. Lastly, we also investigate the neuropharmacological profile of some novel piperazine derivatives and the mechanisms of action.

Acknowledgments

In the name of Alláh, the Most Gracious, and the most merciful, I praise him for his reconcile and guidance. Behind this work, many supportive people helped and encouraged me to achieve this step of education. First, I would like to thank my advisor Dr. Muralikrishnan Dhanasekaran for his continuous support and encouragement. Also, I would like to express my gratitude to my research advisors: Dr. Randall Clark, Dr. Jack Deruiter, and Dr. Timothy Moore, for their valuable advice, support, and encouragement in every step of my research career. Also, I would like to thank my brothers and friends Mohammed Majrashi and Ahmad Almalki, for their patience with me, and I learned a lot from them. My appreciation is extended to my labmate, Dr. Younis Abaidallah; thank you for your support and guidance. My other lab mate, Mansour Alturki, Suhurd Pathak, Sindhu Ramesh, Logan Neel. In addition, I would like to thank the Saudi Arabian Cultural Mission for the financial support they provided me, which made this possible. Finally, the most grateful goes to my family, my mom Asma Almaghrabi, my queen Fatimah Almaghrabi who gave me strength and handled me during this journey. My children, Meshaal, Hamed, and my little princess Dana gave me the reason to be happy. Thank you to those who were the cause of every good that happened to me, Mom and Dad. Thank you to my brother, sisters, and everyone.

Table of Contents

Table of Contents

Abstract.....	ii
Acknowledgments	iii
Table of Contents.....	iv
List of Figures.....	xii
List of Schemes	xv
List of tables	xvii
List of Abbreviation.....	xviii
1. Literature review.....	1
1.1. Introduction	1
1.2. Piperazine derivatives as drugs of abuse	2
1.3. Dark web	4
1.4. Piperazine moiety as a promising therapeutic tool	4
1.4.1. Piperazines as anticancer	5
1.4.2. Piperazine as Antibacterial, antifungal, and antiviral agents	6
1.4.3. Piperazine as antidepressant and anti-anxiolytic	7
1.4.4. Piperazine as cardioprotective	7
1.4.5. Piperazine as a cognitive enhancer	8
1.4.6. Piperazine as Anti-inflammatory	9
1.5. Pharmacology of piperazine compounds	11
1.5.1. Pharmacodynamics and pharmacokinetic of benzylpiperazine (BZP)	11

1.5.2. Pharmacodynamics and pharmacokinetic of TFMPP	13
1.5.3. Pharmacodynamics and pharmacokinetic of mCPP	15
1.5.4. Pharmacodynamics and pharmacokinetic of MDBP	15
1.6. Toxicokinetic and treatment of piperazines toxicity	16
1.7. Piperazine Chemistry	17
1.8. Piperazines dosage form	18
1.9. Analysis and identification of piperazines	18
1.9.1. Colorimetric tests	19
1.9.2. Immunoassays	19
1.9.3. Gas chromatography-mass spectrometry (GC-MS).....	19
1.9.4. Gas chromatography with infrared detection (GC-IRD)	20
1.9.5. high-performance liquid chromatography (HPLC).....	20
1.9.6. Nuclear magnetic resonance (NMR)	21
1.10. Knowledge gap & Project rational.....	21
1.11. Aims	22
2. Design and synthesis of novel Regioisomeric Piperazines	26
2.1. Synthesis of 1-[N-(trifluoromethyl)phenyl]-4-benzylpiperazine	27
2.1.1. Synthesis of 1-[2-(trifluoromethyl)phenyl]-4-benzylpiperazine and 1-[4-(trifluoromethyl)phenyl]-4-benzylpiperazine	27
2.2. Synthesis of 1-[2-(trifluoromethyl)benzyl]-, 1-[3-(trifluoromethyl)benzyl], and 1-[4-(trifluoromethyl)benzyl]-4-phenylpiperazine.....	29
2.3. Synthesis of 1-[2-(methoxybenzyl)]-, 1-[3-(methoxybenzyl)]-, and 1-[4- methoxybenzyl]-4-[3-(trifluoromethyl)phenyl]piperazine	29
2.4. Synthesis of 1-[N-(dimethoxybenzyl)]- 4-[3-(trifluoromethyl)phenyl]piperazine	30

2.4.1. Synthesis of 1-[2,3-(dimethoxybenzyl)]-, and 1-[2,5-(dimethoxybenzyl)]-4-[3-(trifluoromethyl)phenyl]piperazine	30
2.4.2. Synthesis of 1-[2,4-(dimethoxybenzyl)]-, 1-[2,6-(dimethoxybenzyl)]-, and 1-[3,4-(dimethoxybenzyl)]-4-[3-(trifluoromethyl)phenyl]piperazine	31
2.4.3. Synthesis of 1-[3,5-dimethoxybenzyl]-4-[3-(trifluoromethyl)phenyl]piperazine	32
2.5. Synthesis of Synthesis of 1-[2,3-(methylenedioxybenzyl)]-4-[3-(trifluoromethyl)phenyl]piperazine and 1-[3,4-(methylenedioxybenzyl)]-4-[3-(trifluoromethyl)phenyl] piperazine	32
2.6. Synthesis of 1-[N-(bromo-dimethoxy benzyl)]-4-[3-(trifluoromethyl)phenyl]piperazine	33
2.7. Synthesis of 1-(3-chlorophenyl)-4-[(N-methoxybenzyl)piperazine	35
2.8. Synthesis of 1-(chlorophenyl)-4-[(N-(dimethoxybenzyl)piperazine	35
2.9. Synthesis of 1-[N-(methoxybenzyl)]-4-[4-(methoxyphenyl)piperazine	36
2.9.1 Synthesis of 1-[2-(methoxybenzyl)- and 1-[3-(methoxybenzyl)-4-[4-(methoxyphenyl)piperazine	36
2.9.2 Synthesis of 1-[4-(methoxybenzyl)-4-[4-(methoxyphenyl)piperazine	37
2.10. Synthesis of 1-[N-(dimethoxybenzyl)]-4-[4-(methoxyphenyl) piperazine	38
2.10.1. Synthesis of 1-[2,3-(dimethoxybenzyl)]-, 1-[2,5-(dimethoxybenzyl)]-, and 1-[2,6-(dimethoxybenzyl)- 4-[4-(methoxyphenyl)piperazine	38
2.10.2. Synthesis of 1-[2,4-(dimethoxybenzyl)]-, 1-[3,4-(dimethoxybenzyl)]-, and 1-[3,5-(dimethoxybenzyl)- 4-[4-(methoxyphenyl)piperazine	39
2.11. Synthesis of 3,4-methylenedioxybenzylpiperazine	39
2.12. Synthesis of 4-Bromo-2,5-dimethoxybenzylpiperazine	40
3. Analytics studies of piperazine derivatives	42
3.1. Analysis of 1-[N-(trifluoromethyl)phenyl]-4-benzylpiperazine (Group1)	43
3.1.1. Mass spectral studies	43
3.1.2. Gas Chromatographic Separation	46

3.1.3. Vapor-phase Infra-Red Spectrophotometry	47
3.1.4. Conclusion	49
3.2. Analysis of 1-[N-(trifluoromethyl)benzyl]-4-phenylpiperazine (Group 2).....	50
3.2.1. Mass spectral studies	50
3.2.2. Gas Chromatographic Separation	53
3.2.3. Vapor-phase Infra-Red Spectrophotometry	54
3.2.4. Conclusions	56
3.3. Analysis of 1-[N-(methylenedioxybenzyl)]-4-[3-(trifluoromethyl)phenyl]piperazine (Group 3).....	57
3.3.1. Mass spectral studies	57
3.3.2. Gas Chromatographic Separation	59
3.3.3. Vapor-phase Infra-Red Spectrophotometry	60
3.3.4. Conclusions	62
3.4. Analysis of 1-[N-methoxybenzyl]-4-[3-(trifluoromethyl)phenyl]piperazine (Group 4).....	62
3.4.1. Mass spectral studies	63
3.4.2. Gas Chromatographic Separation	66
3.4.3. Vapor-phase Infra-Red Spectrophotometry	67
3.4.4. Conclusion	69
3.5. Analysis of 1-[N-dimethoxybenzyl]-4-[3-(trifluoromethyl)phenyl]piperazine (Group 5).....	70
3.5.2. Gas Chromatographic Separation	78
3.5.3. Vapor-phase Infra-Red Spectrophotometry	79
3.5.4. Conclusions	83
3.6. Analysis of 1-[N-(bromo-dimethoxy)benzyl]-4-[3-(trifluoromethyl)phenyl]piperazine (Group 6)	84
3.6.1. Mass spectral studies	85

3.6.2. Gas Chromatographic Separation	91
3.6.3. Vapor-phase Infra-Red Spectrophotometry	93
3.6.4. Conclusions	96
3.7. Analysis of 1-(3-chlorophenyl)-4-[(N-methoxybenzyl)piperazine (Group 7)	97
3.7.1. Mass spectral studies	97
3.7.2. Gas Chromatographic Separation	100
3.7.3. Vapor-phase Infra-Red Spectrophotometry	101
3.7.3. Conclusion	103
3.8. Analysis of 1-(chlorophenyl)-4-[(N-(dimethoxybenzyl)piperazine (Group 8)	104
3.8.1. Mass spectral studies	104
3.8.2. Gas Chromatographic Separation	109
3.8.3. Vapor-phase Infra-Red Spectrophotometry	111
3.8.4. Conclusions	114
3.9. Analysis of N-(methoxybenzyl)-4-methoxyphenylpiperazine (Group 9)	115
3.9.1. Mass spectral studies	115
3.9.2. Gas Chromatographic Separation	119
3.9.3. Vapor-phase Infra-Red Spectrophotometry	120
3.9.4. Conclusion	122
3.10. Analysis of 1-[N-(dimethoxybenzyl)-4-[4-(methoxyphenyl)piperazine (Group 10)	122
3.10.1. Mass spectral studies	123
3.10.2. Gas Chromatographic Separation	127
3.10.3. Vapor-phase Infra-Red Spectrophotometry	128
3.10.4. Conclusions	131

4. Materials and Methods of pharmacology	133
4.1. Chemicals and Reagents of pharmacology	133
4.2. Rat dopaminergic neuron cells (N27)	133
4.3. Treatment design	134
4.4. Cytotoxicity Assay	134
4.5. Protein quantification.....	135
4.6. Quantifying Reactive Oxygen Species	135
4.7. Nitrite assay	135
4.8. Quantification of hydrogen peroxide	136
4.9. Tyrosine hydroxylase (TH) activity.....	136
4.10. Monoamine oxidase (MAO) activity	137
4.11. Quantification of NADH content.....	137
4.12. Glutathione Content.....	137
4.13. Mitochondrial Complex-I Activity	138
4.14. Statistical Analysis	138
5. Pharmacology result	139
5.1. Piperazine derivatives induced Dose-Dependent and Time-Dependent reduction of dopaminergic (N27) Cell viability.....	139
5.2. MDBP and MDBzTFMPP generated ROS production	144
5.3. MDBzTFMPP significantly increased the nitrite production	145
5.4. MDBP and MDBzTFMPP increased the production of H ₂ O ₂	146
5.5. MDBP significantly increased the GSH content.....	147
5.6. MDBP and MDBzTFMPP did not affect the Tyrosine Hydroxylase activity	148

5.7. MDBP and MDBzTFMPP decreased Monoamine oxidase (MAO) activity	149
5.8 MDBzTFMPP significantly decreased the Mitochondrial Complex-I activity.....	150
6. Discussion of pharmacology part	152
7. Conclusion	155
8. Experimental.....	156
8.1. Materials	156
8.2. Instruments	157
8.3. GC-Columns.....	158
8.4. Temperature Programs.....	159
8.5. Synthesis of Piperazine Regioisomers	161
8.5.1. Synthesis of 1-[N-(trifluoromethyl) phenyl]-4-benzylpiperazine	161
8.5.1.1. Synthesis of 1-[2-(trifluoromethyl) phenyl]-4-benzylpiperazine and 1-[4-(trifluoromethyl) phenyl]- 4-benzylpiperazine.....	161
8.5.1.2. Synthesis of 1-[3-(trifluoromethyl) phenyl]-4-benzylpiperazine.....	162
8.5.2. Synthesis of 1-[2-(trifluoromethyl)benzyl]-, 1-[3-(trifluoromethyl)benzyl], and 1-[4-(trifluoromethyl)benzyl]-4-phenylpiperazine	163
8.5.3. Synthesis of 1-[2-(methoxybenzyl)]-, 1-[3-(methoxybenzyl)]-, and 1-[4-(methoxybenzyl)]-4-[3-(trifluoromethyl)phenyl]piperazine	164
8.5.4. Synthesis of 1-[N-(dimethoxybenzyl)]-4-[3-(trifluoromethyl)phenyl]piperazine	165
8.5.4.1. Synthesis of 1-[2,4-(dimethoxybenzyl)]-, 1-[2,6-(dimethoxybenzyl)]-, and 1-[3,4-(dimethoxybenzyl)]-4-[3-(trifluoromethyl)phenyl]piperazine	165
8.5.4.2. Synthesis of 1-[2,3-(dimethoxybenzyl)]-, and 1-[2,5-(dimethoxybenzyl)]- 4-[3-(trifluoromethyl)phenyl]piperazine	167
8.5.4.3. Synthesis of 1-[3,5-(dimethoxybenzyl)]-4-[3-(trifluoromethyl phenyl piperazine).....	168

8.5.5. Synthesis of Synthesis of 1-[2,3-(methylenedioxybenzyl)]-4-[3-(trifluoromethylphenyl) piperazine and 1-[3,4-(methylenedioxybenzyl)]-4-[3-(trifluoromethyl)phenyl]piperazine.....	169
8.5.6. Synthesis of 1-[N-(bromo-dimethoxybenzyl)]- 4-[3-(trifluoromethyl) phenyl]piperazine.....	170
8.5.7. Synthesis of 1-(3-chlorophenyl)-4-[(N-methoxybenzyl)piperazine.....	172
8.5.8. Synthesis of 1-(chlorophenyl)-4-[(N-(dimethoxybenzyl)piperazine	173
8.5.9. Synthesis of 1-[N-(methoxybenzyl)]-4-[4-(methoxyphenyl)piperazine	175
8.5.9.1. Synthesis of 1-[2-(methoxybenzyl)-, and 1-[3-(methoxybenzyl)]-4-[4-(methoxyphenyl)piperazine	175
8.5.9.2. Synthesis of 1-[4-(methoxybenzyl)]-4-[4-(methoxyphenyl)piperazine	176
8.5.10. Synthesis of 1-[N-(dimethoxybenzyl)]-4-[4-(methoxyphenyl)piperazine	177
8.5.10.1. Synthesis of 1-[2,3-(dimethoxybenzyl)-, 1-[2,5-(dimethoxybenzyl)-, and 1-[2,6-(dimethoxybenzyl)]-4-[4-(methoxyphenyl)piperazine	177
8.5.10.2. Synthesis 1-[2,4-(dimethoxybenzyl)-, 1-[3,4-(dimethoxybenzyl)-, and 1-[3,5-(dimethoxybenzyl)- 4-[4-(methoxyphenyl) piperazine	178
8.5.11. Synthesis of 3,4- methylenedioxybenzyl piperazine.....	180
8.5.12. Synthesis of 1-(4-Bromo-2,5-dimethoxybenzyl)piperazine.....	180
9. References	182

List of Figures

Figure 1. Chemical structure of 3-TFMPP and BZP	2
Figure 2. General structure of piperazine derivatives	26
Figure 3. Piperazine derivatives	27
Figure 4. Substituted N-bromo dimethoxy benzaldehyde	34
Figure 5. 1-[N-(Bromo-Dimethoxy benzyl)-4-[3-(trifluoromethylphenyl)piperazine compounds.....	34
Figure 6. EI mass spectra of 1-[N-(trifluoromethyl)phenyl]-4-benzylpiperazine (Group 1)	45
Figure 7. Gas chromatographic separation of 1-[N-(trifluoromethyl)phenyl]-4-benzylpiperazine using TP-1 program (Group 1)	46
Figure 8. Vapor phase IR spectra of 1-[N-(trifluoromethyl)phenyl]-4-benzylpiperazine (Group 1)	49
Figure 9. EI mass spectra of 1-[N-(trifluoromethyl)benzyl]-4-phenylpiperazine (Group 2)	52
Figure 10. Gas chromatographic separation of 1-[N-(trifluoromethyl)benzyl]-4-phenylpiperazine using TP-2 program (Group 2).....	53
Figure 11. Vapor phase IR spectra of 1-[N-(trifluoromethyl)benzyl]-4-phenylpiperazine (Group 2)	56
Figure 12. EI mass spectra of 1-[N-(methylenedioxybenzyl)]-4-[3-(trifluoromethylphenyl)piperazine (Group 3).....	58
Figure 13. Gas chromatographic separation of 1-[N-(methylenedioxybenzyl)]-4-[3-(trifluoromethylphenyl)piperazine (trifluoromethylphenyl) piperazine using TP-1 program (Group 3).....	60
Figure 14. Vapor phase IR spectra of 1-[N,N-methylenedioxybenzyl]-4-[3-(trifluoromethylphenyl)piperazine (Group 3)	61
Figure 15. EI mass spectra of 1-[N-methoxybenzyl]-4-[3-(trifluoromethyl)phenyl]piperazine (Group 4)	65
Figure 16. Gas chromatographic separation of 1-[N-methoxybenzyl]-4-[3-(trifluoromethylphenyl)piperazine using TP-3 program (Group 4).....	66
Figure 17. Vapor phase IR spectra of 1-[N-methoxybenzyl]-4-[3-(trifluoromethyl)phenyl]piperazine (Group 4)	69
Figure 18. EI mass spectrum for the 2,3-dimethoxybenzyl regioisomer m/z 310 to m/z 370 region	73
Figure 19. EI mass spectra 1-[N-dimethoxybenzyl]-4-[3-(trifluoromethyl phenyl piperazine) (Group 5).....	76
Figure 20. EI-MS of 3,5-dimethoxybenzylpiperazine and 3,5-dimethoxybenzylpiperazine-D8	77

Figure 21. Gas chromatographic separation of 1-[N-dimethoxybenzyl]-4-[3-(trifluoromethyl phenyl piperazine) using TP-3 program (Group 5)	78
Figure 22. Vapor phase IR spectra of 1-[N-dimethoxybenzyl]-4-[3-(trifluoromethyl phenyl piperazine) (Group 5) .	82
Figure 23. 1[-N-(Bromo-Dimethoxy benzyl) - 4-[3-(trifluoromethyl phenyl piperazine) compounds.....	84
Figure 24. EI mass spectra of 1[-N-(Bromo-Dimethoxy) benzyl-4-[3-(trifluoromethyl phenyl piperazine) (Group 6)	90
Figure 25. Gas chromatographic separation of 1[-N-(Bromo-Dimethoxy) benzyl-4-[3-(trifluoromethyl phenyl piperazine) (Group 6) on (Rxi®-17Sil MS) using TP-4 program.....	91
Figure 26. Gas chromatographic separation of 1[-N-(Bromo-Dimethoxy) benzyl-4-[3-(trifluoromethyl phenyl piperazine) (Group 6) Rtx-5 using TP-3 program	92
Figure 27. Vapor phase IR spectra of 1[-N-(Bromo-Dimethoxy) benzyl-4-[3-(trifluoromethyl phenyl piperazine) (Group 6)	96
Figure 28. EI mass spectra of 1[-(N-methoxy-, 4- [3-chloro phenyl piperazine) (Group 7).....	99
Figure 29. Gas chromatographic separation of 1-[N-(methoxybenzyl)-, 4- [3-chloro phenyl piperazine) using TP-1 program (Group 7).....	101
Figure 30. Vapor phase IR spectra of 1[-(N-methoxy-, 4- [3-chloro phenyl piperazine) (Group 7)	103
Figure 31. EI mass spectra of 1[N-dimethoxy- 4- [3-chloro phenyl piperazine) (Group 8)	108
Figure 32. Gas chromatographic separation of 1[N-dimethoxy- 4- [3-chloro phenyl piperazine) (Group 8) Rxi®-17Sil MS using TP-5 program	110
Figure 33. Gas chromatographic separation of 1[N-dimethoxy- 4- [3-chloro phenyl piperazine) (Group 8) (Rtx-200) using TP-6 program	111
Figure 34. Vapor phase IR spectra of 1[N-dimethoxy- 4- [3-chloro phenyl piperazine) (Group 8)	114
Figure 35. EI mass spectra of N-(methoxy) benzyl-4-methoxyphenylpiperazine (Group 9).....	118
Figure 36. Gas chromatographic separation of N-(methoxy) benzyl-4-methoxyphenylpiperazine (Group 9) using TP-1 program.....	119
Figure 37. Vapor phase IR spectra of N-(methoxy) benzyl-4-methoxyphenylpiperazine (Group 9)	121
Figure 38. EI mass spectra of 1[-(N- dimethoxybenzyl- 4- [4-methoxy phenyl piperazine) (Group 10)	126

Figure 39. Gas chromatographic separation of 1[-(N- dimethoxybenzyl- 4- [4-methoxy phenyl piperazine) (Group 10) using TP-7 program.....	128
Figure 40. Vapor phase IR spectra of 1[-(N- dimethoxybenzyl- 4- [4-methoxy phenyl piperazine) (Group 10)	131
Figure 41. Effect of 3-TFMPP and 3-TFMPPBz on dopaminergic (N27).....	140
Figure 42. Effect of MDBP and MDBzTFMPP on dopaminergic (N27)	142
Figure 43. Effect of BrDMBP and BrDMBzTFMPP on dopaminergic (N27)	143
Figure 44. Effect of MDBP and MDBzTFMPP on ROS generation in N27 dopaminergic neuronal cells	145
Figure 45. Effect of MDBP and MDBzTFMPP on Nitrite production in N27 cells	146
Figure 46. Effect of MDBP and MDBzTFMPP on H2O2 production in N7 cells	147
Figure 47. Effect of MDBP and MDBzTFMPP derivatives on GSH content in N27 cells dopaminergic neuronal cells	148
Figure 48. Effect of MDBP and MDBzTFMPP on the tyrosine hydroxylase TH activity in N27	149
Figure 49. Effect of MDBP and MDBzTFMPP on mitochondrial monoamine oxidase (MAO) activity in N27.....	150
Figure 50.a. Effect of MDBP and MDBzTFMPP on Mitochondrial Complex-I activity in N27 cells.....	151
Figure 501.b. Effect of MDBP and MDBzTFMPP on NADH activity in N27	151

List of Schemes

Scheme 1. Proposed scheme for the metabolism of BZP (Staack 2007)	13
Scheme 2. Proposed scheme for the metabolism of 3-TFMPP (Staack et al, 2004).....	14
Scheme 3. Synthetic approach of 1-[N-(trifluoromethyl)phenyl]-4-benzylpiperazine	28
Scheme 4. Synthetic approach of 1-[3-(trifluoromethyl)phenyl]-4-benzylpiperazine	28
Scheme 5. Synthetic approach of 1-[N-(trifluoromethyl)benzyl]-4-phenylpiperazine	29
Scheme 6. Synthetic approach of 1-[N-(methoxybenzyl)]-4-[3-(trifluoromethyl)phenyl]piperazine.....	30
Scheme 7. Synthetic approach of 1-[N-(dimethoxybenzyl)]-4-[3-(trifluoromethyl)phenyl]piperazine	31
Scheme 8. Synthetic approach of 1-[N-(dimethoxybenzyl)]-4-[3-(trifluoromethyl)phenyl]piperazine	31
Scheme 9. Synthetic approach of 1-[3,5 dimethoxybenzyl]- 4-[3-(trifluoromethyl)phenyl]piperazine	32
Scheme 10. Synthetic approach of 1-[N-(methylenedioxybenzyl)]-4-[3-(trifluoromethyl)phenyl]piperazine.....	33
Scheme 11. Synthetic approach of 1-[N-(bromo-dimethoxybenzyl)]-4-[3-(trifluoromethyl)phenyl]piperazine	34
Scheme 12. Synthetic approach of 1-(3-chlorophenyl)-4-[(N-methoxybenzyl)piperazine.....	35
Scheme 13. Synthetic approach of 1-(chlorophenyl)-4-[(N-(dimethoxybenzyl)piperazine.....	36
Scheme 14. Synthetic approach of 1-[N-(methoxybenzyl)-4-[4-(methoxyphenyl)]piperazine.....	37
Scheme 15. Synthetic approach of 1-[4-(methoxybenzyl)-4-[4-(methoxyphenyl)]piperazine	37
Scheme 16. Synthetic approach of 1-[N-(dimethoxybenzyl)- 4-[4-(methoxyphenyl)]piperazine	38
Scheme 17. Synthetic approach of 1-[N-(dimethoxybenzyl)-4-[4-(methoxyphenyl)]piperazine	39
Scheme 18. Synthetic approach of 3,4-methylenedioxybenzyl piperazine.....	40
Scheme 19. Synthetic approach of 4-Bromo-2,5-dimethoxybenzylpiperazine.....	41
Scheme 20. EI mass spectral fragmentation pattern of 1-[N-(trifluoromethyl)phenyl]-4-benzylpiperazine (Group 1)	45
Scheme 21. EI mass spectral fragmentation pattern of 1-[N-(trifluoromethyl)benzyl]-4-phenylpiperazine (Group 2).....	52
Scheme 22. EI mass spectral fragmentation pattern of 1-[N-(methylenedioxybenzyl)]-4-[3- trifluoromethyl)phenyl]piperazine (Group 3).....	59

Scheme 23. EI mass spectral fragmentation pattern of 1-[N-methoxybenzyl]-4-[3-(trifluoromethyl)phenyl]piperazine (Group 4)	65
Scheme 24. Mechanism for the formation of the m/z 136 ion in the mass spectra of the 2,3-dimethoxybenzyl regioisomer	71
Scheme 25. Mechanism for the formation of the m/z 152 ion in the mass spectra of the 3,5-dimethoxybenzyl regioisomer	72
Scheme 26. EI mass spectral fragmentation pattern of 1-[N-dimethoxybenzyl]-4-[3-(trifluoromethyl)phenyl]piperazine (Group 5).....	76
Scheme 27. Mechanism for the formation of the base peak at m/z 229	85
Scheme 28. Mechanism for the formation of the fragment m/z 257/259	86
Scheme 29. Mechanism for the formation of the fragment m/z 214/216	86
Scheme 30. EI mass spectral fragmentation pattern of 1-[N-(bromo-dimethoxy)benzyl]-4-[3-(trifluoromethyl)phenyl]piperazine (Group 6).....	90
Scheme 31. EI mass spectral fragmentation pattern of 1-(3-chlorophenyl)-4-[(N-methoxybenzyl)piperazine (Group 7).....	100
Scheme 32. EI mass spectral fragmentation pattern of 1-(chlorophenyl)-4-[(N-(dimethoxybenzyl)piperazine (Group 7).....	109
Scheme 33. EI mass spectral fragmentation pattern of N-(methoxy) benzyl-4-methoxyphenylpiperazine (Group 9)	118
Scheme 34. EI mass spectral fragmentation pattern of 1-(N-dimethoxybenzyl)-4-[4-methoxy phenyl piperazine) (Group 10)	127

List of tables

Table 1. Piperazines moiety as promising therapeutic tool	10
Table 2. Structural formula of piperazine derivatives.....	26
Table 3. List of columns used and their composition.	159
Table 4. List of temperature programs used	160
Table 5. Yields and crystallization solvents for the 1-[N-(trifluoromethyl) phenyl]-4-benzylpiperazine	162
Table 6. Table 3. Yields and Crystallization Solvents for the 1-[3-(trifluoromethyl) phenyl]-4-benzylpiperazine...	163
Table 7. Yields and Crystallization Solvents for 1-[N-(trifluoromethyl)benzyl]-4-phenylpiperazine.....	164
Table 8. Yields and crystallization solvents for 1-[N-(methoxybenzyl)]-4-[3-(trifluoromethyl) phenyl]piperazine.	165
Table 9. Yields and crystallization solvents for.....	166
Table 10. Yields and crystallization solvents for 1-[N-(dimethoxybenzyl)]- 4-[3-(trifluoromethyl)phenyl]piperazine	167
Table 11. Yields and crystallization solvents for 1-[3,5-(dimethoxybenzyl)]- 4-[3-(trifluoromethyl)phenyl]piperazine	168
Table 12. Yields and crystallization solvents for 1-[N-(methylenedioxybenzyl)]-4-[3-(trifluoromethylphenyl)piperazine.....	170
Table 13. Yields and crystallization solvents for 1-[N-(bromo-dimethoxy benzyl) - 4-[3-(trifluoromethyl phenyl) piperazine	171
Table 14. Yields and crystallization solvents for 1-[N-(methoxybenzyl)-4-[3-(chlorophenyl)piperazine	173
Table 15. Yields and crystallization solvents for.....	174
Table 16. Yields and crystallization solvents for 1-[N-(methoxybenzyl)-4-[4-(methoxyphenyl)piperazine.....	176
Table 17. Yields and crystallization solvents for 1-[4-(methoxybenzyl)-4-[4-(methoxyphenyl)piperazine.....	177
Table 18. Yields and crystallization solvents for 1-[N-(dimethoxybenzyl)-4-[4-(methoxyphenyl)piperazine.....	178
Table 19. Yields and crystallization solvents for 1-[N-(dimethoxybenzyl)-4-[4-(methoxyphenyl)piperazine.....	179
Table 20. Yields and crystallization solvents for 3,4-methylenedioxybenzyl piperazine.....	180
Table 21. Yields and crystallization solvents for 1-(4-Bromo-2,5-dimethoxybenzyl)piperazine.....	181

List of Abbreviation

5-HT	5-hydroxytryptamine (Serotonin)
ACTH	Adrenocorticotropin
AVP	Arginine Vasopressin
BZP	N-benzylpiperazine
CAT	Catalase
CNS	Central Nervous System
CYP	Cytochrome P450
DA	Dopamine
DCF-DA	2', 7-Dichlorofluoresceindiacetate
DMSO	Dimethylsulfoxide
FBS	Fetal Bovine Serum
GC/MS	Gas Chromatography/Mass Spectrometry
GSH	Glutathione
GSH-Px	Glutathione Peroxidase
H ₂ O ₂	Hydrogen Peroxide
LC/MS	Liquid Chromatography/Mass Spectrometry
MAO	Monoamine Oxidase
mCPP	1-(3-chlorophenyl) piperazine
MDA	Malondialdehyde
MDBP	1-(3,4-methylenedioxybenzyl) piperazine
MDMA	Methylenedioxymethamphetamine
MPTP	1-methyl-4-phenyl-1,2,3,6-tetrahydropyridine

NA	Noradrenaline
NADH	Nicotinamide Adenine Dinucleotide
NO	Nitric Oxide
OPA	O-Phthalaldehyde
PBS	Phosphate Buffer Saline
PNS	Peripheral Nervous System
ROS	Reactive Oxygen Species
SCN	Suprachiasmatic Nucleus
TBA	Thiobarbituric Acid
TBARS	Thiobarbituric Acid-Reactive Substances
TCA	Trichloroacetic Acid
TFMPP	Trifluoromethylphenylpiperazine
TFMBzPP	Trifluoro-Methyl-Benzyl-Phenylpiperazine
BzPP	Benzyl-Phenylpiperazine
μl	Micro liter
μm	Micrometer
°C	Degree centigrade
Da	Dalton
DMF	Dimethylformamide
EI	Electron Ionization
GC	Gas chromatography
GC-IRD	Gas chromatography coupled to infrared detection
GC-MS	Gas chromatography- mass spectrometry

MDBP 3,4-Methylenedioxybenzylpiperazines

MDBzTFMPP 3,4-Methylenedioxybenzyl-3-trifluoromethylphenylpiperazines

BrDMBP 4-bromo-2,5-dimethoxybenzylpiperazines

BrDMBTFMPP 4-bromo-2,5-dimethoxybenzyl-3-trifluoromethylphenylpiperazines

1. Literature review

1.1. Introduction

New psychoactive substances (NPS) or designer drugs gained massive attention in recent years worldwide due to the alarming consumption and widespread abuse/use between variant groups of ages. The abuse of illegal drugs is expanding globally, with 269 million people reported to have tried these kinds of drugs at least once in their past. This number represents almost 1 in every 19 or 5.4% of the global population. Consequently, the mortality rate due to the use of illegal substances has been escalating over the past decade, with approximately 450,000 deaths in 2015 (“World Drug Report 2020” n.d.). Meanwhile, the number of NPS is continuously growing; more than 1000 substances have been reported up to December 2020 (Kranenburg et al. 2021). Numerous factors have led to the popularity of designer drugs, especially among young people, such as availability on the street, online access, and lack of legal controls. The rapid growth in designer drug manufacturing and the number of consumers can lead to global health issues due to the ambiguous profile of pharmacological properties and unexplored adverse effects, which can significantly affect the public health (Luethi and Liechti 2020). Designer drugs are structurally modified analogues of well-known drugs of abuse, mainly designed and synthesized to mimic the psychoactive properties without any legal restrictions. These chemicals are often synthesized in clandestine laboratories to avoid legislative control. The commercial availability of precursors may allow the clandestine chemists to produce endless numbers of chemically modified drugs (Monitoring Centre for Drugs and Addiction, n.d.). Designer drugs are classified based on the chemical structure; the most common groups are Phenethylamines, Piperazines, Tryptamines,

synthetic cannabinoids, synthetic cathinones, and synthetic opioids (Carroll et al. 2012). Most groups of designer drugs are structurally related to classic drugs of abuse, except the piperazine group with a unique chemical structure that is not associated with any classical drugs of abuse (Katz et al. 2016a). Piperazine compounds appeared in the illicit drugs market in Europe in 1999 and were marketed as safe alternatives to illegal drugs (Wikström, Holmgren, and Ahlner 2004). Benzylpiperazine (BZP) and 3-trifluoromethylphenylpiperazine (3-TFMPP) are the most frequently abused drugs in this group Figure (1). These compounds have psychostimulant effects similar to amphetamine and MDMA, as well as hallucinogen potent (De Boer et al. 2001).

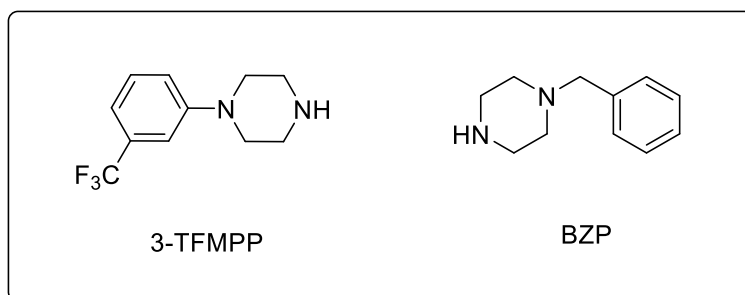


Figure 1. Chemical structure of 3-TFMPP and BZP

1.2. Piperazine derivatives as drugs of abuse

In the U.S., the first reported case of abuse on piperazine derivatives occurred with N-benzylpiperazine (BZP) in 1996. This was followed by many cases of piperazine compound misuse in different countries, primarily European countries and Australasia. Around millions of piperazine tablets were seized in Europe in 2006, while more than eight million of piperazines products were consumed in New Zealand between 2000-2005 (Johnstone et al. 2007) (Arbo, Bastos, and Carmo 2012a). The reasons behind the misuse of piperazine compounds include

resemblance of the psychotropic effects as compared to the well-known classical drugs of abuse such as amphetamine and MDMA, easy access, availability on the street in some countries, and different dosage formulation. The main goal for chemical structure modification of compounds is to mimic the psychoactive and hallucinogenic effects. The abuse of piperazines compounds for recreational use arises from the fact that recognized piperazines of abuse like BZP and TFMPP produce similar effects to well-known psychostimulants drugs but with slower onset. Accordingly, the abusers may ingest multiple doses or overdose to achieve the desired stimulatory effect. For instance, the action of BZP lasts for 6 to 8 hours with usual doses ranging from 50 to 250 mg. Concerning the onset, the psychostimulant influence of BZP is delayed for up to two hours. Thus, the potential of repeated doses or overdoses is escalating, as reported in many studies that the BZP level in some cases reached up to 1000mg (Welz and Koba 2020) (Cohen and Butler 2011). Additionally, the piperazines compounds are usually consumed in combination with other drugs, like BZP and TFMPP, to mimic MDMA. Similarly, piperazine compounds are also used in combination with other psychoactive drugs, like amphetamine, ecstasy, ketamine, cocaine, cannabis, cathinone, and alcohol. The stimulatory influence of consuming the BZP may escalate when used with amphetamine while using the BZP with cannabis most likely leads to relaxation and increased appetite (Welz and Koba 2020) (Wood et al. 2008). There are many formulations of piperazine compounds on the street, tablets, powder, capsules, injections, liquid mixture, and even smoking material. Unfortunately, numerous contaminations have also been reported in combination with piperazines like detergents, bleach, hydrogen peroxide, plant parts, and animal poison (Welz and Koba 2020).

1.3. Dark web

The old fashion or traditional market of drug distribution has been changed recently; with use of the internet as marketing tool. One of the significant reasons for the increase in the popularity of recreational drugs like piperazine is the availability through the internet. As a result, different age groups of people, especially the younger age group, have easy access to piperazines compounds. In fact, internet drug trafficking is reported to motivate clandestine laboratories to create new kinds of recreational drugs or produce novel compounds (Davies et al. 2010). The secret labs are advertising these compounds as safe or legal high substances, ignoring the regulations, or taking the advantages of control absence. The final products of designer drugs are designed to be attractive to abusers with colorful packaging. However, these products lack the content information and directions for use (Davies et al. 2010). Piperazines compounds are traded through the internet under different names like; “party pills” , “legal Ecstasy”, Strong as Hell”, “XXX”, “Head Rush”, ” Herbal ecstasy”, “A2”, and “Legal E.” (Musselman and Hampton 2014) (Rosenbaum, Carreiro, and Babu 2012). In fact, piperazines products are considered as one of the highest-selling psychological drugs through the internet, especially in New Zealand, Europe, and North America. Consequently, there is a considerable profit resulting from the wide-ranging distribution. For instance, in New Zealand, the annual financial revenue of the BZP sale is estimated at NZ\$50 million (C Wilkins et al. 2006).

1.4. Piperazine moiety as a promising therapeutic tool

Designing, synthesizing, and exploring promising new therapeutic agents that may help prevent or treat various diseases is a major goal of medicinal chemistry. Numerous diseases are still required

proper therapeutic agents to help manage and cure. The piperazine moiety is a promising therapeutic scaffold with pharmacological values that will help address many diseases (Brito et al. 2019). The chemical alteration of piperazine core has encouraged many researchers and industrial laboratories to design and investigate novel piperazine analogues due to the wide variety of piperazine ring substituents that can be added (A. Sharma et al. 2020). The piperazine ring has a role in many therapeutic drugs with various pharmacological activities such as antifungal, anticancer, anticonvulsant, antibacterial antidepressant, antimycobacterial, antimalarial, anthelmintic etc (Shaquiquzzaman et al. 2015). Additionally, piperazine moiety has a commercial role for many industries as starting material in neuroprotective iron chelators, tubulin polymerization inhibitors, novel charge-transfer polymers in solar cells, organic-inorganic nano-hybrid polyoxometalates, and brain receptor imaging agents (A. Sharma et al. 2020).

1.4.1. Piperazines as anticancer agents

Cancer is uncontrolled, abnormal cell growth and spread, multifactorial, and is one of the major global health issues that fascinated the whole world's attention. Researchers around the world have dedicated enormous efforts to achieve curable medications for this scourge. The piperazine core ring has been extensively evaluated for antitumor activity, and it is involved in many remarkable anticancer drug development. The piperazine ring present in promising anticancer agents reveals in vitro cytotoxicity on sixty human cancer cells originated from breast cancer, leukemia, liver cancer, non-small cell lung, colon, melanoma, ovarian, renal, prostate (Shaquiquzzaman et al. 2015). Starting from ciprofloxacin based compounds which has piperazine core, many studies illustrate antiproliferation against various cancer cell lines including HeLa and Caski cancer cells (W. X. Sun et al. 2017). In a computational study combined with in vitro study by (Chetan et al.

2010) and his colleague against three cancer cell-lines (NCIH460; HCT116; U251), the piperazines exerted anticancer activity. The study illustrates a potential inhibition against HL60 human promyelocytic leukemia cell line. Another report presents piperazine moiety's ability to improve the natural herb antitumor activity against Bel-7402 and RKO cell lines. These studies describe the antiproliferative activity of merging piperazine ring with matrine (alkaloid) in vitro and in vivo study by using H22 tumor-bearing mice models (Xu et al. 2019).

1.4.2. Piperazines as Antibacterial, antifungal, and antiviral agents

Bacterial infection is an invasion of the body by a pathogenic strain of bacteria, and is one of the leading global mortality and morbidity causes. Antibiotics are usually the first-line therapeutic plan to fight and overcome bacterial infections. Many piperazines based compounds have been developed and evaluated for their antibacterial activity. These piperazines-based compounds oxazilodinone derivatives demonstrate superior antibacterial activity when compared to the present antibacterial treatment (Lohray et al. 2006), Table (1). Takhi et al have synthesized some piperazine compounds that exhibit 3-4 times more potential activity against Gram-positive and Gram-negative strains compared to current line of treatment linezolid (Takhi et al. 2006). Also, Foroumadi et al. designed a series of hybrid compounds of levofloxacin and thiadiazol that have higher activity against *Bacillus subtilis* than the reference drug N-desmethyl levofloxacin (Foroumadi et al. 2006). Piperazine-based compounds exhibit potential activity as antifungal agents. Sun et al. synthesized series of piperazine compounds, these compounds illustrate parallel antifungal activity to the reference drug (Fluconazole) against *Candida krusei*, *C. parapsilosis* *C.*, *albicans*, and *C. krusei* (Q. Y. Sun et al. 2007). Similarly, Upadhayaya et al., Che et al., and Yu et al. designed and synthesized piperazine derivatives to examine their antifungal activity versus

many fungal species such as *Candida albicans*, *Candida tropicalis*, *Candida parapsilosis*, and *Cryptococcus neoformans*, *Rhizoctonia solani*, *C. albicans*, *C. parapsilosis*, and *Torulopsis glabrata* (Che et al. 2009) (Upadhayaya et al. 2004) (Yu et al. 2009). Piperazine-based compounds motivated researchers to develop and evaluate series of antiviral agents. Some of these compounds exhibit comparable activity against viral infections, especially HIV-1, human rhinovirus, and hepatitis C virus (Tagat et al. 2001) (Wang et al. 2011) (Bassetto et al. 2017).

1.4.3. Piperazines as antidepressant and anti-anxiolytic agents

The imbalance of monoamine neurotransmitters is a significant cause of depression which affect almost 350 million of people worldwide. Piperazine compounds alter the monoamines pathways by their receptor agonist action or reuptake inhibition of monoamines. Several antidepressant chemical structures contain piperazine ring, including Amoxapine, Etoporidone, Nefazadone, Trazodone, Vilazadone, and Vortioxetine (Brito et al. 2019). Similarly, piperazine-based compounds have been tested for their activity in treatment anxiety disorders. Some studies also identified piperazine compounds with an anti-anxiolytic profile (Pytko et al. 2016) (Khatri et al. 2009).

1.4.4. Piperazines as cardioprotective agents

Cardiovascular diseases are a major health problem and one of the top causes of death globally. The elevated prevalence of cardiovascular diseases is due to numerous factors and causes (Balakumar, Maung-U, and Jagadeesh 2016). Many researchers have investigated piperazine-based drugs to discover cardioprotective activity. They developed various piperazine-based

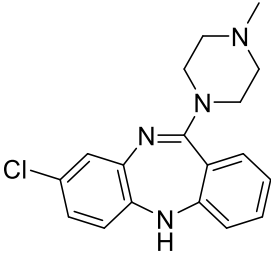
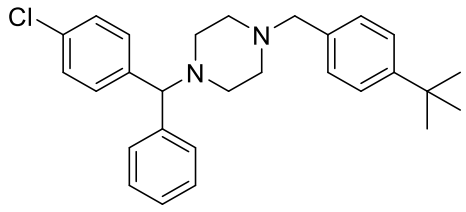
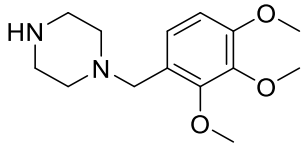
compounds with antihypertensive, antiarrhythmic, antiplatelet aggregation activity, and rennin inhibitory activity (Nakamura et al. 2012) (Kulig et al. 2009). A series of substituted piperazine compounds were synthesized and investigated (Di Braccio et al. 2013) for their inhibitory activity on human platelet aggregation; nine of fifteen compounds showed significant promising results. Also, (Romeiro et al. 2011) and (Nakamura et al. 2012) designed piperazine compounds that exhibit encouraging adrenergic receptor blocking activity and renin inhibitory activity.

1.4.5. Piperazines as cognitive enhancer agents

Cognition is the mental process of thinking, knowing, remembering, and many crucial functions to sustain human life. For decades, scientists have developed drugs that improve cognition status since it connected with several mental diseases. Alzheimer's disease (AD), schizophrenia, Parkinson's disease (PD), depression, and epileptic disorders are linked with cognition disturbance. Dementia, which is the umbrella of neurodegenerative diseases, is the ideal target for cognition enhancers. Furthermore, notably, progress on cognition enhancer agents have been established, and piperazine-based compounds are part of that progress (P. Sharma et al. 2020) (M. K. Sun, Nelson, and Alkon 2015). Piplani et al. and colleges were determined excellent AChE inhibitory agents derived from piperazine moiety. The synthesized piperazines by Piplani et al. illustrate a scopolamine reverse effect using a step-down passive avoidance model (Piplani and Danta 2015). Similarly, alteration of piperazine ring of potent cognition enhancer DM235 by Martino et al showed many modified piperazine compounds with encouraging *in vivo* results as a cognitive enhancer (Martino et al. 2017).

1.4.6. Piperazines as Anti-inflammatory agents

Inflammation is the response of the body to which immune system to an invader, usually accompanied by numerous symptoms such as redness, pain, heat, and swelling. The first line of inflammation treatment is non-steroidal anti-inflammatory drugs, which may cause significant side effects in a long period of usage (Shaquiquzzaman et al. 2015). Recently, scientists established the potential anti-inflammatory activity of piperazine-based compounds. Saeed et al. and his team developed a series of piperazine compounds with potent anti-inflammatory effects compared to indomethacin (Saeed et al. 2012). Another study by (Hatnapure et al. 2012), established the anti-inflammatory activity of novel piperazine-based compounds.

<p>Clozapine (Shaquiquzzaman et al. 2015)</p>		<p>Antipsychotic</p>
<p>Buclizine (G. E. Gaillard 1955)</p>		<p>Antihistamine</p>
<p>Trimetazidine (Kálai et al. 2006)</p>		<p>Antianginal</p>

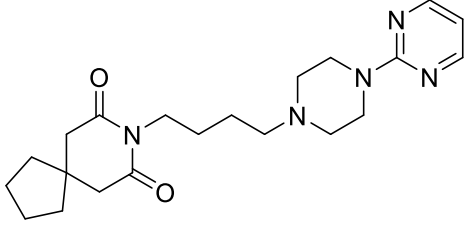
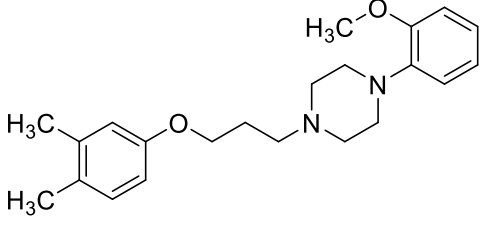
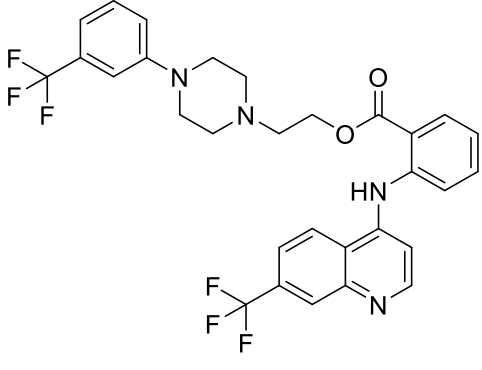
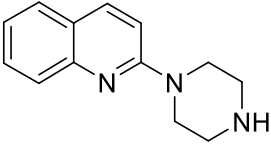
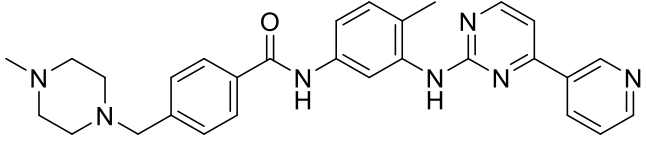
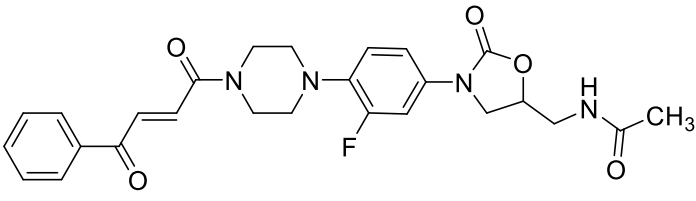
<p>Buspirone</p> <p>(Chilmonczyk, Krajewski, and Cybulski 2002)</p>		<p>Antidepressant</p>
<p>HBK-18</p> <p>(Kubacka et al. 2013)</p>		<p>Cardioprotective</p>
<p>Antrafenine</p> <p>(Saeed et al. 2012)</p>		<p>Analgesic & Anti-inflammatory</p>
<p>Quipazine</p> <p>(Cappelli et al. 2005)</p>		<p>Serotonin receptor agonist</p>
<p>Imatinib</p> <p>(Manley et al. 2013)</p>		<p>Anticancer</p>
<p>oxazilodinone derivative</p> <p>(Lohray et al. 2006)</p>		<p>Antibacterial</p>

Table 1. Piperazines moiety as a promising therapeutic tool

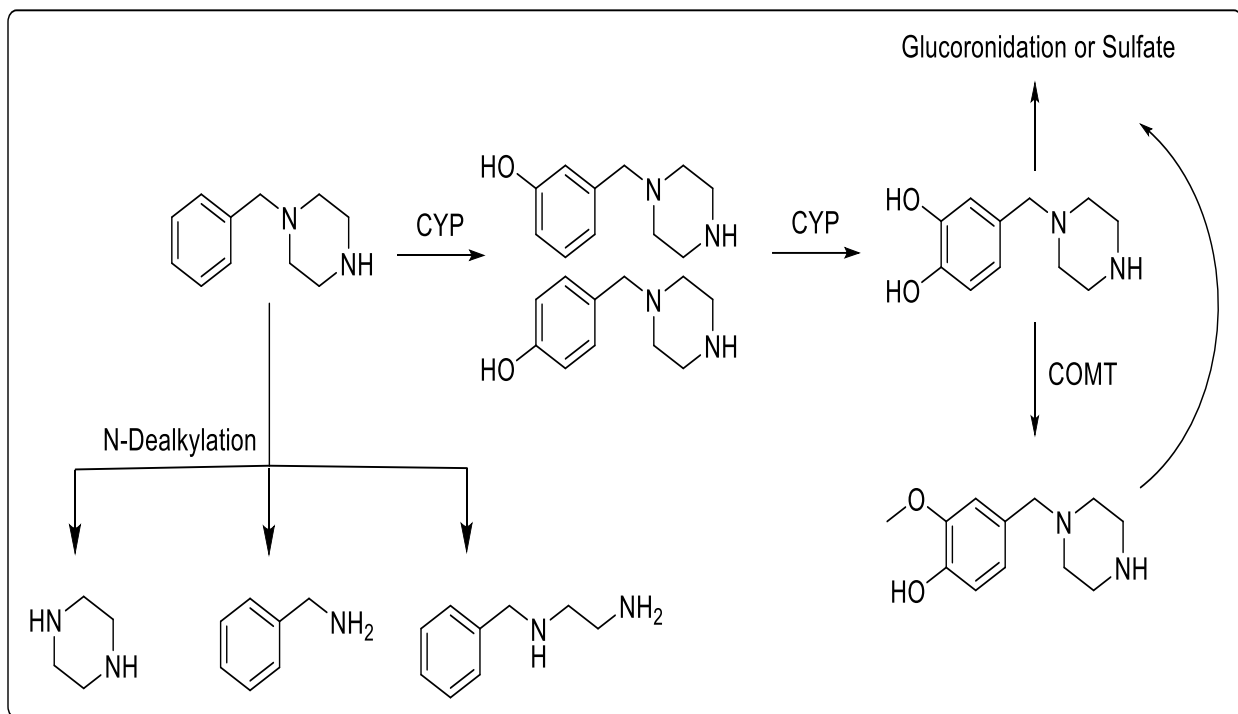
1.5. Pharmacology of piperazine compounds

The new psychoactive substances or designer drugs affect the central nervous system, but little is known about their pharmacological profile. The influence of designer drugs appears to result from the interaction with monoamines neurotransmitters; norepinephrine (NE), serotonin (5-HT), dopamine (DA), and their transporters (NET, SERT, and DAT). Consequently, the pharmacological characteristics of designer drugs are considered a significant research area for many scientists due to the widespread and high probability of abuse. Designer drugs with piperazine moiety in their structures illustrate variable interactions with monoamine neurotransmitters. The piperazine derivatives are presumed to cause hallucination and stimulation effects by elevating the synaptic serotonin and dopamine level.

1.5.1. Pharmacodynamics and pharmacokinetics of benzylpiperazine (BZP)

Benzylpiperazine (BZP) has a similar mode of action to MDMA with mixed action on serotonergic and dopaminergic receptors. BZP blocks the serotonin reuptake in the synapse with a 5-HT₁ agonist, leading to serotoninomimetic action. The common side effects of BZP consumption are hallucination, peripheral side influence of nausea and stomach pain, and headache arise from binding profile to 5-HT_{2A}, 5-HT_{2B}, and 5-HT₃, respectively (Yeap et al. 2010), (Monteiro et al. 2013). *In vivo* studies show that BZP elevates the DA and 5-HT extracellularly compared to *in vitro* studies for 5-HT release (BAUMANN et al. 2004). In addition, Baumann and his team found that BZP with EC₅₀ = 175nM released monoamines through the DAT-mediated mechanism. Besides the DA and 5-HT activity, BZP is also antagonizes alpha -2- adrenoreceptor releasing

noradrenaline. Consequently, 100 mg of BZP consumption by the human results in an equal cardiostimulant effect produced by 7.5-10 mg of amphetamine (Simmler et al., 2014). Behavioral studies of BZP on animals described powerful locomotor stimulants, hyperactivity, involuntary head movements on rats. While on rhesus monkeys, BZP showed jaw chattering, flycatching, involuntary head movements, bizarre body postures, hyperactivity, and self-administered (Fantegrossi et al. 2005), (Campbell et al. 1973). Nikolova and Danchev have reported numerous side effects of BZP, such as; insomnia, dryness of the mouth, tremor, dystonia, headache, dilated pupils, extreme alertness, pruritus, confusion, agitation, dizziness, anxiety, insomnia, vomiting, chest pain, palpitations, collapse, tachycardia, hypertension, hyperventilation, hyperthermia (Nikolova and Danchev 2008a). Metabolism of piperazine compounds appears to occur mainly in the liver, where piperazine exposure occurs first. Piperazine compounds are absorbed from the gastrointestinal tract. However, the pharmacokinetic profile of BZP is not fully understood in human since few studies clarify the metabolism process of BZP. BZP has three metabolic targets: the aromatic ring, the benzyl carbon, and the piperazine ring. Studies on male Wistar rats identified metabolic pathways of BZP, but most of the BZP dose was excreted unchanged (Arbo, Bastos, and Carmo 2012b). The proposed metabolic pathways include hydroxylation of the aromatic ring by CYP 450, then methylation by catechol-O-methyltransferase (COMT). The previous step is to form the substrate of the glucuronides and/or sulfates conjugations. Dealkylation involves BZP metabolism, leading to form piperazine, N-benzylethylenediamine and benzylamine Scheme (1) (Staack 2007).

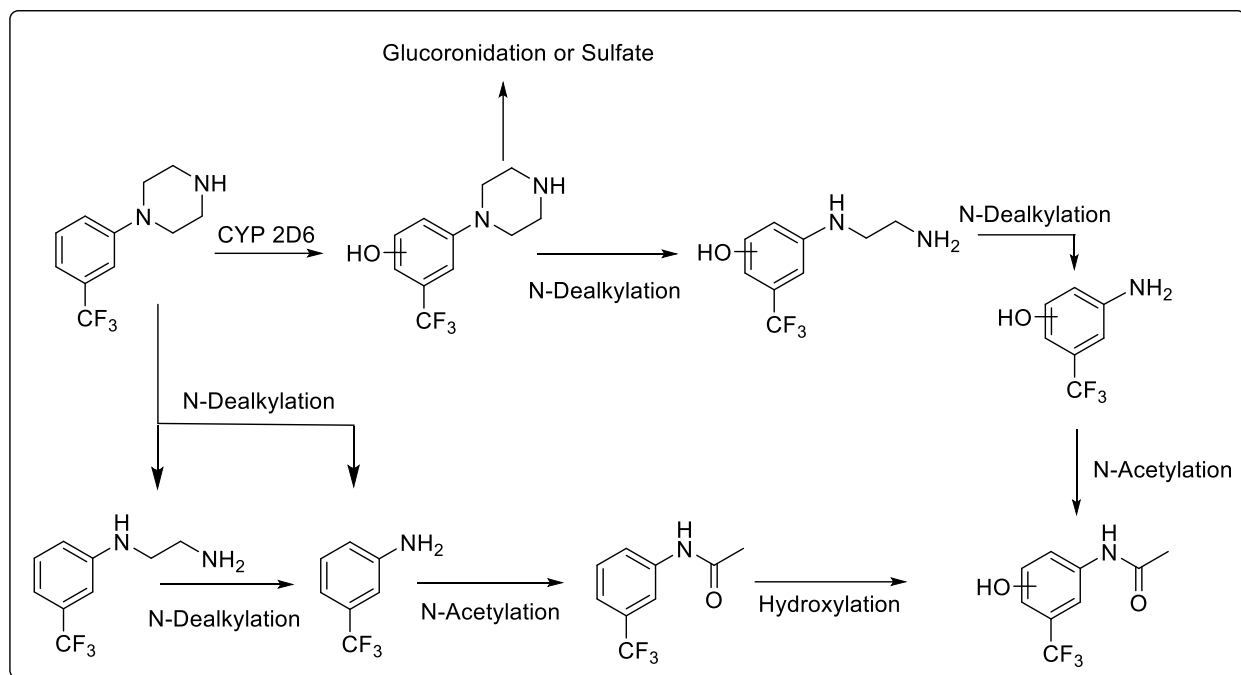


Scheme 1. Proposed scheme for the metabolism of BZP (Staack 2007)

1.5.2. Pharmacodynamics and pharmacokinetics of TFMPP

The effect of TFMPP on monoaminergic neurotransmission by a mixed agonist, partial agonist, and antagonist at 5-HT receptors with no relevant effect on dopaminergic activity. TFMPP with $EC_{50} = 121\text{nM}$ released $[3\text{H}]$ 5-HT through SERT-mediated mechanism (BAUMANN et al. 2004). TFMPP derivatives have shown in vitro and in vivo stimulation of 5-HT release from presynaptic neurons with limited binding affinity to 5-HT₁ and 5-HT₂ (Auerbach, Rutter, and Juliano 1991) (Pettibone and Williams 1984). Since TFMPP is rarely used alone, there is a limited clinical trial on humans demonstrating the TFMPP effects. However, TFMPP alone causes slight psychedelic effects like LSD and dysphoria (Lin et al. 2011). The metabolic pathway of TFMPP in animal is similar to the BZP but with a significantly higher rate of metabolism. The aromatic hydroxylation for TFMPP is the major pathway mainly by CYP2D6 to form N- (hydroxy-3-

trifluoromethylphenyl)ethylenediamine or hydroxy-3 trifluoromethylaniline. Hydroxylation of an aromatic ring is usually followed by glucuronidation or sulfation. Another metabolic route of TFMPP involves N-dealkylation to form N-(3-trifluoromethylphenyl)ethylenediamine or 3-trifluoromethylaniline. This step is followed by N-acetylation in some reports Scheme (2) (Staack et al. 2004). The combination of TFMPP and BZP has demonstrated a synergistic effect that remarkably increases the dopamine and serotonin level in rat diencephalon, which mimics the pharmacological effect of MDMA (Baumann et al. 2004).



Scheme 2. Proposed scheme for the metabolism of 3-TFMPP (Staack et al, 2004)

1.5.3. Pharmacodynamics and pharmacokinetics of mCPP

meta-chlorophenylpiperazine (mCPP) has similar pharmacological actions to TFMPP with direct and indirect agonistic activity at 5-HT receptors. mCPP elevates the 5-HT extracellularly in the hippocampus of SH rats. Likewise, mCPP has shown limited dopamine boost in the nucleus accumbens and in the striatum of SH rats and SD strain rats. Interestingly, mCPP has a negligible effect on dopamine and acutely depleted serotonin (Bossong et al. 2010), (Eriksson et al. 1999). Adverse effects of mCPP include dizziness, anxiety, hallucinations, nausea, warm and cold flushes, panic attacks, and migraine (Tancer and Johanson 2001) (Gijsman, Cohen, and Van Gerven 2004). The metabolism of mCPP is very similar to other designer drugs piperazines like BZP and TFMPP. Aromatic hydroxylation of mCPP is the major metabolic pathway, followed by phase II glucuronidation or sulfation. Other metabolic pathways include degradation with N-dealkylation to form N-(3-chlorophenyl) ethylenediamine or to 3-chloroaniline. mCPP is the active metabolite for some drugs like mepiprazol, nefazodone, etoperidone, and trazodone (Staack and Maurer 2005).

1.5.4. Pharmacodynamics and pharmacokinetics of MDBP

The pharmacological profile of 1-(3,4-methylenedioxybenzyl) piperazine has not been extensively investigated, although some reports suggest the modest inhibition of serotonin uptake of MDBP. The metabolic pathways of MDBP differ from other previous piperazine compounds. MDBP metabolism has demethylation methylenedioxy scaffold as the main metabolic pathway. The demethylation of MDBP leads to form catechol followed by methylation to N - (4-hydroxy-

3-methoxybenzyl) piperazine. Glucuronidation or sulfation is the further step as phase II metabolites. The N-dealkylation pathway was also reported for MDBP to form piperazine. Interestingly, the use of fipexide, a psychoactive drug, was discontinued due to the adverse effects of its primary metabolite, which is MDBP (Sleno et al. 2007) (Staack and Maurer 2004).

1.6. Toxicokinetics and treatment of piperazines toxicity

Most studies demonstrate the toxicity of piperazine derivatives have focused on “party bills” BZP, TFMPP, and the BZP/TFMPP combination. Even though, there are few studies on human and animals which validate and investigate the toxicity profile of piperazines. Many of these reports depend on collecting data from users by surveys and self-reporting, which may not lead to accurate results (Schep et al. 2011). However, the limited reports on piperazines toxicity show moderate adverse effects with some rare severe side effects. Mild effects related to piperazines toxicity wnot requiring medical care include nausea, headache, insomnia (Chris Wilkins, Sweetsur, and Girling 2008) (Gee et al. 2008a). In contrast, the clinical manifestations of the CNS intoxications involve hallucinations, anxiety, paranoia, confusion, short temper. In addition to tachycardia, hypertension, chest pain (Chris Wilkins, Sweetsur, and Girling 2008). Severe toxicity of piperazine compounds may lead to respiratory failure, seizure, hyperventilation, collapse (Gee, Jerram, and Bowie 2010), (Gee et al. 2008b). *In vitro* studies on piperazines predict hepatotoxicity in human hepatic (HepaRG & HepG2) cells and primary rat hepatocytes (Katz et al. 2016b). Piperazines also exhibit a neurotoxic effect on rat's dopaminergic neuron cells (Majrashi et al. 2018b). Since BZP and TFMPP both have serotonergic activity, some reports indicate serotonin syndrome as a toxic effect of piperazines (Gee, Jerram, and Bowie 2010). The current management approaches for piperazines toxicity is providing the supportive care and monitoring the vital signs. There is no

particular antidote for piperazines toxicity at present time. The first line treatment of piperazine induced seizure and agitation is benzodiazepine, while for oral ingestion toxicity is charcoal. Other treatment practices include rapid cooling, thermoregulation, fluid therapy, and patients should receive electrodiagram test (Balmelli et al., 2001), (Wood et al., 2007), (Schep et al., 2011b)

1.7. Piperazine Chemistry

Piperazine is a heterocyclic organic molecule with two opposing nitrogen atoms within a six-membered ring. Piperazine or 1, 4-hexahydropyrazine has a structural similarity with piperidine observed in the black pepper plant (*Piper nigrum*) (Singh et al. 2015). The piperazine ring's dinitrogen moiety and hydrogen bonding allow this scaffold to be an efficient backbone in many therapeutic agents (A. Sharma et al. 2020). Piperazines are colorless, volatile, freely soluble in water, and available in salt form. Piperazine incorporation in drug structures is interesting for many researchers due to several characteristics: high yields, short reaction times, simple procedure, and availability (A. Sharma et al. 2020). The piperazine designer drug derivatives are divided into two classes: benzylpiperazine and phenylpiperazine. The benzylpiperazines include N-benzylpiperazine (BZP) and 1-(3,4-methylenedioxybenzyl)-piperazine (MDBP), the methylenedioxy analogues. And phenylpiperazines such as 1-(3-chlorophenyl) piperazine (mCPP), 1-(3-trifluoromethylphenyl) piperazine (TFMPP), and 1-(4-methoxyphenyl) piperazine (MeOPP) (Arbo, Bastos and Carmo, 2012). Interestingly, Chemical structures of piperazines are not related to other psychoactive substances, and it's completely synthetic compounds (Katz et al. 2016b).

1.8. Piperazines dosage form

Piperazines designer drugs are usually consumed in various forms such as capsules, pills, tablets, liquid, or powder form. Other minor forms of piperazines administration include insufflation, inhalation, smoking, snorting, liquid mixture, and intravenous to escalate the onset of action (Nikolova and Danchev 2008b) (Katz et al. 2016a). The piperazine derivatives are primarily found in combination with other piperazines reach in some samples to four products of piperazines derivatives (Y. P. Gaillard et al. 2013). Additionally, piperazines are use with other psychoactive substances like amphetamines, ecstasy, cannabis, and alcohol to increase the stimulant effect or decrease the sobering impact of piperazines (Butler and Sheridan 2007), (Katz et al. 2016a). Several reports indicate the dose range of BZP in party pills is typically between 50 to 200 mg, but this range is varied according to the origin of party pills. Some BZP samples reach 1000 mg (Cohen and Butler 2011). While the 3-TFMPP is used in doses ranging between 5 to 60 mg, but that TFMPP is rarely used alone. Regularly, BZP and TFMPP are combined in ratios 2:1 to 10:1 (Welz and Koba 2020).

1.9. Analysis and identification of piperazines

The rapid appearance of new psychoactive substances in the illicit drug market makes analytical identification challenging because of the structural diversity and the large number of novel compound possibilities. Consequently, escalating the piperazines abuse has necessitated organizations and forensic labs to detect and identify piperazine derivatives (Dickson et al. 2010). Many techniques are utilized to detect the piperazines derivatives, such as colorimetric tests, immunoassays, and chromatographic analysis (De Boer et al. 2001).

1.9.1. Colorimetric tests

In forensic labs, the colorimetric reactions are used as a quick tool to detect the potential presence or absence of a specific compound in seized samples. There are many reagents used for preliminary drug screening, like Marquis reagent, Simon's reagent, and Dragendorff reagent. However, there is no specific colorimetric test for piperazines compounds (Namera et al. 2011).

1.9.2. Immunoassays

Piperazines derivatives do not have commercially available immunoassays for qualitative analysis tests. Therefore, amphetamine detection assays as the fluorescence polarization immunoassay (FPIA) are used to identify some piperazines compounds as BZP. Still, a false positive result is usually expected results (De Boer et al. 2001).

1.9.3. Gas chromatography-mass spectrometry (GC-MS)

GC-MS is the principal primary analytical tool that is used to identify and validate different substances in the forensic field. The combination of GC with MS provides the advantages of compounds separation by GC and accurate data for identification and quantification by MS. The simplicity, reliability, affordability, and sensitivity of GC-MS in forensic analysis make this device the first choice for piperazine detection (Tsutsumi et al. 2005b). The GC-MS technique developed by Peters et al. has succeeded in detecting piperazines derivatives in human plasma samples using characteristic fragments ions. (Peters et al. 2003) and his team had applied mixed-mode solid-phase extraction (SPE) and derivatization with heptafluorobutyric anhydride (HFBA) to screen

many designer drugs, including BZP, TFMPP, and mCPP. In a study to clarify MDMA positive urine sample content, the team has detected piperazines derivatives BZP, TFMPP, and mCPP (Dickson et al. 2010). The task was executed on 251 samples, and they concluded that piperazines derivatives BZP, TFMPP, and mCPP were validated in 15%, 7%, 1% percentage of samples, respectively.

1.9.4. Gas chromatography with infrared detection (GC-IRD)

Gas chromatography coupled with infrared spectroscopy is a powerful technique that combines the separation of the component by GC with detection of IR by vapor phase infrared absorption. GC-Infrared spectroscopy technique allows characterizing the isomers and functional group to provide confirmatory data profile of target molecule, without further modification (Abdel-Hay, DeRuiter, and Randall Clark 2012). The infrared spectroscopy is nondestructive and provides unique absorption bands at the fingerprint region of compounds. The differentiation between piperazine compounds had been successfully approved by (Maher, Awad, and Clark 2009) and (Abdel-Hay et al.) for many piperazines compounds such as TFMPP derivatives and methylbenzylpiperazines (MBPs).

1.9.5. High-performance liquid chromatography (HPLC)

HPLC is one of the most used analytical procedures to separate, identify, and quantify each element in a mixture. The numerous advantages of HPLC, including low temperature, underivatized compounds, no need for volatility, and coupling with many other analytical

techniques, make it one of the primary instruments in forensic labs (Koves 1995). Determination of piperazine compounds has been reported in many studies, Tsutsumi and his colleague succeeded in detect BZP, TFMPP, and their metabolite in human urine samples (Tsutsumi et al. 2005a). Takahashi and his team created a library of 104 kinds of psychoactive substances like piperazines using LC/PDA and GC/EI/MS. The library's goal is to confirm suspects designer drugs quickly (Takahashi et al. 2009).

1.9.6. Nuclear magnetic resonance (NMR)

NMR is an analytical method that elucidates the molecular structure and can determine the purity and content of a sample. The NMR methods can characterize the suspicious samples in forensic laboratories since most of these samples have unknown origins or structures. Uncontrolled substances are considered a major challenging issue for forensic specialty, but NMR could help identify these substances' fingerprints. Also, NMR spectroscopy does not require derivatization, isolation procedures, and the ability to quantify several mixture components in a single spectrum. However, the high cost and low sensitivity are disadvantages of the NMR technique (Santos et al. 2018), (Groombridge 1996). NMR confirmed piperazine derivatives in many seized samples by (Westphal et al. 2009), (Tennant et al. 2020), (Alver, Parlak, and Şenyel 2007).

1.10. Knowledge gap & Project rationale

The black market of designer drugs or psychoactive substances is drastically growing globally for many reasons. Lack of regulations and easy access to these substances through the internet are the

main reasons. Many piperazines derivatives have been detected in forensic laboratories, and many clinical toxicology cases have been reported worldwide. The chemical modification on drugs of abuse is continuously producing new psychoactive substances each year. The clandestine chemists are willing to continue these operations due to the availability of chemical precursors and the desire to overcome the legal controls. Piperazines derivatives can be readily synthesized in underground labs and marketed for their psychostimulant activity properties. The two nitrogen atoms in the piperazine ring allow endless possibilities to install substituents groups that may produce psychoactive substances. However, the analytical profile of these potential designer drugs and the pharmacological and /or toxic effects have not been clearly elucidated. Hence, in this study, we designed and synthesized novel piperazine compounds depending on the general model of many drugs of abuse and will create new/ precise analytical methods for identification and differentiation profiles. Our study will also investigate the analytical properties of some prospective future designer drugs. This study's analytical data and methods outcomes will be practical tools that will assist in forensic chemistry development. This work aims to provide reference data and methods for differentiation and quick identification among these designers regioisomeric and isobaric substances and make these data accessible to assist in drug identification. Additionally, *in vitro* effect on monoaminergic (dopamine) neuronal viability and their associated mechanisms were identified.

1.11. Aims

One of the major goals of forensic science is recognizing the potential hazards of unknown substances. To effectively prevent the damage behind the various psychoactive substances, it is mandatory to analyze and characterize the threat of these kinds of substances to public health. The

current study aims to develop comprehensive analytical research of potential new/novel piperazine designer drugs and investigate the pharmacodynamic/neuropharmacological effects of these piperazines on the neuronal cell line. The aims for this project will be accomplished by:

Aim 1: Create an analytical data library for potential psychoactive substances by

Aim 1-1: Design and synthesize hybrid derivatives of designer piperazine drugs (BZP and 3-TFMPP) - Several disubstituted piperazine rings were synthesized with different substitution patterns on the piperazine nitrogen atoms.

Aim1-2: Create an analytical profile for each compound using the

Gas Chromatography-Mass Spectrometry (GC-MS) and.

Gas Chromatography-Infrared Detection (GC-IRD).

Aim 2-1: Evaluate the *in vitro* the effect of novel piperazine designer drugs on N27 dopaminergic neuronal cell viability.

Aim 2-2: Elucidate the mechanism of action of novel piperazine compounds.

Aim 1-1: Design and synthesize hybrid derivatives of designer piperazine drugs (BZP and 3-TFMPP) To elevate the psychoactive influence, the users of piperazine drugs are combining the BZP and 3-TFMPP (Arbo, Bastos, and Carmo 2012a) (Yeap et al. 2010). The above observation encouraged our group to design compounds with the structural elements of BZP and 3-TFMPP in a single hybrid molecule. Many reports proved that the main constituents of the party pills are the combination of BZP and 3-TFMPP. This combination of BZP and 3-TFMPP in a ratio (1:2) or (1:10) is to mimic the psychostimulant influence of MDMA (Cohen and Butler 2011) (De Boer et

al. 2001). Therefore, the clandestine labs may produce new hybrid compounds of BZP and 3-TFMPP. Incorporating the two structural elements of BZP and 3-TFMPP is feasible and accessible due to two secondary nitrogen atoms in the piperazine ring (DeRuiter et al. 2017). These novel compounds are substituted by common functional groups that present in designer drugs that are commercially available such as methoxy-, dimethoxy-, and methylenedioxy-, halogens, methyl aromatic substituents.

Aim1-2: Create an analytical profile for each compound using the GC-MS and GC-IRD

The clandestine labs apparently will continue the distribution of designer drugs on the black market. Evasion of the laws is the primary motivation for these secret illegal labs to produce new analogs of classical drugs of abuse. Consequently, the extensive development in designer drug production is presenting a significant challenge for forensic laboratories. Since these designer drugs analogs or regioisomers with almost identical molecular weight, functional groups, elemental composition, and frequently identical mass fragments, they could be misidentified with related control drugs. The capability to differentiate the analytical characteristics between these regioisomers will improve the specificity of identification for reported drugs of abuse. In addition, the analytical profile for the novel designer drugs will create an analytical library that will accelerate the identification of prospective designer drugs in the future.

Aim 2-1: Evaluate the *in vitro* effect of novel piperazine designer drugs on N27 dopaminergic neuronal cell viability

The prime targets for psychoactive substances to produce their pharmacological action or toxic effects are the monoaminergic neurons in the central and peripheral nervous system. Piperazine compounds are designer drugs that are structurally modified to exert stimulant effect, which

resembles the well-known drugs of abuse (amphetamine, MDMA). By interacting with monoamines (serotonin, dopamine, and norepinephrine), the piperazines produce psychological symptoms in addition to stimulant effects. Piperazine derivatives have shown neurotoxic activity that led to dopaminergic neuron depletion. Furthermore, this group of drugs has a wide range of popularity worldwide often targeting teenagers (Party pills). Benzylpiperazine BZP and 3-trifluoromethyl phenyl piperazine 3-TFMPP are considered the main abused piperazines available in the black market. Abusing piperazine compounds will alter monoaminergic neurons and directly deplete neurotrophic factors leading to dopaminergic neurotoxicity.

Aim 2-2: Elucidate the mechanism of action of novel piperazine compounds

This approach will address the mechanism of piperazines compounds' mechanism on markers of oxidative stress and mitochondrial functions. Oxidative stress and has been implicated in the etiology of dopaminergic neuronal neurodegeneration. Earlier studies with stimulants and neurotoxins have shown that these substances can generate reactive oxygen species, induce oxidative stress and inhibit mitochondrial respiration leading to dopaminergic neurotoxicity (Majrashi et al. 2018c). We propose that the neurotoxic effects of piperazine derivatives will directly correlate with the initiation of oxidative stress and resulting in the neurodegeneration of monoaminergic neurons. Oxidative stress, mitochondrial dysfunction, and depletion of neurotrophic factors contribute to the neuronal insults associated with several cognitive and movement-related disorders. Consequently, chronic use of stimulants or drugs of abuse can alter neurotransmission, induce neurotoxicity, and thereby act as catalytic factors for the emergence of dopaminergic neurodegenerative disorders.

2. Design and synthesis of novel Regioisomeric Piperazines

Analytical studies for regioisomers compounds are critical to identify and discover the chemical properties of these compounds. This considerable demand is increasing, particularly when the regioisomers compounds are related to controlled substances. The forensic analysis of abused drugs is directly augmented by analytical methods to distinguish between regioisomers. Whereas the mass spectrum is the confirmatory device for substance identification, some substances may have very similar mass spectra but different pharmacological activity. Since the 1960s, piperazine compounds have emerged to illicit market with many various forms of compounds. The main base structure of most piperazine derivatives in this study is shown in Figure (2) with a substitution pattern in the phenyl and benzyl rings. Most piperazine derivatives in this study are synthesized by utilizing the reductive amination approach. While some compounds are synthesized by direct displacement alkylation to yield the aimed products. Figure (3) shows the piperazines derivatives included in this project.

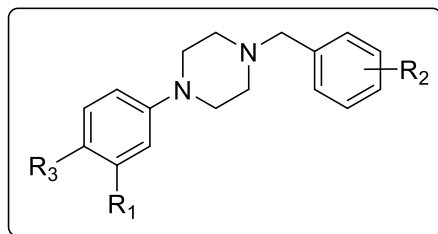


Figure 2. General structure of piperazine derivatives

R₁	R₂	R₃
3-trifluoromethyl	OMe, diOMe, Br-diOMe, MD	H
3-chloro	OMe, diOMe, Br-diOMe, MD	H
H	OMe, diOMe, Br-diOMe, MD	4-OMe

Table 2. The structural formula of piperazine derivatives

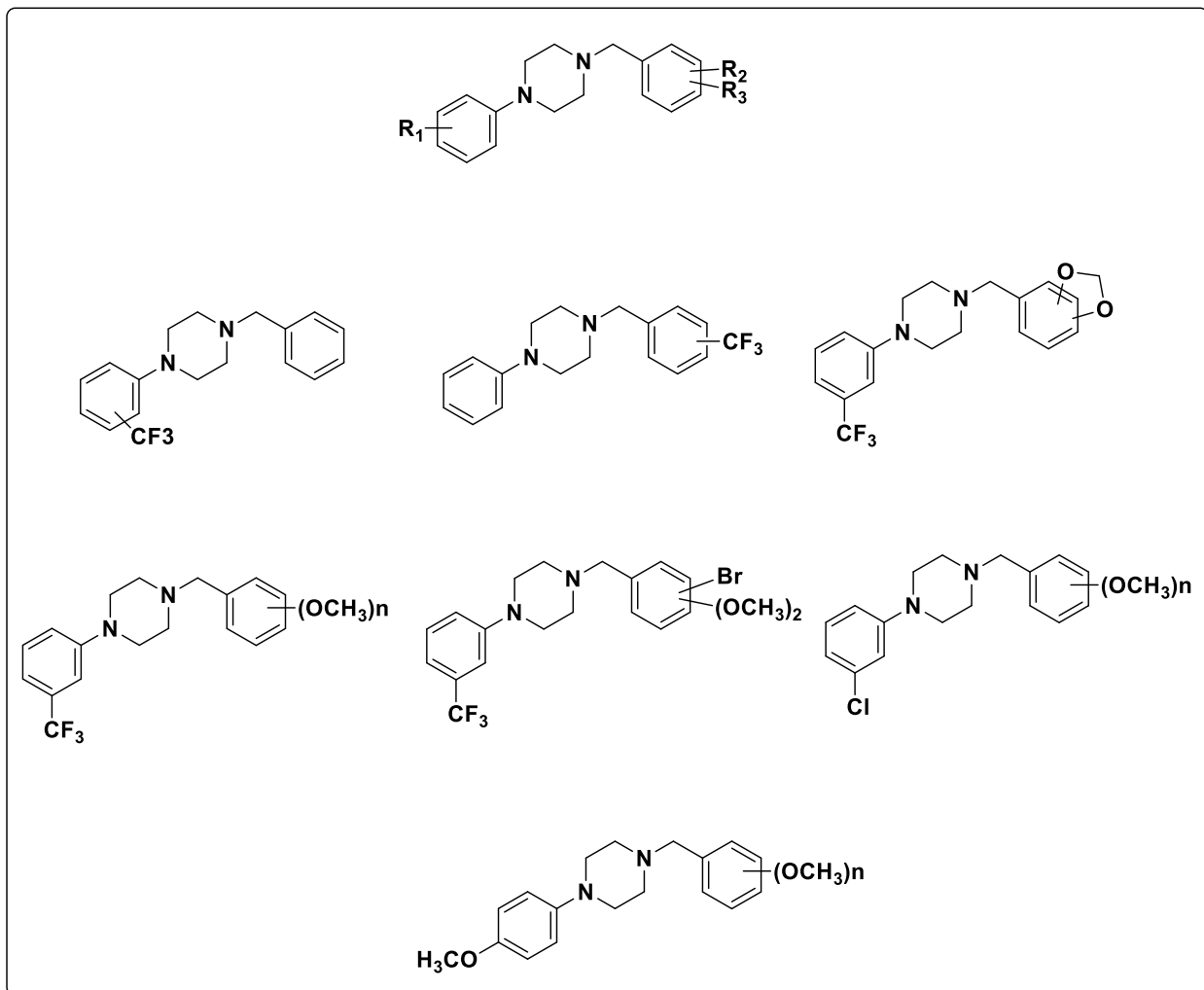


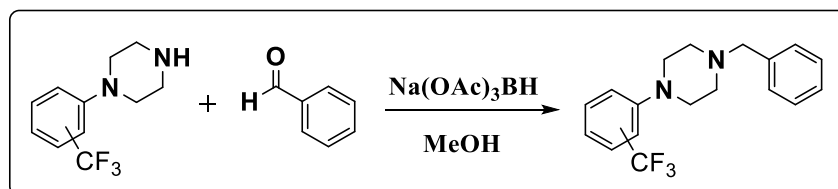
Figure 3. Piperazine derivatives

2.1. Synthesis of 1-[N-(trifluoromethyl)phenyl]-4-benzylpiperazine

2.1.1. Synthesis of 1-[2-(trifluoromethyl)phenyl]-4-benzylpiperazine and 1-[4-(trifluoromethyl)phenyl]-4-benzylpiperazine

The Synthesis of 1-[2-(trifluoromethyl) phenyl]-4-benzylpiperazine and 1-[4-(trifluoromethyl) phenyl]- 4-benzylpiperazine depends on reductive alkylation reaction of commercially available 2- and 4-trifluoromethylphenyl piperazine with benzaldehyde as shown in Scheme (3). Initially,

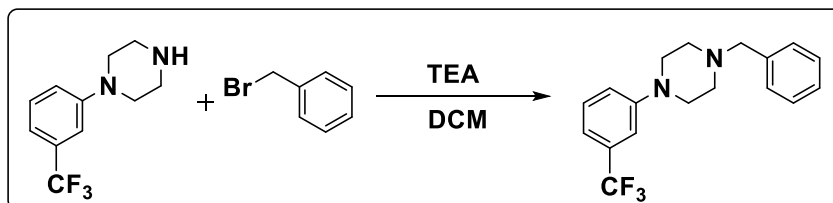
one equivalent of 2- or 4-trifluoromethylphenyl was heated with an equal molar amount of benzaldehyde in methanol for 2 hours to form the intermediate imine. The imine intermediate was then reduced with two equivalents of sodium triacetoxyborohydride at room temperature for 24 hours to yield the crude products. The products were isolated from the reaction mixture by evaporation of the reaction solvent followed by acid-base extraction as described in the experimental section and converted to their hydrochloride salts with ethereal HCl.



Scheme 3. Synthetic approach of 1-[N-(trifluoromethyl)phenyl]-4-benzylpiperazine

2.1.2. Synthesis of 1-[3-(trifluoromethyl)phenyl]-4-benzylpiperazine

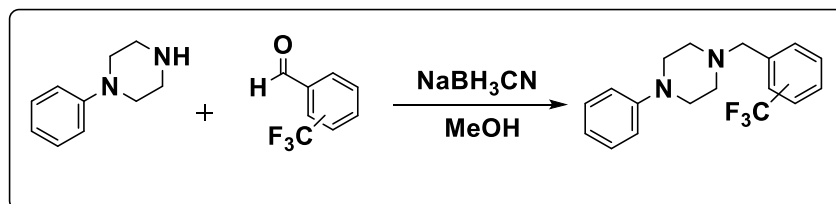
The synthesis of 1-[3-(trifluoromethyl)phenyl]-4-benzylpiperazine was accomplished by direct nucleophilic displacement as shown in Scheme (4). In this reaction, one equivalent of the 1-[3-(trifluoromethyl)phenyl]piperazine is reacted with one equivalent of benzyl bromide in dichloromethane with an equivalent of the base triethylamine at room temperature over 24 hours. The product was isolated from the reaction mixture by evaporation of the reaction solvent followed by acid-base extraction as described in the experimental section and converted to the hydrochloride salts with ethereal HCl.



Scheme 4. Synthetic approach of 1-[3-(trifluoromethyl)phenyl]-4-benzylpiperazine

2.2. Synthesis of 1-[2-(trifluoromethyl)benzyl]-, 1-[3-(trifluoromethyl)benzyl], and 1-[4-(trifluoromethyl)benzyl]-4-phenylpiperazine

The synthesis of 1-[2-(trifluoromethyl) benzyl]-, 1-[3-(trifluoromethyl) benzyl], and 1-[4-(trifluoromethyl)benzyl]-4-phenylpiperazine was accomplished by a reductive alkylation reaction with commercially available 1-phenylpiperazine and commercially available 2-, 3- or 4-trifluoromethylbenzaldehyde as shown in Scheme (5). One equivalent of 1-phenylpiperazine was initially heated with an equal molar amount of 2-, 3- or 4-trifluoromethylbenzaldehyde in methanol for 2 hours to form the intermediate imine. The intermediate imine was then reduced with three equivalents of sodium cyanoborohydride at room temperature for 24 hours to yield the crude products. The products were isolated from the reaction mixture by evaporation of the reaction solvent followed by acid-base extraction as described in the experimental section and converted to their hydrochloride salts with ethereal HCl.

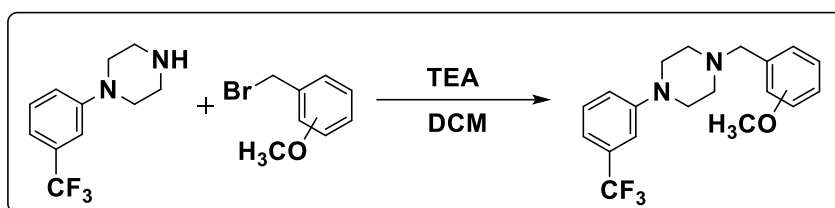


Scheme 5. Synthetic approach of 1-[N-(trifluoromethyl)benzyl]-4-phenylpiperazine

2.3. Synthesis of 1-[2-(methoxybenzyl)-, 1-[3-(methoxybenzyl)-, and 1-[4-(methoxybenzyl)-4-[3-(trifluoromethyl)phenyl]piperazine

The synthesis 1-[2- methoxybenzyl]-, 1-[3- methoxybenzyl]-, and 1-[4- methoxybenzyl]- 4-[3-(trifluoromethyl) phenyl]piperazine was achieved by direct N-alkylation of the secondary amine of 3-trifluoromethylphenylpiperazine with 2-, 3- or 4-methoxybenzyl bromide as illustrated in

scheme (6). In this reaction, one equivalent of 1-[3-(trifluoromethyl) phenyl]piperazine is reacted with one equivalent of 2-methoxy or 3-methoxy or 4-methoxybenzyl bromide in dichloromethane with an equivalent of the base triethylamine at room temperature over 24 hours. The product was isolated from the reaction mixture by evaporation of the reaction solvent followed by acid-base extraction as described in the experimental section and converted to the hydrochloride salts with ethereal HCl.

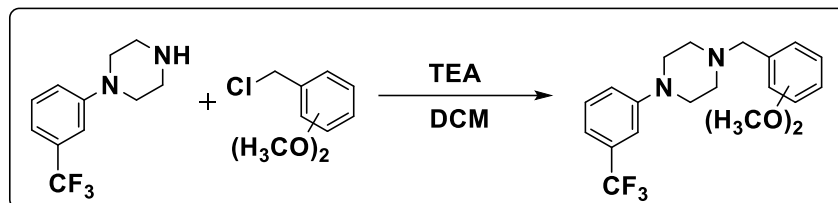


Scheme 6. Synthetic approach of 1-[N-(methoxybenzyl)]-4-[3-(trifluoromethyl)phenyl]piperazine

2.4. Synthesis of 1-[N-(dimethoxybenzyl)]- 4-[3-(trifluoromethyl)phenyl]piperazine

2.4.1. Synthesis of 1-[2,3-(dimethoxybenzyl)]-, and 1-[2,5-(dimethoxybenzyl)]-4-[3-(trifluoromethyl)phenyl]piperazine

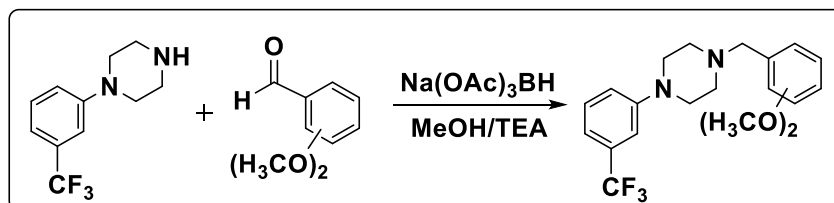
The synthesis 1-[2,3- dimethoxybenzyl]-, and 1-[2,5- dimethoxybenzyl]-4-[3-(trifluoromethyl) phenyl piperazine was associated with direct nucleophilic displacement as illustrated in scheme (7). In this reaction, one equivalent of 3-trifluoromethylphenylpiperazine is reacted with one equivalent of 2,3- dimethoxy or 2,5- dimethoxybenzyl chloride in DCM with one equivalent of triethyl triethylamine at room temperature over 24 hours. The product was isolated from the reaction mixture by evaporation of the reaction solvent followed by acid-base extraction as described in the experimental section and converted to the hydrochloride salts with ethereal HCl.



Scheme 7. Synthetic approach of 1-[N-(dimethoxybenzyl)]-4-[3-(trifluoromethyl)phenyl]piperazine

2.4.2. Synthesis of 1-[2,4-(dimethoxybenzyl)]-, 1-[2,6-(dimethoxybenzyl)]-, and 1-[3,4-(dimethoxybenzyl)]-4-[3-(trifluoromethyl)phenyl]piperazine

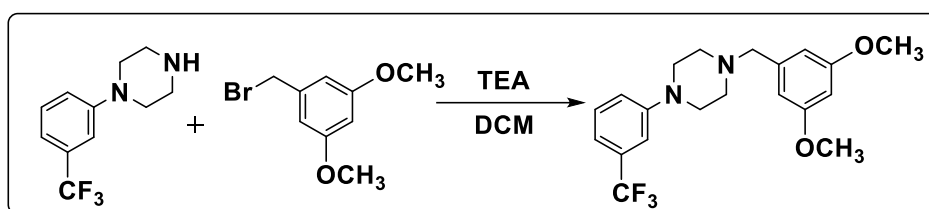
Synthesis of 1-[2,4-dimethoxybenzyl]-, 1-[2,6-dimethoxybenzyl]-, and 1-[3,4-dimethoxybenzyl]-4-[3-(trifluoromethyl)phenyl]piperazine depends on condensation reaction of the 3-trifluoromethylphenylpiperazine hydrochloride with substituted benzaldehyde as illustrated in scheme (8). Intermediate imine will be produced when treated with the substituted benzaldehyde with 3-(trifluoromethyl)phenylpiperazine hydrochloride and triethylamine (all in one equivalent amount) under reductive amination conditions in methanol for 2 hours. This intermediate imine can be reduced by sodium triacetoxyborohydride (two equivalent) at room temperature for 24 hours to yield the crude products. The product was isolated from the reaction mixture by evaporation of the reaction solvent followed by acid-base extraction as described in the experimental section and converted to the hydrochloride salts with ethereal HCl.



Scheme 8. Synthetic approach of 1-[N-(dimethoxybenzyl)]-4-[3-(trifluoromethyl)phenyl]piperazine

2.4.3. Synthesis of 1-[3,5-dimethoxybenzyl]-4-[3-(trifluoromethyl)phenyl]piperazine

The synthesis of 1-[3,5-dimethoxybenzyl]-4-[3-(trifluoromethyl)phenyl]piperazine was accomplished with direct nucleophilic displacement as illustrated in scheme (9). In this reaction, one equivalent of 3-trifluoromethylphenylpiperazine is reacted with 3,5-dimethoxybenzyl bromide in DCM with one equivalent of triethylamine at room temperature over 24 hours. The product was isolated from the reaction mixture by evaporation of the reaction solvent followed by acid-base extraction as described in the experimental section and converted to the hydrochloride salts with ethereal HCl.

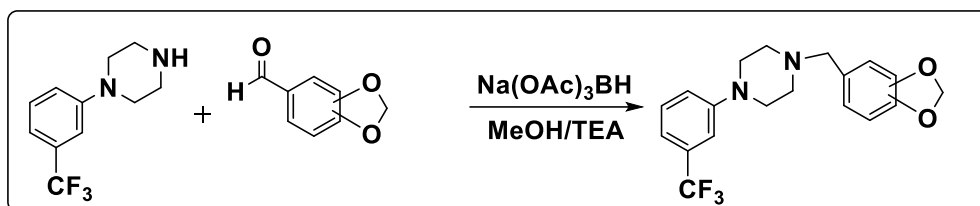


Scheme 9. Synthetic approach of 1-[3,5-dimethoxybenzyl]-4-[3-(trifluoromethyl)phenyl]piperazine

2.5. Synthesis of 1-[2,3-(methylenedioxybenzyl)]-4-[3-(trifluoromethyl)phenyl]piperazine and 1-[3,4-(methylenedioxybenzyl)]-4-[3-(trifluoromethyl)phenyl]piperazine

The synthesis of 1-[2,3-methylenedioxybenzyl]-, and 1-[3,4-methylenedioxybenzyl]-4-[3-(trifluoromethyl)phenyl]piperazine depends on the condensation reaction of the commercially available 2,3-methylenedioxy or 3,4-methylenedioxy benzaldehyde with 3-trifluoromethylphenylpiperazine as illustrated in scheme (10). In this reaction, one equivalent of 1-[3-(trifluoromethyl)phenyl]piperazine was heated with an equal molar amount of 2,3-methylenedioxy or 3,4-methylenedioxy benzaldehyde in methanol for 2 hours to form the

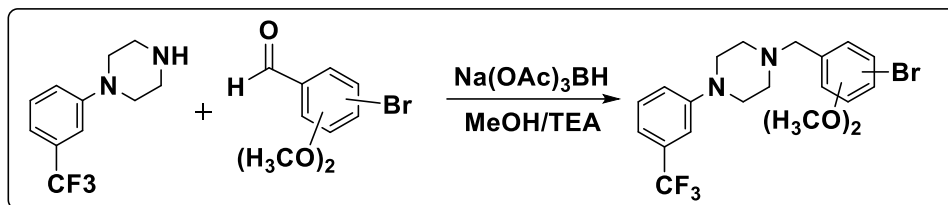
intermediate imine. The intermediate imine was then reduced with 1.5 equivalents of sodium triacetoxyborohydride at room temperature for 24 hours to yield the crude products. The products were isolated from the reaction mixture by evaporation of the reaction solvent followed by acid-base extraction as described in the experimental section and converted to their hydrochloride salts with ethereal HCl.



Scheme 10. Synthetic approach of 1-[N-(methylenedioxybenzyl)]-4-[3-(trifluoromethyl)phenyl]piperazine

2.6. Synthesis of 1-[N-(bromo-dimethoxy benzyl)]-4-[3-(trifluoromethyl)phenyl]piperazine

Synthesis of 1-[N-(bromo-dimethoxy benzyl)] - 4-[3-(trifluoromethyl) phenyl] piperazine depends on condensation reaction of the commercially available substituted benzaldehyde with 3-trifluoromethylphenylpiperazine as illustrated in scheme (11). In this reaction, one equivalent of 1-[3-(trifluoromethyl) phenyl]piperazine was heated with an equal molar amount of substituted benzaldehyde figure (4) in methanol for 2 hours to form the intermediate imine. The intermediate imine was then reduced with three equivalents of sodium triacetoxyborohydride at room temperature for 24 hours to yield the crude products. The products were isolated from the reaction mixture by evaporation of the reaction solvent followed by acid-base extraction as described in the experimental section and converted to their hydrochloride salts with ethereal HCl, all products list in the Figure (5)



Scheme 11. Synthetic approach of 1-[N-(bromo-dimethoxybenzyl)-4-[3-(trifluoromethyl)phenyl]piperazine

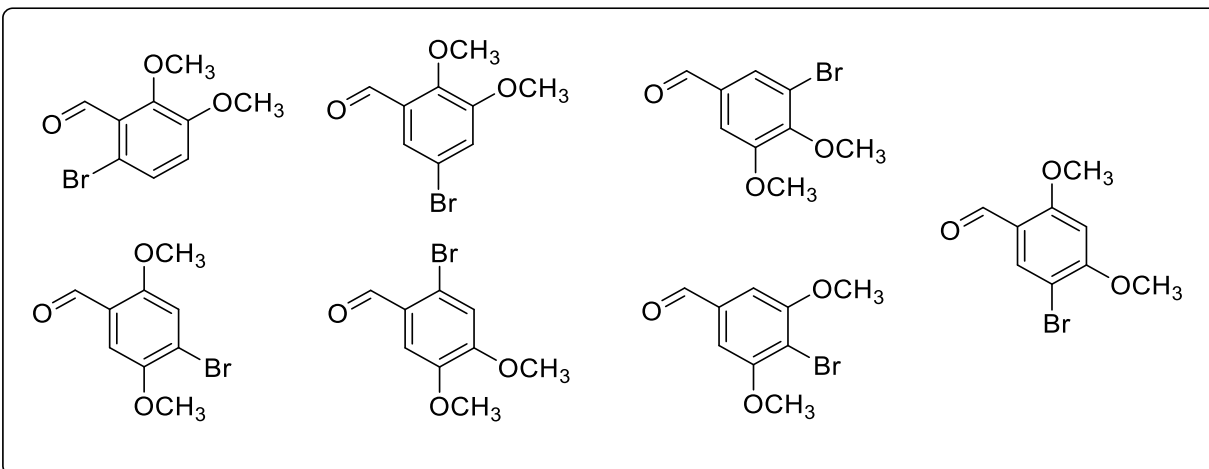


Figure 4. Substituted N-bromo dimethoxy benzaldehyde

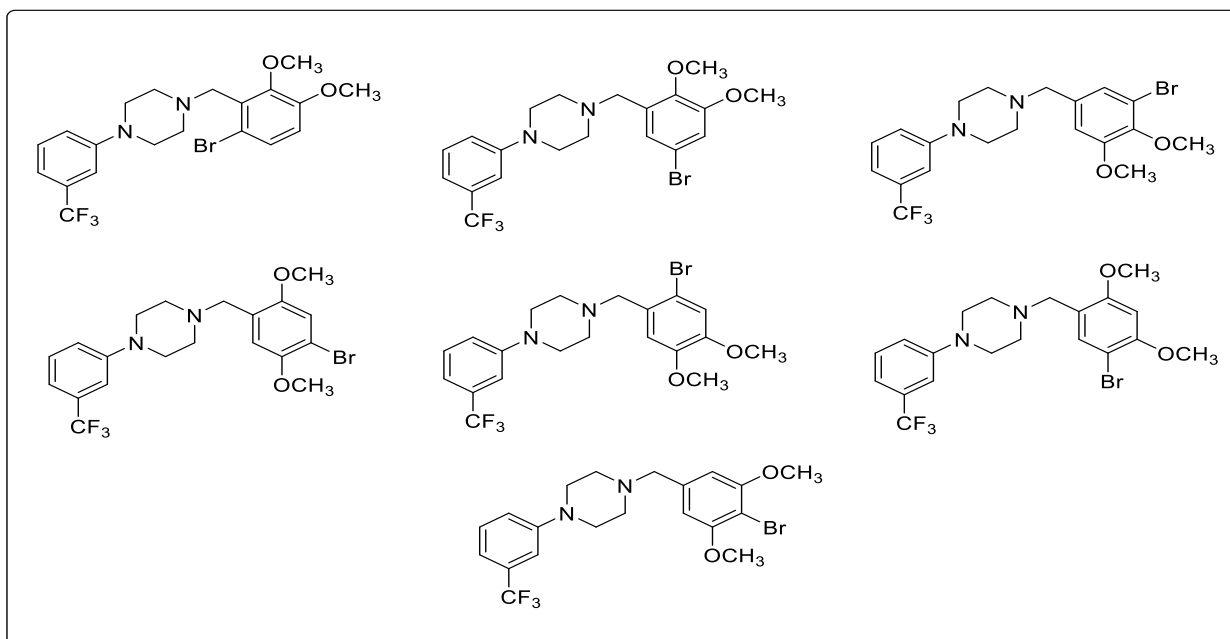
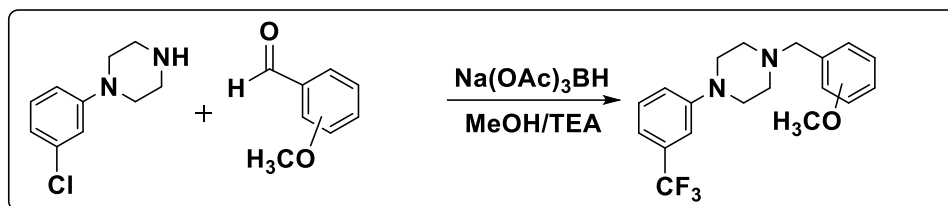


Figure 5. 1-[N-(Bromo-Dimethoxy benzyl)-4-[3-(trifluoromethyl)phenyl]piperazine compounds

2.7. Synthesis of 1-(3-chlorophenyl)-4-[(N-methoxybenzyl)piperazine

Synthesis of 1-(3-chlorophenyl)-4-[2-(methoxybenzyl), -[3-(methoxybenzyl), and -[4-(methoxybenzyl)piperazine depends on reductive alkylation reaction of commercially available substituted benzaldehyde with 3-chlorophenylpiperazine as illustrated in scheme (12). In this reaction, one equivalent of 3-chlorophenylpiperazine was heated with an equal molar amount of 2-methoxy or 3-methoxy or 4-methoxybenzaldehyde and an equivalent of the base triethylamine in methanol for 2 hours to form the intermediate imine. The intermediate imine was then reduced with 1.5 equivalents of sodium triacetoxyborohydride at room temperature for 24 hours to yield the crude products. The products were isolated from the reaction mixture by evaporation of the reaction solvent followed by acid-base extraction as described in the experimental section and converted to their hydrochloride salts with ethereal HCl.

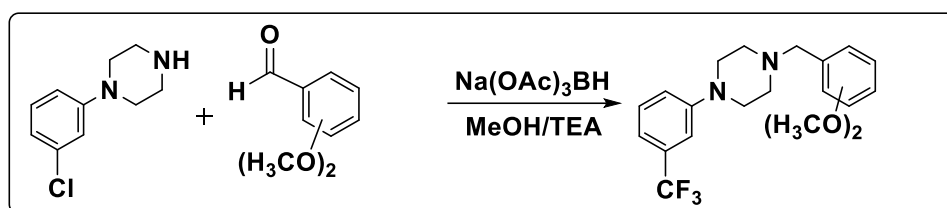


Scheme 12. Synthetic approach of 1-(3-chlorophenyl)-4-[(N-methoxybenzyl)piperazine

2.8. Synthesis of 1-(chlorophenyl)-4-[(N-(dimethoxybenzyl)piperazine

Synthesis of 1-(chlorophenyl)-4-[2,3-(dimethoxybenzyl)-, [2,4-(dimethoxybenzyl)-, [2,5-(dimethoxybenzyl)-, [2,6-(dimethoxybenzyl)-, [3,4-(dimethoxy)-, and [3,5-(dimethoxybenzyl)piperazine depends on reductive alkylation reaction of commercially available substituted benzaldehyde with 3-chlorophenylpiperazine as illustrated in scheme (13). In this reaction, one equivalent of 3-chlorophenylpiperazine was heated with an equal molar amount of

substituted benzaldehyde and an equivalent of the base triethylamine in methanol for 2 hours to form the intermediate imine. The intermediate imine was then reduced with 1.5 equivalents of sodium triacetoxyborohydride at room temperature for 24 hours to yield the crude products. The products were isolated from the reaction mixture by evaporation of the reaction solvent followed by acid-base extraction as described in the experimental section and converted to their hydrochloride salts with ethereal HCl.



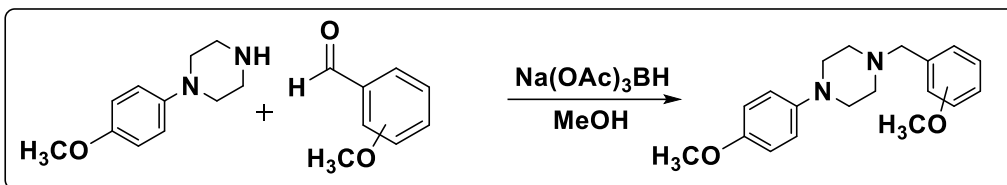
Scheme 13. Synthetic approach of 1-(chlorophenyl)-4-[(N-(dimethoxybenzyl))piperazine

2.9. Synthesis of 1-[N-(methoxybenzyl)]-4-[4-(methoxyphenyl)piperazine

2.9.1 Synthesis of 1-[2-(methoxybenzyl)- and 1-[3-(methoxybenzyl)-4-[4-(methoxyphenyl)piperazine

The synthesis of 1-[2-(methoxybenzyl)- and 1-[3-(methoxybenzyl)-4-[4-(methoxyphenyl)piperazine depends on reductive alkylation reaction of commercially available substituted benzaldehyde with 4-methoxyphenylpiperazine as illustrated in scheme (14). In this reaction, one equivalent of 1-[4-(methoxy) phenylpiperazine was heated with an equal molar amount of 2-methoxy or 3-methoxy benzaldehyde in methanol for 2 hours to form the intermediate imine. The intermediate imine was then reduced with three equivalents of sodium triacetoxyborohydride at room temperature for 24 hours to yield the crude products. The products

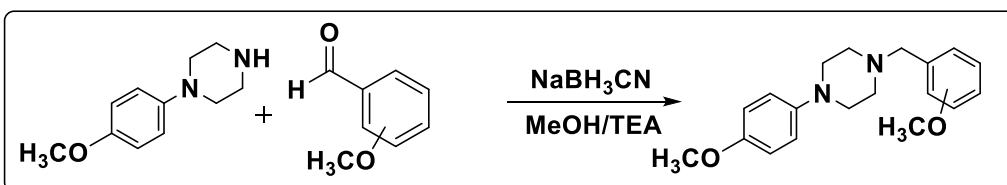
were isolated from the reaction mixture by evaporation of the reaction solvent followed by acid-base extraction as described in the experimental section and converted to their hydrochloride salts with ethereal HCl.



Scheme 14. Synthetic approach of 1-[N-(methoxybenzyl)-4-[4-(methoxyphenyl)]piperazine

2.9.2 Synthesis of 1-[4-(methoxybenzyl)-4-[4-(methoxyphenyl)]piperazine

The synthesis of 1-[4-(methoxybenzyl)-4-[4-(methoxyphenyl)]piperazine depends on reductive alkylation reaction of commercially available substituted benzaldehyde with 4-methoxyphenylpiperazine as illustrated in scheme (15). In this reaction, one equivalent of 4-methoxyphenylpiperazine was heated with an equal molar amount of 4-methoxybenzaldehyde and two equivalents of the base triethylamine in methanol for 2 hours to form the intermediate imine. The intermediate imine was then reduced with three equivalents of sodium cyanoborohydride at room temperature for 24 hours to yield the crude products. The products were isolated from the reaction mixture by evaporation of the reaction solvent followed by acid-base extraction as described in the experimental section and converted to their hydrochloride salts with ethereal HCl.

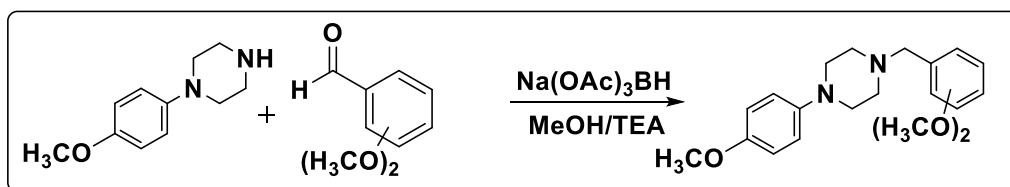


Scheme 15. Synthetic approach of 1-[4-(methoxybenzyl)-4-[4-(methoxyphenyl)]piperazine

2.10. Synthesis of 1-[N-(dimethoxybenzyl)]-4-[4-(methoxyphenyl) piperazine

2.10.1. Synthesis of 1-[2,3-(dimethoxybenzyl)-, 1-[2,5-(dimethoxybenzyl)-, and 1-[2,6-(dimethoxybenzyl)- 4-[4-(methoxyphenyl)piperazine

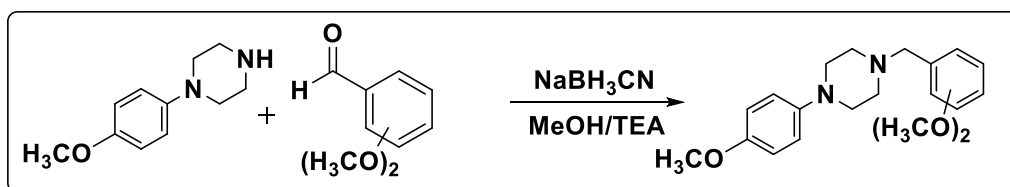
The synthesis of 1-[2,3-(dimethoxybenzyl)-, 1-[2,5-(dimethoxybenzyl)-, and 1-[2,6-(dimethoxybenzyl)- 4-[4-(methoxyphenyl) piperazine depends on reductive alkylation reaction of commercially available substituted benzaldehyde the with 4-methoxyphenylpiperazine as illustrated in scheme (16). In this reaction, one equivalent of 4-methoxyphenylpiperazine dihydrochloride was heated with an equal molar amount of 2,3-methoxy or 2,5-methoxy or 2,6-methoxy benzaldehyde and two equivalent of triethylamine in methanol for 2 hours to form the intermediate imine. The imine intermediate was then reduced with three equivalents of sodium triacetoxyborohydride at room temperature for 24 hours to yield the crude products. The products were isolated from the reaction mixture by evaporation of the reaction solvent followed by acid-base extraction as described in the experimental section and converted to their hydrochloride salts with ethereal HCl.



Scheme 16. Synthetic approach of 1-[N-(dimethoxybenzyl)- 4-[4-(methoxyphenyl)piperazine

2.10.2. Synthesis of 1-[2,4-(dimethoxybenzyl)-, 1-[3,4-(dimethoxybenzyl)-, and 1-[3,5-(dimethoxybenzyl)- 4-[4-(methoxyphenyl)piperazine

The synthesis of Synthesis of 1-[2,4-(dimethoxybenzyl)-, 1-[3,4-(dimethoxybenzyl)-, and 1-[3,5-(dimethoxybenzyl)- 4-[4-(methoxyphenyl) piperazine depends on reductive alkylation reaction of commercially available substituted benzaldehyde the with 4-methoxyphenylpiperazine as illustrated in scheme (17). In this reaction, one equivalent of 4-methoxyphenylpiperazine dihydrochloride was heated with an equal molar amount of 2,4-methoxy or 3,4-methoxy or 3,5-methoxybenzaldehyde and two equivalent of the base triethylamine in methanol for 2 hours to form the intermediate imine. The intermediate imine was then reduced with three equivalents of sodium cyanoborohydride at room temperature for 24 hours to yield the crude products. The products were isolated from the reaction mixture by evaporation of the reaction solvent followed by acid-base extraction as described in the experimental section and converted to their hydrochloride salts with ethereal HCl.

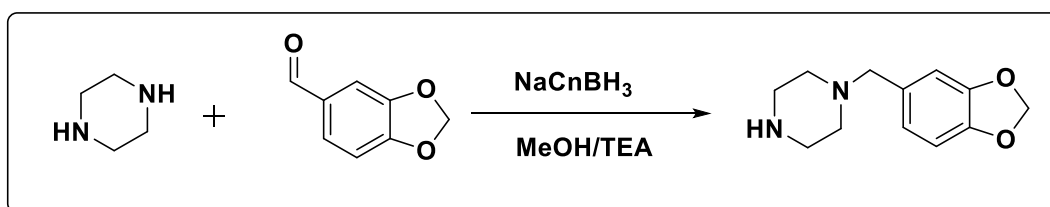


Scheme 17. Synthetic approach of 1-[N-(dimethoxybenzyl)-4-[4-(methoxyphenyl)piperazine

2.11. Synthesis of 3,4-methylenedioxybenzylpiperazine

The synthesis of 3,4-methylenedioxybenzylpiperazine depends on reductive alkylation reaction of commercially available substituted benzaldehyde the with piperazine as illustrated in scheme (18). In this reaction, two equivalents of piperazine were heated with one equivalent amount of 3,4-

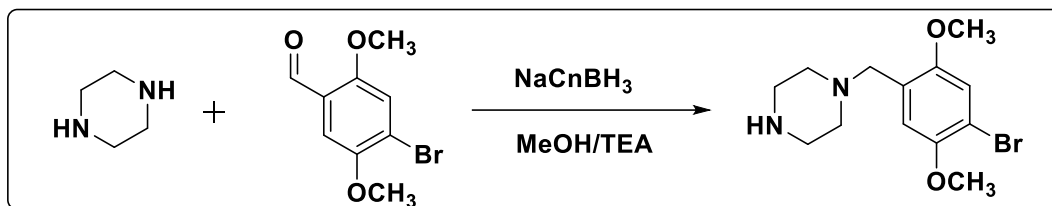
methylenedioxybenzaldehyde in methanol for 2 hours to form the intermediate imine. The imine intermediate was then reduced with three equivalents of sodium cyanoborohydride at room temperature for 24 hours to yield the crude products. The products were isolated from the reaction mixture by evaporation of the reaction solvent followed by acid-base extraction as described in the experimental section and converted to their hydrochloride salts with ethereal HCl.



Scheme 18. Synthetic approach of 3,4-methylenedioxybenzyl piperazine

2.12. Synthesis of 4-Bromo-2,5-dimethoxybenzylpiperazine

The synthesis of 4-Bromo-2,5-dimethoxybenzylpiperazine depends on reductive alkylation reaction of commercially available substituted benzaldehyde with piperazine as illustrated in scheme (19). In this reaction, two equivalents of piperazine were heated with one equivalent amount of 4-bromo-2,5-dimethoxybenzaldehyde in methanol for 2 hours to form the intermediate imine. The imine intermediate was then reduced with three equivalents of sodium cyanoborohydride at room temperature for 24 hours to yield the crude products. The products were isolated from the reaction mixture by evaporation of the reaction solvent followed by acid-base extraction as described in the experimental section and converted to their hydrochloride salts with ethereal HCl.



Scheme 19. Synthetic approach of 4-Bromo-2,5-dimethoxybenzylpiperazine

3. Analytics studies of piperazine derivatives

Over the past decade, massive numbers of new psychoactive substances or designer drugs have emerged in the illicit drugs market. The identification and characterization of potential illegal substances is a mandatory part of analytical chemistry. Since the underground labs are more likely to continue producing new psychoactive substances analogues. The procedures of delivering these substances are based on substituted amphetamines and related phenethylamines models. Hence, these methods are directly applicable to piperazine derivatives synthesis. Forensic laboratories are mainly the core to discover and classify the new illegal substances in cooperation with advanced instruments. One of the significant challenges for analytical chemists is identifying regioisomers compounds, especially if related to controlled substances. Mass spectrometry is the primary analytical tool to identify compounds; it is not always providing sufficient results when an ambiguous substance is applied. Obstacles can emerge when other substance with unspecified pharmacological activity have similar or identical mass spectra, which may lead to misidentifications. Piperazine derivatives have numerous positional isomers which might produce by clandestine laboratories as uncontrolled substances. Thus, the uncontrolled regioisomers substances may interfere with piperazine analytical profile, leading to misidentified as controlled substances. This chapter has applied some analytical methods such as mass spectrometry studies, gas chromatography separation, and Infrared spectroscopy to elucidate and characterize many of piperazine regioisomers. These methods will help create a screening profile for potential designer piperazine drugs, which directly enhances the analysis accuracy for the target drugs of abuse.

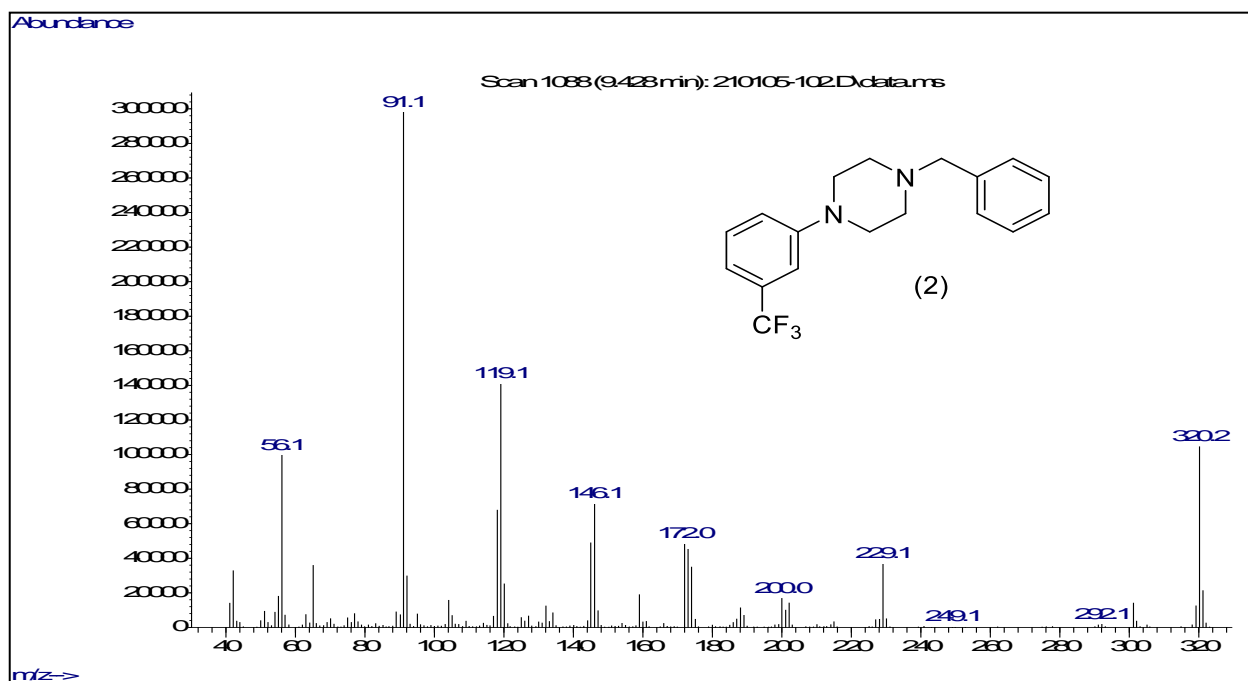
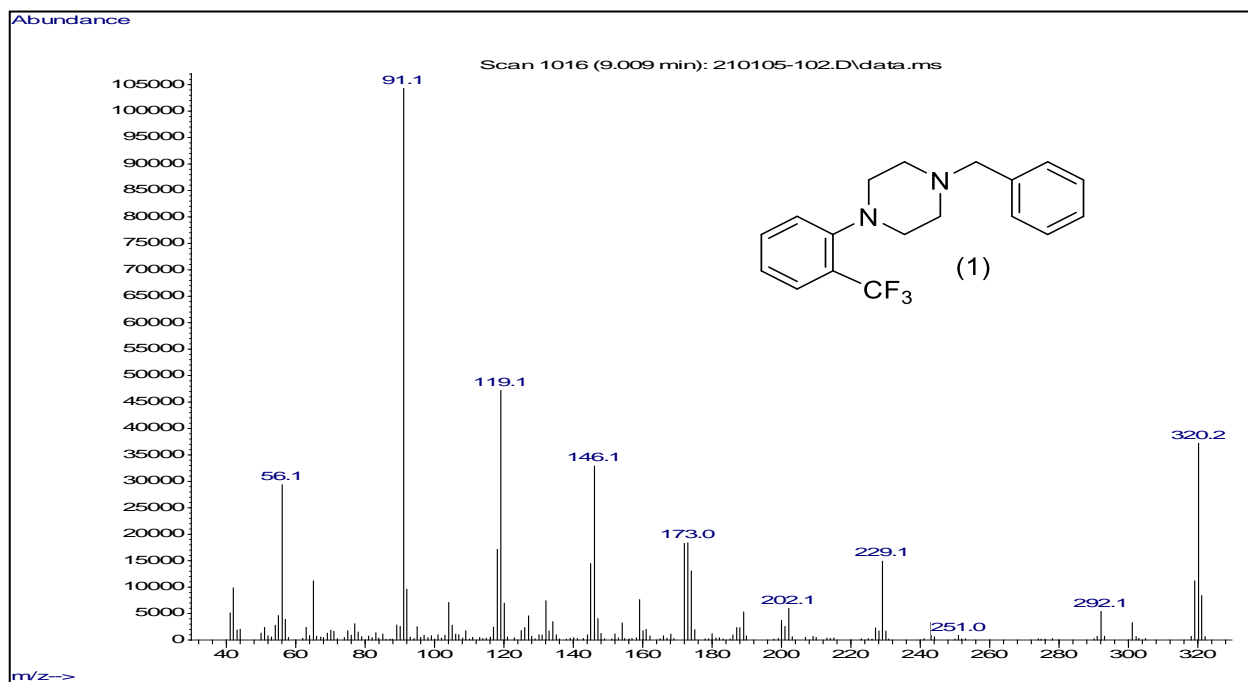
3.1. Analysis of 1-[N-(trifluoromethyl)phenyl]-4-benzylpiperazine (Group1)

The disubstituted piperazines 2-, 3-, and 4-trifluoromethyl phenyl benzyl piperazine structures incorporate well-known drugs of abuse in piperazine class BZP and TFMPP. The position of substituted trifluoromethyl on the phenyl ring is the variation between these compounds in this group. The three regioisomers have identical mass spectra with almost equivalent fragments. Gas chromatographic separation coupled with infrared detection (GC-IRD) provides direct confirmatory data for structural differentiation between the three regioisomers. The mass spectrum combined with the vapor phase infrared spectrum provides for specific confirmation of each of the regioisomeric piperazines. The piperazines derivatives were resolved on a 30-meter capillary column containing an Rxi®-17Sil MS stationary phase.

3.1.1. Mass spectral studies

The EI mass spectra of three regioisomers of trifluoromethyl phenyl benzyl piperazine are shown in Figure (6). The spectra for the trifluoromethylphenyl- N-benzylpiperazines show the fragment ions at m/z 91, 119, 146, 173, and 229 as well as other ions of low relative abundance. The base peak fragment ion at m/z 91 for the benzyl cation, while m/z 229, resulted from the loss of the benzyl radical (91Da). The major fragment at m/z 119 (a radical cation) observed in all regioisomers as indicates this fragment contains the unsubstituted benzyl group common to all regioisomers. The m/z 146 is the unsubstituted benzyl fragment containing four of the atoms of the piperazine ring. The characteristic fragment for piperazine ring is m/z 56. Fragmentation from the trifluoromethylphenyl substituted nitrogen via equivalent processes yields the m/z 173 and the m/z 200 ions. The smaller radical cation fragment (m/z 173) includes two of the piperazine ring atoms

while the higher mass (m/z 200) cation includes four of the atoms from the piperazine ring. The small peak at m/z 301 represent the loss of fluorine radical from the molecular ion. The proposed structures of the major 2-, 3-, and 4-trifluoromethyl phenyl benzyl piperazine fragment ions are shown in Scheme (20).



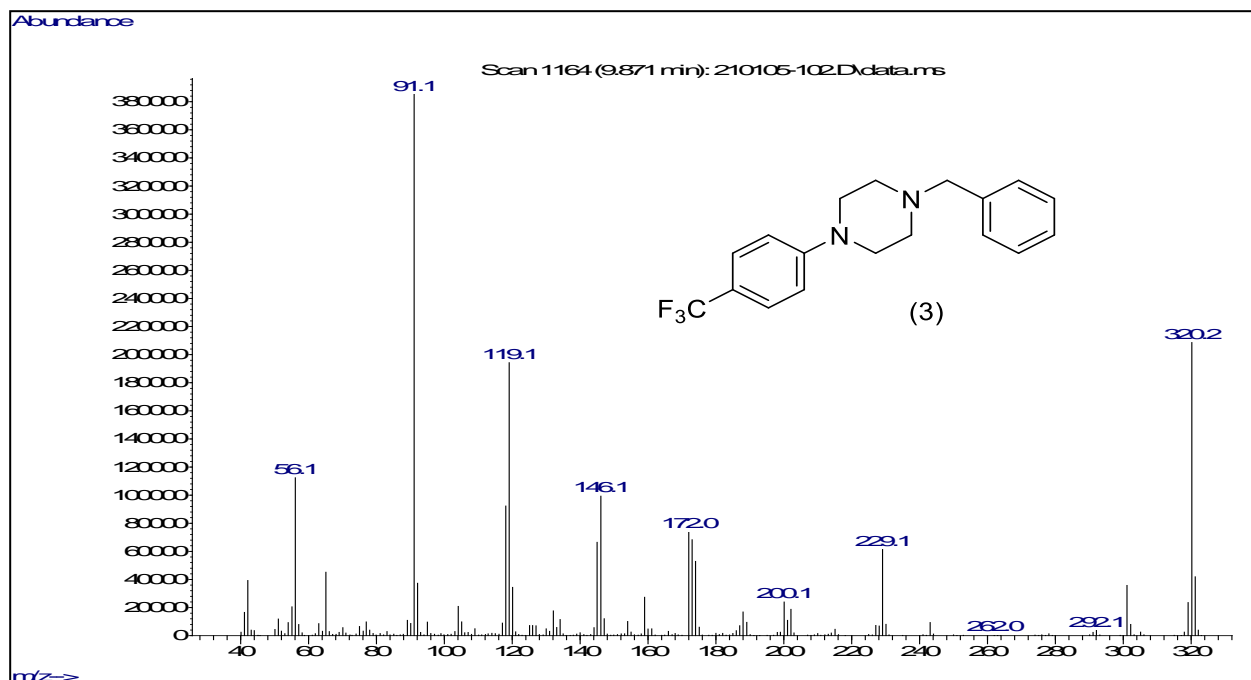
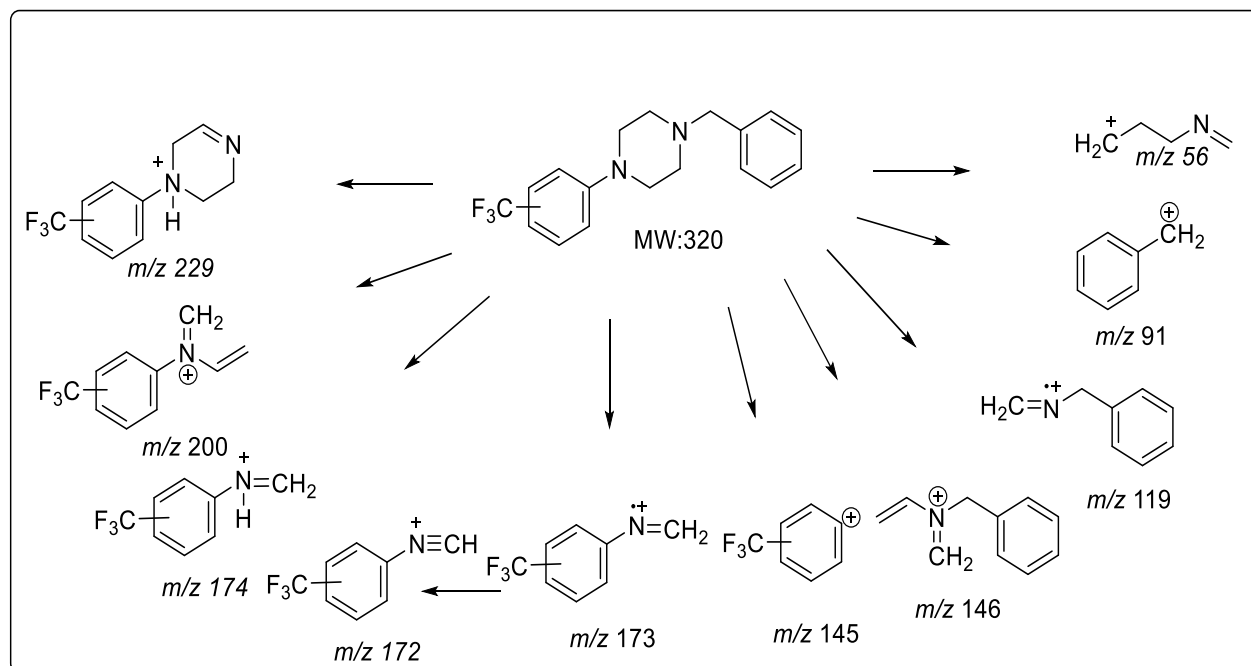


Figure 6. EI mass spectra of 1-[N-(trifluoromethyl)phenyl]-4-benzylpiperazine (Group1)



Scheme 20. EI mass spectral fragmentation pattern of 1-[N-(trifluoromethyl)phenyl]-4-benzylpiperazine (Group1)

3.1.2. Gas Chromatographic Separation

To differentiate the three regioisomers of this group, gas chromatographic separations were performed. The three compounds 2-,3-, and 4-trifluoromethyl phenyl benzyl piperazine differ in the position of phenyl ring substitution with the trifluoromethyl group. Gas chromatographic separation of the three compounds was carried out using a 30-meter capillary column coated with a 0.50 μm film of Rxi®-17Sil MS, a midpolarity phase: similar to 50% phenyl, 50% dimethyl polysiloxane. The compounds elute over approximately a 0.9-minute window using a total run time of just over 16.0 minutes. The 2-trifluoromethyl phenyl benzyl piperazine elutes first, followed by the 3- and 4- trifluoromethyl phenyl benzyl piperazine isomers respectively as shown in Figure (7).

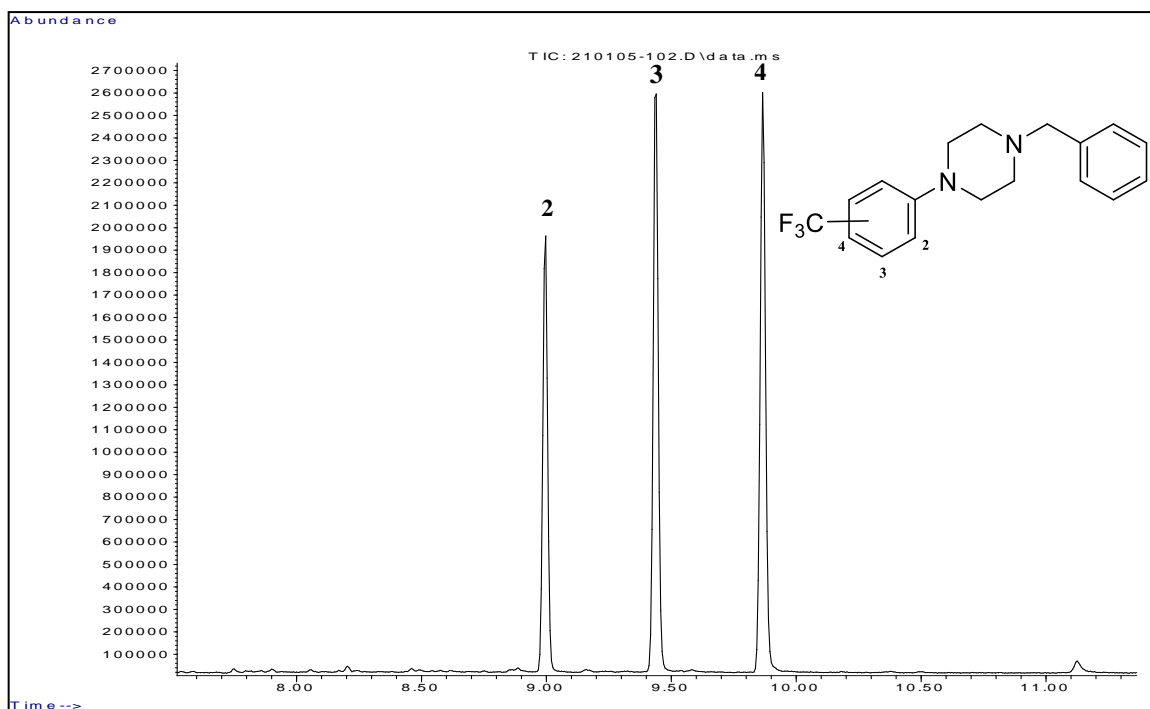
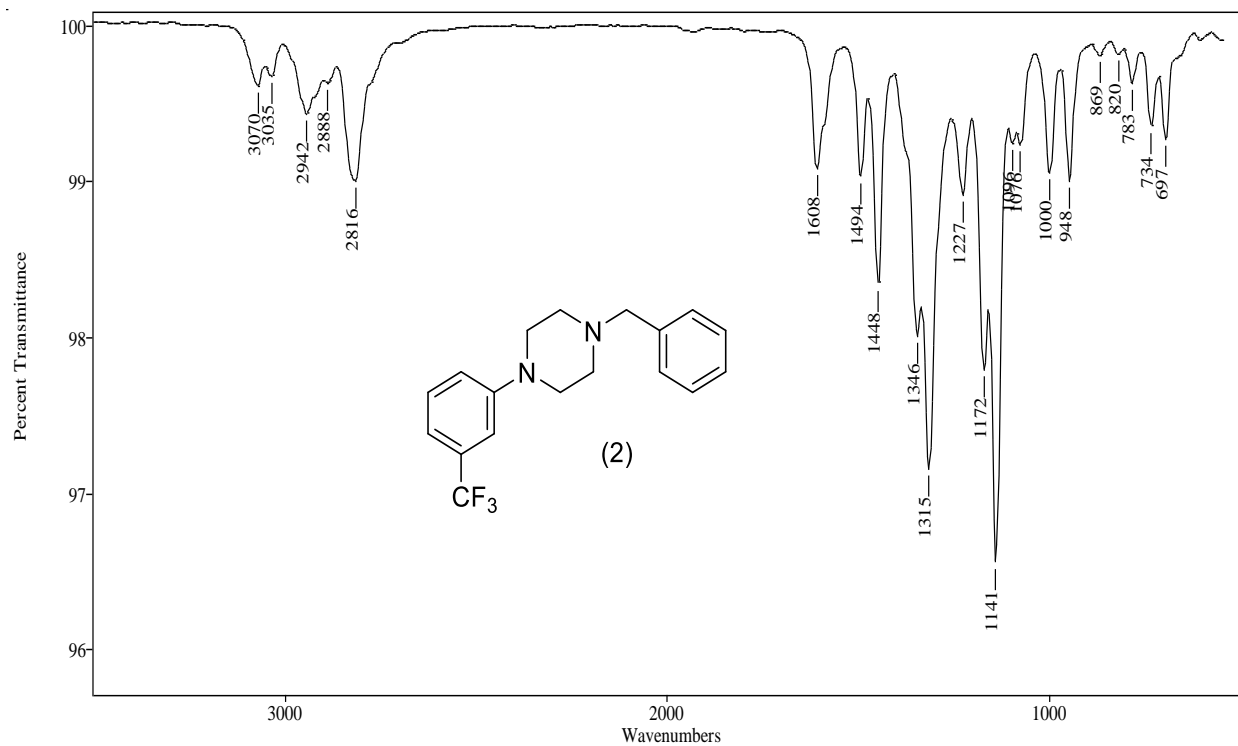
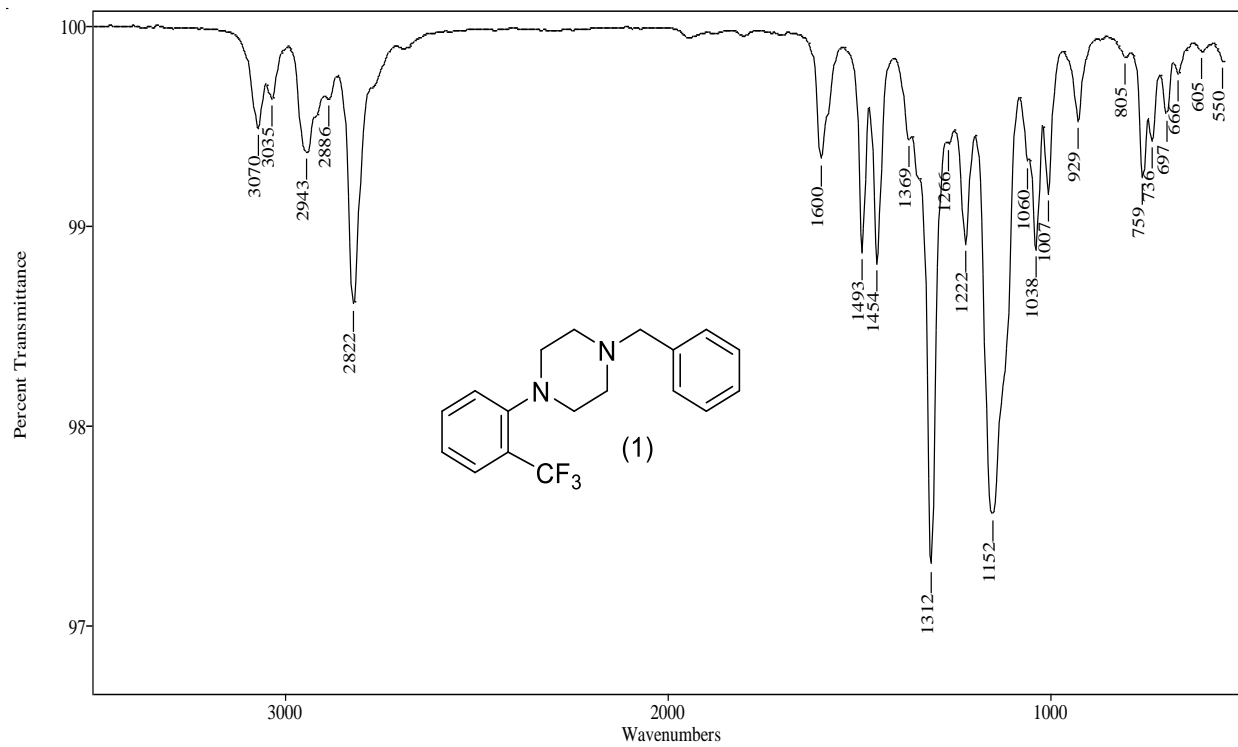


Figure 7. Gas chromatographic separation of 1-[N-(trifluoromethyl)phenyl]-4-benzylpiperazine using TP-1 program (Group1)

3.1.3. Vapor-phase Infra-Red Spectrophotometry

Infrared spectroscopy is one of the main instrumentations in analytical chemistry for drugs identification and confirmation. Gas-chromatography coupled infrared detection (GC-IRD) was performed to differentiate between the three regioisomers trifluoromethylphenyl-N benzylpiperazines. Unique absorption bands were resulted from the vapor phase spectra of the three regioisomers. These bands are differed according to the position of the trifluoromethyl substitution on the phenyl ring. All three compounds have shown vapor phase IR absorption bands in the range 550-1600 and 2800-3100 cm^{-1} , the range 550 to 1000 shows variant low intensity bands and positions for all three regioisomers. The 2-trifluoromethyl phenyl benzyl piperazine isomer exhibits two major bands at 1312 cm^{-1} and 1152 cm^{-1} , the one on 1312 cm^{-1} is a single band while the band centered at 1152 cm^{-1} is very broad. In addition, this compound has almost two identical bands at 1493 cm^{-1} and 1454 cm^{-1} . 3-trifluoromethyl phenyl benzyl piperazine has also two major bands appear as doublet peak at 1315 cm^{-1} and 1141, the first doublet signal is at 1346 cm^{-1} with the more intense component of the doublet at 1315 cm^{-1} . The second doublet at 1172 and 1141 cm^{-1} has a similar relative absorption band profile and the 1141 cm^{-1} is the more intense component. The third compound 4- trifluoromethyl phenyl benzyl piperazine has dissimilarity with the previous two regioisomers, it has only one single sharp band at 1323 cm^{-1} and wide shorter band at 1144 cm^{-1} . The 4- trifluoromethyl phenyl benzyl piperazine can be distinguish by absence the two bands that located at 1493 cm^{-1} and 1454 cm^{-1} Figure (8).



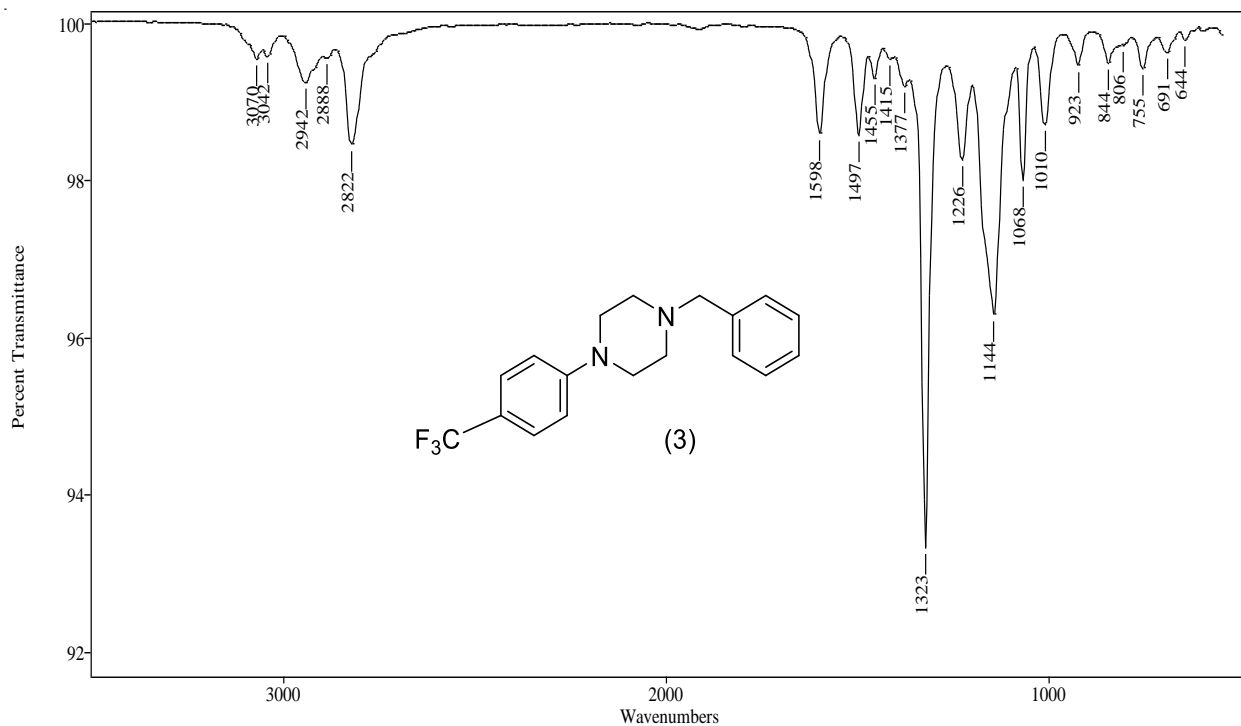


Figure 8. Vapor phase IR spectra of 1-[N-(trifluoromethyl)phenyl]-4-benzylpiperazine (Group1)

3.1.4. Conclusion

The major EI-MS fragment ions occur via processes initiated by one of the two nitrogen atoms of the piperazine ring. The base ion at m/z 91 observed in all three spectra resulted from the loss of the benzyl radical (91Da). The major fragment at m/z 119 (a radical cation) observed in all regioisomers contains the unsubstituted benzyl group common to all regioisomers and the m/z 56 cation (C_3H_6N)⁺ is a characteristic piperazine ring fragment. The EI-MS fragments for the isomers did not show significant fragment ions that could be used for differentiation among them. However, the vpIR studies illustrate different characterization of absorption bands among these three regioisomers. The 2-trifluoromethyl phenyl benzyl piperazine isomer displays two major bands at 1312 cm^{-1} and 1152 cm^{-1} , the one at 1312 cm^{-1} is a single band while the band at 1152 cm^{-1}

¹ is much wider. In addition, this compound has two almost identical bands at 1493 cm⁻¹ and 1454 cm⁻¹. While the isomer 4- triflouromethyl phenyl benzyl piperazine has dissimilarity with the previous two regioisomers, it has only one sharp band at 1323 cm⁻¹ and wide shorter band at 1144 cm⁻¹. The 4- triflouromethyl phenyl benzyl piperazine can be distinguish by absence the two bands that located at 1493 cm⁻¹ and 1454 cm⁻¹

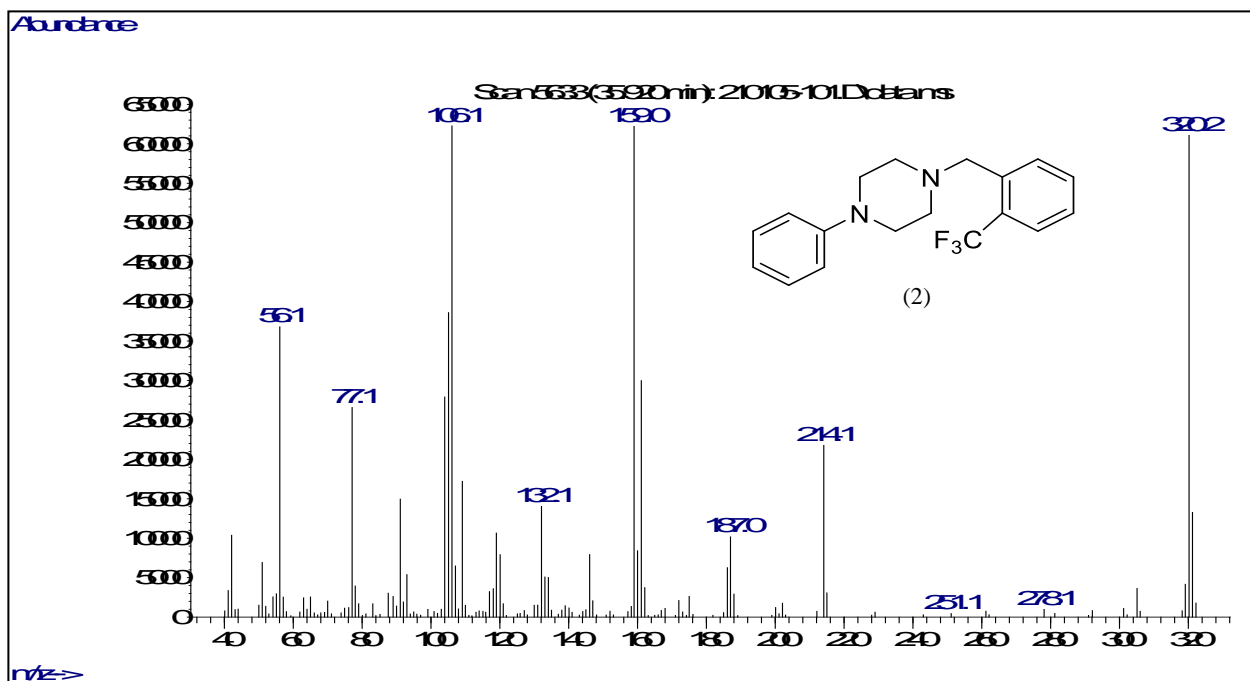
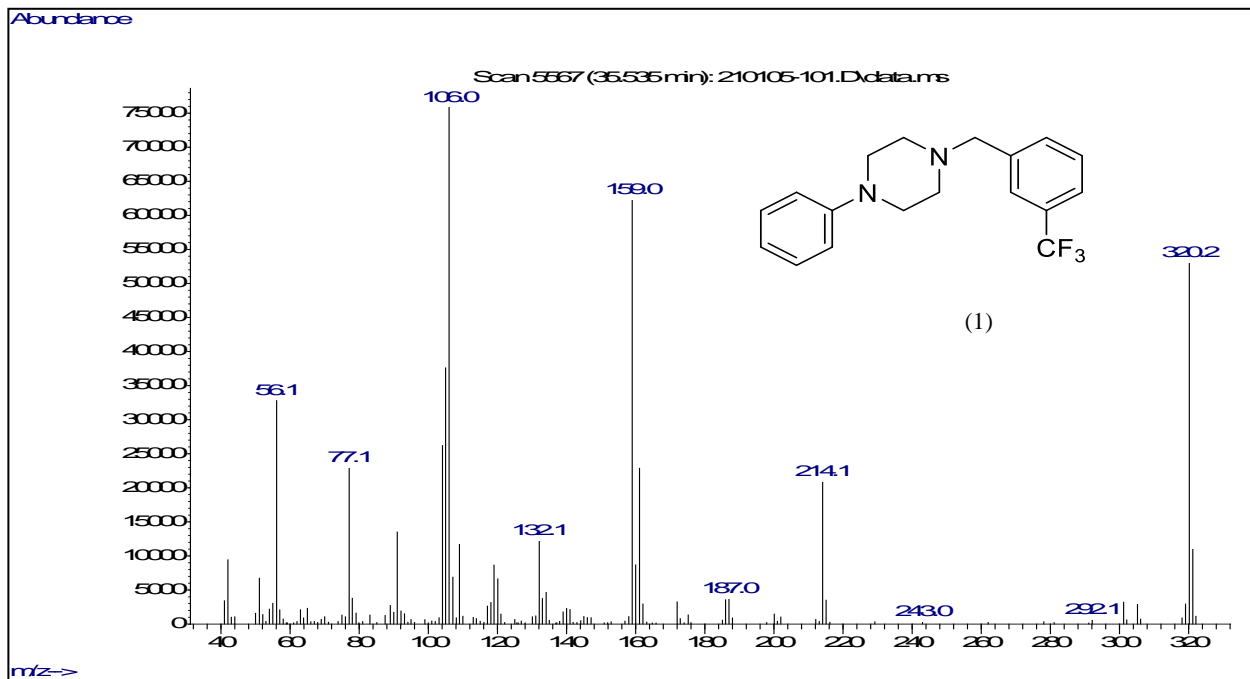
3.2. Analysis of 1-[N-(trifluoromethyl)benzyl]-4-phenylpiperazine (Group 2)

This set of compounds 1-phenyl 2-,3-,4-triflouromethylbenzyl-piperazine are also hybridized compounds of BZP and TFMPP, where the only difference for the previous group is the position of trifluoromethyl substituent on the benzyl ring. The three regioisomers have identical mass spectra with almost equivalent fragments as the earlier group. Gas chromatographic separation coupled with infrared detection (GC-IRD) provides direct confirmatory data for structural differentiation between the three regioisomers. The mass spectrum combined with the vapor phase infrared spectrum provides for specific confirmation of each of the regioisomeric piperazines. The piperazines derivatives were resolved on a 30-meter capillary column containing an Rxi®-17Sil MS stationary phase.

3.2.1. Mass spectral studies

The EI mass spectra of three regioisomers of 1-phenyl 1-4triflouromethylbenzyl-piperazine are shown in Figure (9). The spectra for these regioisomers show fragment ions at m/z 56, 77, 106, 132, 159, and 214 as well as other ions with low relative abundance. The major fragments peaks

at m/z 106 is containing two atoms of piperazine ring, also this fragment is a part of three ion cluster (m/z 104,105, and 106) which are all significant ions. Another significant fragment m/z 159 the trifluoromethyl benzyl cation. Other fragments include m/z 56, 132 and 214 which have four atoms of piperazine ring while m/z 187 has a two-atoms portion of piperazine. The proposed fragments structures of this group are shown in Scheme (21).



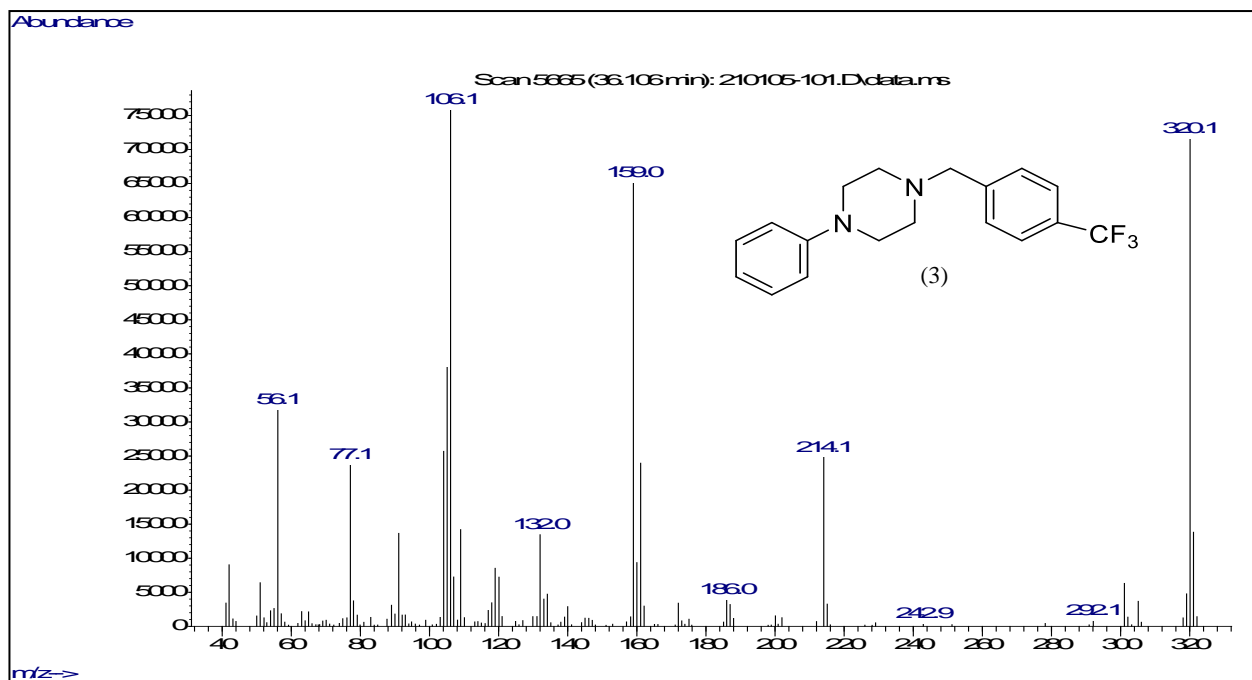
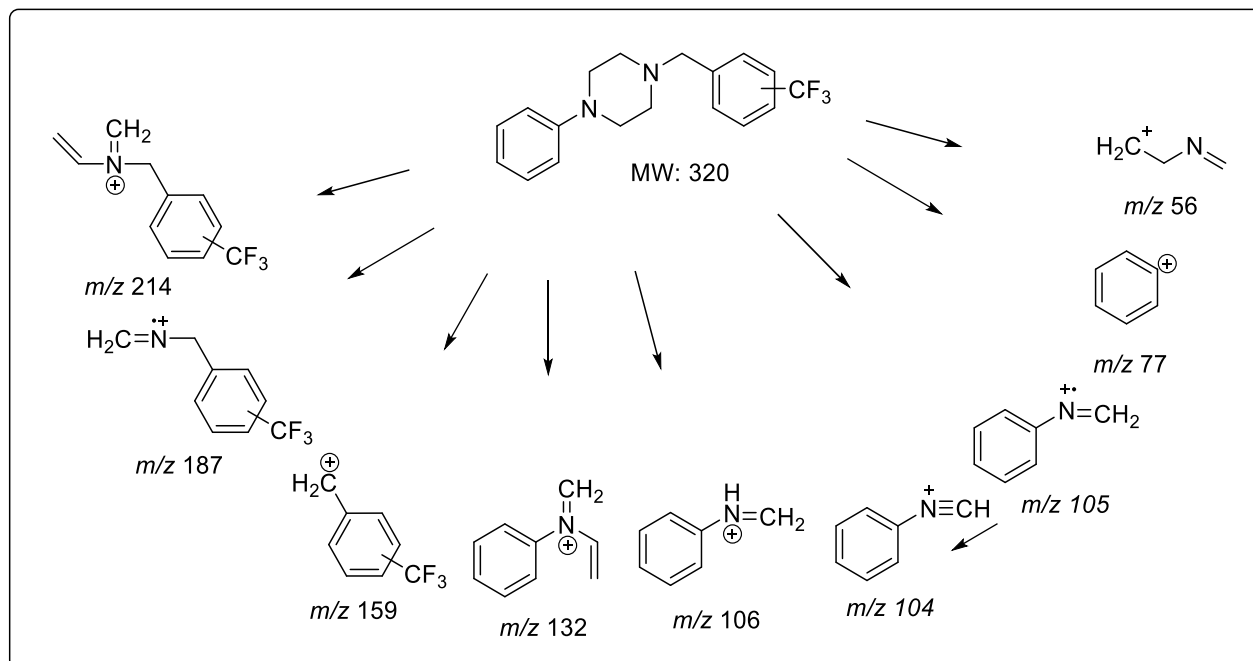


Figure 9. EI mass spectra of 1-[N-(trifluoromethyl)benzyl]-4-phenylpiperazine (Group 2)



Scheme 22. EI mass spectral fragmentation pattern of 1-[N-(trifluoromethyl)benzyl]-4-phenylpiperazine (Group 2)

3.2.2. Gas Chromatographic Separation

To differentiate the three regioisomers of this group, gas chromatographic separations were performed. The three compounds 1-phenyl N-trifluoromethylbenzyl-piperazine differ in the position of benzyl ring substitution with the trifluoromethyl group. Gas chromatographic separation of the three compounds was carried out using a 30-meter capillary column coated with a 0.50 μm film of Rxi®-17Sil MS, a midpolarity phase; similar to 50% phenyl, 50% dimethyl polysiloxane. The compounds elute over approximately a 0.5-minute window using a total run time of just over 68.0 minutes, the three isomers eluted in the 36 minutes range. The 3-trifluoromethylbenzyl-piperazine elutes first, followed by 2- and 4-trifluoromethylbenzyl-piperazine respectively as shown in Figure (10).

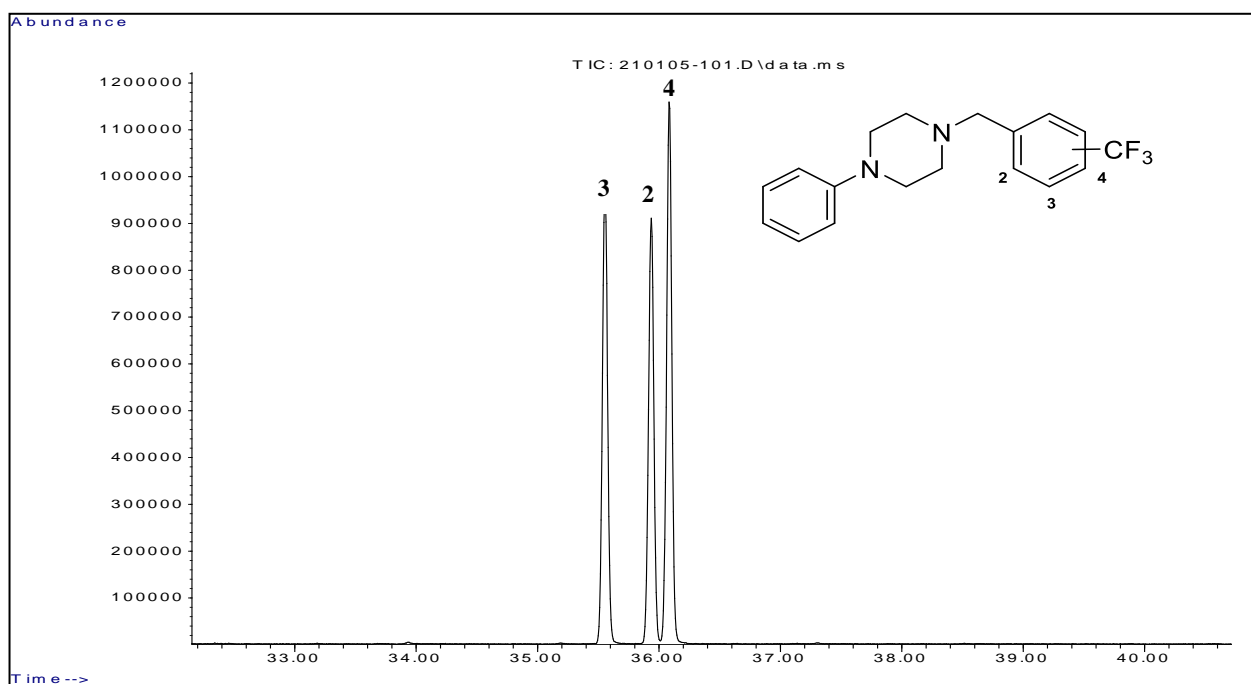
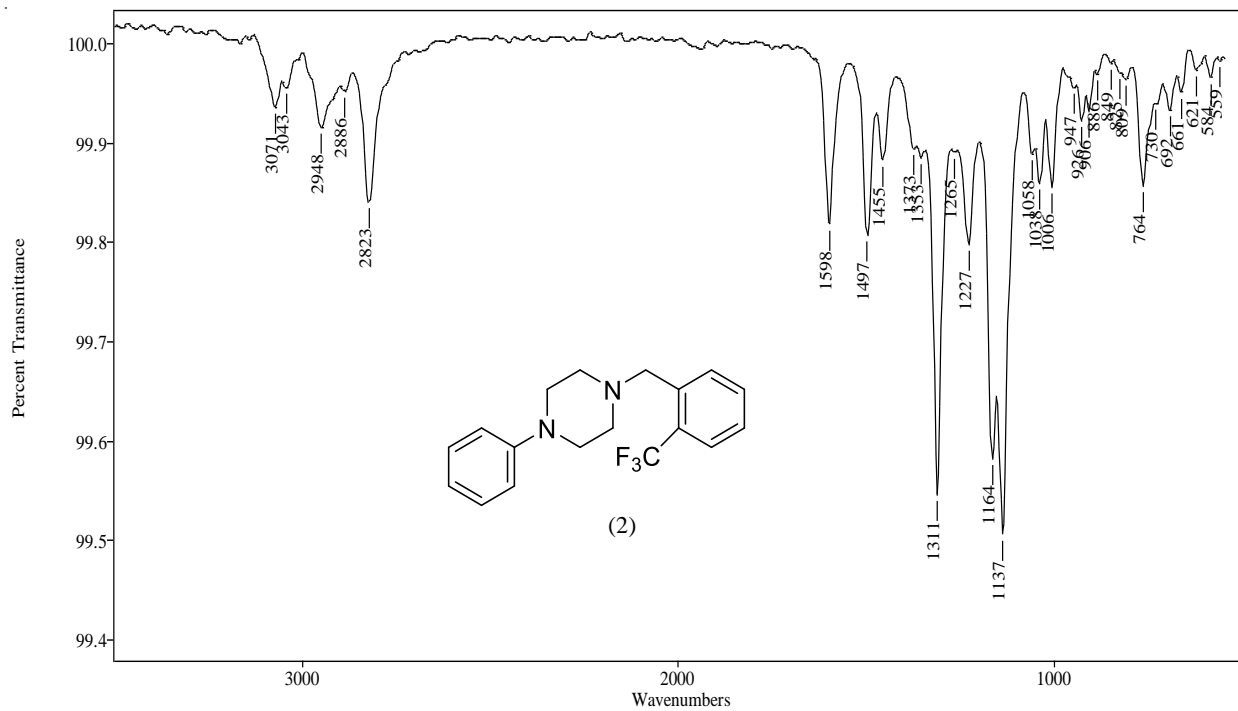
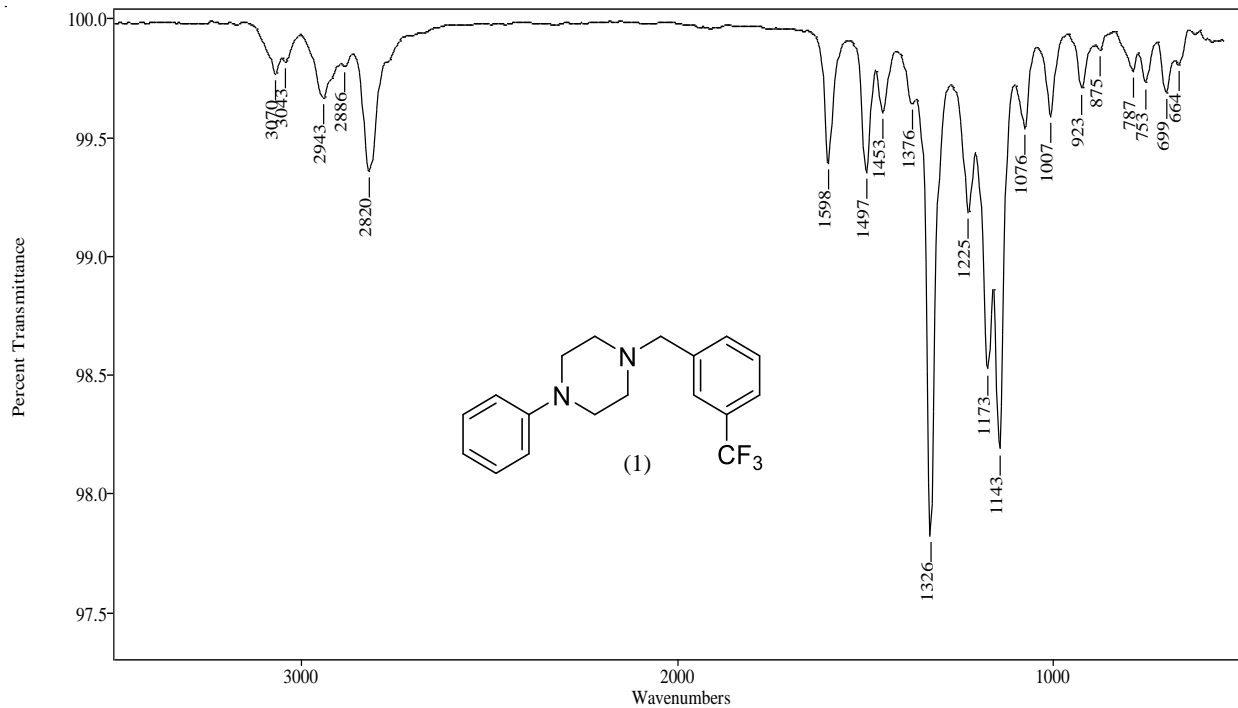


Figure 10. Gas chromatographic separation of 1-[N-(trifluoromethyl)benzyl]-4-phenylpiperazine using TP-2 program (Group 2)

3.2.3. Vapor-phase Infra-Red Spectrophotometry

Infrared spectroscopy is one of the main instrumentations in analytical chemistry for drugs identification and confirmation. Gas-chromatography coupled infrared detection (GC-IRD) was performed to differentiate between the three regioisomers of this group as shown in Figure (11). Unique absorption bands resulted from the vapor phase spectra of the three regioisomers. These bands are different according to the position of the trifluoromethyl substitution on the benzyl ring. All compounds display vapor phase IR spectrum with bands in the regions $550 - 1550 \text{ cm}^{-1}$ and $2800 - 3080 \text{ cm}^{-1}$. The nitrogen substitution in all three regioisomers is the same and IR spectra in the region $2800 - 3080 \text{ cm}^{-1}$ for all regioisomers are almost identical. On the other hand, the region between $550 - 1550 \text{ cm}^{-1}$ shows variable vpIR spectra for this compound group. The compounds show a sharp peak at 1311 , 1326 , and 1327 cm^{-1} for the 2-, 3-, and 4- trifluoromethyl benzyl isomers. This peak is more intense for 3-trifluoromethylbenzyl isomer and 4-trifluoromethylbenzyl isomer. The regions $1130-1170 \text{ cm}^{-1}$ have double absorption bands for 3-, and 2-trifluoromethylbenzyl isomer, but not 4-trifluoromethylbenzyl isomer which has broad absorption band in this region. The distinguish between 3-isomer and 2-isomer could be obvious in the region $550-1100 \text{ cm}^{-1}$.



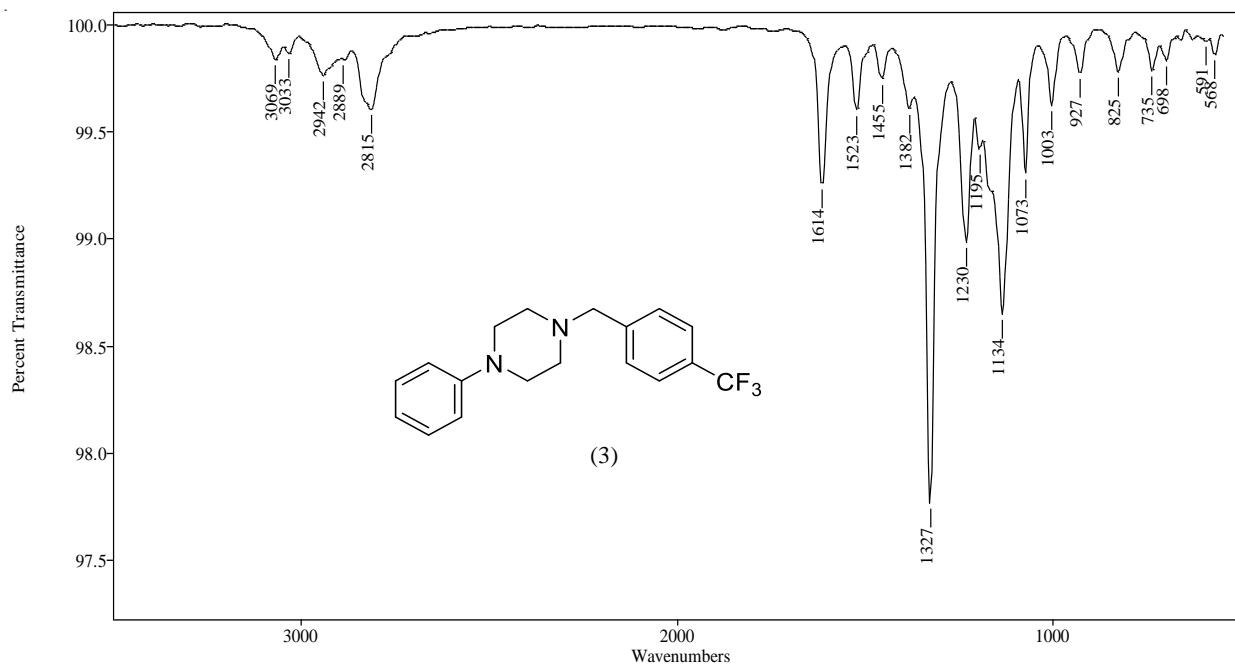


Figure 11. Vapor phase IR spectra of 1-[N-(trifluoromethyl)benzyl]-4-phenylpiperazine (Group 2)

3.2.4. Conclusions

The major EI-MS fragment ions occur via processes initiated by one of the two nitrogen atoms of the piperazine ring. The base ion at m/z 106 observed in all three spectra and the m/z 56 cation (C_3H_6N)⁺ is a characteristic piperazine ring fragment. The EI-MS fragments for the isomers did not show significant fragment ions that could be used for differentiation among them. However, the vpIR studies illustrate different characterization of absorption bands among these three regioisomers. The compounds show individual and characteristic sharp peaks at 1311, 1326, and 1327 cm^{-1} , this peak is more intense for compounds (1) and (3). The regions 1130-1170 cm^{-1} have double absorption bands for 3- and 2- trifluoromethylbenzyl-piperazine isomers, but not the 4-trifluoromethylbenzyl-piperazine isomer which has broad absorption band in this region. The distinguish between compounds 3- trifluoromethylbenzyl-piperazine isomer and 2-trifluoromethylbenzyl-piperazine isomer could be obvious in the region 550-1100 cm^{-1}

3.3. Analysis of 1-[N-(methylenedioxybenzyl)]-4-[3-(trifluoromethyl)phenyl]piperazine (Group 3)

The disubstituted piperazine with 3-TFMP and N-methylenedioxybenzyl regioisomers have identical mass spectra with almost equivalent fragments. They are only differed in the position of methylenedioxy substitution on the benzyl group. The mass spectra for these two compounds did not show characteristic ion fragment for specific identification. Therefore, gas chromatographic separation coupled with infrared detection (GC-IRD) were used to provide direct confirmatory data for structural differentiation between the two regioisomers. The mass spectrum combined with the vapor phase infrared spectrum provides for specific confirmation of each of the regioisomeric piperazines. The piperazines derivatives were resolved on a 30-meter capillary column containing an Rxi®-17Sil MS stationary phase.

3.3.1. Mass spectral studies

The EI mass spectra of the two regioisomers of methylenedioxybenzyl are shown in Figure (12). The spectra for the regioisomers of this group show the fragment ions at m/z 56, 105, 135, 163, 172, 190, and 229 as well as other ions with low relative abundance. The major fragments peaks at m/z 135 which result from methylenedioxybenzyl cation. Another significant fragment is 163 which contains two atoms of the piperazine ring. Other fragments include the characteristic fragment of piperazine ring m/z 56, and 190 which has four atoms of piperazine ring while m/z 229 represent the 3-TFMPP cation. The proposed fragments structures of this group are shown in Scheme (22).

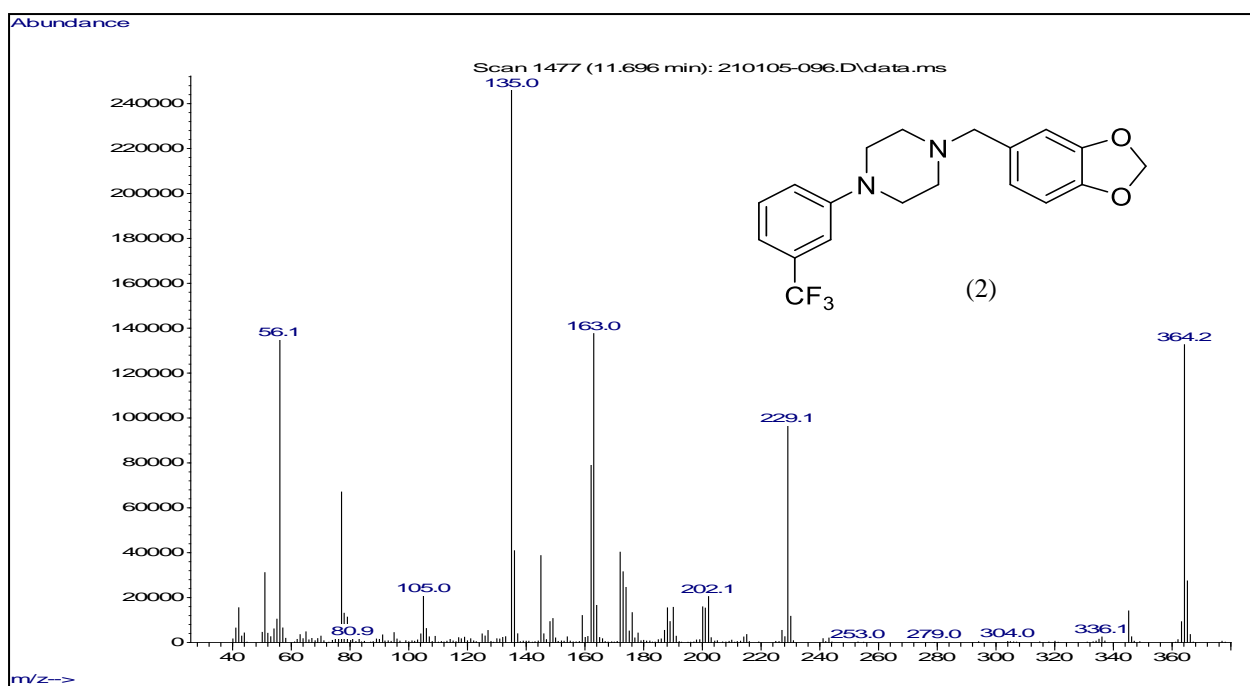
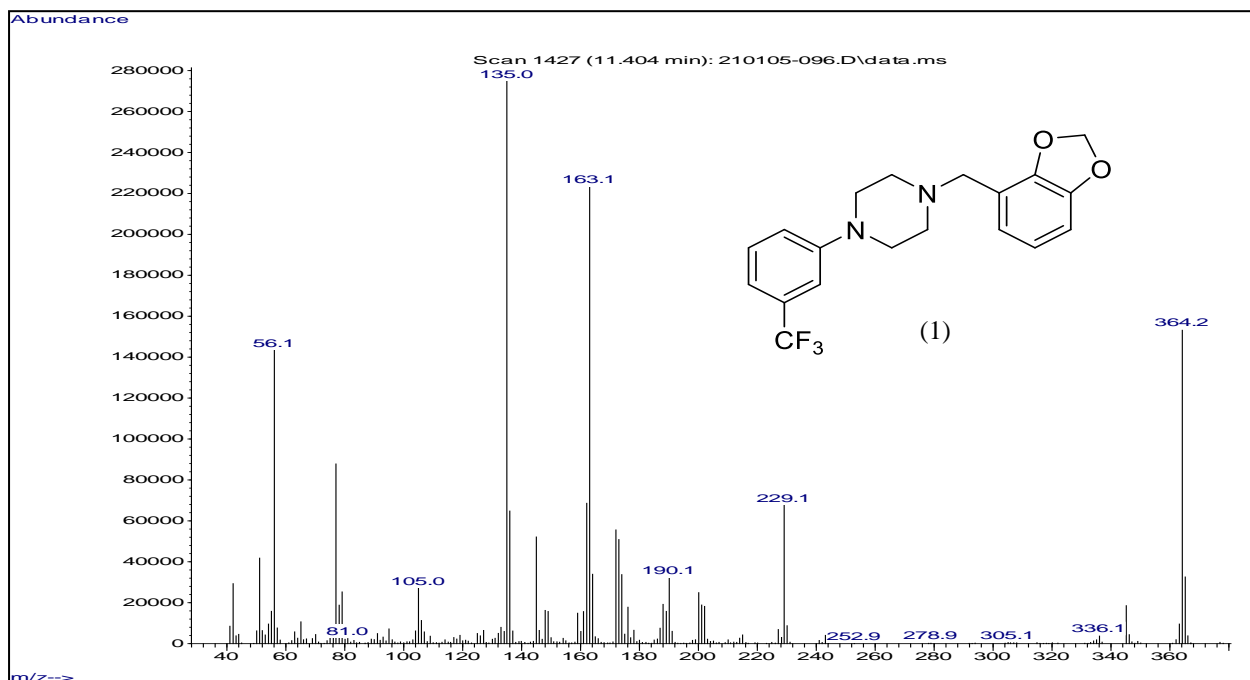
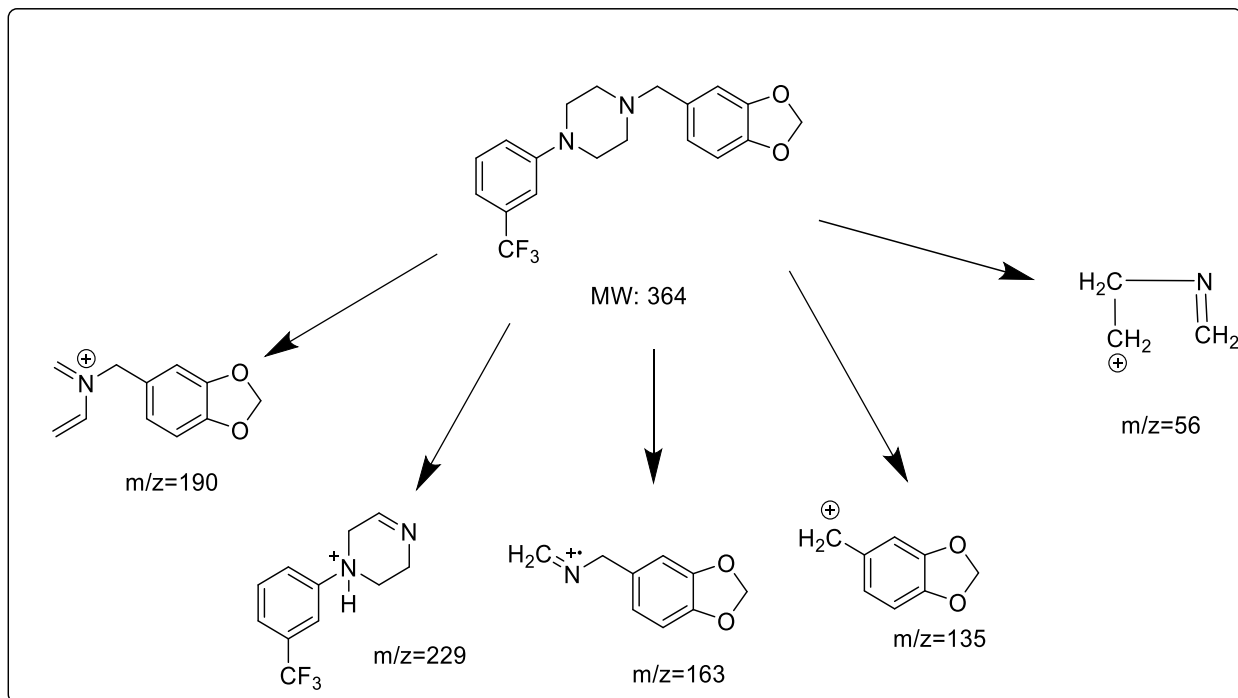


Figure 12. EI mass spectra of 1-[N-(methylenedioxybenzyl)]-4-[3-(trifluoromethyl)phenyl]piperazine (Group 3)



Scheme 23. EI mass spectral fragmentation pattern of 1-[N-(methylenedioxybenzyl)]-4-[3-(trifluoromethyl)phenyl]piperazine (Group 3)

3.3.2. Gas Chromatographic Separation

To differentiate the two regioisomers of this group, gas chromatographic separations were performed. The two regioisomers differ in the methylenedioxy substitution position on the benzyl group. Gas chromatographic separation of the two compounds was carried out using a 30-meter capillary column coated with a 0.50 μm film of Rxi®-17Sil MS, a midpolarity phase; similar to 50% phenyl, 50% dimethyl polysiloxane. The compounds elute over approximately a 0.5-minute window in the 11 minutes require using a total run time of just over 16.0 minutes. The 1-[2,3-(methylenedioxybenzyl)]-4-[3-(trifluoromethylphenyl) piperazine elutes first, followed by 1-[3,4-(methylenedioxybenzyl)]-4-[3-(trifluoromethylphenyl) piperazine as shown in Figure (13).

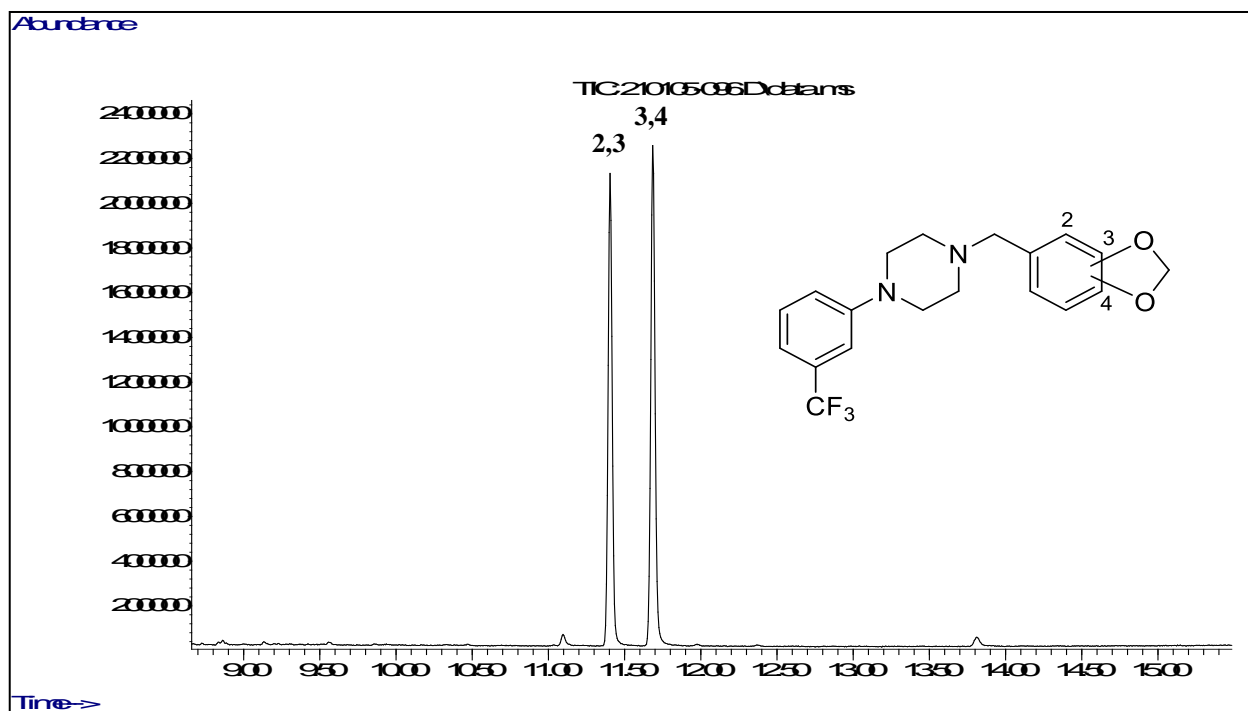


Figure 13. Gas chromatographic separation of 1-[N-(methylenedioxybenzyl)]-4-[3-(trifluoromethylphenyl)piperazine (trifluoromethylphenyl) piperazine using TP-1 program (Group 3)

3.3.3. Vapor-phase Infra-Red Spectrophotometry

Infrared spectroscopy is one of the main instruments in analytical chemistry for drugs identification and confirmation. Gas-chromatography coupled infrared detection (GC-IRD) was performed to differentiate between the two regioisomers of this group as shown in Figure (14). All compounds display vapor phase IR spectrum with transmittance bands in the regions 650 - 1620 cm^{-1} and 2770 - 3080 cm^{-1} . The two regioisomers have nearly indistinguishable bands in the region 2770 - 3080 cm^{-1} . However, the 2,3 methylenedioxy isomer has a unique single sharp absorption band at 1453 cm^{-1} , while the 3,4 methylene dioxy isomer has a doublet bands at 1446 and 1489 cm^{-1} . These characteristic bands are the specific identification for the methylenedioxy

substitution patterns. Both compounds show IR spectra with doublet bands at 1141, 1172 cm^{-1} and 1315,1316,1346, and 1343 cm^{-1} .

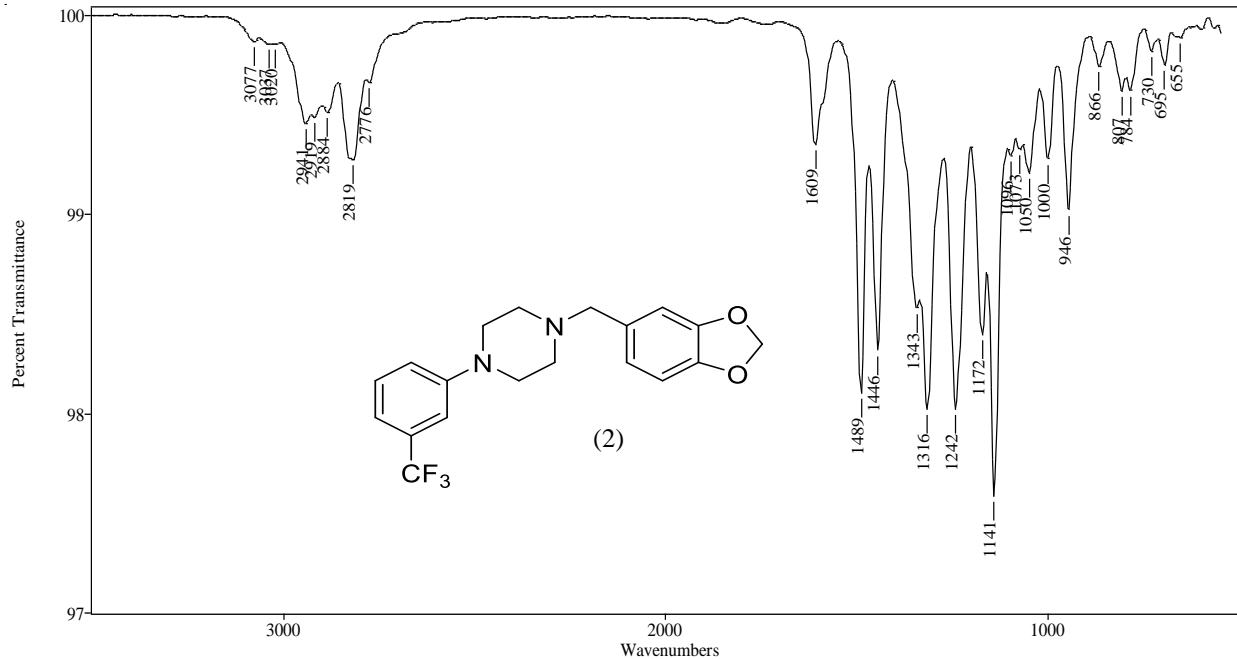
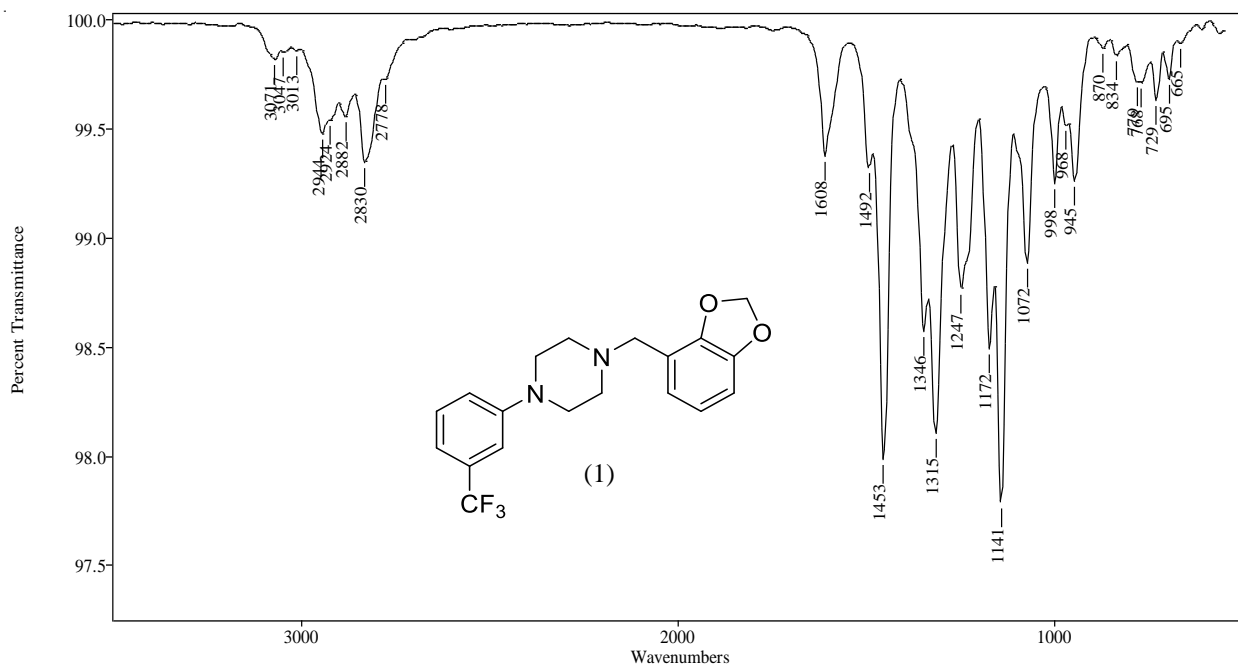


Figure 14. Vapor phase IR spectra of 1-[N,N-methylenedioxybenzyl]-4-[3-(trifluoromethyl)phenyl]piperazine (Group 3)

3.3.4. Conclusions

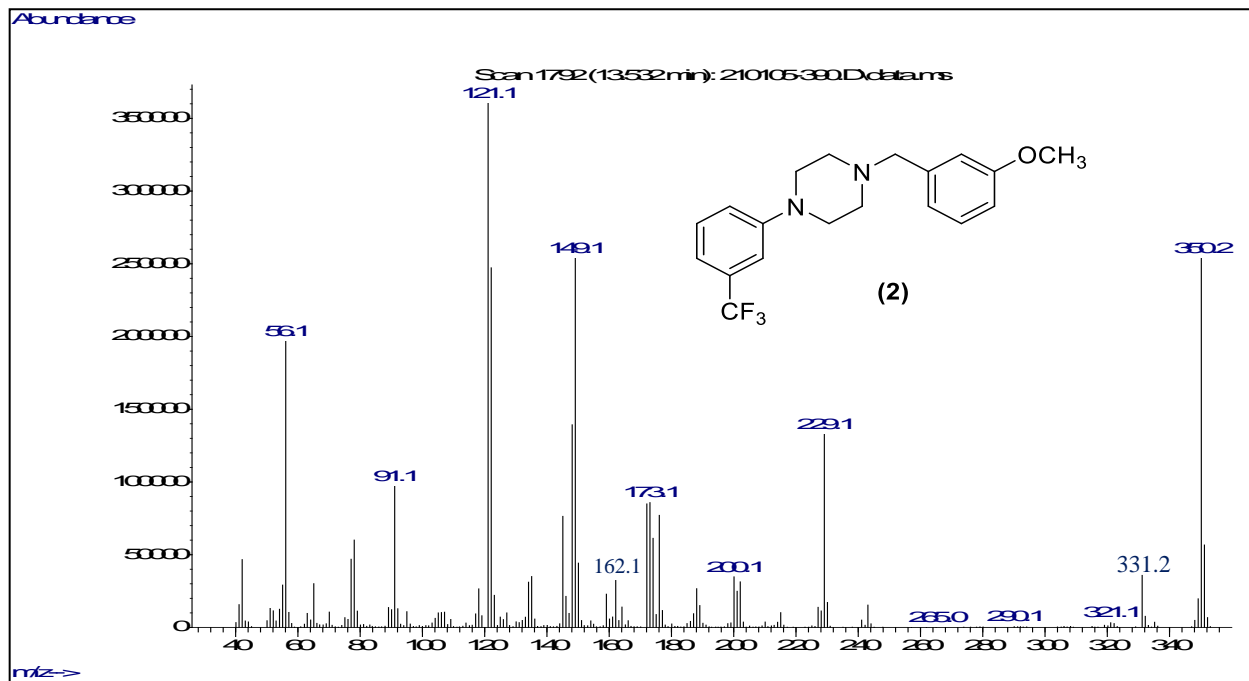
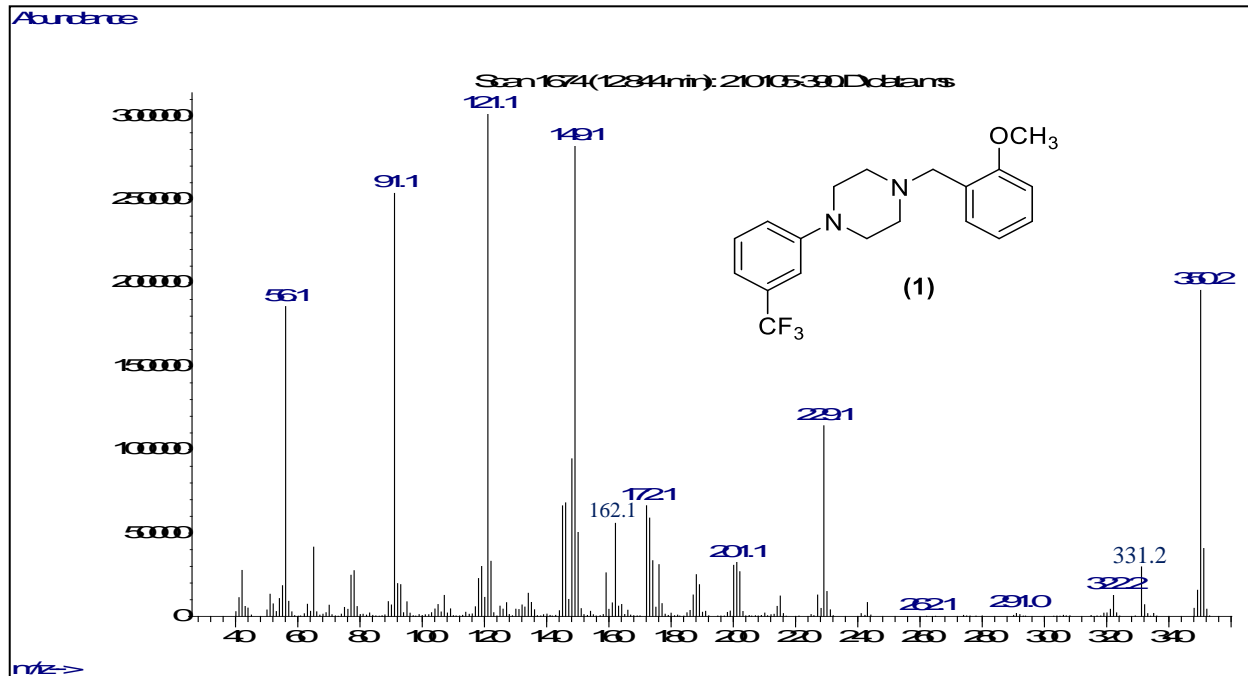
The major EI-MS fragment ions occur via processes initiated by one of the two nitrogen atoms of the piperazine ring. The base ion at m/z 135 was observed in all spectra and the m/z 56 cation (C_3H_6N)⁺ is a characteristic piperazine ring fragment. The EI-MS fragments did not show significant fragment ions that could be used for differentiation between the isomers. However, the vpIR studies illustrate different characterization of absorption bands among these two regioisomers. The 2,3 methylenedioxy isomer has a unique single sharp absorption band at 1453 cm^{-1} , while the 3,4 methylene dioxy isomer has a doublet bands at 1446 and 1489 cm^{-1} .

3.4. Analysis of 1-[N-methoxybenzyl]-4-[3-(trifluoromethyl)phenyl]piperazine (Group 4)

The regioisomers in this group have identical mass spectra with almost equivalent fragments. They only differed in the position of methoxy substitution on the benzyl group. The mass spectra for these three compounds did not show characteristic ion fragment for specific identification. Therefore, gas chromatographic separation coupled with infrared detection (GC-IRD) were used to provide direct confirmatory data for structural differentiation between the three regioisomers. The piperazines derivatives were resolved on a 30-meter capillary column containing an Rxi®-17Sil MS stationary phase.

3.4.1. Mass spectral studies

The electron ionization (EI) mass spectra for these three regioisomers are shown in Figure (15). These compounds share common major fragment ions as expected however there are some differences in relative intensity of ions which could be used for tentative differentiation between these regioisomers. The proposed structures for the major fragment ions are summarized in Scheme (23). All these compounds yield molecular radical cations of significant relative abundance and the loss of the methoxybenzyl radical yields the 3-trifluoromethylphenylpiperazine cation at m/z 229. The high mass fragment ion at m/z 331 results from the loss of fluorine radical from the molecular radical cation. The fragmentation of the piperazine ring from the nitrogen bearing the methoxybenzyl group yields the methoxybenzyl iminium-type radical cation at m/z 149. The m/z 121 cation can form in a direct manner via initial ionization of the methoxybenzyl aromatic ring via loss of the 3-trifluoromethylphenylpiperazine radical species yielding the methoxybenzyl/methoxytropylium cation. Further loss of formaldehyde from this species yields the m/z 91 unsubstituted benzyl/tropylium cation fragment. The m/z 56 ion is a characteristic fragment observed in most mono and disubstituted piperazine compounds originating from the atoms of the piperazine ring. While the base peak ion for all three spectra in Figure (15) is the methoxybenzyl cation, the product ion at m/z 91 (the unsubstituted benzyl/tropylium fragment) is significantly more abundant for the 2-methoxybenzyl isomer and decreases in relative intensity for the 3-methoxybenzyl isomer and is much less significant for the 4-methoxybenzyl isomer. The 3-methoxybenzyl isomer yields a significant 3-methoxybenzyl radical cation at m/z 122 compared to either the 2- or 4-methoxybenzyl isomers. Thus, the very intense m/z 91 ion in the 2-methoxybenzyl isomer and the intense m/z 122 for the 3-methoxybenzyl isomer provides some data for the direct EI-MS differentiation of these three isomeric compounds.



3.4.2. Gas Chromatographic Separation

The chromatogram in Figure (16) shows the separation of the three regioisomeric monomethoxybenzyl-3-TFMPP analogues. The three compounds were separated on an Rxi[®]-17Sil MS midpolarity stationary phase with baseline resolution and the isomers eluted over about a 1-minute time window in the 13 minute range. The elution order was the same as that observed for regioisomeric methoxybenzyl groups in other series of compounds (Davidson and Jackson 2019),(Almalki, Clark, and DeRuiter 2019) with the 2-methoxybenzyl isomer eluting first followed by the 3-methoxy isomer and the 4-methoxybenzyl isomer having the highest retention time.

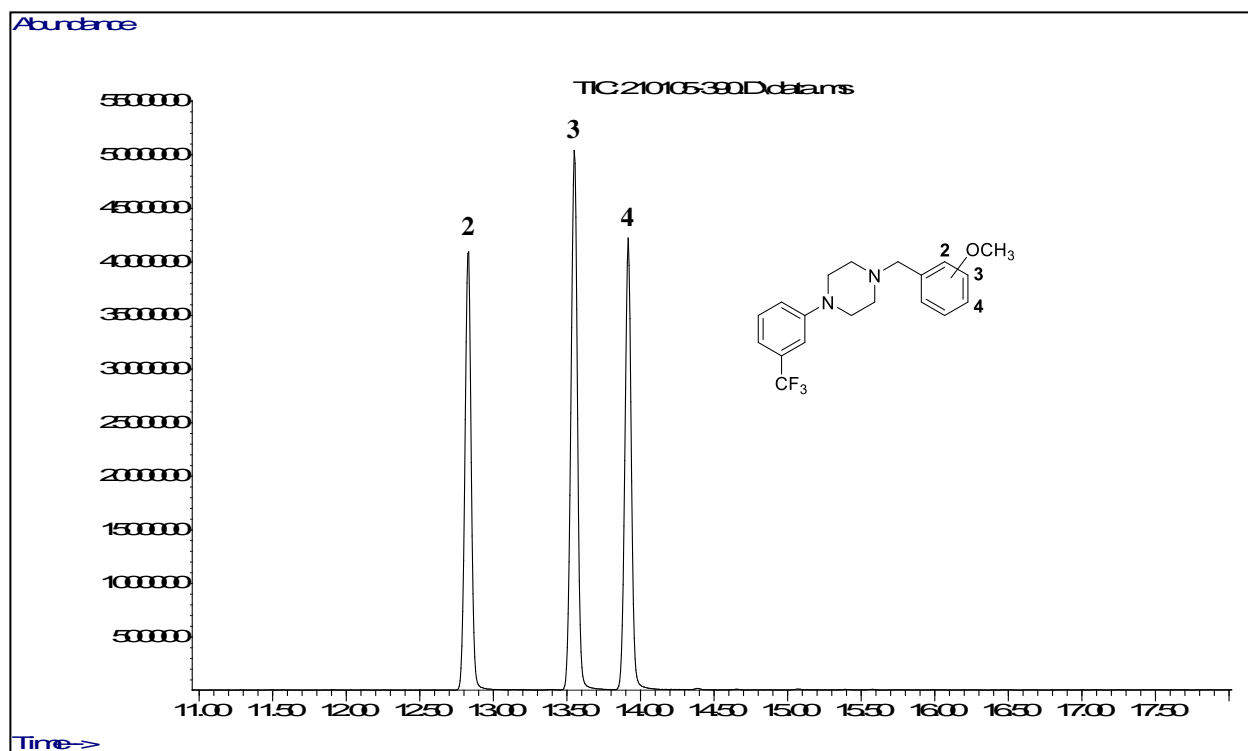
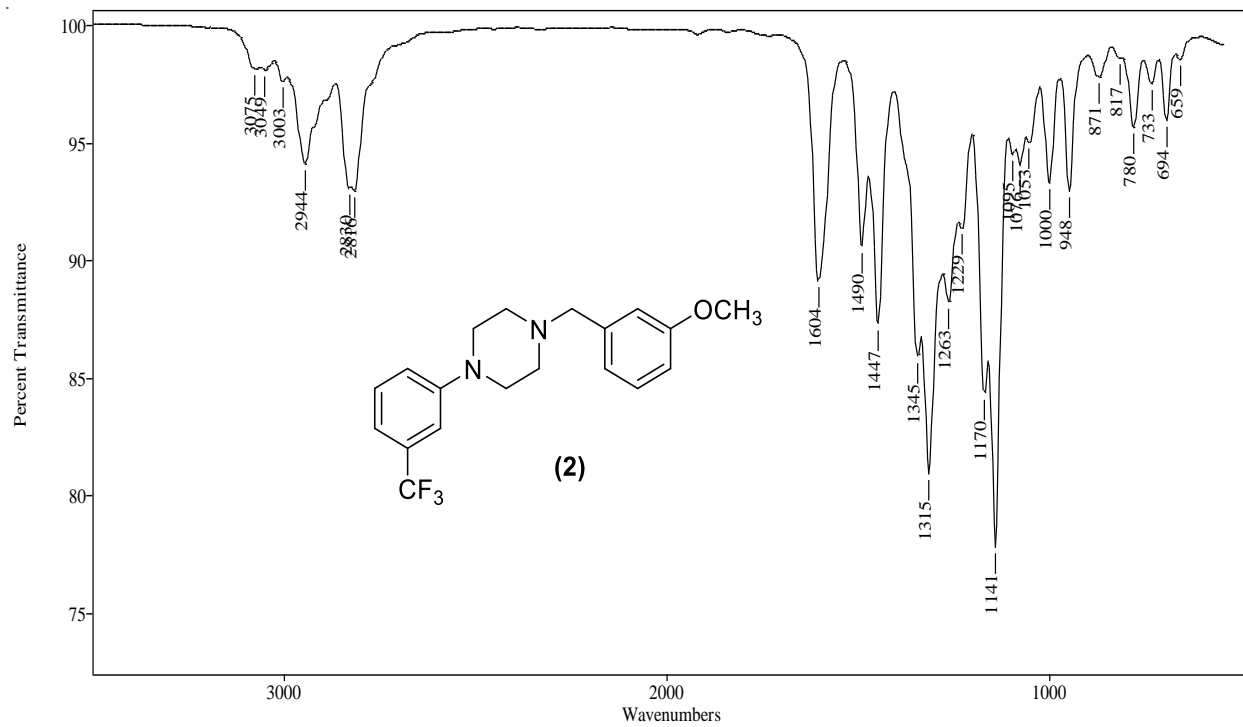
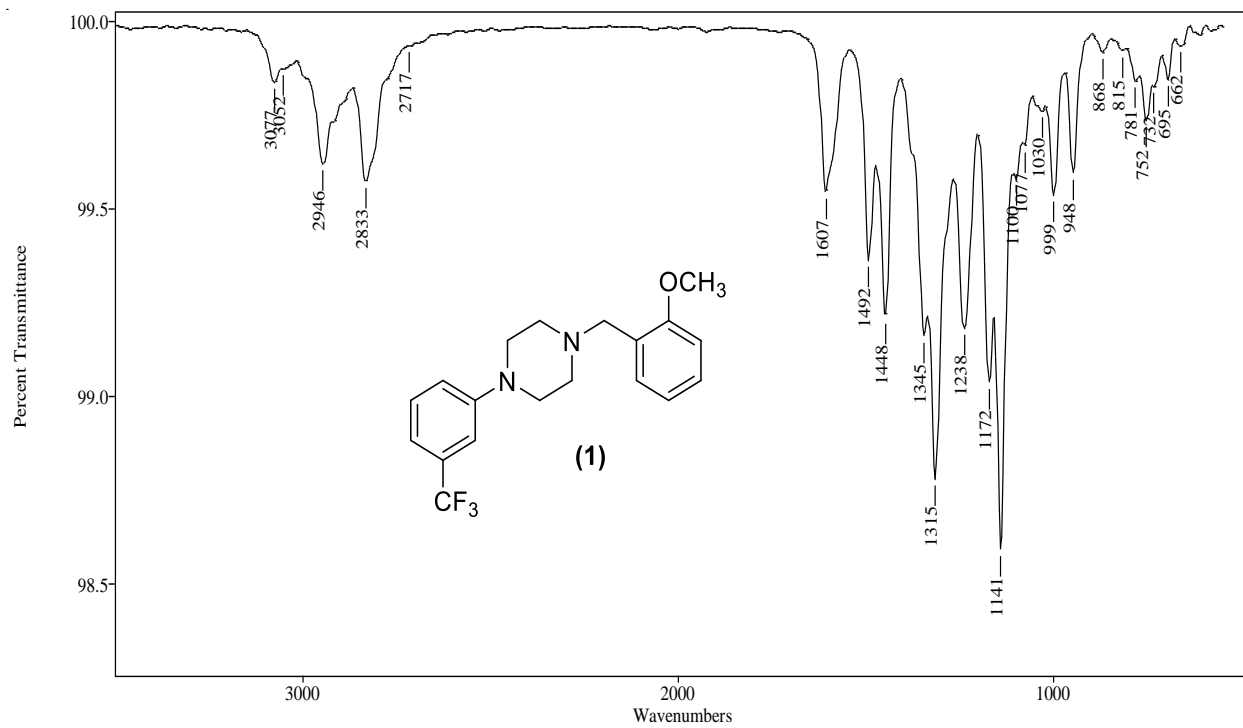


Figure 16. Gas chromatographic separation of 1-[N-methoxybenzyl]-4-[3-(trifluoromethyl)phenyl]piperazine using TP-3 program (Group 4)

3.4.3. Vapor-phase Infra-Red Spectrophotometry

The vapor phase infrared spectra for the three regioisomeric methoxybenzyl-3-TFMPP analogues are provided in Figure (17). These are true vapor phase spectra generated directly as the individual peaks elute from the capillary gas chromatography column, GC–vpIR. The spectral region from just over 1600 cm^{-1} to 1100 cm^{-1} provides several unique absorption bands and relative intensities for further differentiation of these three regioisomeric compounds. The strong bands in this region are aromatic ring carbon-carbon stretching vibrations referred to as Wilson 19a and 19b absorptions. The consistency of absorption position and intensity of several of these bands suggest their origin as the 3-TFMPP portion of the molecular structure common to all these compounds. The absorption bands at $1447/1448\text{ cm}^{-1}$, 1315 cm^{-1} and 1141 cm^{-1} would fall into this category. The vpIR spectrum for the monosubstituted parent molecule 3-TFMPP confirms these assignments showing these major absorption bands at 1447 cm^{-1} , 1315 cm^{-1} and 1141 cm^{-1} . The strong absorption bands at 1508 cm^{-1} and 1245 cm^{-1} are characteristic for the 4-methoxybenzyl isomer as these bands are less intense and centered at 1490 cm^{-1} and 1263 cm^{-1} for the 3-methoxybenzyl isomer and at 1492 cm^{-1} and 1238 cm^{-1} for the 2-methoxybenzyl isomer. These regioisomers specific absorptions coupled with the variations in EI-MS fragment ion intensities provide data for the complete differentiation of these three methoxybenzyl-3-TFMPP regioisomers.



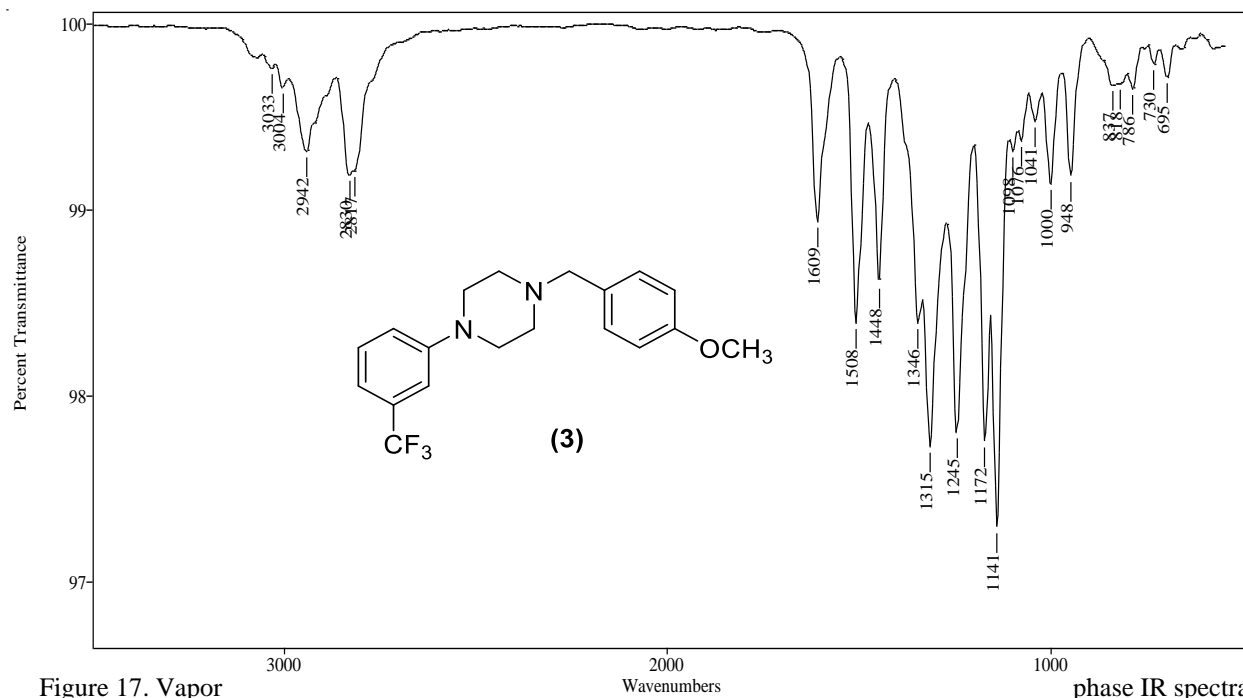


Figure 17. Vapor phase IR spectra of 1-[N-methoxybenzyl]-4-[3-(trifluoromethyl)phenyl]piperazine (Group 4)

3.4.4. Conclusion

The three regioisomers in this group share common major fragment ions, however there are some differences in relative intensity of ions which could be used for tentative differentiation between these regioisomers. While the base peak ion for all three spectra in is m/z 121, the product ion at m/z 91 is significantly more abundant for the 2-methoxybenzyl isomer and decreases in relative intensity for the 3-methoxybenzyl isomer and is much less significant for the 4-methoxybenzyl isomer. The strong absorption bands at 1508 cm^{-1} and 1245 cm^{-1} are characteristic for the 4-methoxybenzyl isomer as these bands are less intense and centered at 1490 cm^{-1} and 1263 cm^{-1} for the 3-methoxybenzyl isomer and at 1492 cm^{-1} and 1238 cm^{-1} for the 2-methoxybenzyl isomer

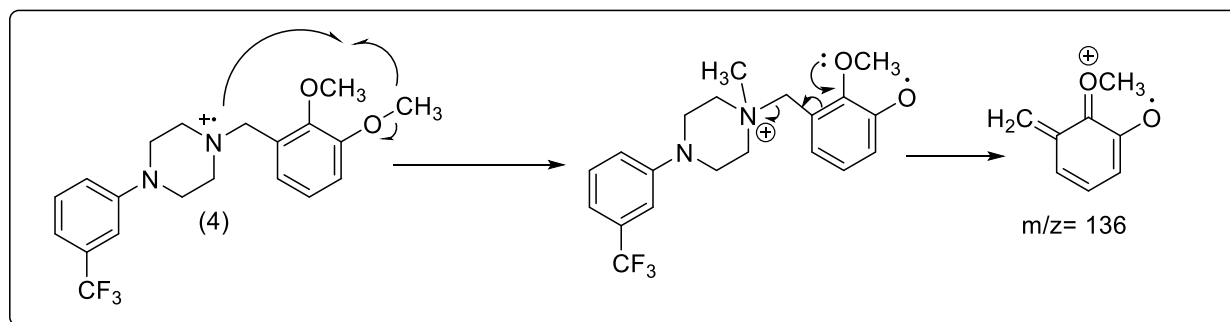
3.5. Analysis of 1-[N-dimethoxybenzyl]-4-[3-(trifluoromethyl)phenyl]piperazine (Group 5)

Six regioisomers of dimethoxybenzyl-3TFMPP have identical mass spectra with almost equivalent fragments. The only difference between these regioisomers is the position of dimethoxy substitution on the benzyl side. The mass spectra for these six compounds did not show characteristic ion fragments for specific identification, except for the 2,3- dimethoxybenzyl isomer with a unique fragment at m/z 136 and 3,5- dimethoxybenzyl isomer which shows a unique major fragment at m/z 152. Therefore, gas chromatographic separation coupled with infrared detection (GC-IRD) were used to provide direct confirmatory data for structural differentiation between the six regioisomers. The piperazine derivatives were resolved on a 30-meter capillary column containing an Rxi®-17Sil MS stationary phase.

3.45.1. Mass spectral studies

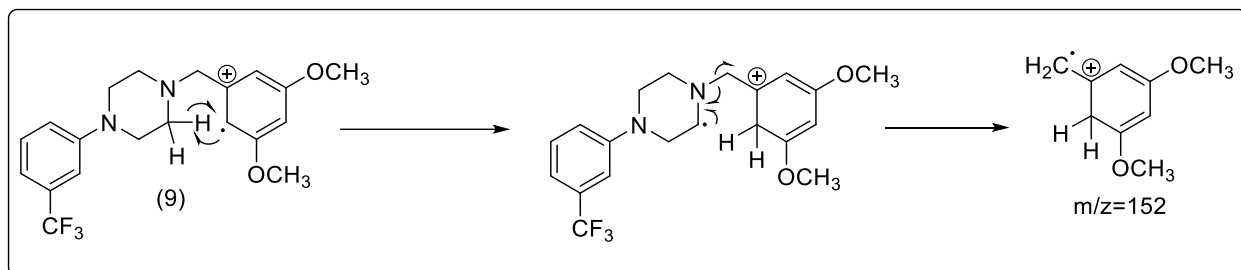
The EI mass spectra for these six regioisomers are available in Figure (19). Some of the major fragments in Figure (19) originating from the 3-TFMPP portion of the molecule occur at identical masses to those already described in the monomethoxybenzyl-3-TFMPP series including the m/z 56 and m/z 229 cations. Some of the major ions originating from the dimethoxybenzylpiperazine portion of the molecule show a 30 Da increase in mass based on the presence of the additional methoxy group compared to the monomethoxybenzyl containing ions described in Figure (15). The major fragment at m/z 179 is the dimethoxybenzyl iminium-type radical cation which occurs via the equivalent process that produces the m/z 149 ion in the monomethoxybenzyl series. Additionally, the m/z 151 peak is the dimethoxybenzyl cation which can undergo the sequential rearrangement loss of formaldehyde producing the product ions at m/z 121 and m/z 91. Most of

the EI mass spectra in Figure (18) show a series of very low intensity ions in the high mass region of the spectrum at m/z 365, 361, 352, 349, and 321. These fragments are the result of molecular radical cation loss of methyl radical (m/z 365), fluorine radical (m/z 361), ethylene (m/z 352), methoxy radical (m/z 349) and the combined loss of neutral ethylene as well as the methoxy radical (m/z 321). The insert within the EI mass spectrum for the 2,3-dimethoxybenzyl regioisomer in Figure (18) shows an enhanced view of these ions in the m/z 310 to m/z 370 region. However, the relative intensity of these ions varies with the dimethoxybenzyl substitution pattern as observed in the other spectra in Figure (19). The spectra in Figure (18) display some significant differences in ion intensities as well as a few unique ions, which provide initial information for differentiation among these regioisomeric substances. The spectrum for the 2,3-dimethoxy isomer shows the m/z 136 which is unique to the 2,3-substitution pattern and represents the rearrangement of a methyl group from an aromatic ring methoxy group to the piperazine nitrogen (4-position) via a six-centered bond migration followed by elimination of the 1-[3-(trifluoromethyl)phenyl]-4-methylpiperazine and the m/z 136 oxymethoxybenzyl radical cation ($C_8H_8O_2$), the Scheme (24) shows the mechanism of this fragment formation.



Scheme 24. Mechanism for the formation of the m/z 136 ion in the mass spectra of the 2,3-dimethoxybenzyl regioisomer

The unique ion and base peak at m/z 152 allows the EI spectrum to differentiate the 3,5-dimethoxy isomer from the other five isomers in this series. This m/z 152 is the 3,5-dimethoxybenzyl radical cation and appears to be a structural uniqueness based on both aromatic ring substituted methoxy groups present in a *meta* relationship to the benzylic methylene group, Scheme (24).



Scheme 25. Mechanism for the formation of the m/z 152 ion in the mass spectra of the 3,5-dimethoxybenzyl regioisomer

Although not the base peak, the equivalent fragment at m/z 122 was observed in the monomethoxy series when the single methoxy group was *meta* to the benzylic methylene. The second methoxy group having the same relative position appears to further stabilize the rearranged radical cation yielding the m/z 152 as the base peak for the 3,5-dimethoxy isomer. The formation of this ion requires a hydrogen migration from the piperazine ring to the benzyl aromatic ring in order to form the m/z 152 radical cation. Some of the other isomers show the m/z 152 ion but none approach the level of a major peak. The model compound 3,5-dimethoxybenzylpiperazine- D_8 was prepared from D_8 -piperazine (2,2,3,3,5,5,6,6-octadeuteropiperazine) and its EI-mass spectrum was compared to the un-deuterated form of this compound Figure (20). The D_8 analogue showed a significant m/z 153 as expected based on migration of the deuterium radical from the piperazine ring. Several other ions for this model compound show appropriate mass shifts based on the number of piperazine ring hydrogens contained in the fragment structure. The dimethoxybenzyl cation at m/z 151 is the base peak for four of these six isomers, the 2,4-, 2,5-, 2,6-, and the 3,4-

dimethoxy isomers. The radical cation at m/z 179 is essentially the co-base peak in the 2,5-isomer, sharing almost equal intensity with the m/z 151 fragment in this spectrum. This m/z 179 radical cation is the base peak in the EI spectrum for the 2,3-dimethoxybenzyl regioisomer. A traditional *N*-benzyl iminium cation ($\text{CH}_2=\text{NH}^+\text{-R}$) would yield a major benzylic/tropylium product ion via loss of the neutral imine, $\text{CH}_2=\text{NH}$. In summary, the EI-mass spectra can clearly differentiate the 2,3- and 3,5-isomers from the other four isomers and from each other based on unique base peaks at m/z 179 and m/z 152, respectively as well as the additional confirmation for the 2,3-dimethoxybenzyl regioisomer provided by the significant m/z 136 ion.

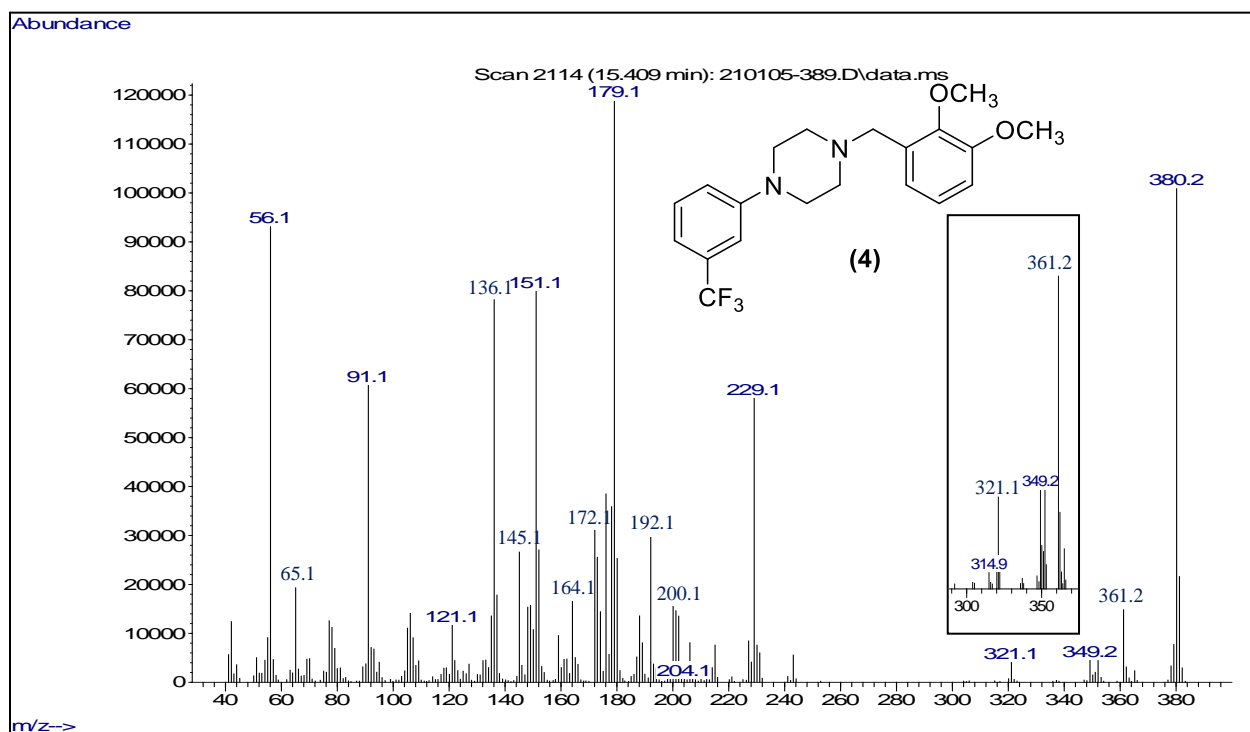
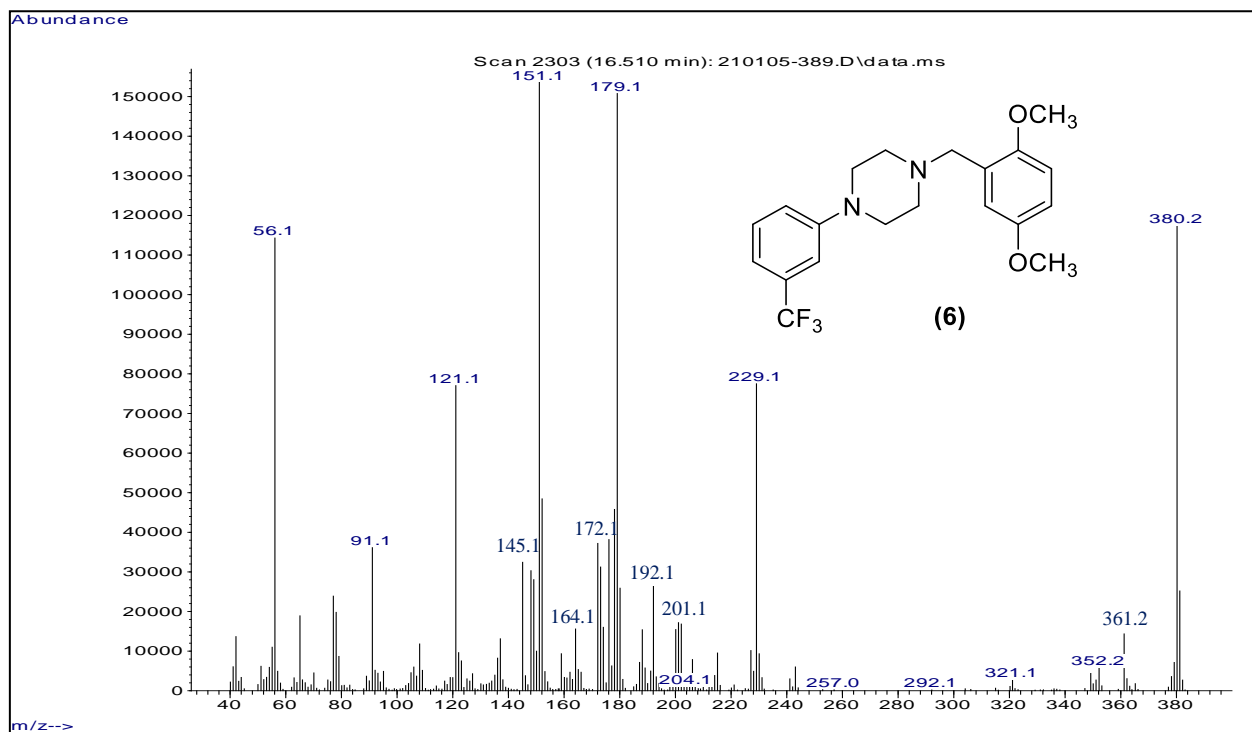
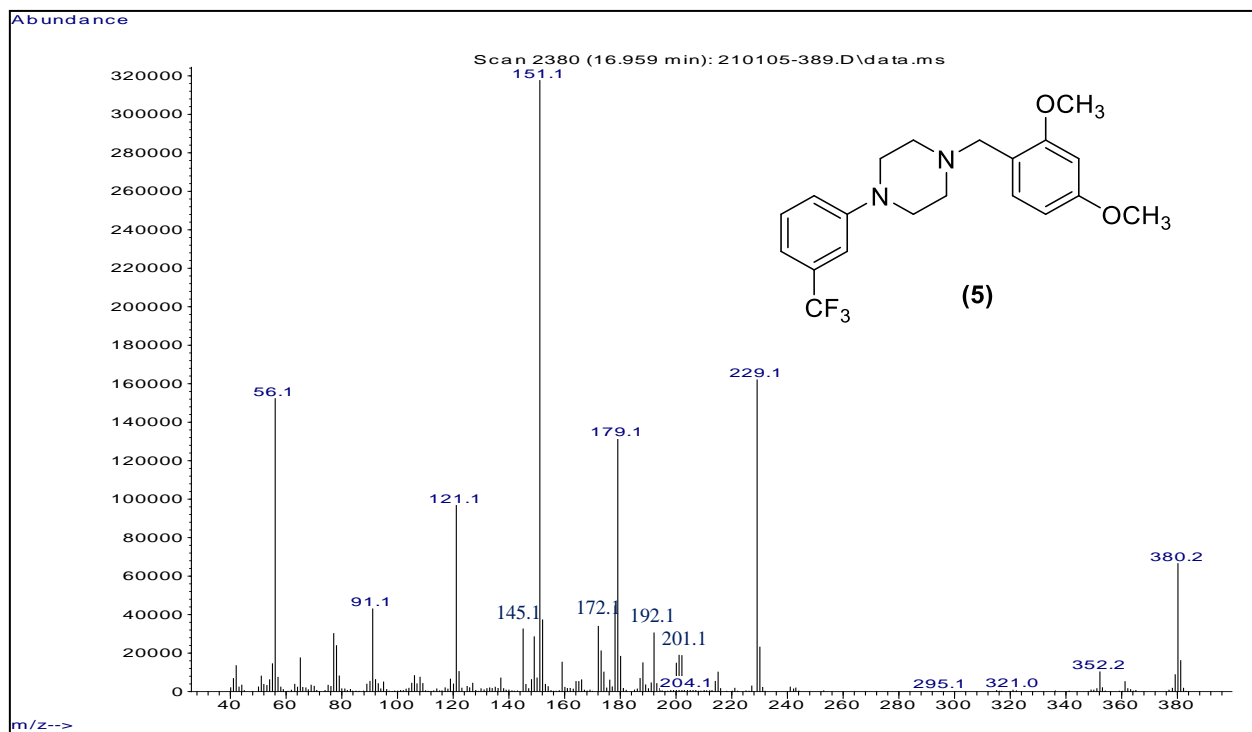
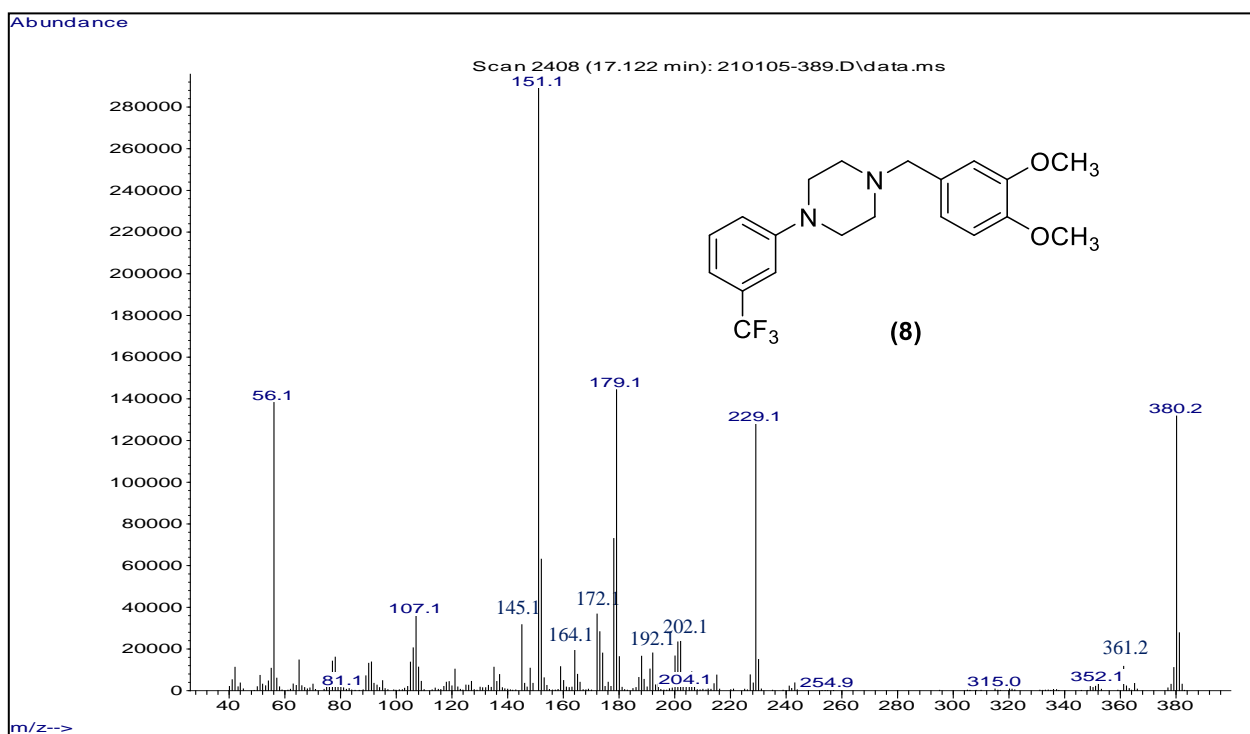
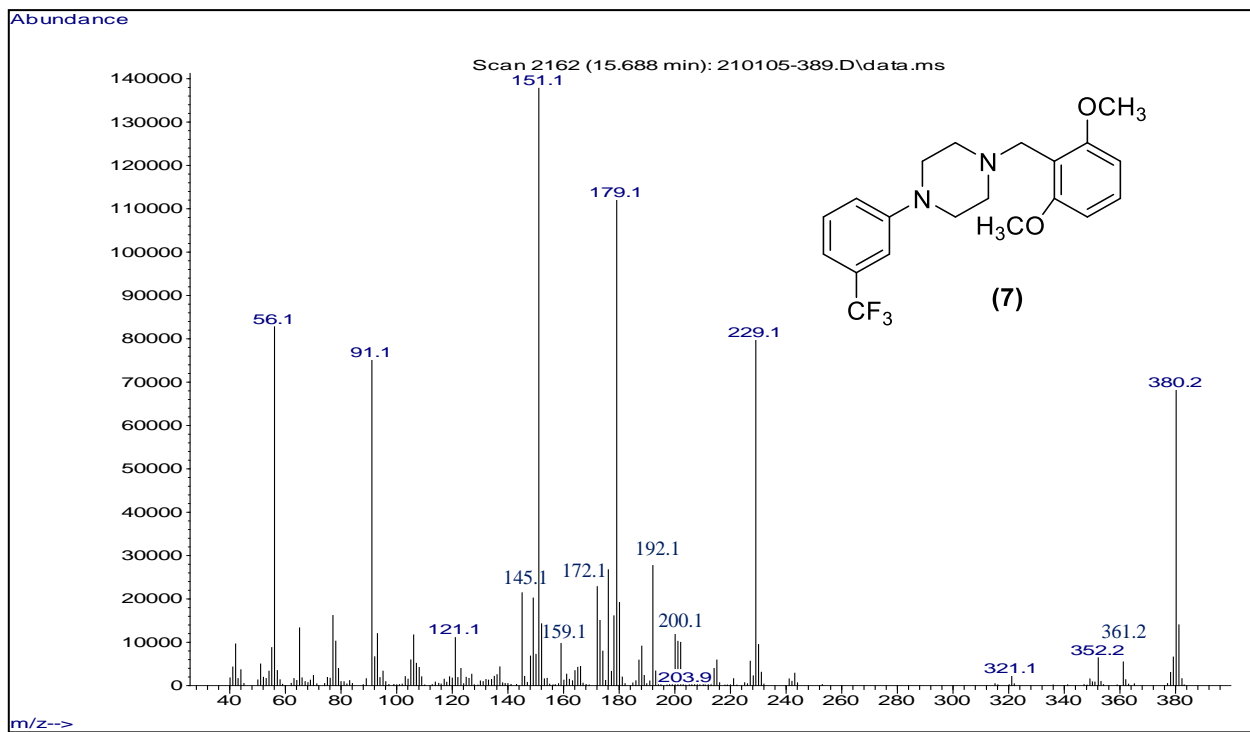


Figure 18. EI mass spectrum for the 2,3-dimethoxybenzyl regioisomer m/z 310 to m/z 370 region





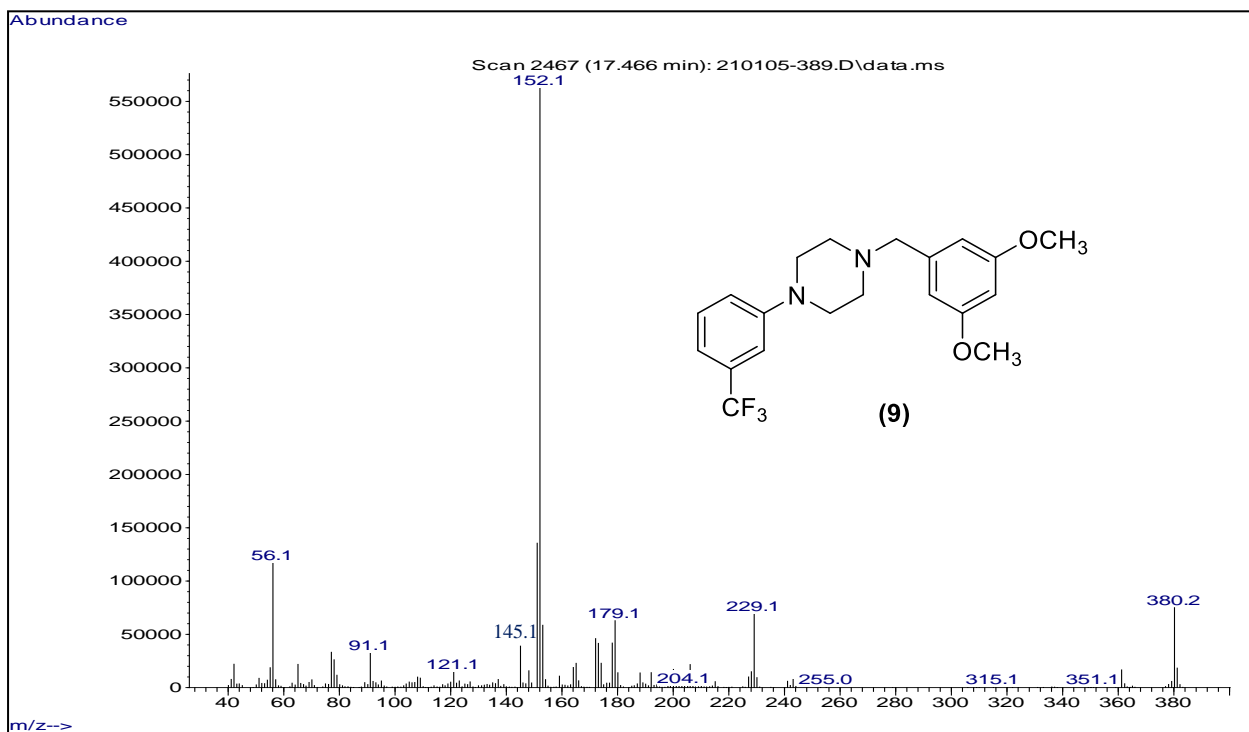
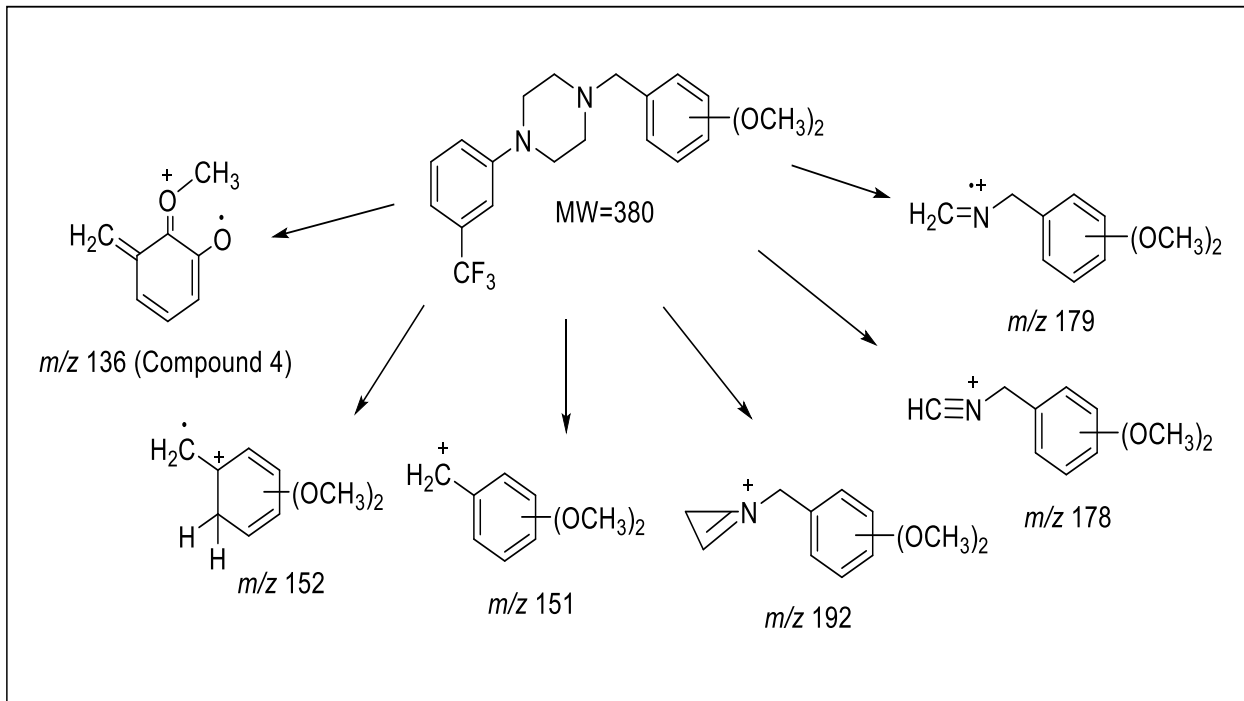


Figure 19. EI mass spectra 1-[N-dimethoxybenzyl]-4-[3-(trifluoromethyl phenyl) piperazine] (Group 5)



Scheme 26. EI mass spectral fragmentation pattern of 1-[N-dimethoxybenzyl]-4-[3-(trifluoromethyl)phenyl]piperazine (Group 5)

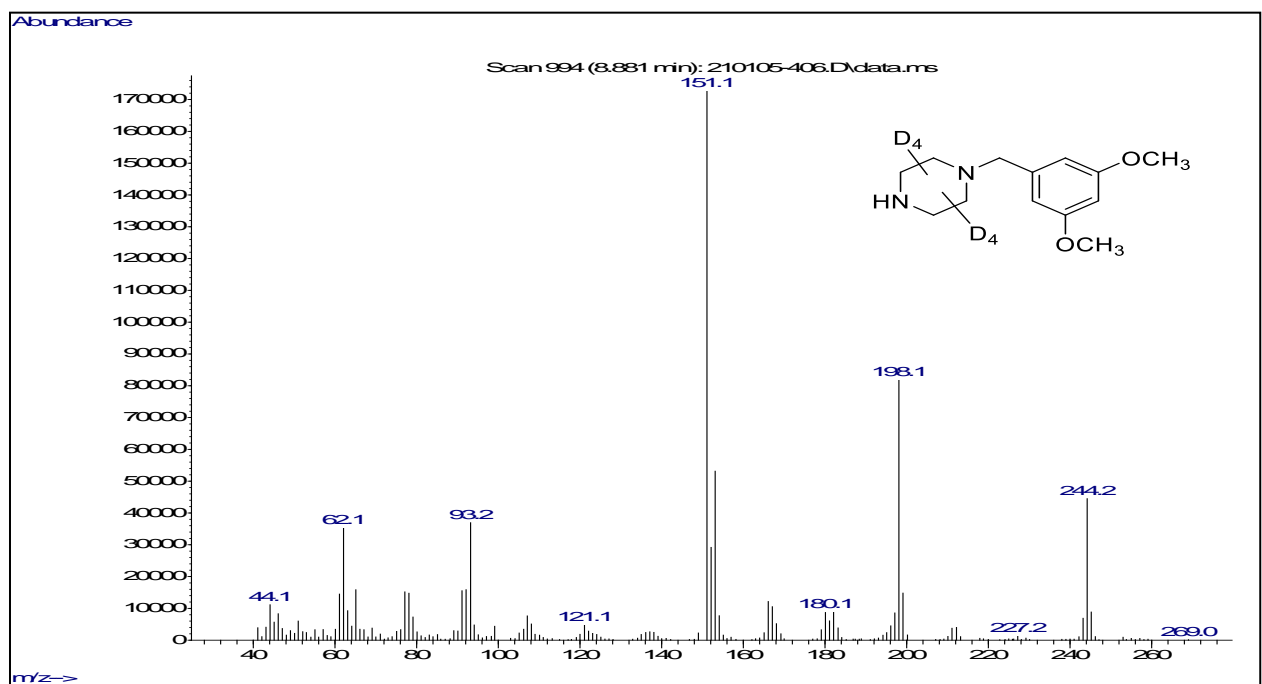
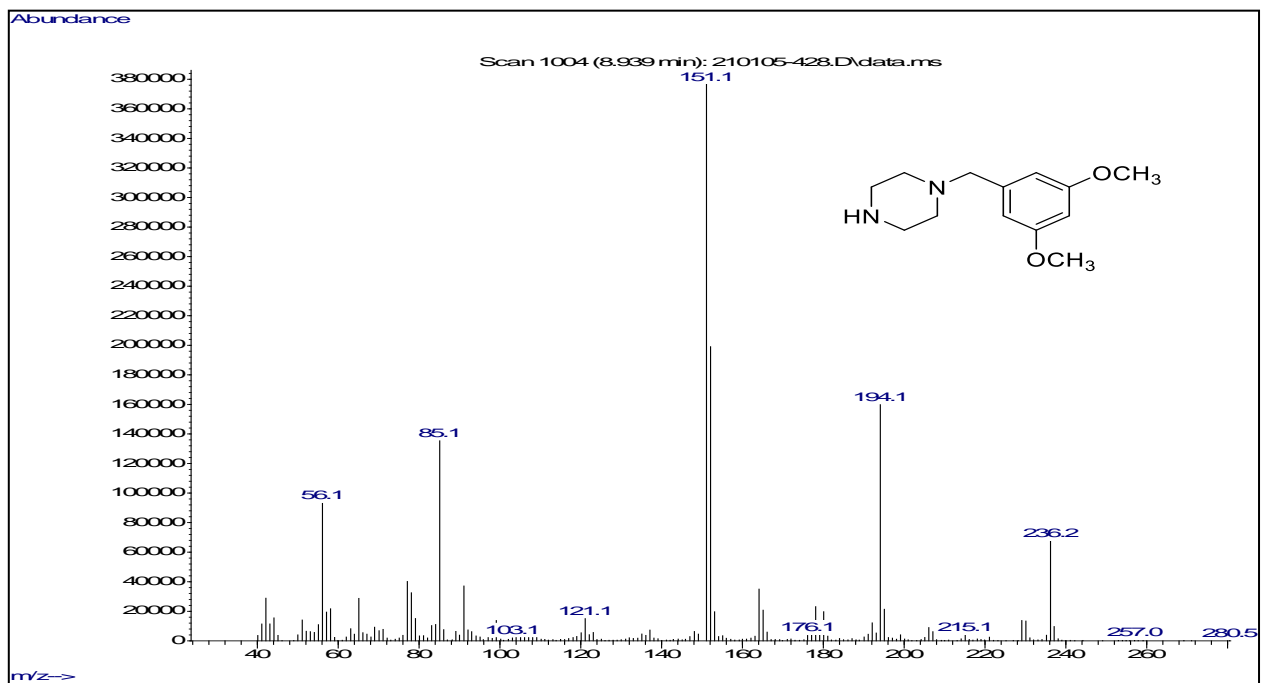


Figure 20. EI-MS of 3,5-dimethoxybenzylpiperazine and 3,5-dimethoxybenzylpiperazine-D8

3.5.2. Gas Chromatographic Separation

The GC separation of the six regioisomeric dimethoxybenzyl-3-TFMPP analogues are provided in Figure (21). The chromatographic separation was achieved under the same conditions as described for the monomethoxybenzyl analogues using a midpolarity Rxi[®]-17Sil MS stationary phase. The compounds eluted in about a 2-minute range from 15.4 to 17.4 minutes with the 2,4- and 3,4-dimethoxybenzyl isomers representing the critical peak pair. The elution order for these six isomers is consistent with other dimethoxybenzyl substituted series of compounds on this stationary phase (Abdel-Hay, Deruiter, and Clark 2013) (Almalki et al. 2020). The relative elution substituent crowding of the benzyl aromatic ring with the 2,3- and 2,6-isomers eluting first while the least crowded substituent pattern the 3,5-dimethoxy isomer elutes last. Furthermore, all four compounds having at least one methoxy group substituted *ortho* to the benzylamine side chain (the 2,3- 2,6-, 2,5- and 2,4-isomers) elute before the two isomers without an *ortho* methoxy group.

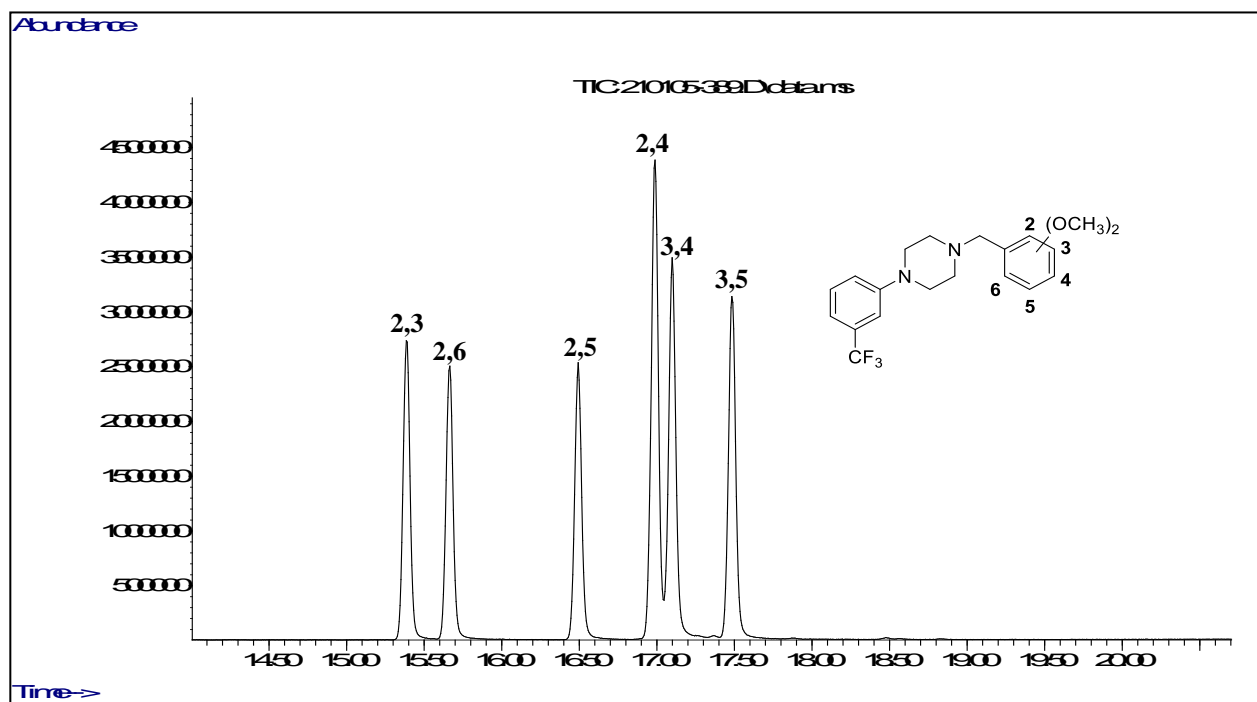
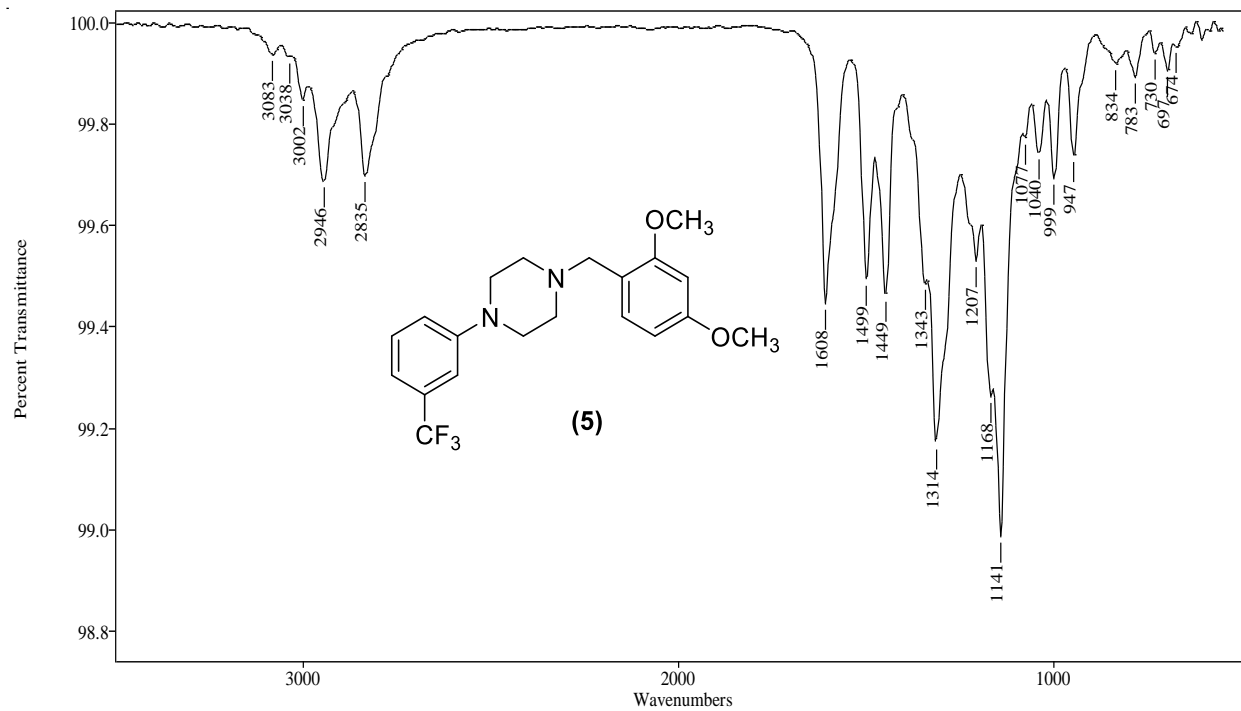
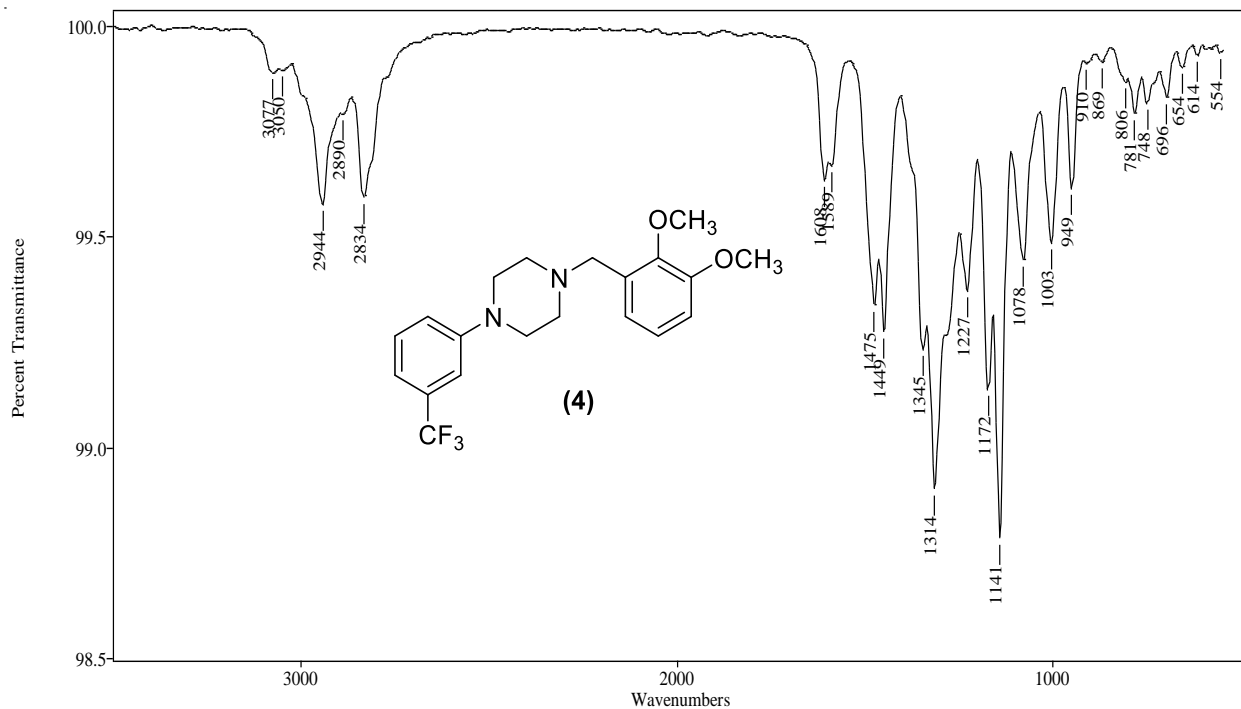


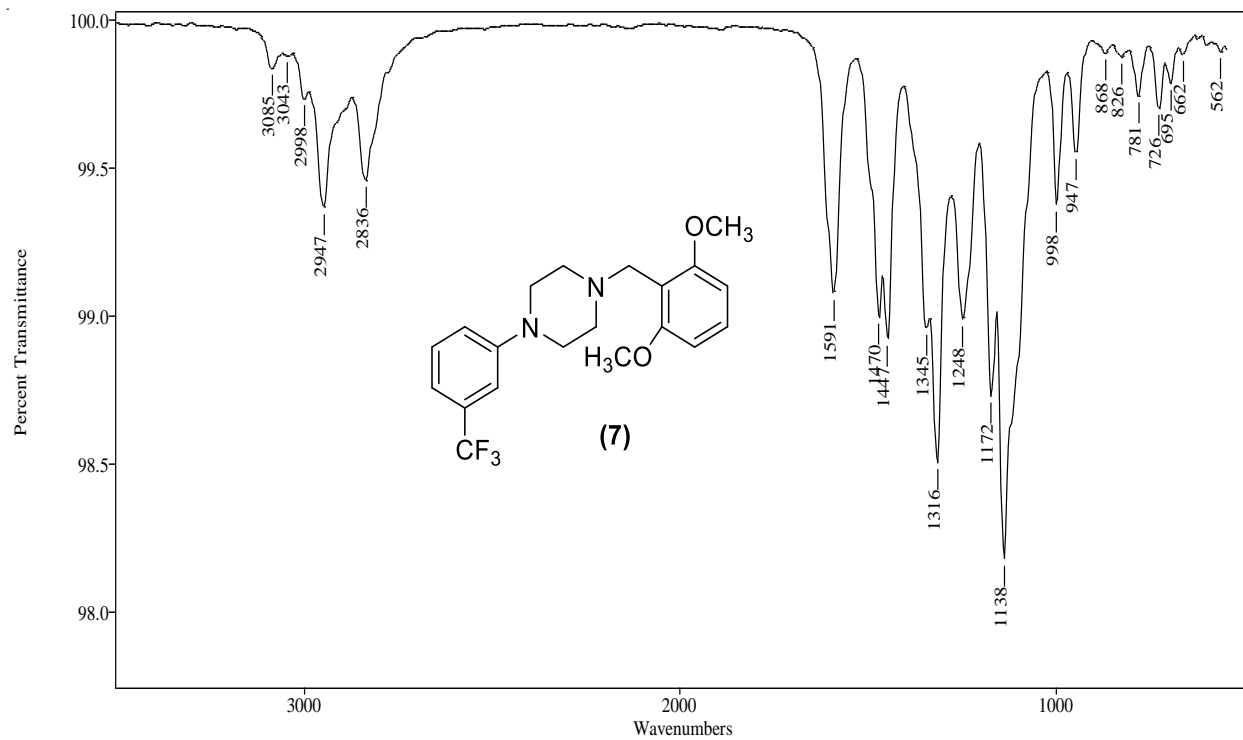
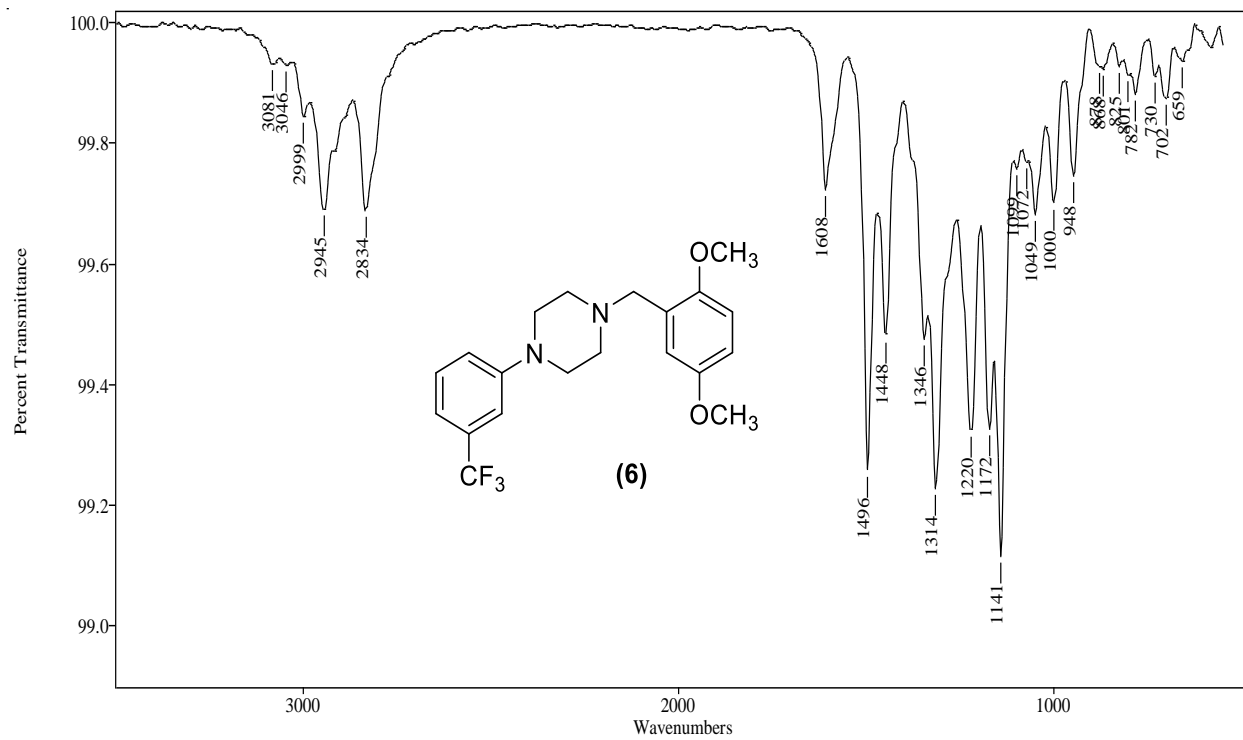
Figure 21. Gas chromatographic separation of 1-[N-dimethoxybenzyl]-4-[3-(trifluoromethyl)phenyl]piperazine using TP-3 program (Group 5)

3.5.3. Vapor-phase Infra-Red Spectrophotometry

The vapor phase infrared spectra for these six regioisomeric dimethoxybenzyl analogues of 3-TFMPP are shown in Figure (22). The absorption bands for the reference compound 3-TFMPP occurring at 1447 cm^{-1} , 1315 cm^{-1} and 1141 cm^{-1} serve as the anchoring points for evaluation of the six vpIR spectra in this series. The equivalent bands in the spectra in Figure () occur over a narrow range with the first band occurring between 1449 and 1447 cm^{-1} and the second from 1314 cm^{-1} to 1316 cm^{-1} and the third anchoring band at 1138 to 1141 cm^{-1} (the 3,5-isomer has a slightly higher absorption band at 1145 cm^{-1}). The two sterically crowded isomers, the 2,3- and 2,6-dimethoxy isomers yield a strong absorption just above the first anchoring band occurring at 1475 and 1470 cm^{-1} , respectively. The 2,5-, 2,4- and 3,4-isomers show this band at 1496 , 1499 and 1504 cm^{-1} , respectively. This absorption occurs as a shoulder band at 1492 cm^{-1} for the 3,5-dimethoxy isomer. The pattern, position and relative intensities of bands on either side of the second (1314 cm^{-1} to 1316 cm^{-1}) and third (1138 cm^{-1} to 1141 cm^{-1}) major anchoring bands provide fingerprint-style information for further correlation with specific dimethoxy substitution patterns. The less intense bands on the high side of each of these major bands is again consistent with the pattern of the monosubstituted model compound 3-TFMPP. For example, these accompanying less intense shoulder bands occur at 1346 cm^{-1} and 1172 cm^{-1} for the 2,5-dimethoxybenzyl analogue. This 2,5-isomer has an additional strong band at 1220 cm^{-1} and the 2,6-isomer is the only other analogue with a band of similar relative intensity centered at 1248 cm^{-1} in this case. Three of these isomers have an aromatic carbon-carbon double bond stretching vibration in the 1600 cm^{-1} region of intensity similar to the first anchoring band at 1448 cm^{-1} . These isomers are the 2,6-, 2,4- and 3,5-dimethoxybenzyl analogues and all three have the two methoxy groups arranged *meta* to each

other, furthermore, the other three isomers do not yield a corresponding band in the 1600 cm^{-1} region approaching the intensity of the first anchoring absorption band.





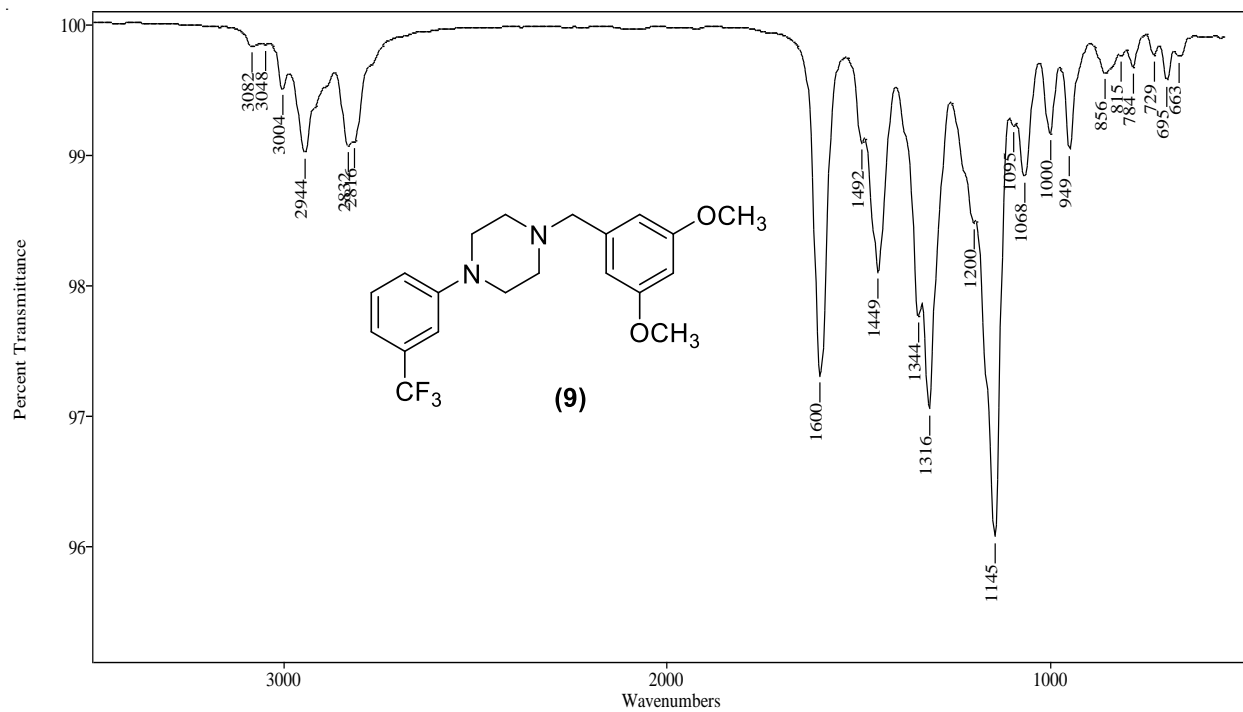
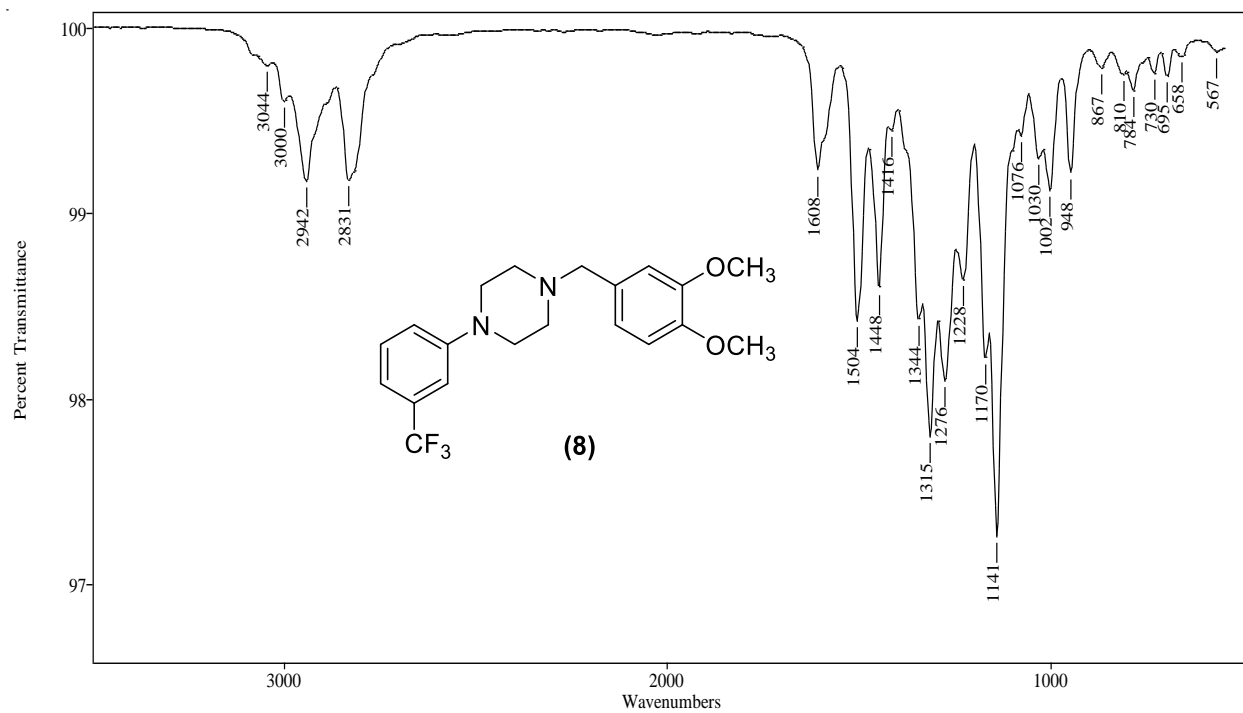


Figure 22. Vapor phase IR spectra of 1-[N-dimethoxybenzyl]-4-[3-(trifluoromethyl)phenyl]piperazine (Group 5)

3.5.4. Conclusions

The major EI-MS fragment ions occur via processes initiated by one of the two nitrogen atoms of the piperazine ring. The ion at m/z 229 observed in all six spectra occurs from the loss of the substituted benzyl radical and the m/z 56 cation (C_3H_6N)⁺ is a characteristic piperazine ring fragment. These dimethoxybenzyl groups provide unique and specific modifications and additions for the strong vpIR anchoring bands of the reference compound 3-TFMPP. These structure-vpIR relationships coupled with the EI-MS vs regioisomeric structure relationships provide complete differentiation for each of these *N,N*-disubstituted piperazine analogues. The unique EI-MS fragments for the 2,3-dimethoxybenzyl- and 3,5-dimethoxybenzyl isomers at m/z 136 and m/z 152, respectively set apart these two compounds. The very strong aromatic ring absorptions in the vpIR at 1608 cm⁻¹ and 1591 cm⁻¹ provide differentiation for the 2,4- and 2,6-dimethoxybenzyl analogues, respectively. The 2,5-dimethoxybenzyl isomer can be identified by the strong band at 1496 cm⁻¹ with an accompanying unique strong band at 1220 cm⁻¹ and the 3,4-isomer is characterized by the 1504 cm⁻¹ band and the triplet absorption pattern at 1344/1315/1276 cm⁻¹. These observations of uniqueness in the vpIR spectrum of each isomer coupled with the general pattern of common EI-MS fragments provide identifying data for each regioisomeric member of this dimethoxybenzyl-3-TFMPP series.

3.6. Analysis of 1-[N-(bromo-dimethoxy)benzyl]-4-[3-(trifluoromethyl)phenyl]piperazine (Group 6)

Seven regioisomeric compounds in this group where the bromo-dimethoxy substitution pattern of the benzyl ring was varied and constant trifluoromethyl group on the meta position of phenylpiperazine ring Figure (23). The only difference between these regioisomers is the position of bromo-dimethoxy substitution on the benzylic side. The mass spectra for these seven compounds did not show characteristic ion fragments for specific identification. Therefore, gas chromatographic separation coupled with infrared detection (GC-IRD) were used to provide direct confirmatory data for structural differentiation between the seven regioisomers. The mass spectrum combined with the vapor phase infrared spectrum provides specific confirmation for regioisomeric piperazines. The bromo dimethoxy piperazines derivatives were resolved on a 30-meter capillary column containing an Rxi®-17Sil MS stationary phase.

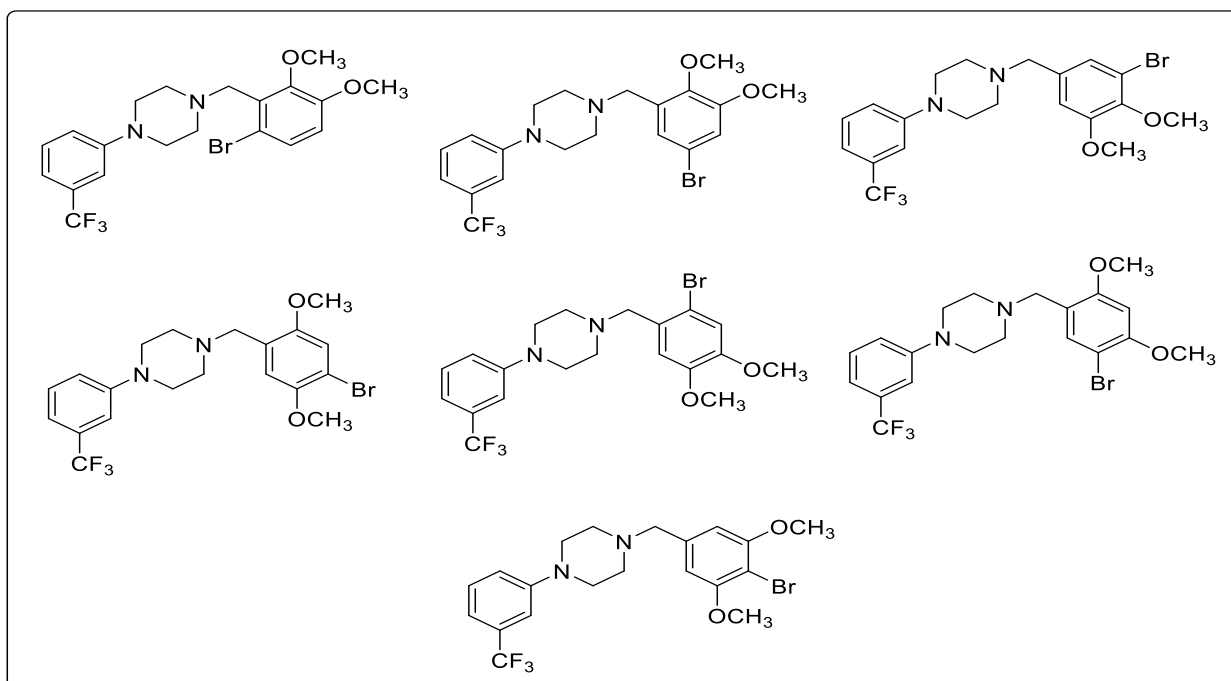
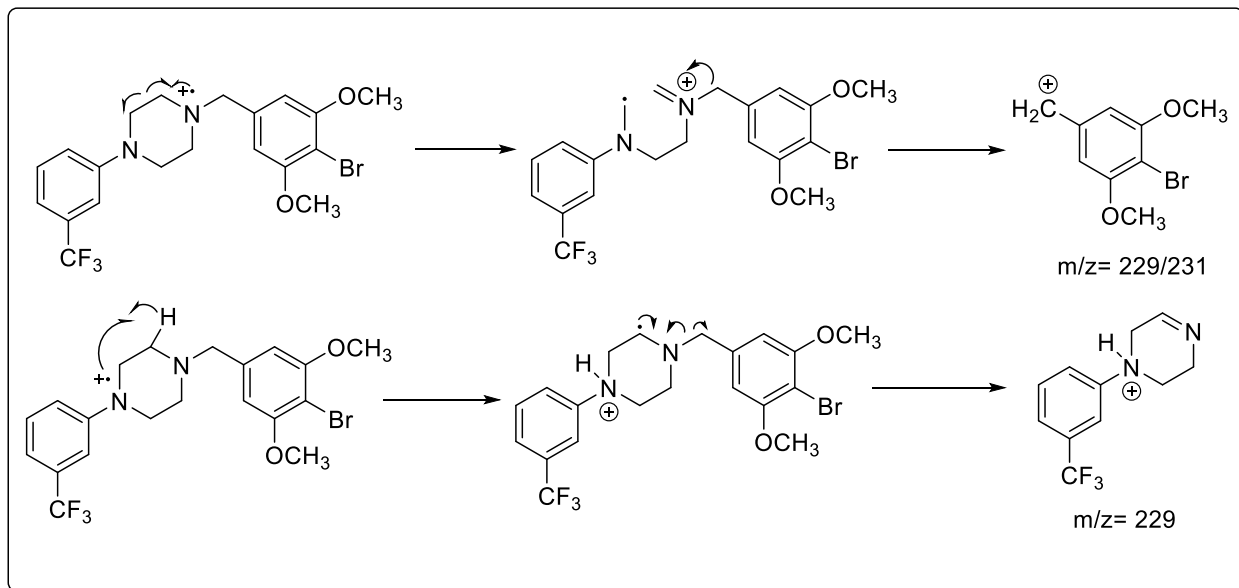


Figure 23. 1-[N-(bromo-dimethoxy benzyl) - 4-[3-(trifluoromethyl)phenyl]piperazine compounds

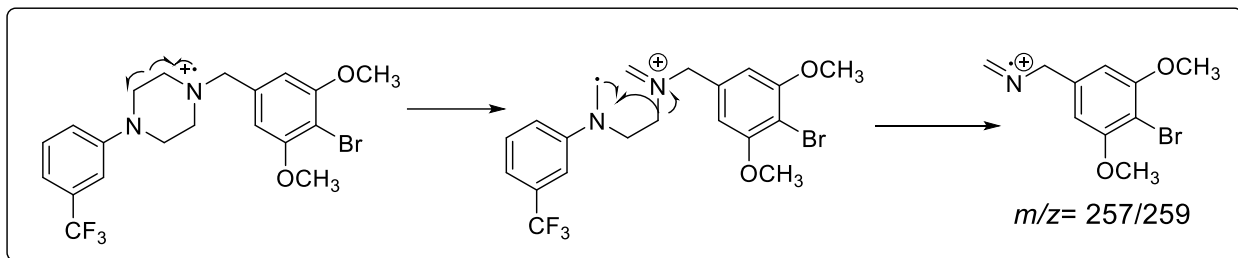
3.6.1. Mass spectral studies

Mass spectrometry is the primary analytical method for confirming the identity of drugs in forensic laboratories. Figure (24) shows the EI mass spectra of all regioisomers belong to this group. The seven regioisomers of N-(bromo-dimethoxy) benzyl-3-TFMP have almost identical mass spectra which may lead to misidentification in forensic samples. The dominant ions in EI-MS spectrum for these compounds detected at m/z 229, 259, and the characteristic molecular ion of piperazine ring at m/z 56. The base peak ion for most regioisomers is m/z 229 the which can be formed by breaking the N-C bond to produce two species the 3-trifluoromethylphenyl-piperazine cation and m/z 229/231 bromo dimethoxybenzylic cation Scheme (27)



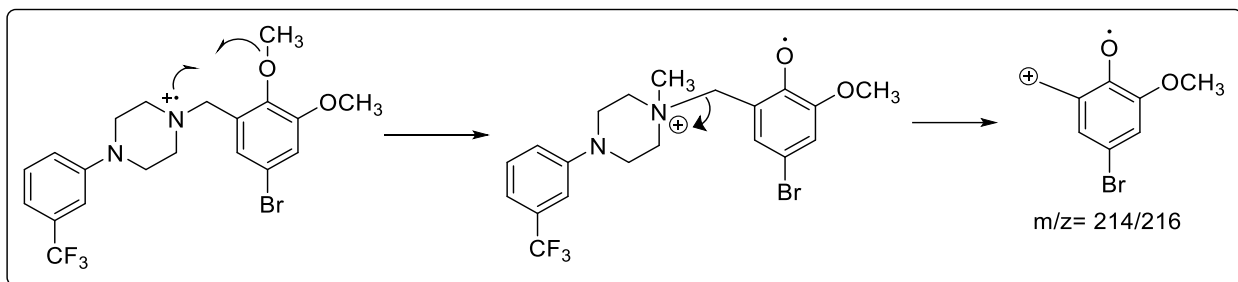
Scheme 27. Mechanism for the formation of the base peak at m/z 229

While the base peak for 6-Bromo-2,3-isomer and 5-Bromo-2,3-isomer is the characteristic piperazine fragment at m/z 56. The fragment ion at m/z 257/259 is bromine isotope based produced by cleavage of N-C bond to yield a species with two atoms of the piperazine ring Scheme (28).



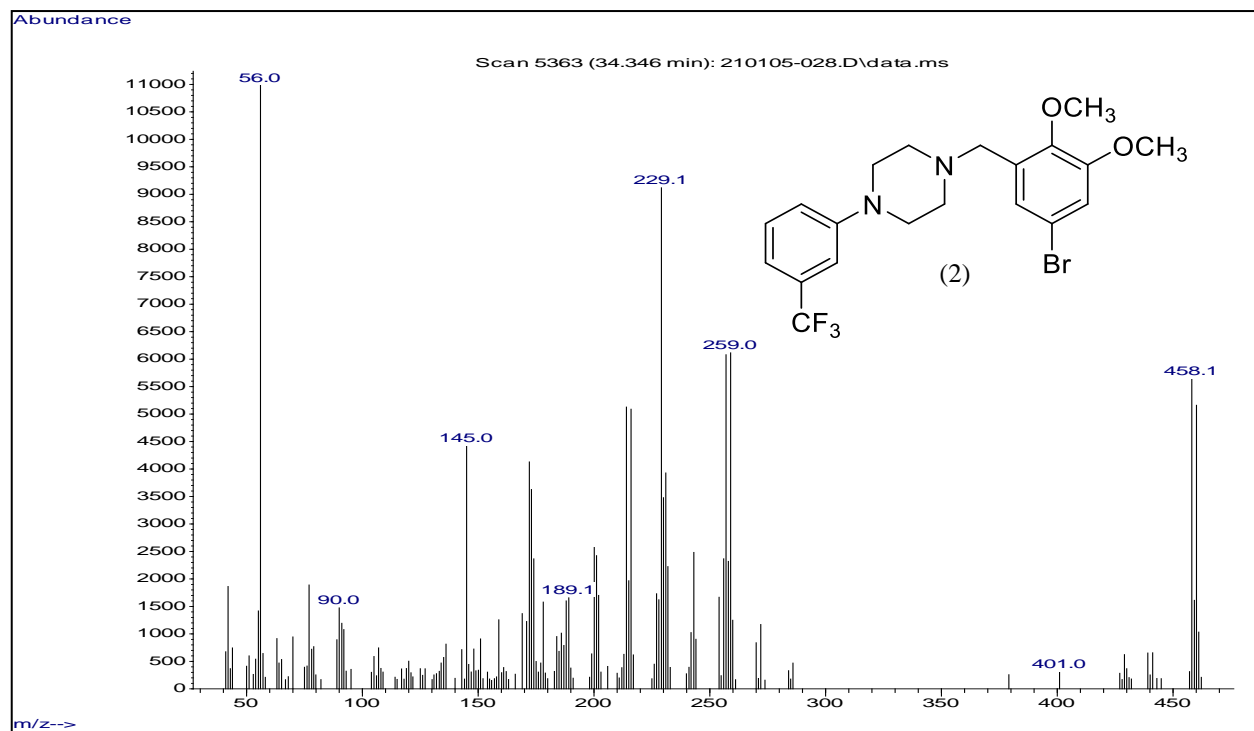
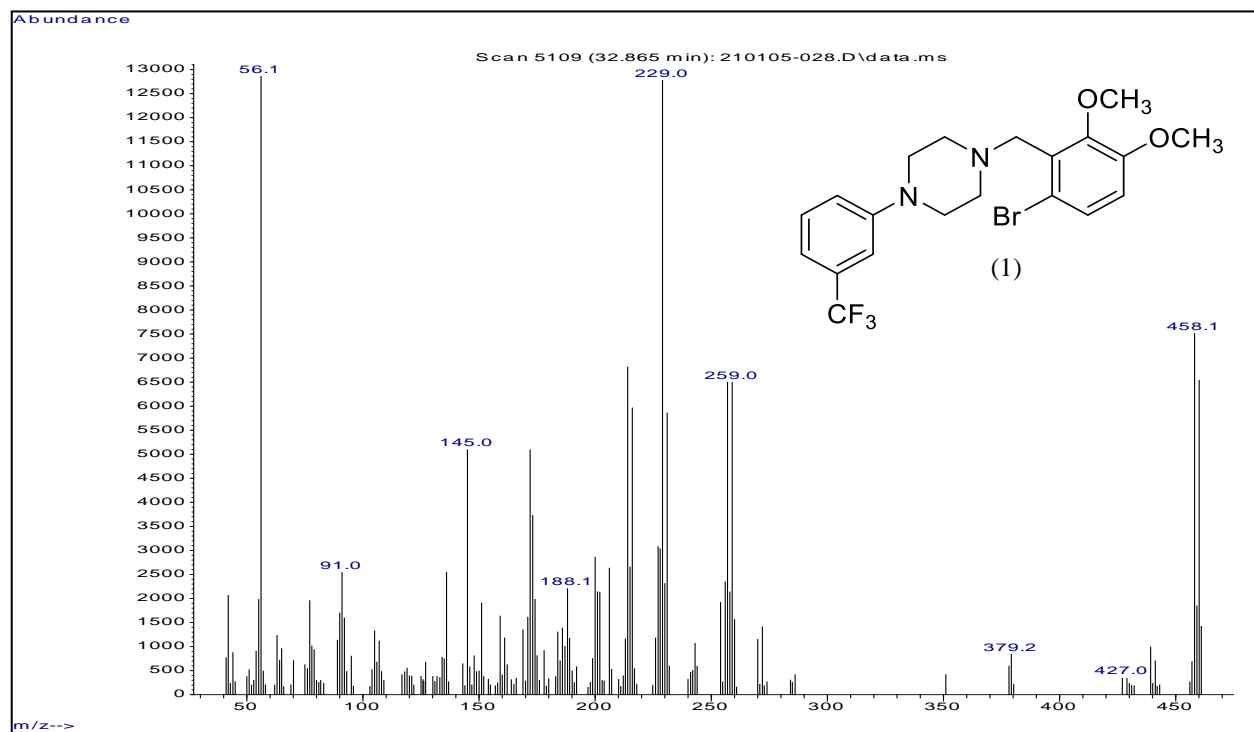
Scheme 28. Mechanism for the formation of the fragment m/z 257/259

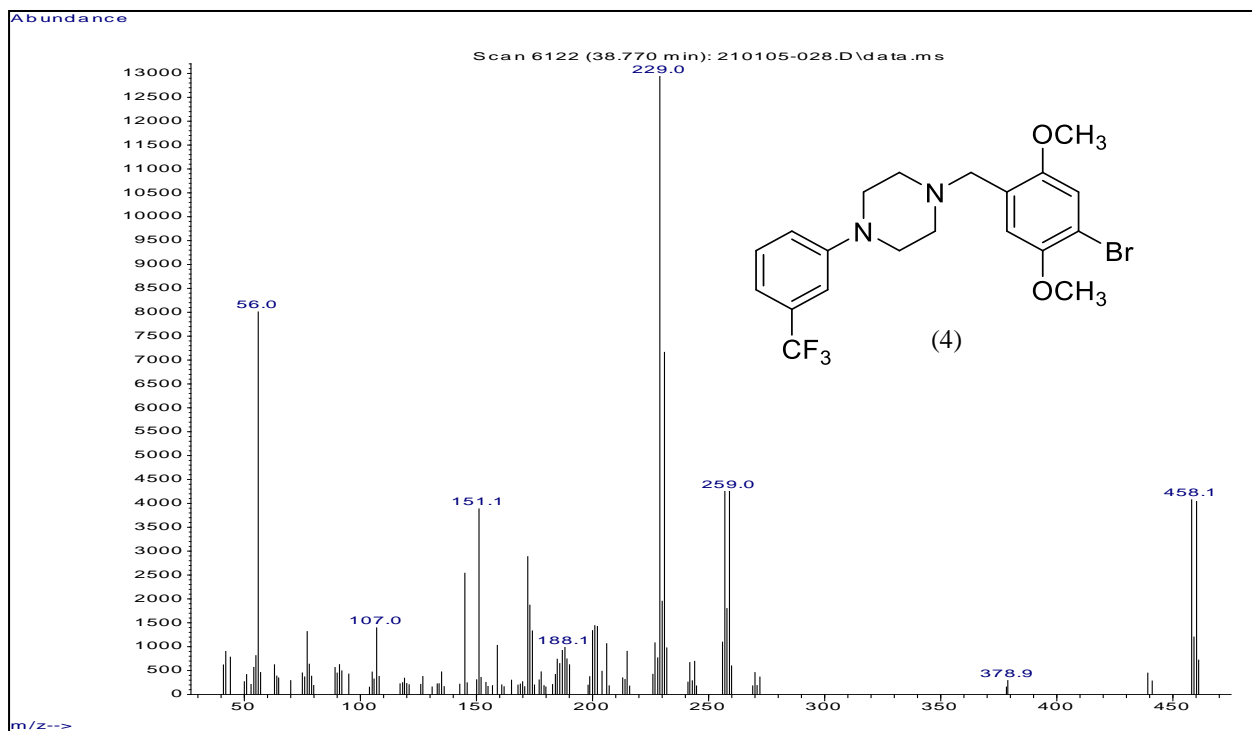
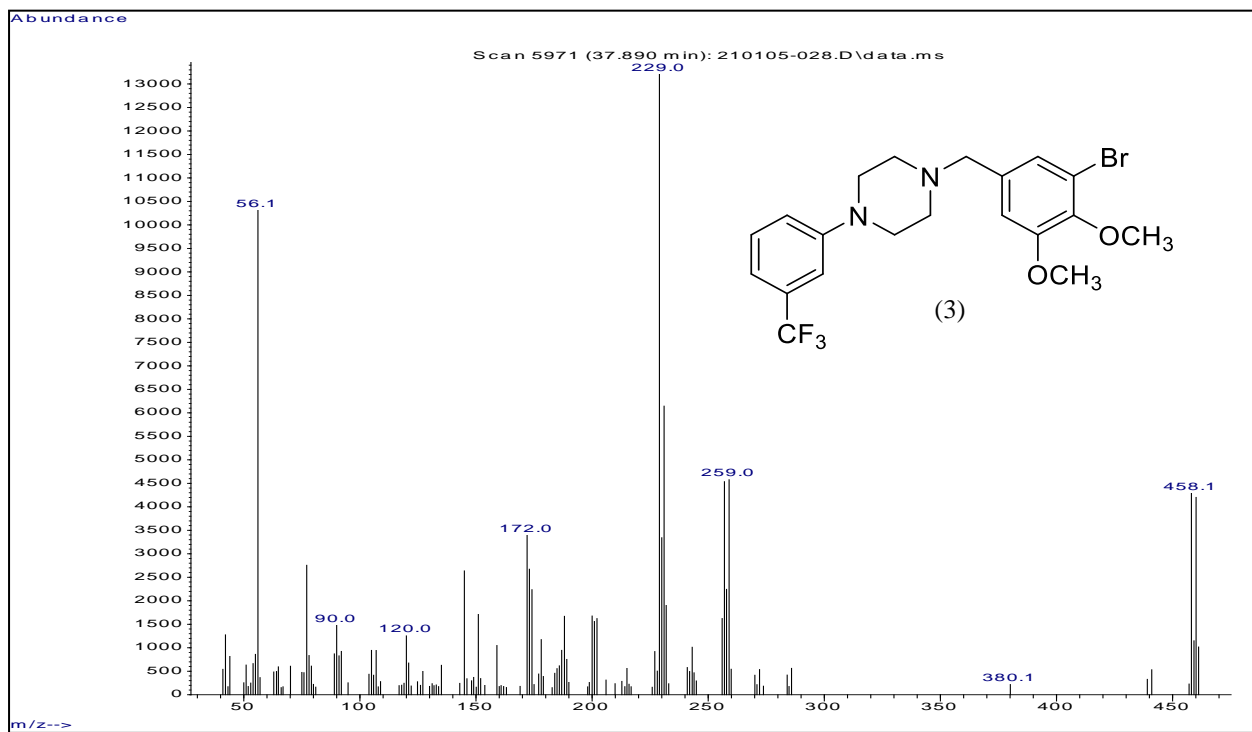
Similarly, the radical cation fragment at m/z 214/216 the Scheme (29) shows the proposed mechanism for this fragment.

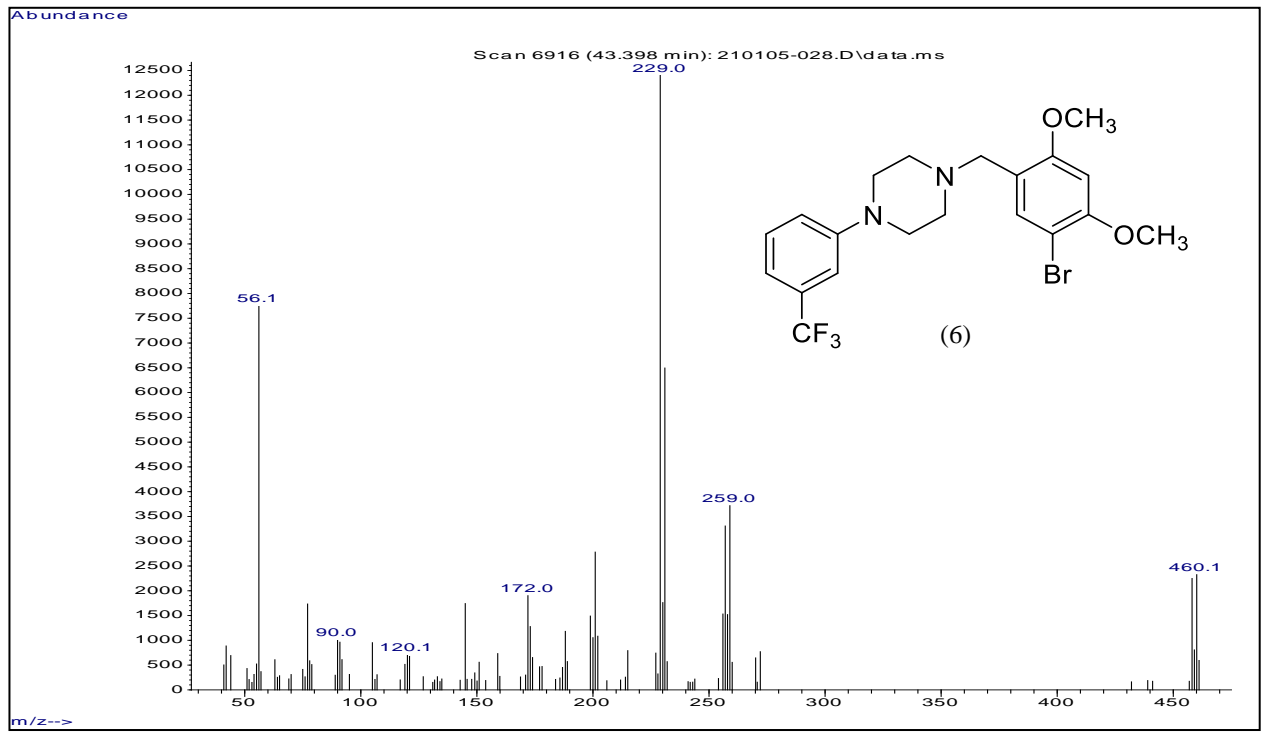
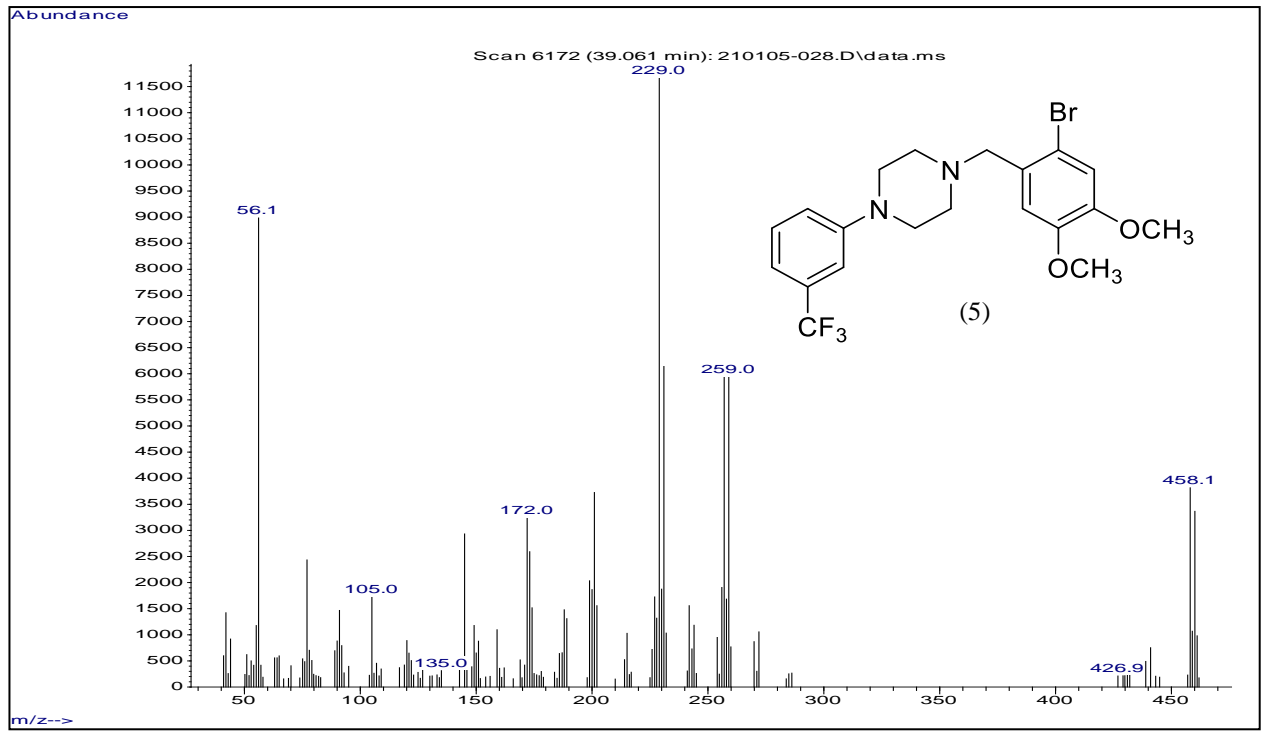


Scheme 29. Mechanism for the formation of the fragment m/z 214/216

Other fragments of this set of compounds include 90, 91, 105, 121, 145, 172, 173 as well as other ions with low relative abundance. The product ion m/z 145 is trifluoromethyl-phenyl cation which produced from parent ion m/z 229 found with high abundant in compound (1) and (2). Another common fragments at m/z 172 and 173 are composed of the substituted phenyl ring with two atoms of piperazine ring. The proposed fragments structures of this group are shown in Scheme (29).







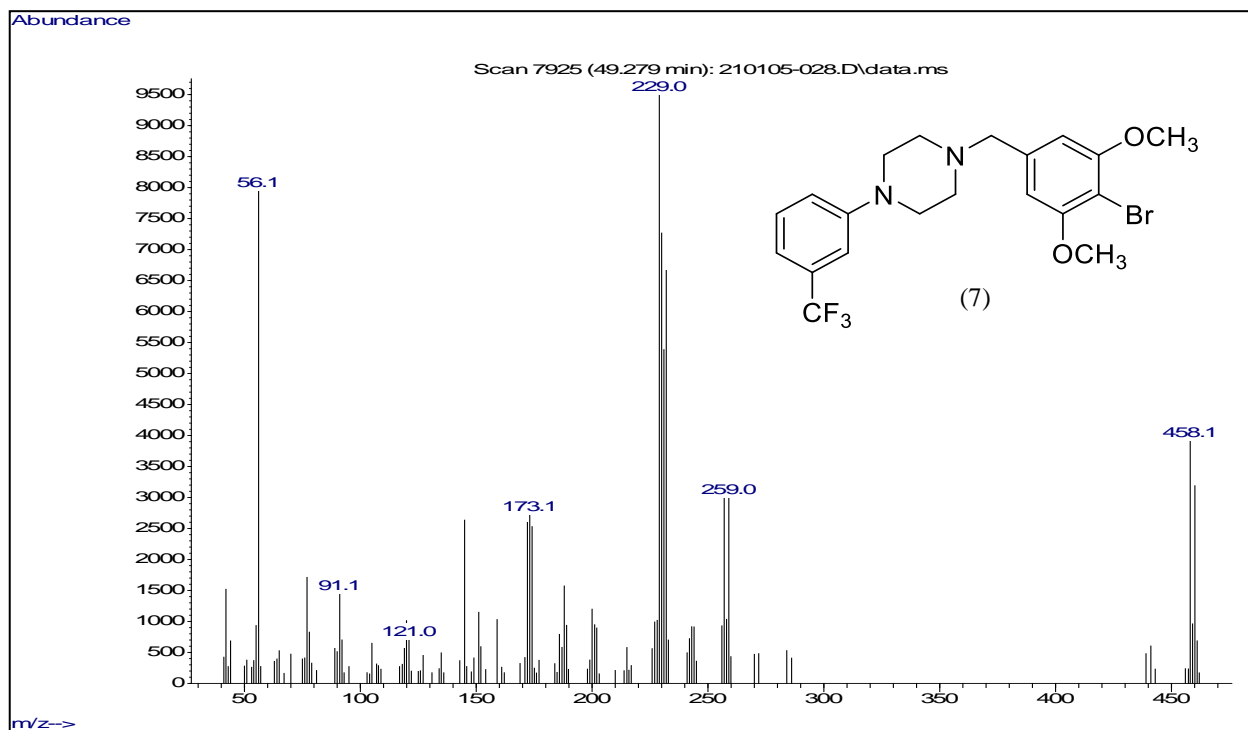
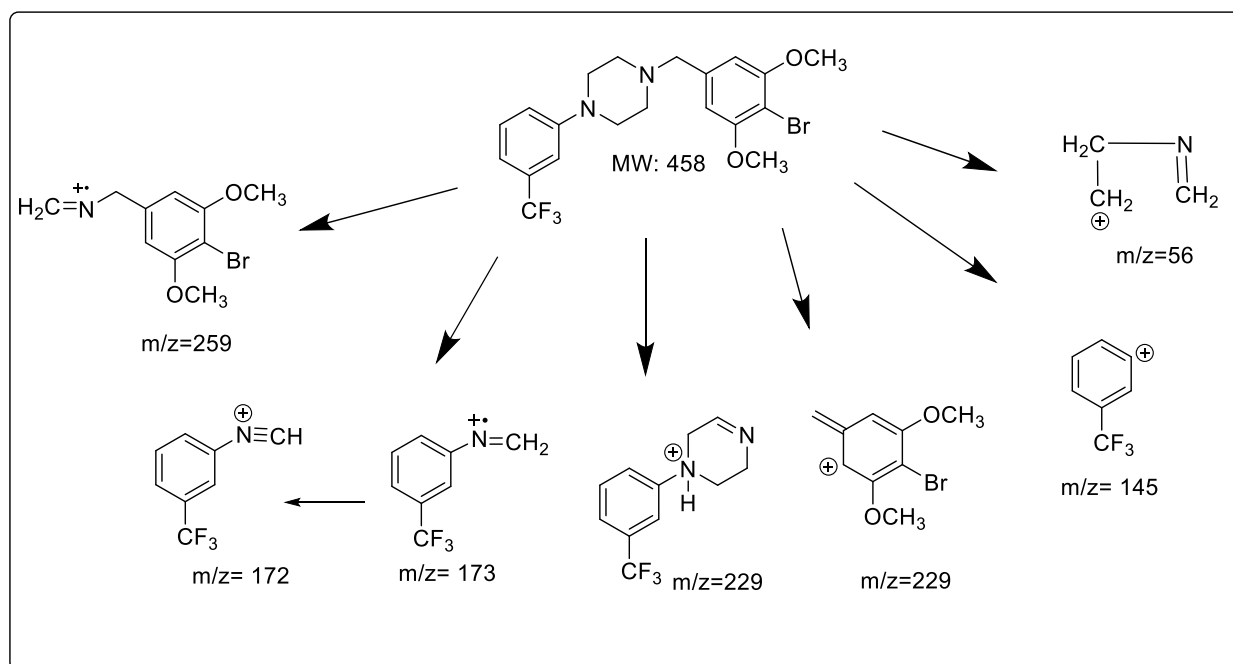


Figure 24. EI mass spectra of 1-[N-(bromo-dimethoxy)benzyl]-4-[3-(trifluoromethyl)phenyl]piperazine (Group 6)



Scheme 26. EI mass spectral fragmentation pattern of 1-[N-(bromo-dimethoxy)benzyl]-4-[3-(trifluoromethyl)phenyl]piperazine (Group 6)

3.6.2. Gas Chromatographic Separation

For better identification for the of 1-[N-(bromo-dimethoxybenzyl)-4-[3-(trifluoromethylphenyl) piperazine regioisomers, gas chromatographic separations were performed. The seven compounds of N-(bromo-dimethoxybenzyl)-3-TFMPP differ in the bromo-dimethoxy substitution on the benzylic side side. Gas chromatographic separation of the seven compounds was carried out using a 30-meter capillary column coated with a 0.50 μm film of Rxi®-17Sil MS, a midpolarity phase: similar to 50% phenyl, 50% dimethyl polysiloxane. The compounds elute over approximately 18 minutes window requiring a total run time of just over 58.0 minutes. The 1[-6-(Bromo-2,3dimethoxybenzyl-4-[3-(trifluoromethyl phenyl piperazine) elutes first, followed by 5-Br-2,3-dimethoxy isomer, and lastly 4-Br-3,5- dimethoxy isomer respectively as shown in Figure (25). The tow isomers 4-Br-2,5-dimethoxy and 2-Br-4,5- dimethoxy are critical base pair and sharing same substitution in positions 2, 4, and 5.

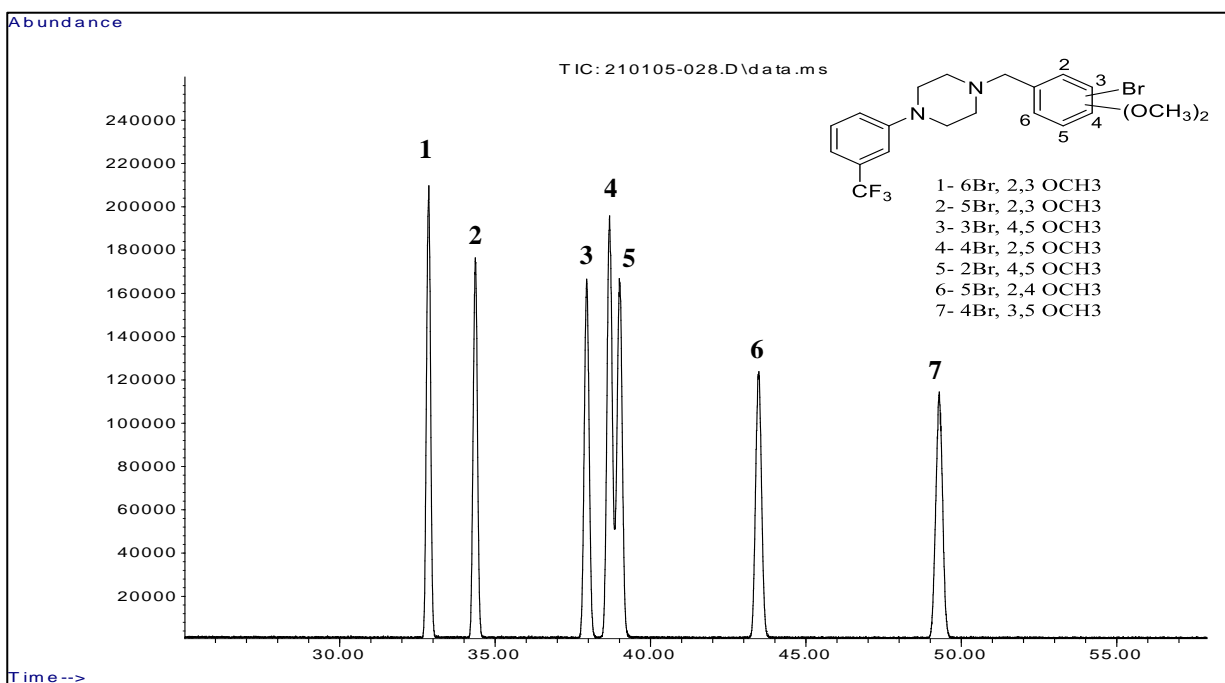


Figure 25. Gas chromatographic separation of 1-[N-(bromo-dimethoxy)benzyl-4-[3-(trifluoromethyl)phenyl]piperazine (Group 6) on (Rxi®-17Sil MS) using TP-4 program

Another chromatogram was accomplished on a capillary column 30 m × 0.25 mm i.d. coated with 0.50 μm of 5% diphenyl and 95% dimethyl polysiloxane (Rtx-5), Figure (26). The (Rtx-5) shows lower retention time and almost same elution order of previous Rxi®-17Sil MS, except for the 2-Br-4,5- and 4-Br-2,5-dimethoxybenzyl isomer, the 2-Br-4,5-dimethoxybenzyl isomer elutes before the 4-Br-2,5-isomer in as shown in Figures (25-26). The compounds elute over approximately 2.5 minutes window using total run time of just over 49.0 minutes. The tow isomers 3-Br-4,5-dimethoxy and 2-Br-4,5- dimethoxy are critical base pair and sharing same substitution in positions 4 and 5.

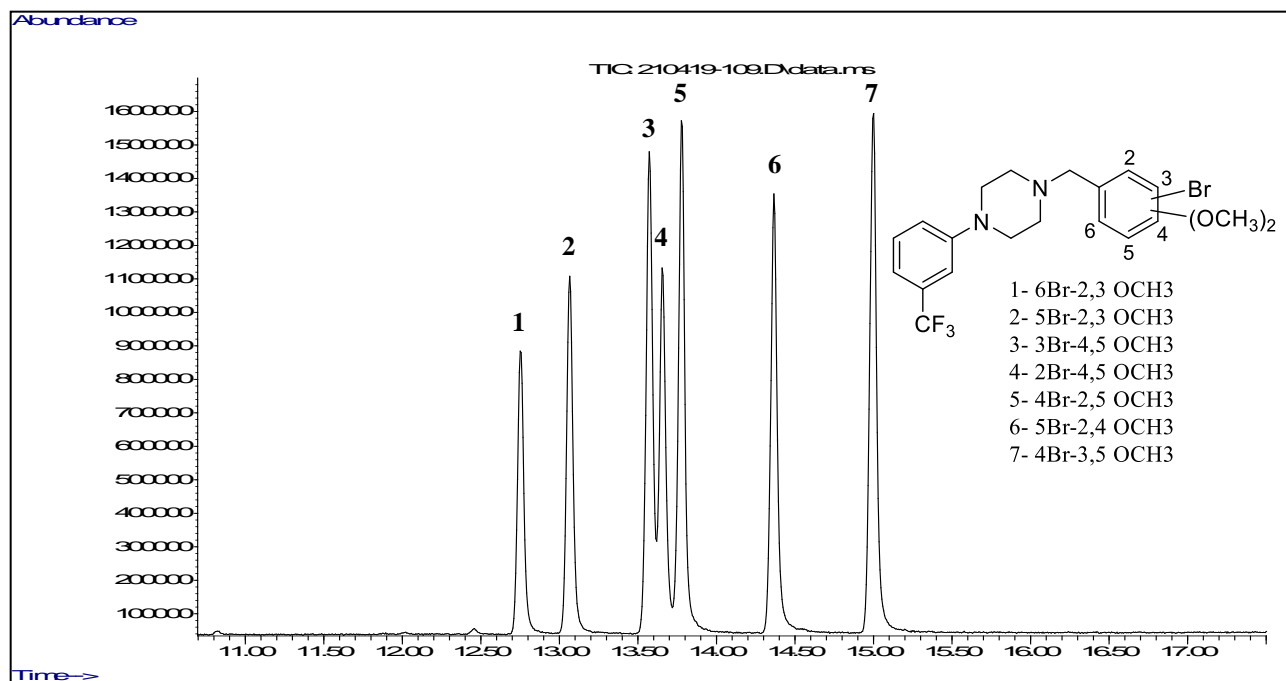
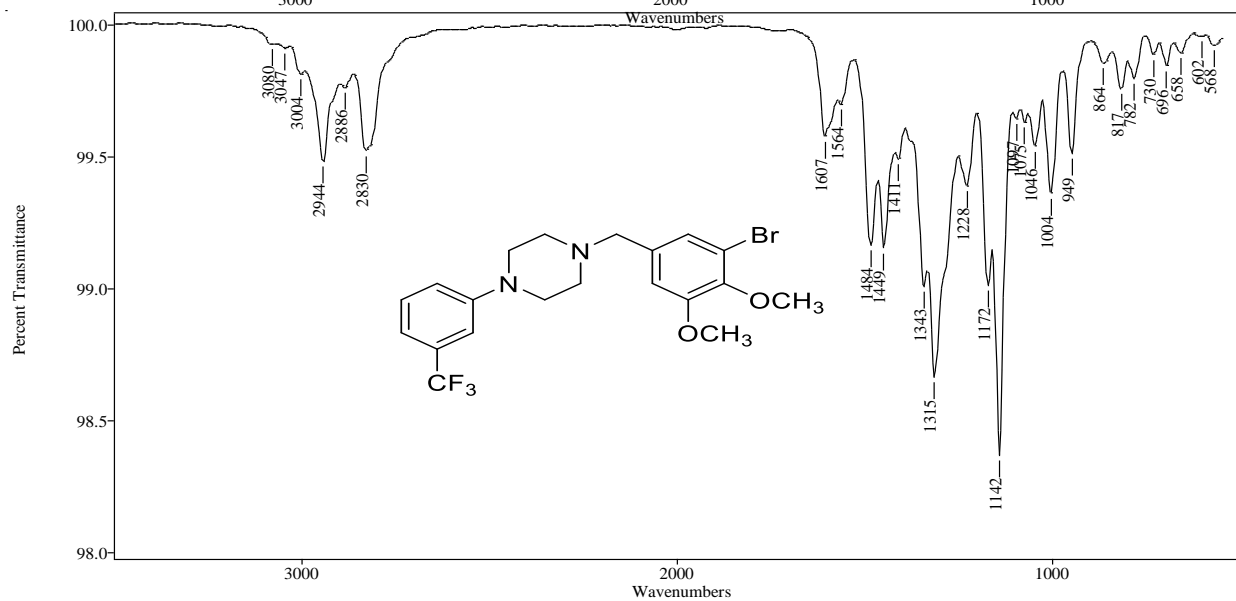
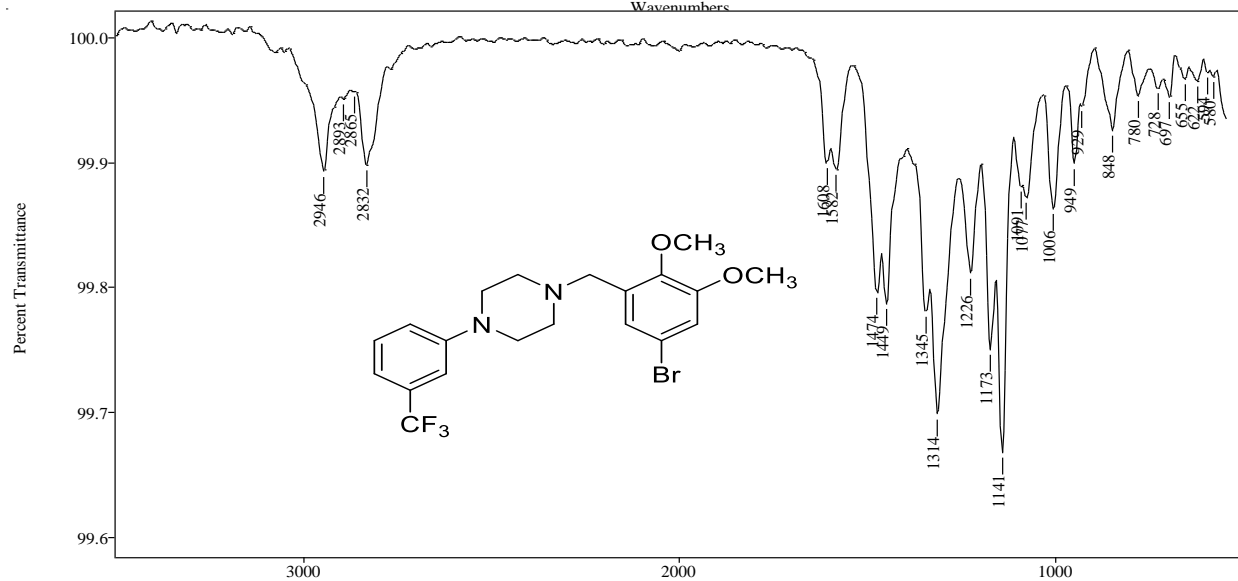
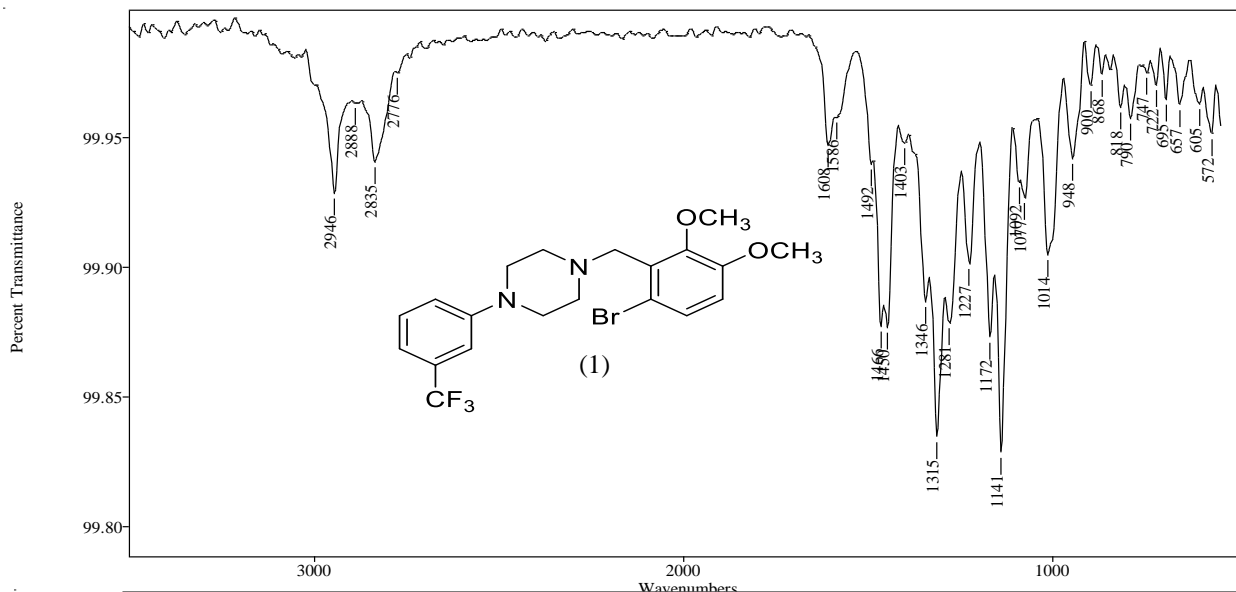
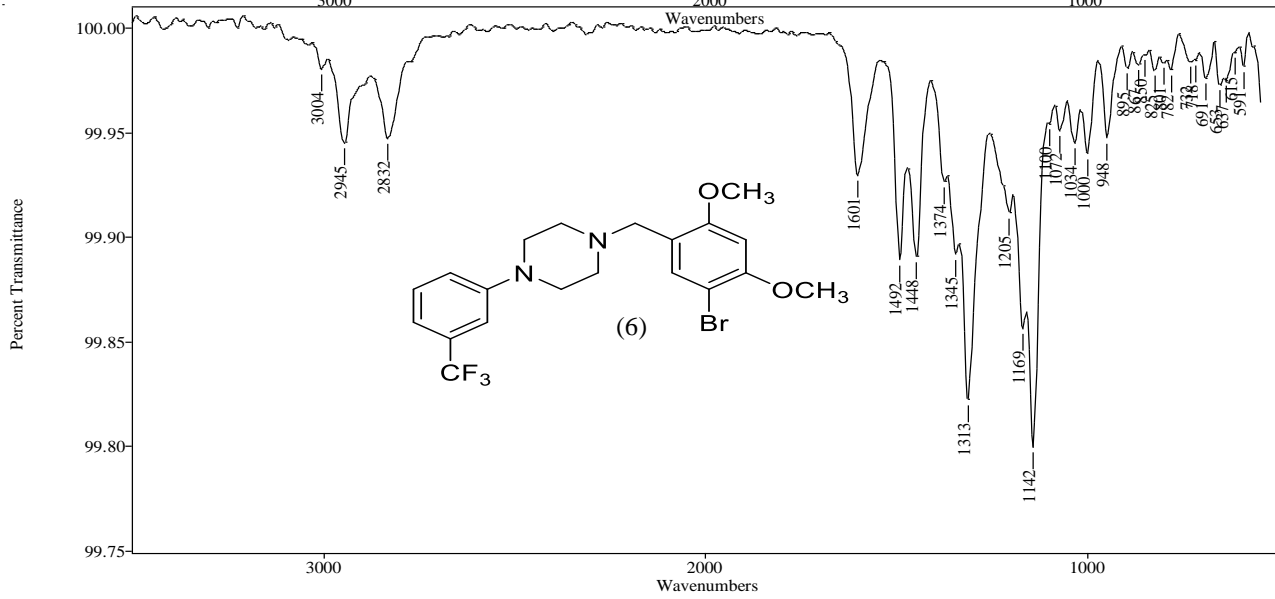
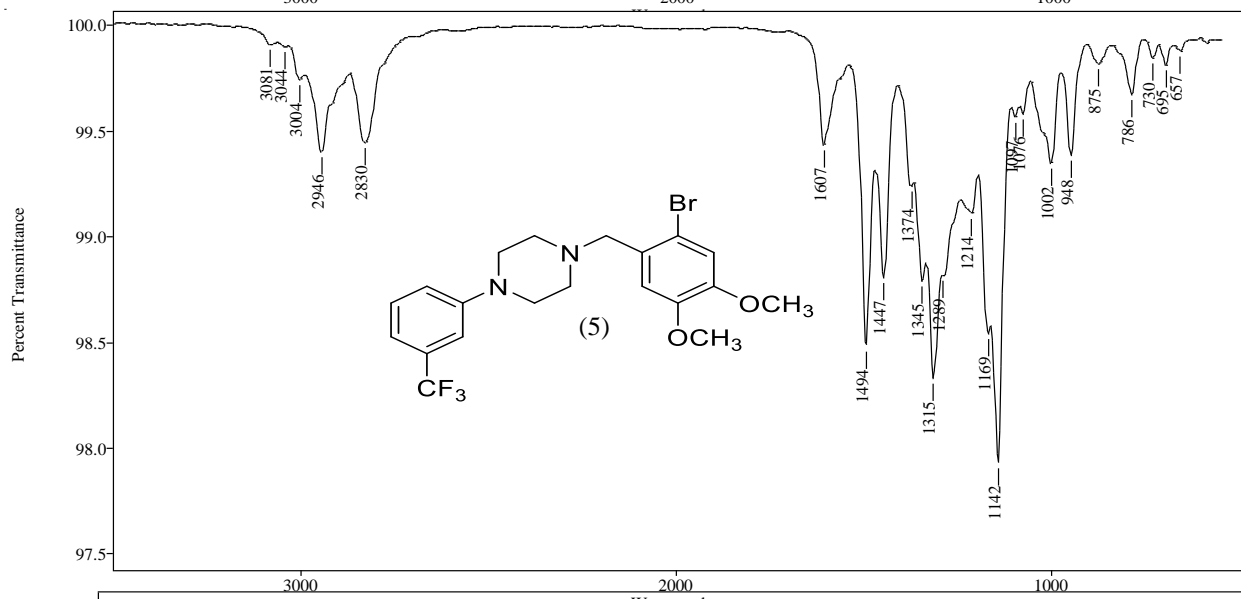
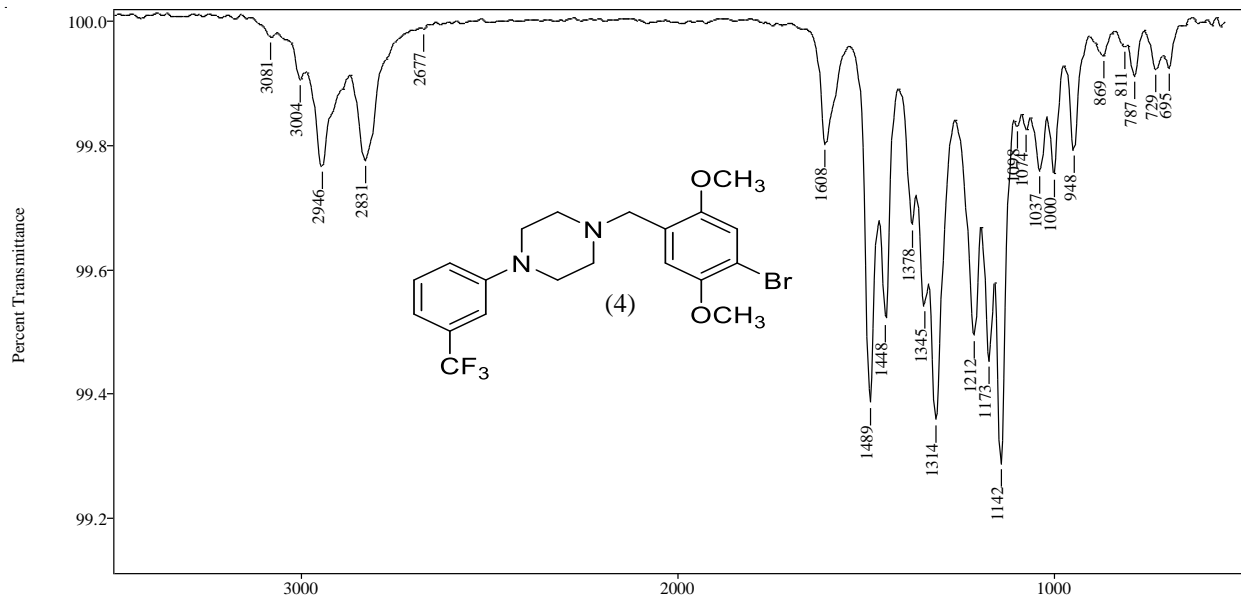


Figure 26. Gas chromatographic separation of 1-[N-(bromo-dimethoxy)benzyl-4-[3-(trifluoromethyl)phenyl]piperazine (Group 6) Rtx-5 using TP-3 program

3.6.3. Vapor-phase Infra-Red Spectrophotometry

In forensic drug analysis, the Infra-Red Spectrophotometry tool is used to provide compounds identification specificity. Gas-chromatography coupled infrared detection (GC-IRD) was performed to differentiate between the seven regioisomers of this group Figure (27). The N-(bromo-dimethoxy) benzyl-3-TFMP regioisomers display vapor phase IR spectrum with transmittance bands in the regions $550 - 1620 \text{ cm}^{-1}$ and $2710 - 3250 \text{ cm}^{-1}$. All seven regioisomers have almost similar absorption bands in the region $2710 - 3250 \text{ cm}^{-1}$. The isomer 6-Br-2,3-dimethoxy has broad triple absorption bands in the region 1281 cm^{-1} , 1315 cm^{-1} , and 1345 cm^{-1} . The 5-Br-2,3-isomer characterized by presence low intensity doublet band at 1582 cm^{-1} and 1608 cm^{-1} . While 3-Br-4,5-dimethoxy isomer has a sharp absorption band at 1142 cm^{-1} , with equal intensity double bands at 1449 and 1484 cm^{-1} . The isomer 4-Br-2,5-dimethoxy has also broad triple bands but in the region 1142 cm^{-1} , 1173 cm^{-1} , and 1212 cm^{-1} . The 4-Br-3,5-dimethoxy isomer has a single absorption band at 1450 cm^{-1} , while the rest of compounds are displaying double bands in the region 1449 cm^{-1} and 1490 cm^{-1} . In the same region the 5-Br-2,4-dimethoxy isomer has almost identical double band with medium intensity, but the 3-Br-4,5-dimethoxy has low intensity double bands.





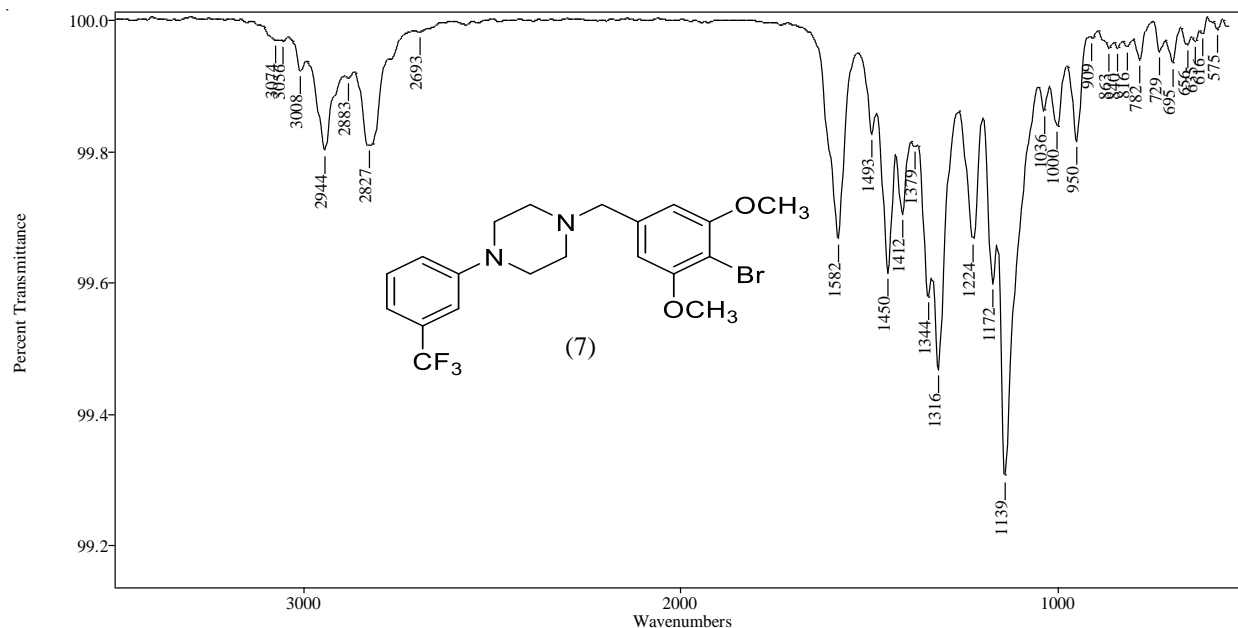


Figure 27. Vapor phase IR spectra of 1-[N-(bromo-dimethoxy)benzyl]-4-[3-(trifluoromethyl)phenyl]piperazine (Group 6)

3.6.4. Conclusions

The major EI-MS fragment ions occur via processes initiated by one of the two nitrogen atoms of the piperazine ring. The ion at m/z 229 observed in all seven spectra occurs from the loss of the substituted benzyl radical and the m/z 56 cation (C_3H_6N)⁺ is a characteristic piperazine ring fragment. The EI-MS fragments for the bromo-dimethoxy isomers did not show significant fragment ions that could be used for differentiation among them. However, the vpIR analysis affords some characterization absorption bands that can be utilized in the differentiation between the regioisomers in this group. The isomer 6-Br-2,3-dimethoxy has broad triple absorption bands in the region 1281 cm⁻¹, 1315 cm⁻¹, and 1345 cm⁻¹. The 5-Br-2,3-isomer is characterized by presence of a low intensity doublet band at 1582 cm⁻¹ and 1608 cm⁻¹. While the 3-Br-4,5-dimethoxy isomer has a sharp absorption band at 1142 cm⁻¹, with equal intensity double bands at 1449 and 1484 cm⁻¹. The

isomer 4-Br-2,5-dimethoxy has also broad triple bands but in the region 1142 cm^{-1} , 1173 cm^{-1} , and 1212 cm^{-1} .

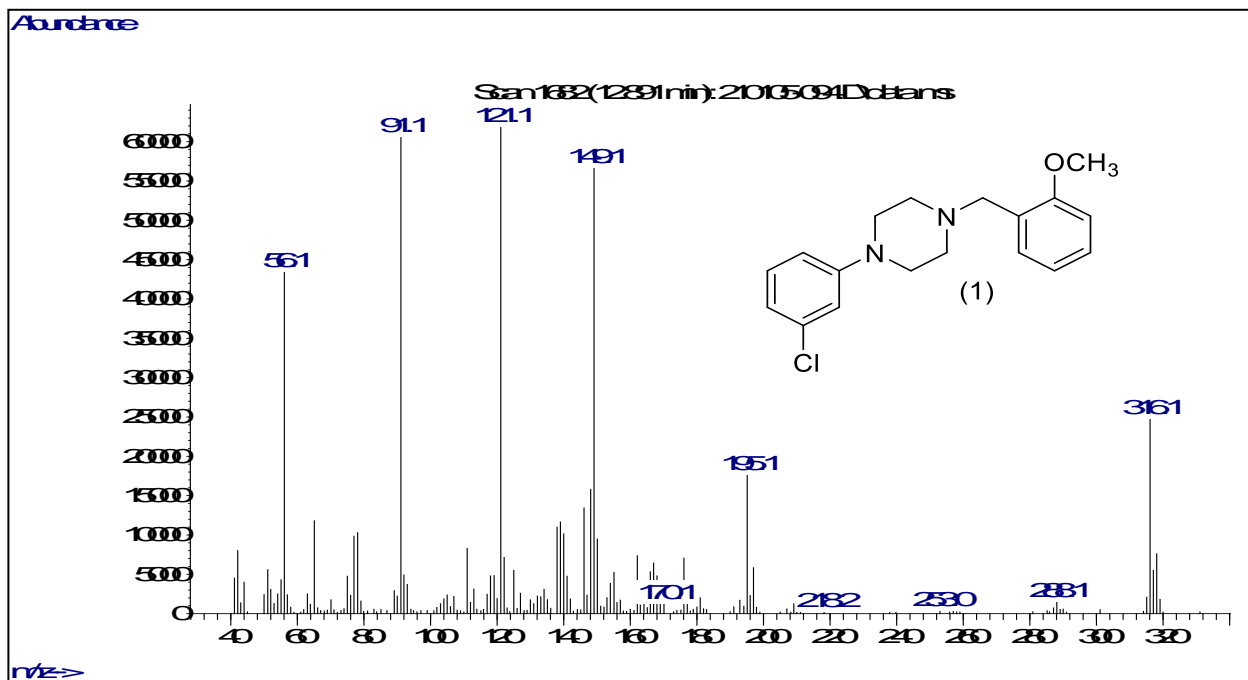
3.7. Analysis of 1-(3-chlorophenyl)-4-[(N-methoxybenzyl)piperazine (Group 7)

The compounds in this group are hybrid analogues containing the structural fragments of 1-[3-(chlorophenyl)] piperazine (3-CIPP) and methoxy benzylpiperazines in a single molecule. Three regioisomers of monomethoxybenzyl-3-chloro phenyl piperazine have identical mass spectra with almost equivalent fragments. They are only differed in the position of methoxy substitution on the benzylic group. The mass spectra for these three regioisomers did not show characteristic ion fragment for specific identification. Therefore, gas chromatographic separation coupled with infrared detection (GC-IRD) were used to provide direct confirmatory data for structural differentiation between the three regioisomers. The three regioisomers piperazines derivatives were resolved on a 30-meter capillary column containing an Rxi®-17Sil MS stationary phase.

3.7.1. Mass spectral studies

The electron ionization (EI) mass spectra for these three regioisomers are shown in Figure (28). These compounds have similar major fragment ions. However, there are some differences in relative intensity of ions which could be used for to differentiate between these regioisomers. The proposed structures for the major fragment ions are summarized in Scheme (31). The base peak at m/z 121 cation can form in a direct manner via initial ionization of the methoxybenzyl aromatic ring via loss of the 3-chlorophenylpiperazine radical species yielding the methoxybenzyl cation. Further loss of formaldehyde from this species yields the m/z 91 unsubstituted benzyl cation

fragment. All the three regioisomers lose the methoxybenzyl radical to yield the 3-chlorophenyl-piperazine cation at m/z 195. The fragmentation of the piperazine ring from the nitrogen bearing the methoxybenzyl group yields the methoxybenzyl iminium-type radical cation at m/z 149. The m/z 56 ion is a characteristic fragment observed in most mono and disubstituted piperazine compounds originating from the atoms of the piperazine ring (C_3H_6N)⁺. The 2-methoxybenzyl regioisomer has the product ion at m/z 91 as most abundant fragment, while in 3-methoxybenzyl isomer the m/z 91 has lower relative abundance and is much less significant for the 4-methoxybenzyl isomer. The 3-methoxybenzyl isomer yields a significant 3-methoxybenzyl radical cation at m/z 122 compared to either the 2- or 4-methoxybenzyl isomers. Thus, the very intense m/z 91 ion in the 2-methoxybenzyl isomer and the intense m/z 122 for the 3-methoxybenzyl isomer provides some data for the direct EI-MS differentiation of these three isomeric compounds.



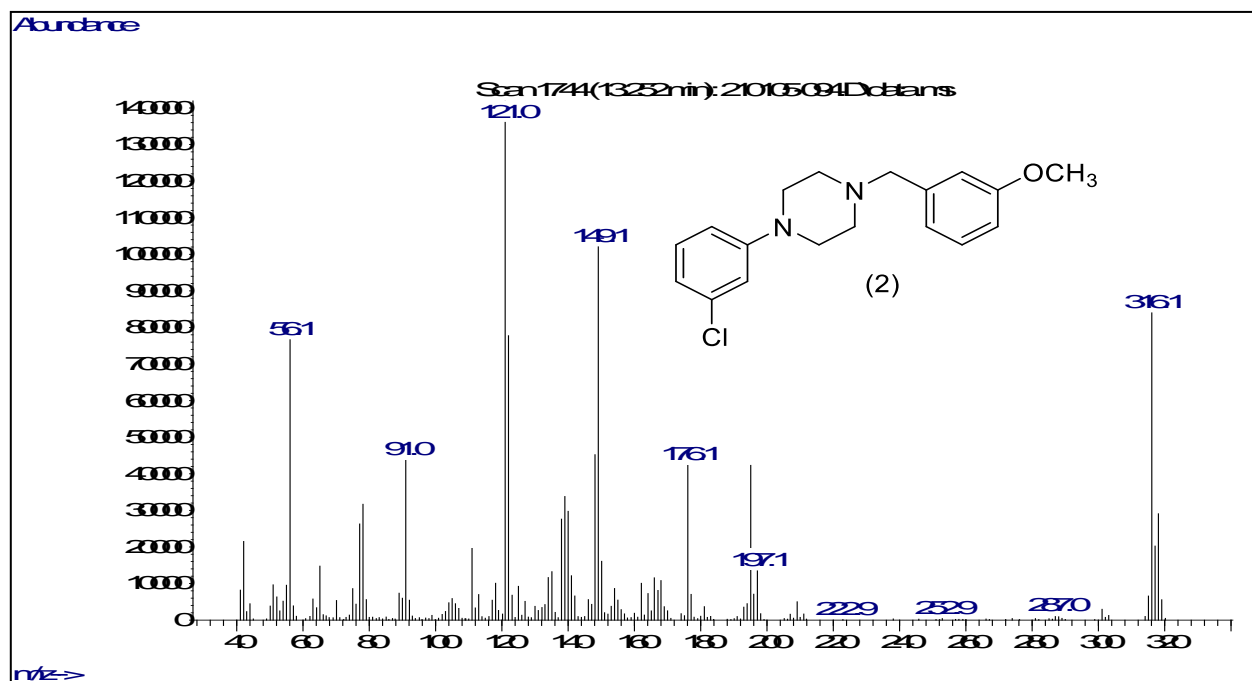
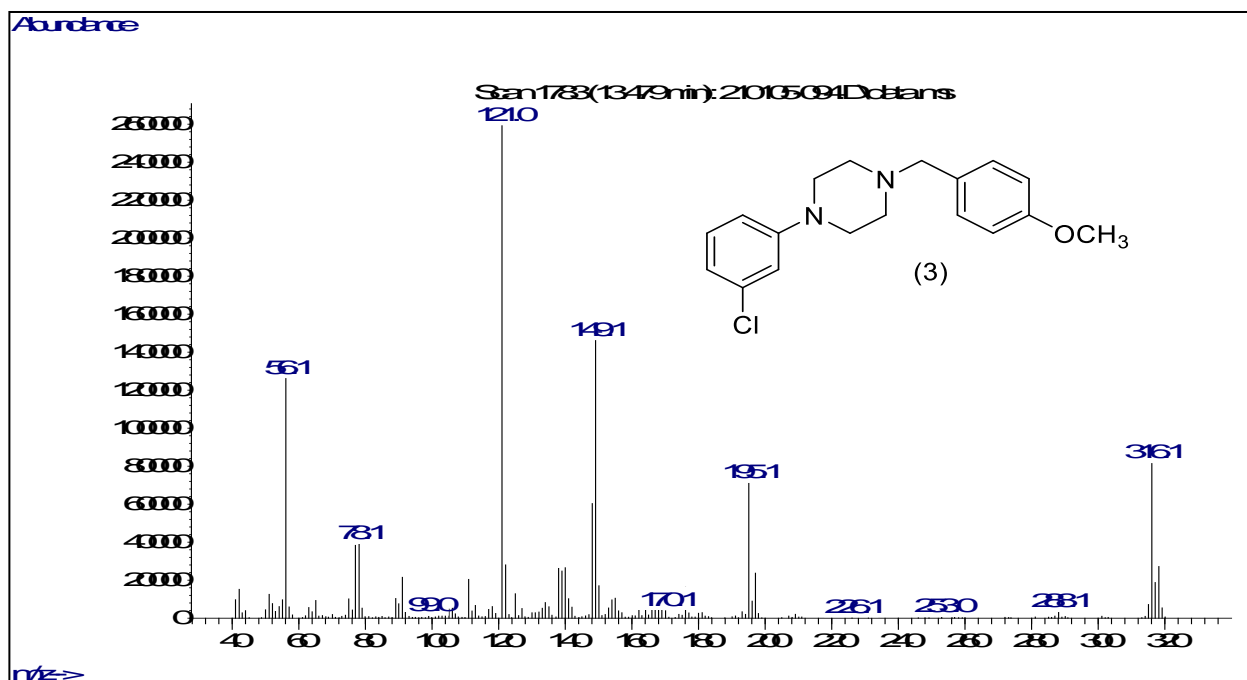
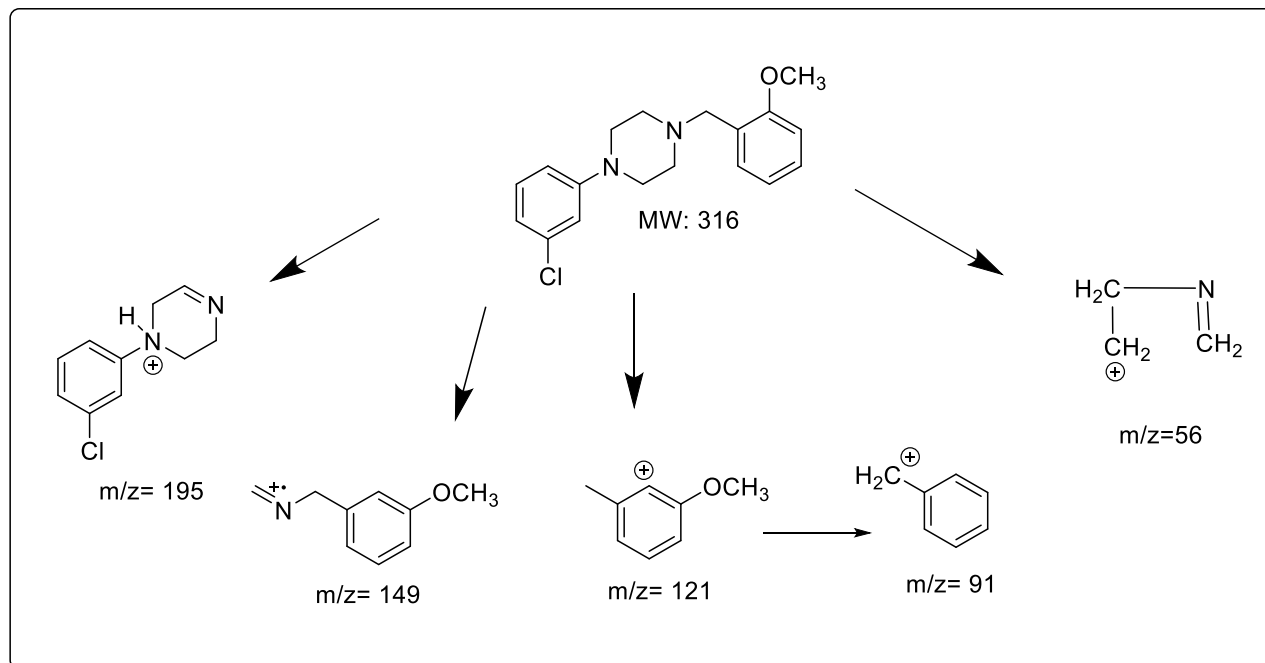


Figure 28. EI mass spectra of 1-(3-chlorophenyl)-4-[(N-methoxybenzyl)piperazine] (Group 7)



Scheme 31. EI mass spectral fragmentation pattern of 1-(3-chlorophenyl)-4-[(N-methoxybenzyl)piperazine (Group 7)

3.7.2. Gas Chromatographic Separation

To differentiate between the three regioisomers of monomethoxybenzyl-3-chlorophenyl piperazine, gas chromatographic separations were performed. The three compounds differ in the methoxy substitution on the benzyl group. The chromatogram in Figure (29) shows the separation of the three regioisomeric monomethoxybenzyl-3-chloro phenyl piperazine. The three compounds were separated on an Rxi®-17Sil MS midpolarity stationary phase with baseline resolution and the isomers eluted over about a 1-minute time window in the 14-minute range. The 1[-(2-methoxybenzyl - , 4-[3-chloro phenyl piperazine) elutes first, followed by 1[-(3-methoxybenzyl-, 4-[3-chloro phenyl piperazine) and lastly 1[-(4-methoxybenzyl-, 4-[3-chloro phenyl piperazine) respectively as shown in Figure (29).

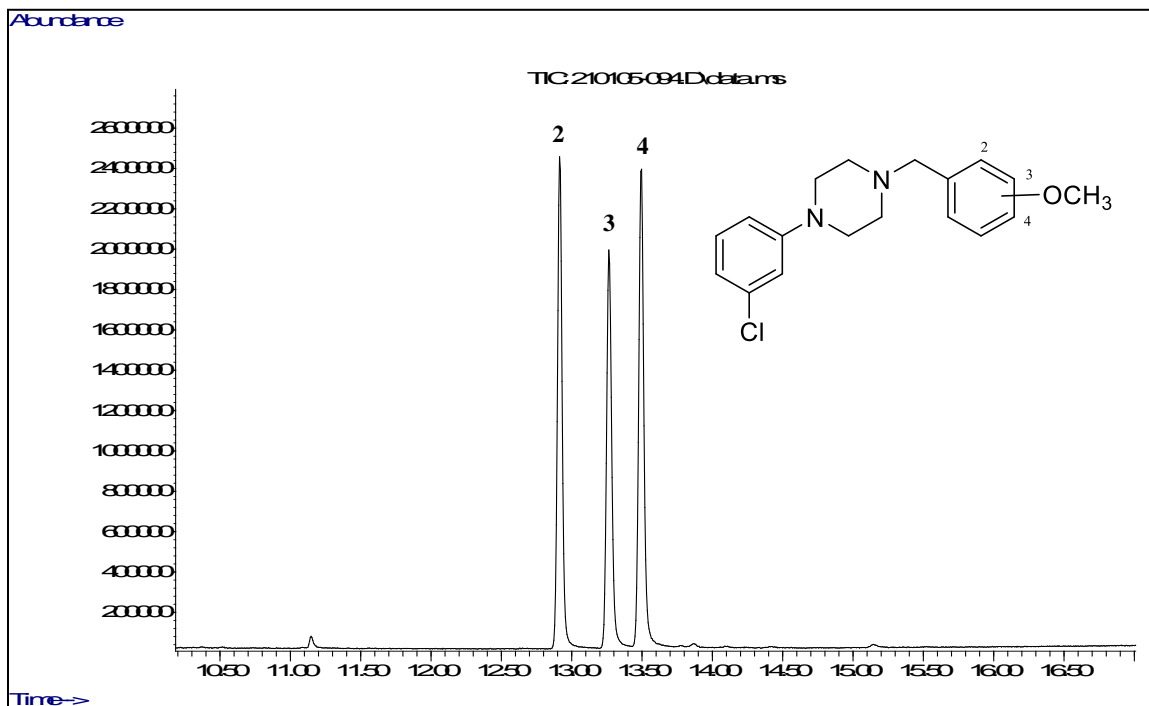
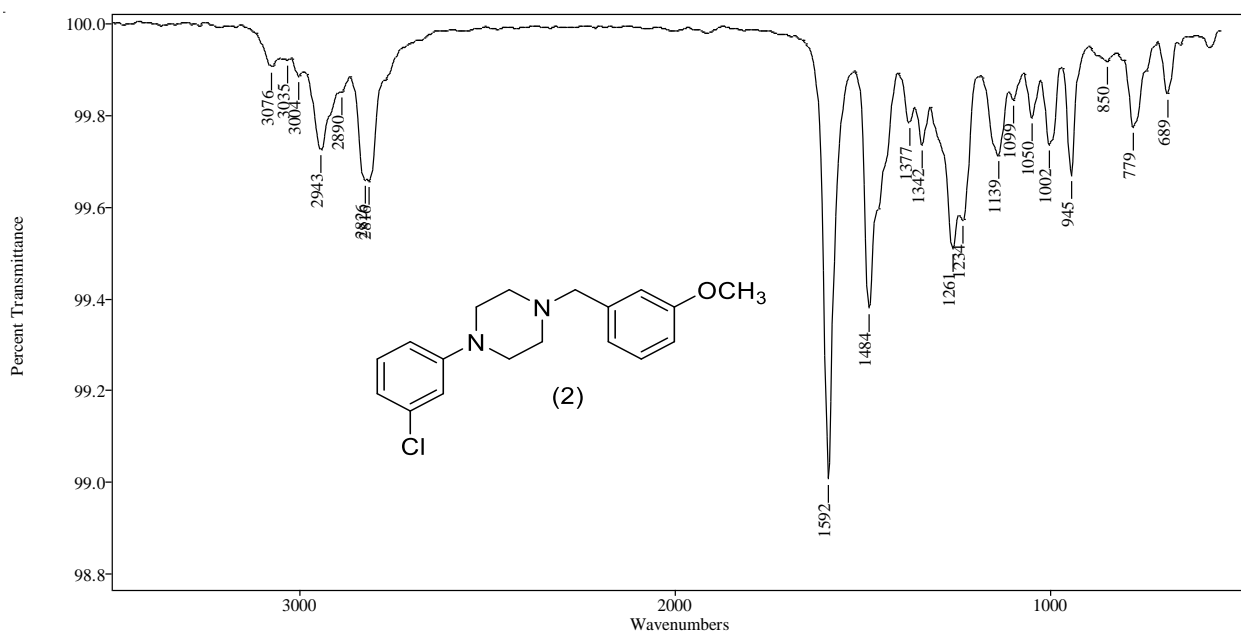
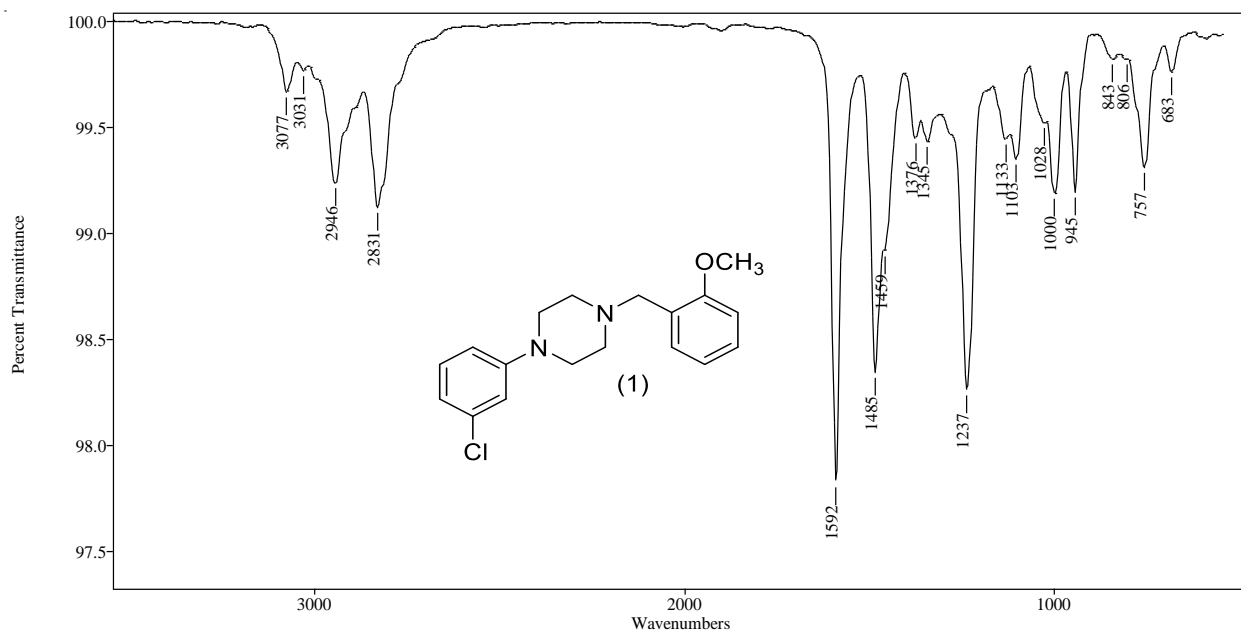


Figure 29. Gas chromatographic separation of 1-(3-chlorophenyl)-4-[(N-methoxybenzyl)piperazine using TP-1 program (Group 7)

3.7.3. Vapor-phase Infra-Red Spectrophotometry

Gas-chromatography coupled infrared detection (GC-IRD) was performed to differentiate between the three regioisomers of this group Figure (30). These are true vapor phase spectra generated directly as the individual peaks elute from the capillary gas chromatography column, GC-vpIR. The spectral region from just over 1592 cm^{-1} to 645 cm^{-1} provides several unique absorption bands and relative intensities for further differentiation of these three regioisomeric compounds. All three regioisomers have nearly similar absorption bands in the region 550 - 1600 cm^{-1} . All compounds are sharing a sharp intense absorption band at 1592 cm^{-1} , also double bands at 945-1002 cm^{-1} which almost identical in 2-methoxybenzyl isomer and 4-methoxybenzyl isomer nor

3-methoxybenzyl isomer . The 2-methoxybenzyl isomer has a small unique doublet band at 1103 cm^{-1} and 1133 cm^{-1} . The 3-methoxybenzyl isomer is the only isomer in this group with doublet band at 1234 cm^{-1} and 1261 cm^{-1} . While 4-methoxybenzyl isomer has wide triple bands at 1459 cm^{-1} , 1484 cm^{-1} , and 1509 cm^{-1} . Thus provide numerous points for differentiation among these three regioisomers.



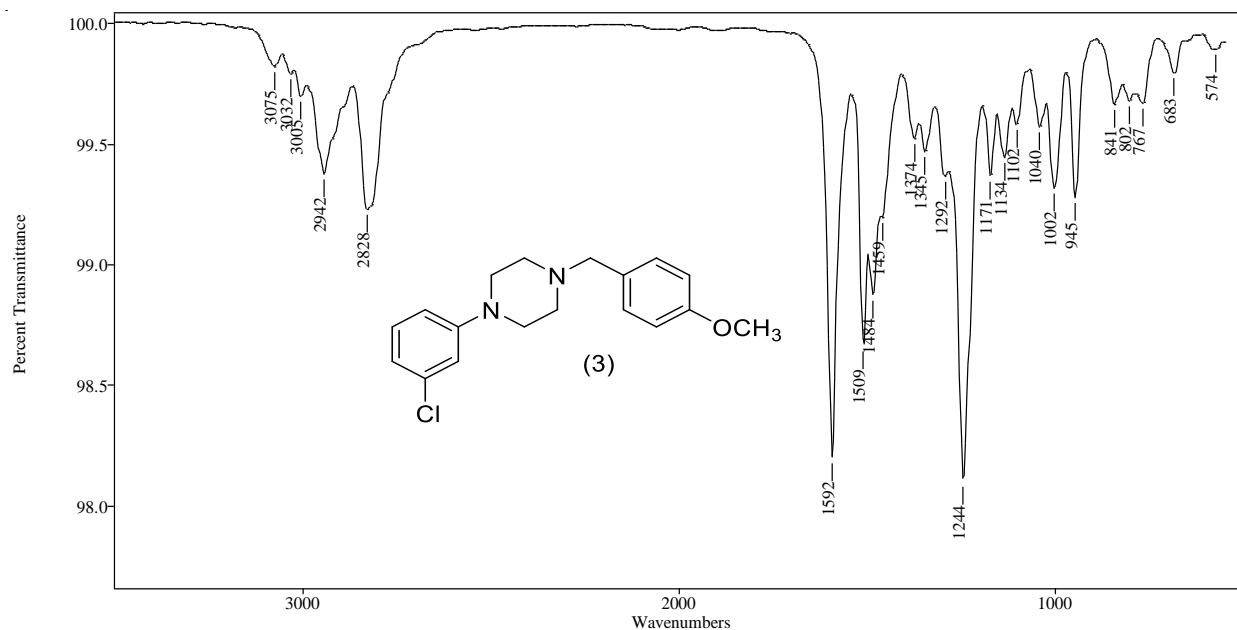


Figure 30. Vapor phase IR spectra of 1-(3-chlorophenyl)-4-[(N-methoxybenzyl)piperazine (Group 7)

3.7.3. Conclusion

The three regioisomers in this group share common major fragment ions, but there are some differences in relative intensity of ions which could be used for differentiation between these regioisomers. The base peak ion for all three spectra in is m/z 121, the product ion at m/z 91 is significantly more abundant for the 2-methoxybenzyl isomer and decreases in relative intensity for the 3-methoxybenzyl isomer and is much less significant for the 4-methoxybenzyl isomer. The (GC-IRD) result provides characteristic absorption bands that used to differentiate between the three regioisomers. The 2-methoxybenzyl isomer has a small unique doublet band at 1103 cm^{-1} and 1133 cm^{-1} . The 3-methoxybenzyl isomer is the only isomer in this group with doublet band at 1234 cm^{-1} and 1261 cm^{-1} . While 4-methoxybenzyl isomer has wide triple bands at 1459 cm^{-1} , 1484 cm^{-1} , and 1509 cm^{-1} .

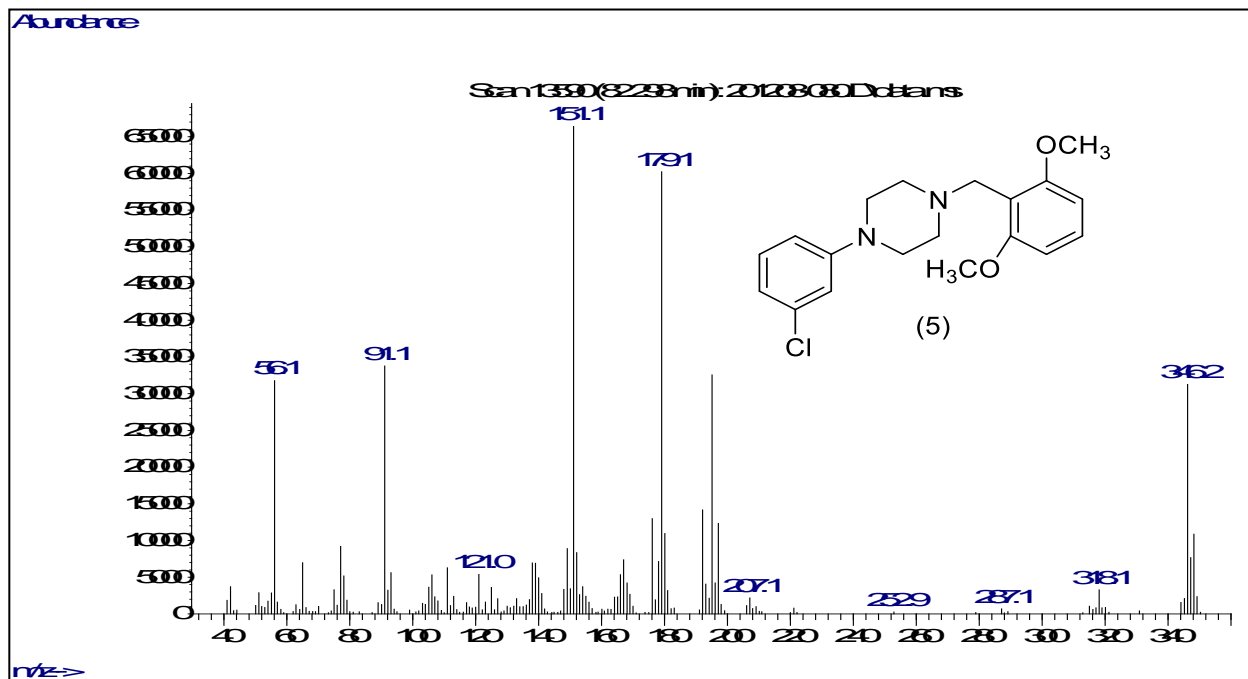
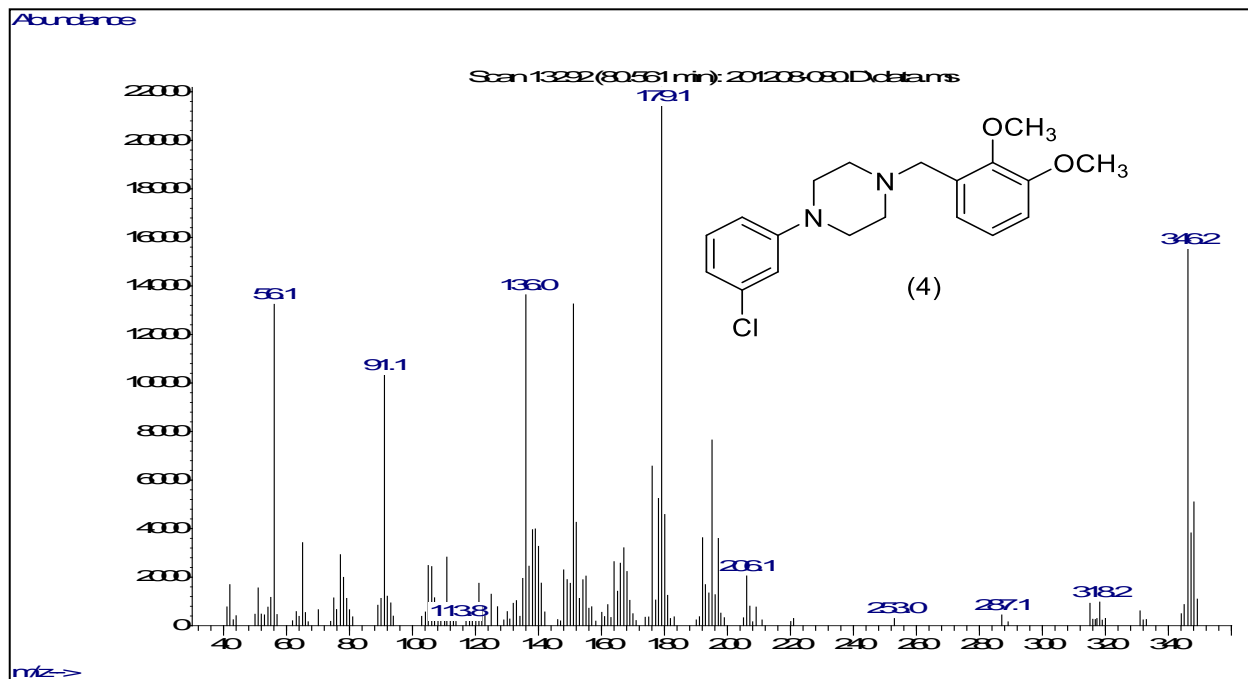
3.8. Analysis of 1-(chlorophenyl)-4-[(N-(dimethoxybenzyl)piperazine (Group 8)

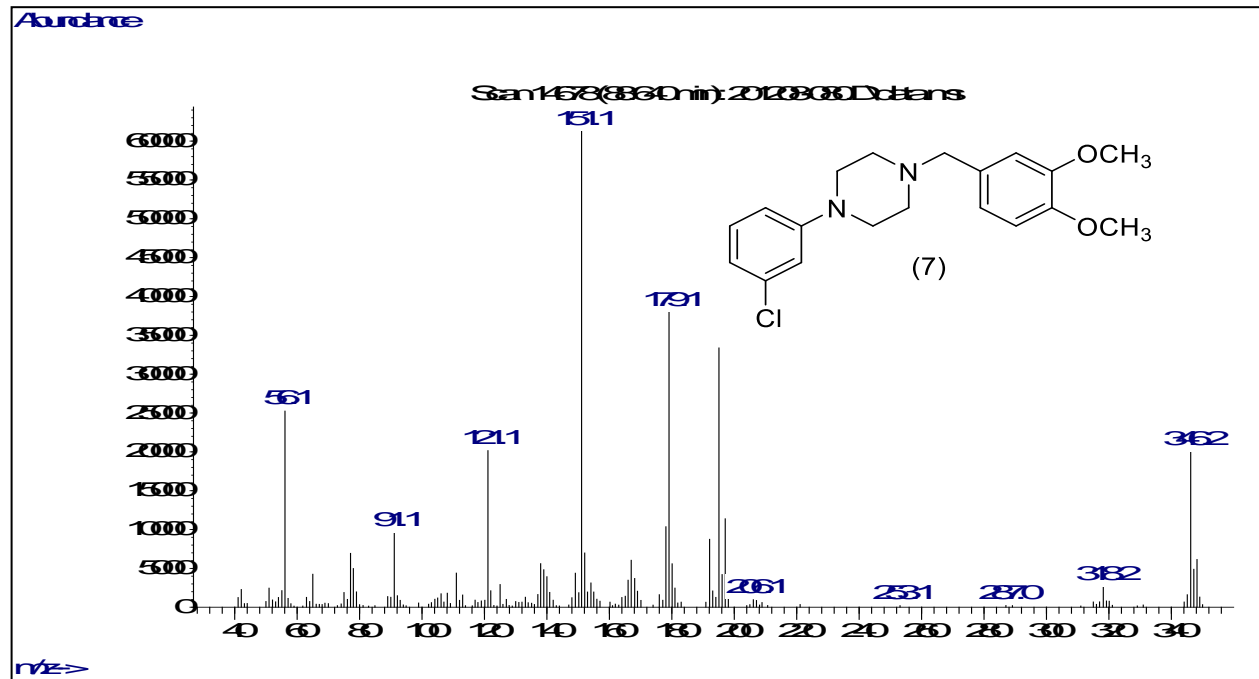
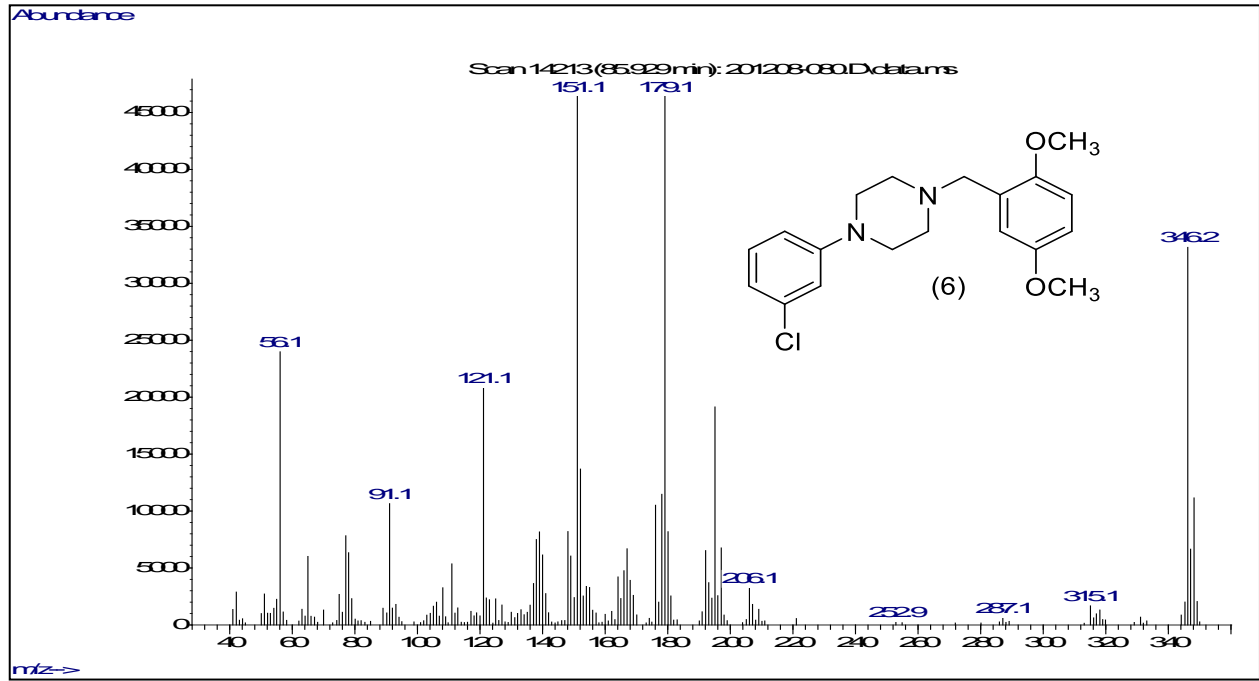
Six regioisomers of N-(dimethoxybenzyl)-3-chlorophenylpiperazine have identical mass spectra with almost equivalent fragments. The only difference between these regioisomers is the position of dimethoxy substitution on the benzylic side. The mass spectra for these six compounds did not show characteristic ion fragment for specific identification, except for 2,3-dimethoxybenzyl isomer which shows a unique major fragment at m/z 136, and 3,5 dimethoxybenzyl isomer which has another unique major fragment at m/z 152. Therefore, gas chromatographic separation coupled with infrared detection (GC-IRD) were used to provide direct confirmatory data for structural differentiation between the six regioisomers. The piperazines derivatives were chromatographed on a 30-meter capillary column containing an Rxi®-17Sil MS stationary phase and on a Rtx-200.

3.8.1. Mass spectral studies

The EI mass spectra for these six regioisomers are available in Figure (31). Some of the major ions originating from the dimethoxybenzyl portion of the molecule show a 30 Da increase in mass based on the presence of the additional methoxy group compared to the monomethoxy benzyl containing ions. The proposed structures for the major fragment ions are summarized in Scheme (32). The major fragment at m/z 179 is the dimethoxybenzyl iminium-type radical cation which occurs via the equivalent process that produces the m/z 149 ion in the monomethoxybenzyl series. This fragment is the base peak for 2,3-isomers. Additionally, the m/z 151 peak is the dimethoxybenzyl cation which can undergo the sequential rearrangement loss of formaldehyde producing the product ions at m/z 121 and m/z 91. The spectrum for the 2,3-dimethoxy isomer

shows the m/z 136 which is unique to the 2,3-substitution pattern and represents the rearrangement of a methyl group from an aromatic ring methoxy group to the piperazine nitrogen (4-position) via a six-centered bond migration followed by elimination of the 1-[3-(chloro)phenyl]-4-methylpiperazine and the m/z 136 oxymethoxybenzyl radical cation ($C_8H_8O_2$) will be formed. The unique ion and base peak at m/z 152 allow the EI spectrum to differentiate the 3,5-dimethoxy isomer from the other five isomers in this series. This m/z 152 is the 3,5-dimethoxybenzyl radical cation and appears to be a structural uniqueness based on both aromatic rings substituted methoxy groups present in a *meta* relationship to the benzylic methylene group. The formation of this ion requires a hydrogen migration from the piperazine ring to the benzyl aromatic ring in order to form the m/z 152 radical cation. The dimethoxybenzyl cation at m/z 151 is the base peak for four of these six isomers, the 2,4-, 2,5-, 2,6-, and the 3,4-dimethoxy isomers. The radical cation at m/z 179 is essentially the co-base peak in the 2,5-isomer, sharing almost equal intensity with the m/z 151 fragment in this spectrum. This m/z 179 radical cation is the base peak in the EI spectrum for the 2,3-dimethoxybenzyl regioisomer. Thus, the m/z 151 ion is the result of direct fragmentation initiated at the dimethoxybenzyl aromatic ring. In summary, the EI-mass spectra can clearly differentiate the 2,3- and 3,5-isomers from the other four isomers and from each other based on unique base peaks at m/z 179 and m/z 152, respectively as well as the additional confirmation for the 2,3-dimethoxybenzyl regioisomer provided by the significant m/z 136 ion.





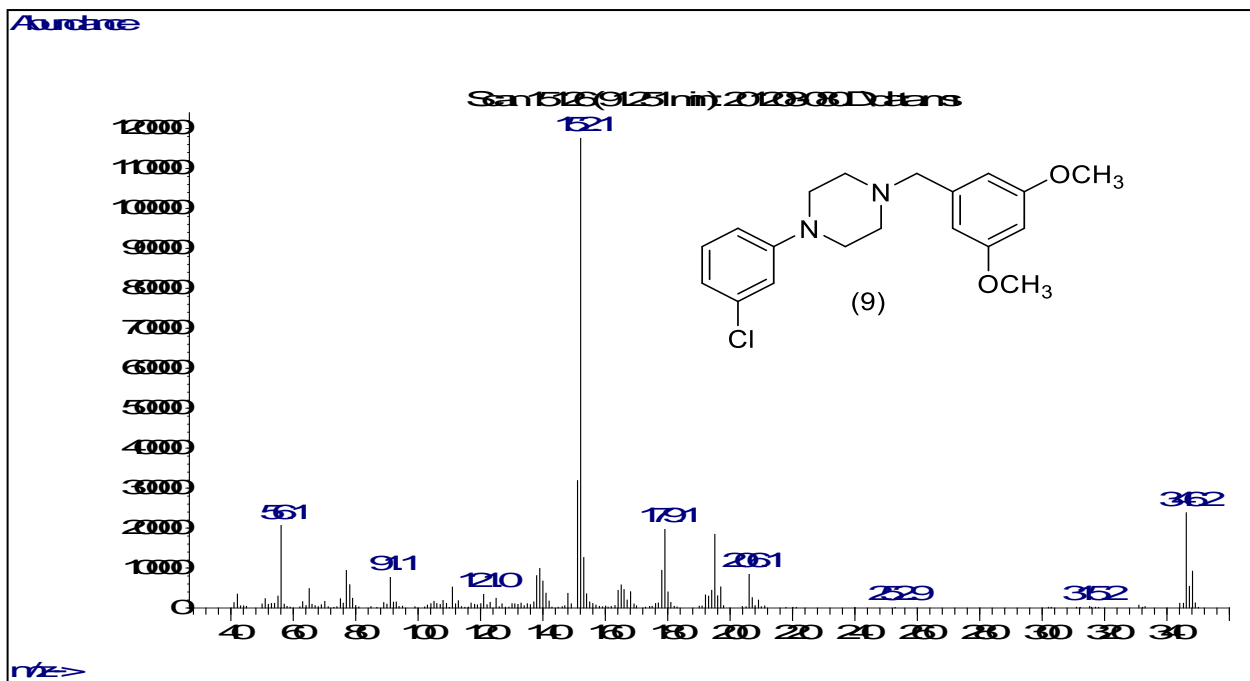
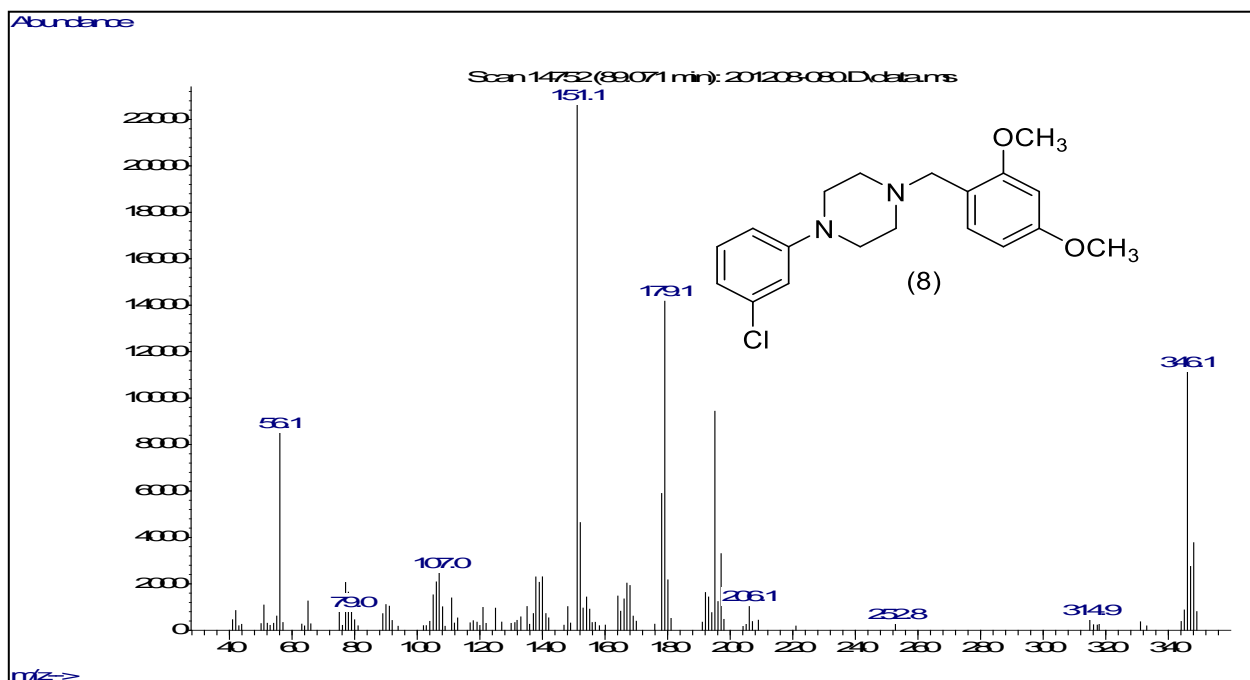
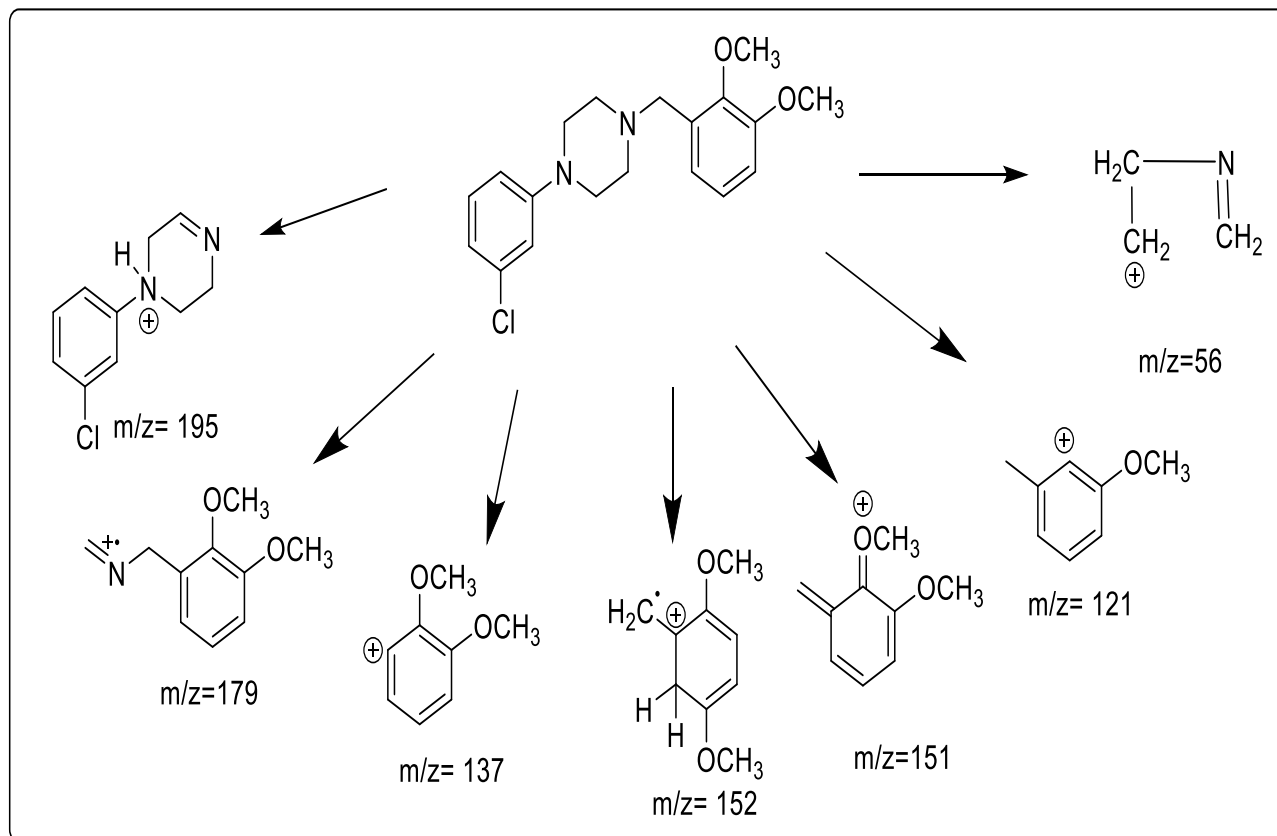


Figure 31. EI mass spectra of 1-(chlorophenyl)-4-[(N-(dimethoxybenzyl)piperazine (Group 8)



Scheme 27. EI mass spectral fragmentation pattern of 1-(chlorophenyl)-4-[(N-(dimethoxybenzyl))piperazine (Group 7)

3.8.2. Gas Chromatographic Separation

To differentiate the six regioisomers of this group, gas chromatographic separations were performed as provided in Figure (32). The six compounds N-(dimethoxybenzyl)-3-CIPP are different in the dimethoxy substitution on the benzyl group. Gas chromatographic separation of the six compounds was carried out using a 30-meter capillary column coated with a 0.50 μm film of Rxi®-17Sil MS, a midpolarity phase; similar to 50% phenyl, 50% dimethyl polysiloxane. The compounds elute over approximately a 12-minute window using a total run time of just over 92.0 minutes. The elution order for these six isomers shows 1-[2,3- dimethoxy- 4- [3-chloro phenyl

piperazine) elutes first, followed by 2,6-dimethoxybenzyl isomer , 2,5-dimethoxybenzyl isomer, 3,4- dimethoxybenzyl isomer, 2,4- dimethoxybenzyl isomer, and lastly the 3,5- dimethoxybenzyl isomer respectively. The two isomers 3,4-dimethoxy and 2,4-dimethoxy are critical base pair and sharing same substitution in position 4.

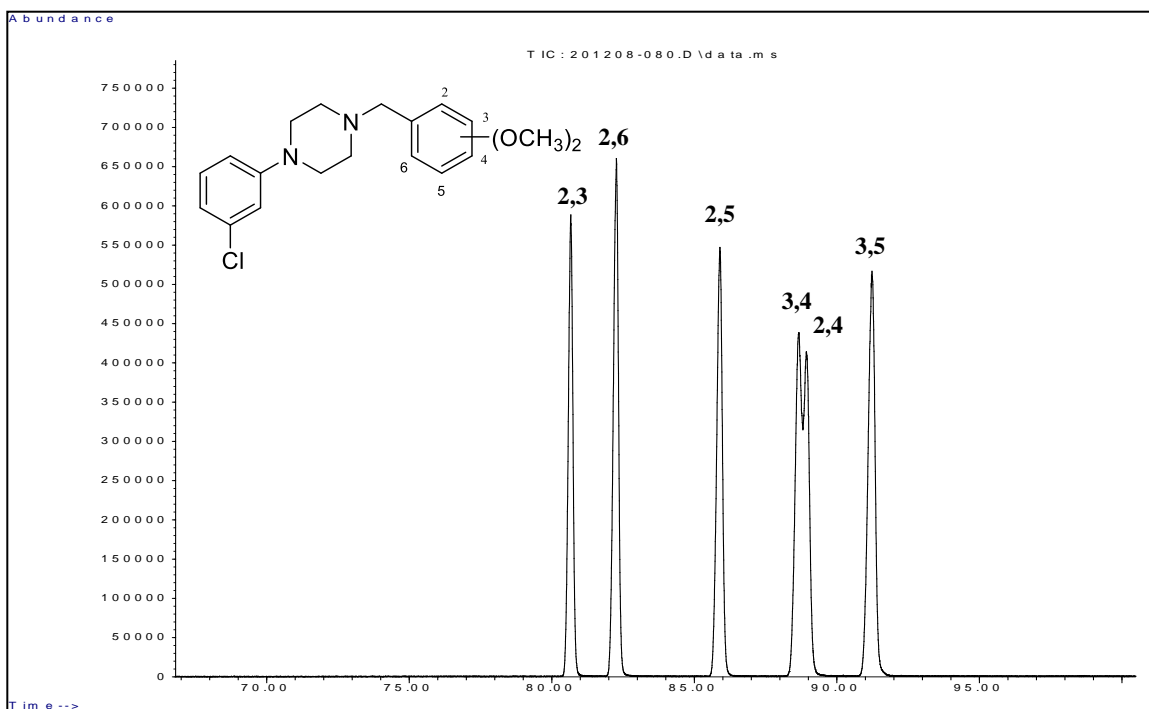


Figure 32. Gas chromatographic separation of 1-(chlorophenyl)-4-[(N-(dimethoxybenzyl)piperazine (Group 8)
Rxi®-17Sil MS using TP-5 program

Another chromatogram of the six regioisomers was carried out using a capillary column of dimensions 30 m × 0.25 mm and 0.5- μ m film depth of the relatively polar stationary phase, 100% trifluoropropyl methyl polysiloxane (Rtx-200). The second column shows better and much lower retention time in resolving the six regioisomers, in addition to different elution order. The elution order for these six isomers shows the 2,3-dimethoxybenzyl isomer elutes first, followed by 2,6-

dimethoxybenzyl isomer, 2,5-dimethoxybenzyl isomer, 2,4-dimethoxybenzyl isomer, 3,4-dimethoxybenzyl isomer, , and lastly 3,5- dimethoxybenzyl isomer respectively as shown in Figure (33).

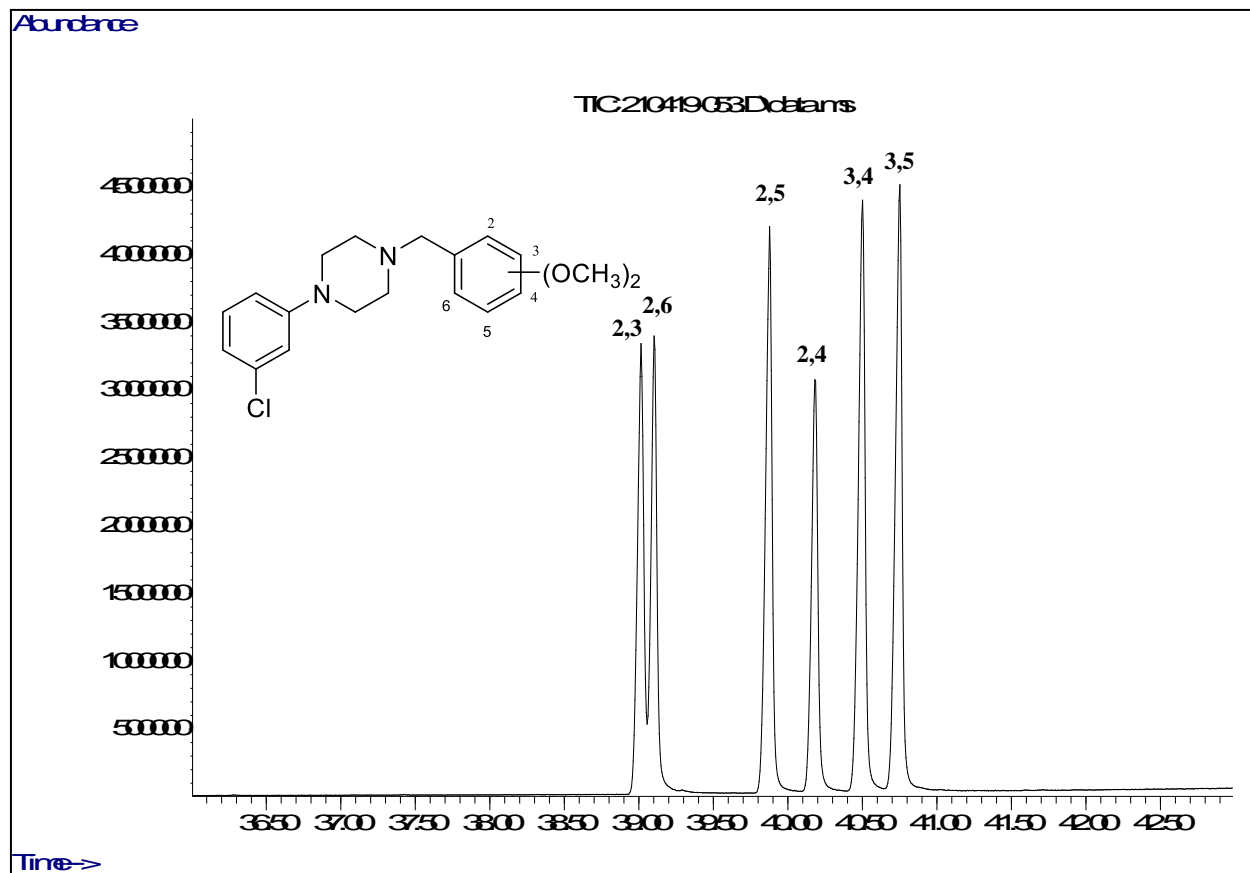
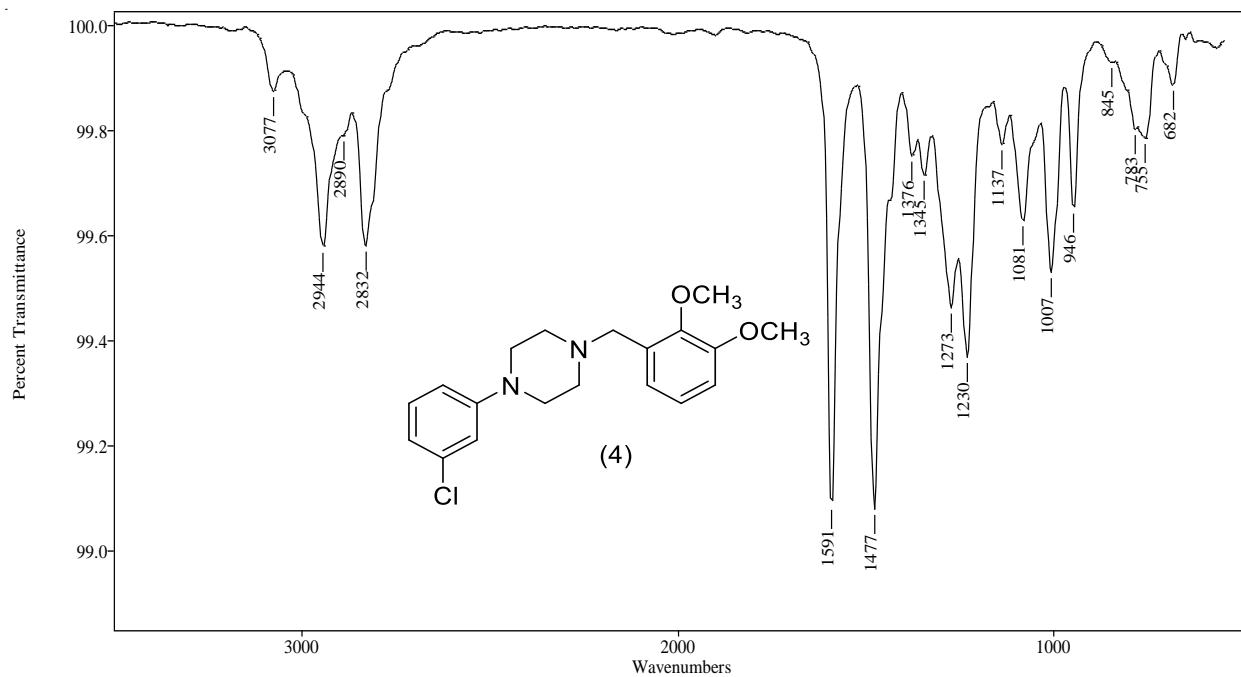


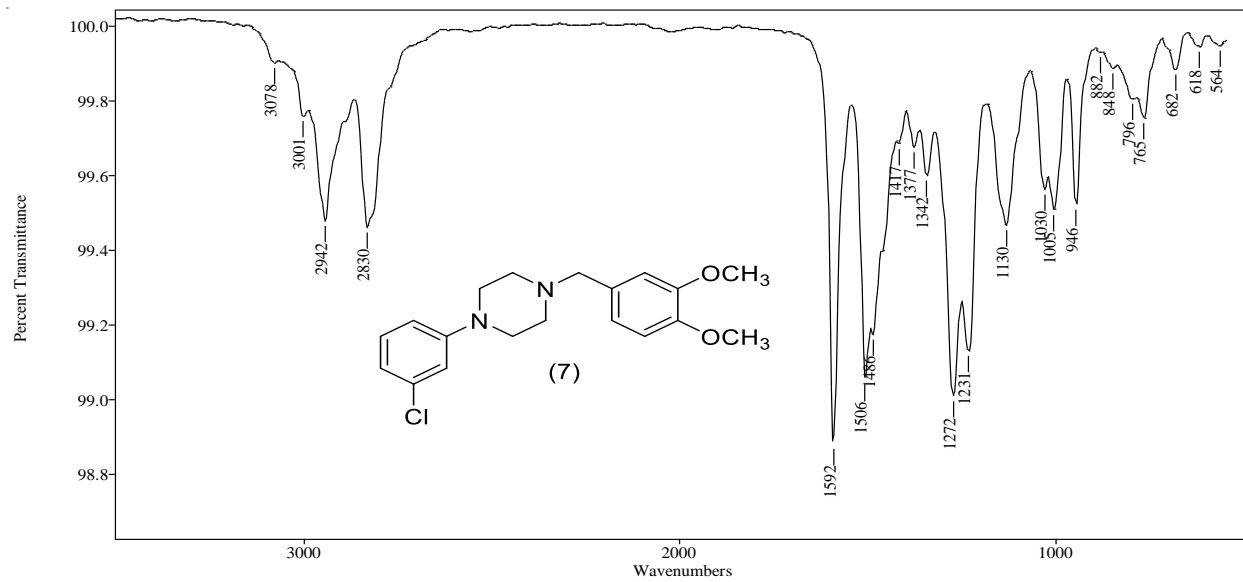
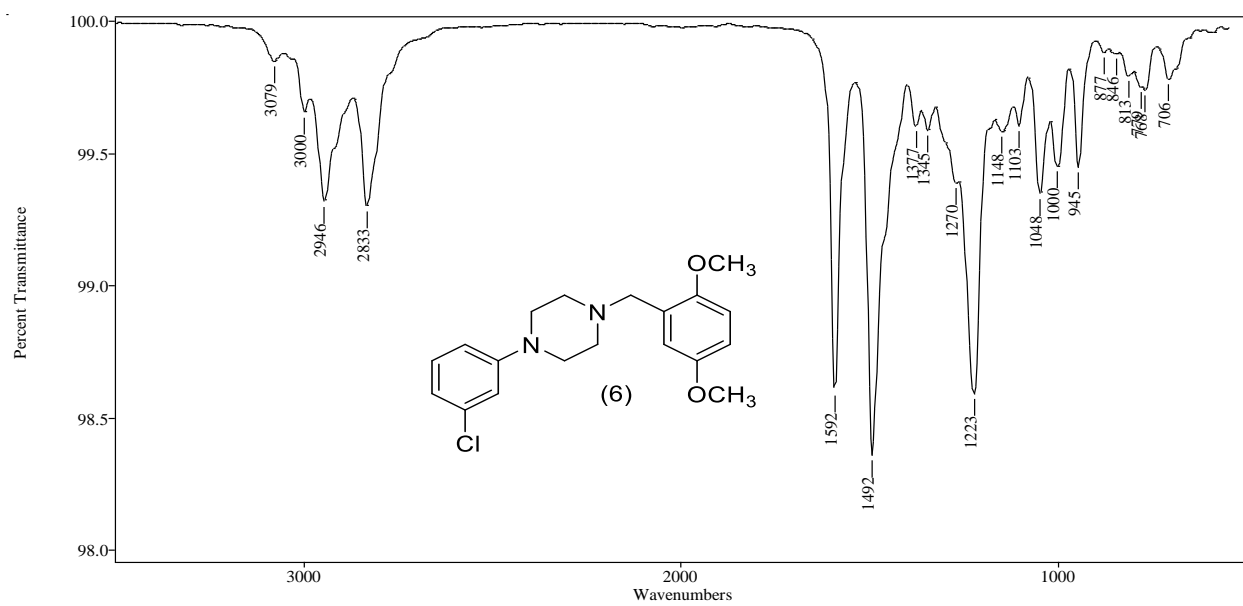
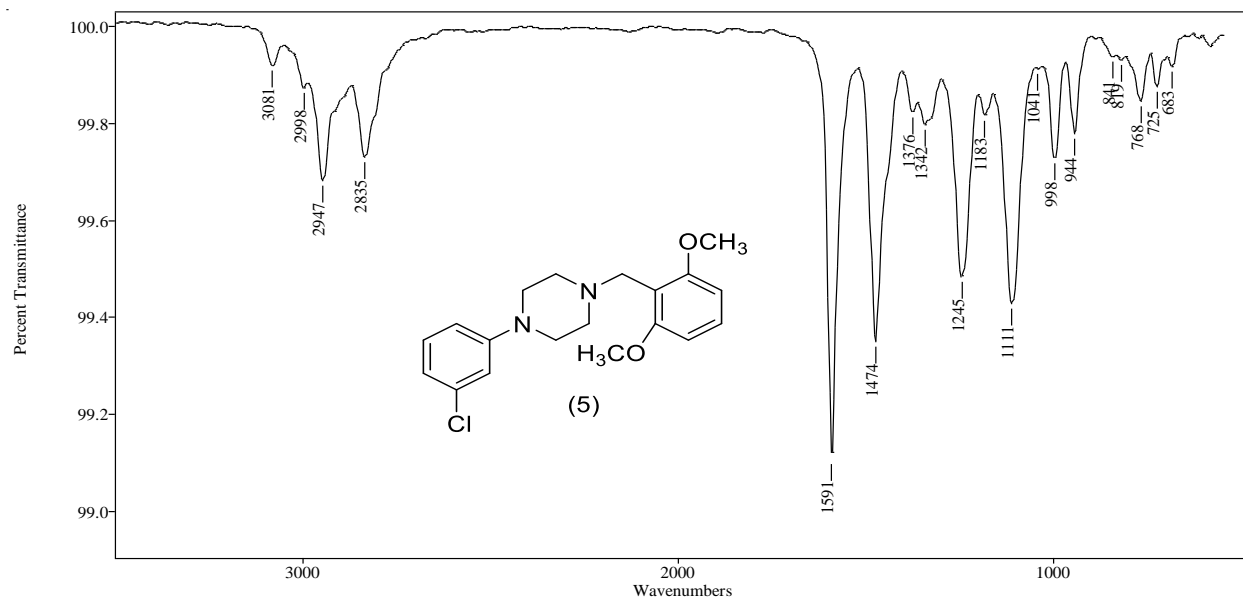
Figure 33. Gas chromatographic separation of 1-(chlorophenyl)-4-[(N-(dimethoxybenzyl))piperazine (Group 8) (Rtx-200) using TP-6 program

3.8.3. Vapor-phase Infra-Red Spectrophotometry

Gas-chromatography coupled infrared detection (GC-IRD) was performed to differentiate between the six regioisomers of this group Figure (34). All compounds display vapor phase IR spectrum with transmittance bands in the regions $550 - 1600 \text{ cm}^{-1}$ and $2810 - 3082 \text{ cm}^{-1}$. All six

regioisomers have similar absorption bands in the region 2810 – 3082 cm^{-1} . The 2,3-dimethoxybenzyl isomer has unique double absorption bands with identical intensity at 1477 cm^{-1} and 1591 cm^{-1} , additionally, a broad doublet bands at 1230 cm^{-1} and 1273 cm^{-1} . The 2,6-dimethoxybenzyl isomer has two major absorption bands at 1111 cm^{-1} and 1245 cm^{-1} . The 2,5-dimethoxybenzyl isomer has three significant IR spectra bands with high intensity at 1223 cm^{-1} , 1492 cm^{-1} , and 1592 cm^{-1} . The 3,4-dimethoxybenzyl isomer has unique two significant absorption bands at 1231 - 1272 cm^{-1} and 1486 – 1506 cm^{-1} appeared as doublet bands. The two isomers' 2,4-dimethoxybenzyl isomer and 3,5-dimethoxybenzyl isomer have low intensity bands in region 1347-948 cm^{-1} , the band at 1153 cm^{-1} in 3,5-dimethoxybenzyl isomer is stronger than that in 2,4-dimethoxybenzyl isomer at the same region. The 2,4-dimethoxybenzyl isomer has three low intensity bands at 945, 999, and 1039 cm^{-1} .





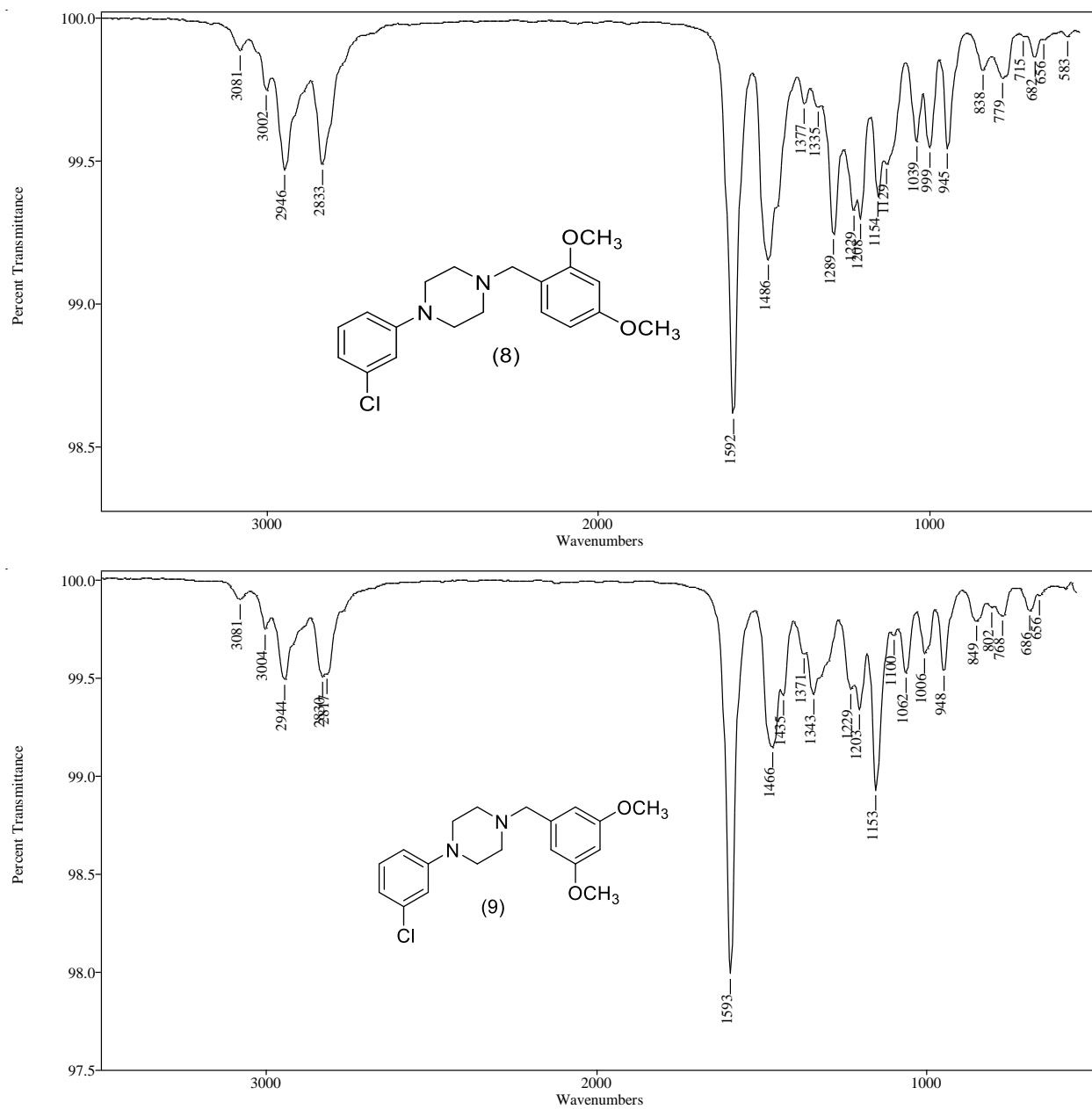


Figure 34. Vapor phase IR spectra of 1-(chlorophenyl)-4-[(N-(dimethoxybenzyl)piperazine (Group 8)

3.8.4. Conclusions

The major EI-MS fragment ions occur via processes initiated by one of the two nitrogen atoms of the piperazine ring. The ion at m/z 195 observed in all nine spectra occurs from the loss of the substituted benzyl radical and the m/z 56 cation ($C_3H_6N^+$) is a characteristic piperazine ring

fragment. The unique EI-MS fragments for the 2,3-dimethoxybenzyl- and 3,5-dimethoxybenzyl isomers at m/z 136 and m/z 152, respectively set apart these two compounds. The 2,3-dimethoxybenzyl isomer can be identified by a unique double absorption bands with identical intensity at 1477 cm^{-1} and 1591 cm^{-1} and the 3,4-isomer is characterized by two unique significant absorption bands at $1231 - 1272\text{ cm}^{-1}$ and $1486 - 1506\text{ cm}^{-1}$ appeared as doublet bands. These observations of uniqueness in the vpIR spectrum of each isomer coupled with the general pattern of common EI-MS fragments provide identifying data for each regioisomeric member of this dimethoxybenzyl-3-chlorophenylpiperazine series.

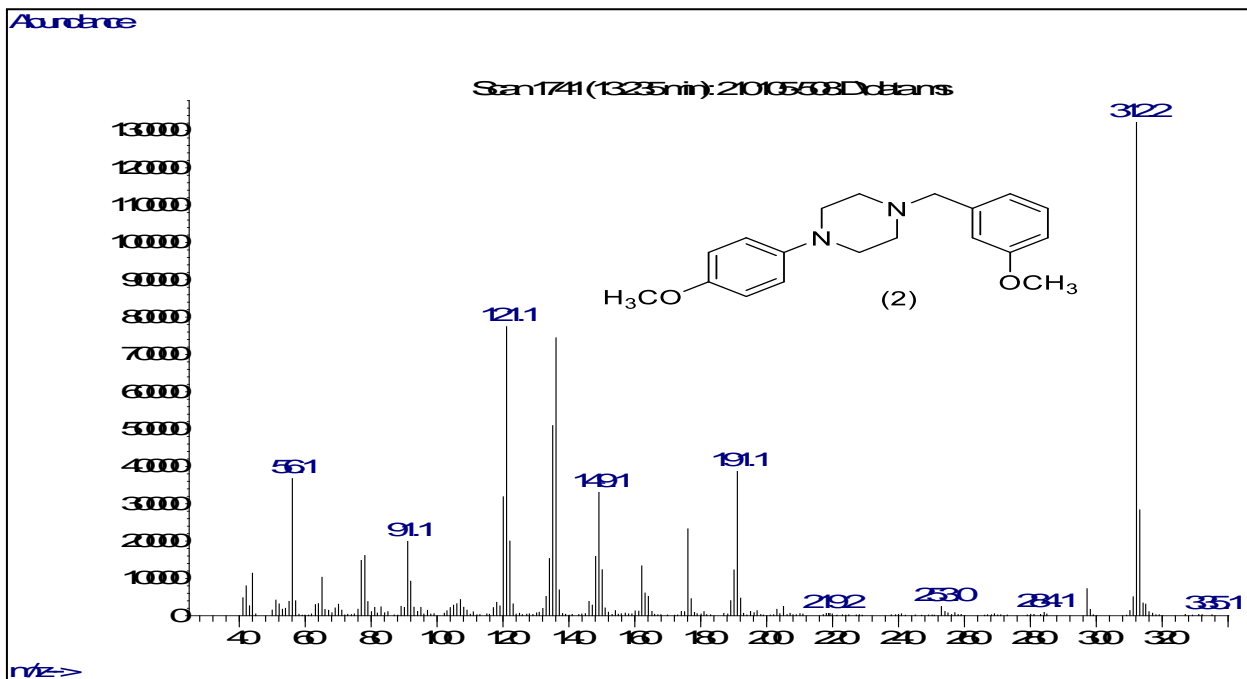
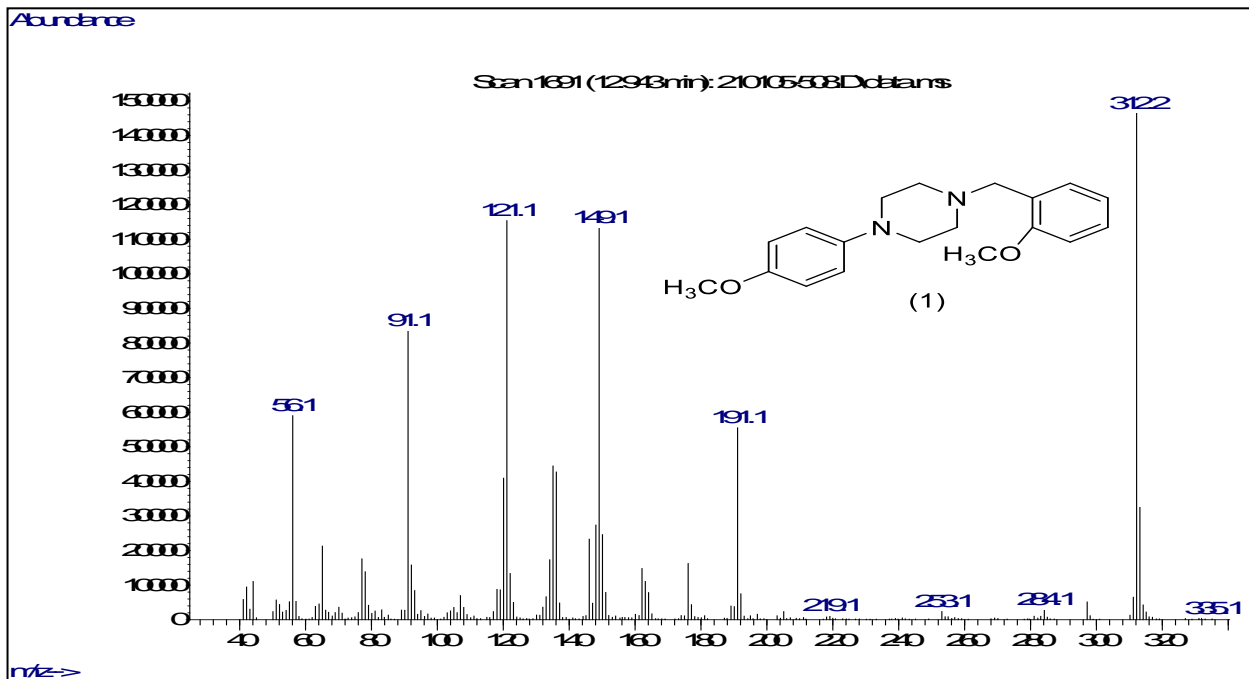
3.9. Analysis of N-(methoxybenzyl)-4-methoxyphenylpiperazine (Group 9)

Three regioisomers of N-(methoxybenzyl)-4-methoxyphenylpiperazines have identical mass spectra with almost equivalent fragments. They only differ in the position of methoxy substitution on the benzylic group. The mass spectra for these three compounds did not show characteristic ion fragment for specific identification. Therefore, gas chromatographic separation coupled with infrared detection (GC-IRD) were used to provide direct confirmatory data for structural differentiation between the three regioisomers. The monomethoxy benzyl-4-methoxyphenylpiperazine derivatives were resolved on a 30-meter capillary column containing an Rxi®-17Sil MS stationary phase.

3.9.1. Mass spectral studies

The electron ionization (EI) mass spectra for these three regioisomers are shown in Figure (35). These compounds have similar major fragment ions. However, there are some differences in

relative intensity of ions which could be used for to differentiate between these regioisomers. The proposed structures for the major fragment ions are summarized in Scheme (33). A major at m/z 121 cation can form in a direct manner via initial ionization of the methoxybenzyl aromatic ring via loss of the 4-methoxyphenylpiperazine radical species yielding the methoxybenzyl cation. Further loss of formaldehyde from this species yields the m/z 91 unsubstituted benzyl cation fragment. All the three regioisomers loss the methoxybenzyl radical to yield the 4-methoxyphenylpiperazine cation at m/z 191. The fragmentation of the piperazine ring from the nitrogen bearing the methoxybenzyl group yields the methoxybenzyl iminium-type radical cation at m/z 149. The m/z 56 ion is a characteristic fragment observed in most mono and disubstituted piperazine compounds originating from the atoms of the piperazine ring . The 2-methoxybenzyl regioisomers has the product ion at m/z 91 as a significant fragment of high relative abundance, while in 3-methoxybenzyl isomer the m/z 91 has lower relative abundance and is much less significant for the 4-methoxybenzyl isomer. The 4-methoxybenzyl isomer yields a significant 3-methoxybenzyl radical cation at m/z 121 compared to either the 2- or 4-methoxybenzyl isomers. Thus, the very intense m/z 91 ion in the 2-methoxybenzyl isomer and the intense m/z 121 for the 4-methoxybenzyl isomer provides some data for the direct EI-MS differentiation of these three isomeric compounds.



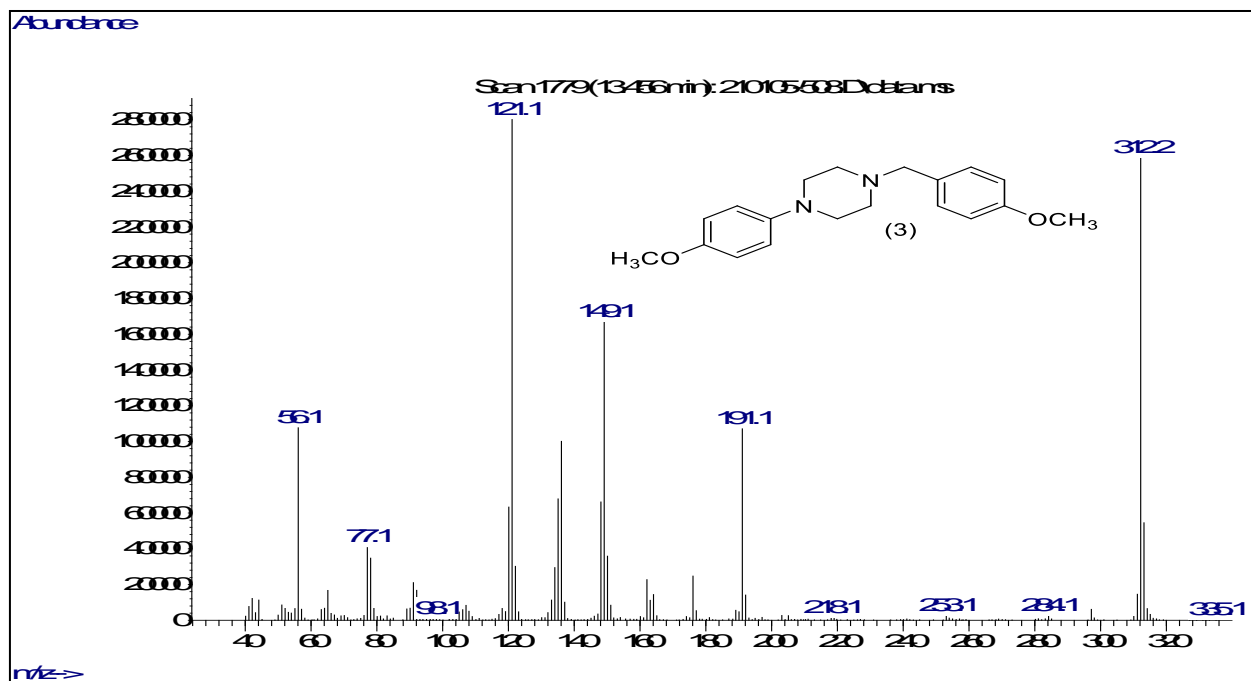
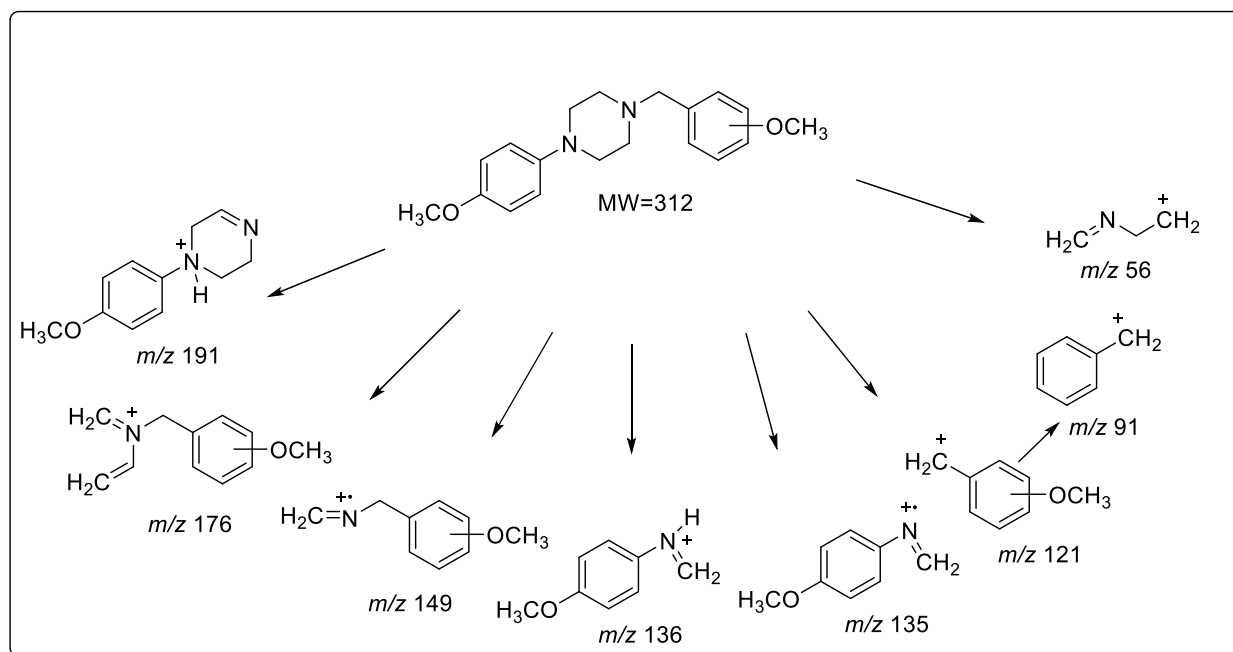


Figure 35. EI mass spectra of N-(methoxy) benzyl-4-methoxyphenylpiperazine (Group 9)



Scheme 28. EI mass spectral fragmentation pattern of N-(methoxy) benzyl-4-methoxyphenylpiperazine (Group 9)

3.9.2. Gas Chromatographic Separation

To differentiate the three regioisomers of this group, gas chromatographic separations were performed. The three regioisomers N-(methoxy) benzyl-4-methoxyphenyl piperazine differ in the methoxy substitution on the benzyl group. The chromatogram in Figure (36) shows the separation of the three regioisomeric monomethoxybenzyl isomers. The three compounds were separated on an Rxi®-17Sil MS midpolarity stationary phase with baseline resolution and the isomers eluted over about a 1-minute time window in the 16-minute range. The 2-(methoxy)benzyl-4-methoxyphenylpiperazine elutes first, followed by 3- methoxy isomer and 4- methoxy isomer respectively.

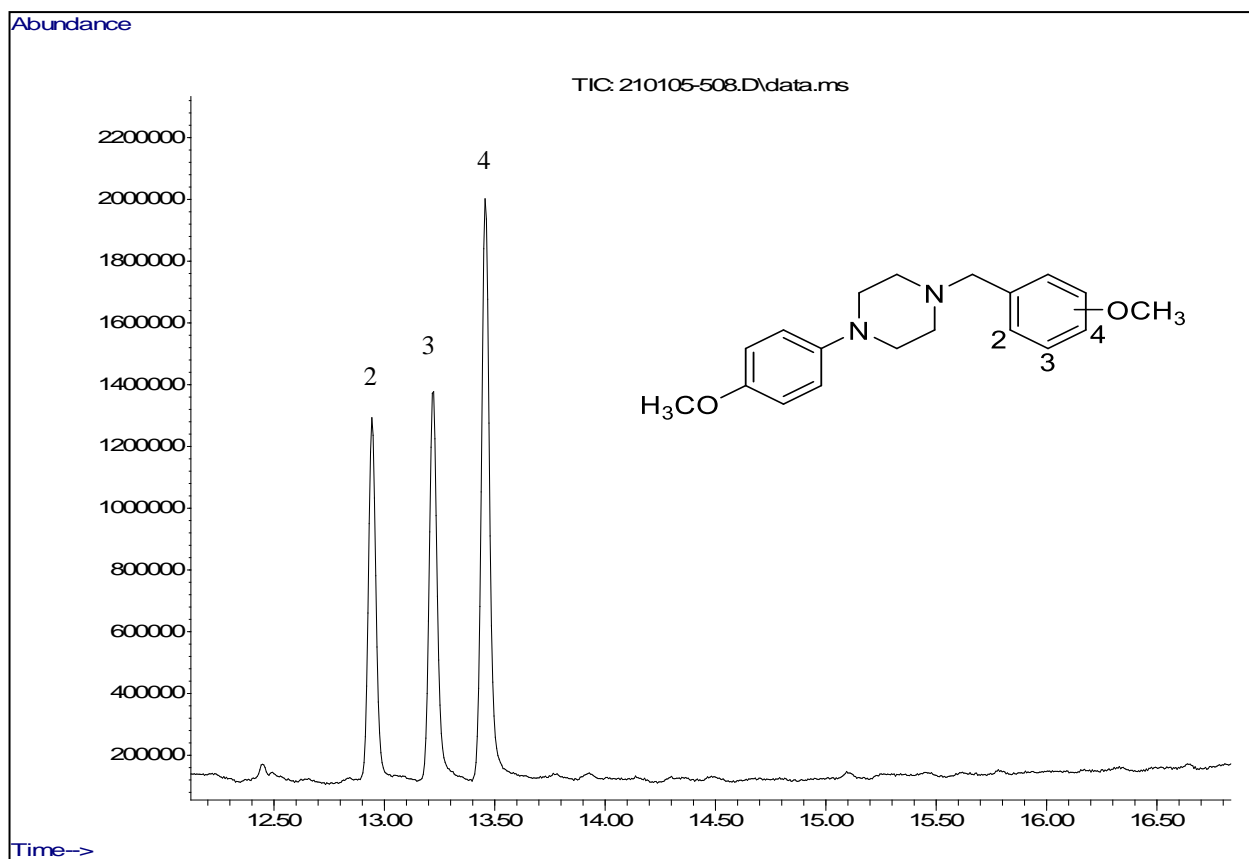
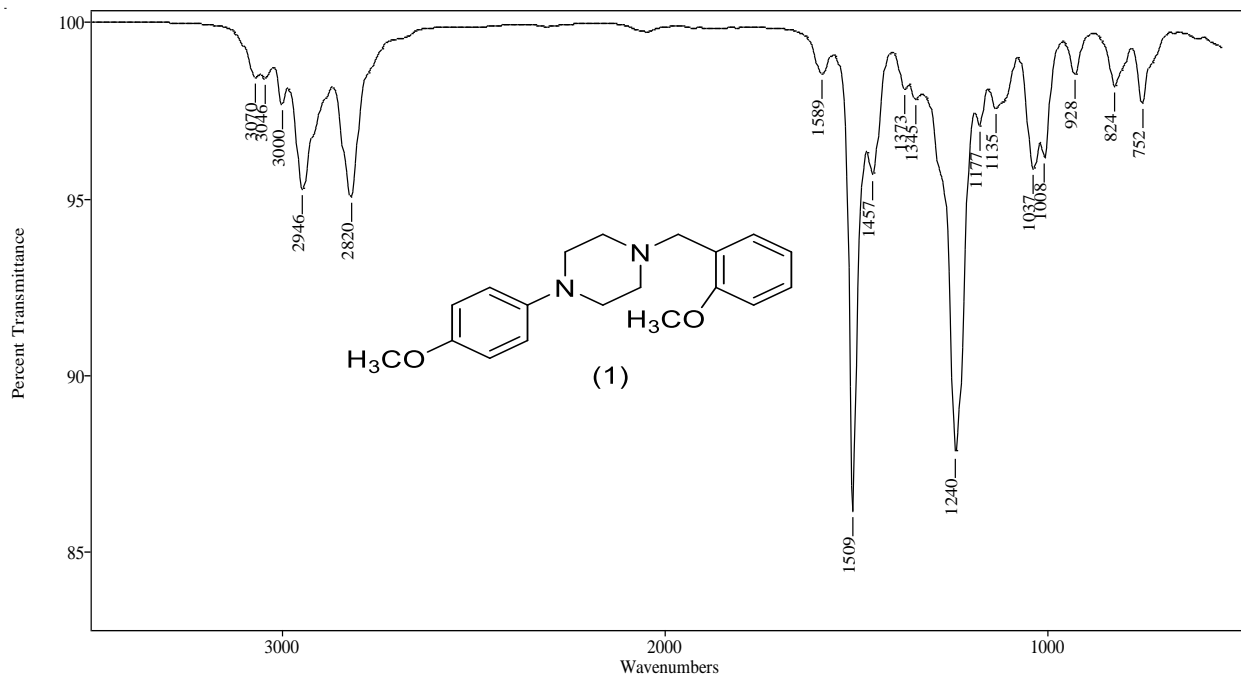


Figure 36. Gas chromatographic separation of N-(methoxy) benzyl-4-methoxyphenylpiperazine (Group 9) using TP-1 program

3.9.3. Vapor-phase Infra-Red Spectrophotometry

Gas-chromatography coupled infrared detection (GC-IRD) was performed to differentiate between the three regioisomers of this group. All compounds display vapor phase IR spectrum with transmittance bands in the regions $560 - 1610 \text{ cm}^{-1}$ and $2810 - 3070 \text{ cm}^{-1}$. All three regioisomers have nearly similar absorption bands in the region $560 - 1610 \text{ cm}^{-1}$. All compounds are sharing a sharp intense absorption band at 1509 cm^{-1} , also double bands at $1007-1040 \text{ cm}^{-1}$. The 3-(methoxy)benzyl has a unique band at 1597 cm^{-1} , this band is smaller in other two compounds. Also, 3-(methoxy)benzyl is the only isomer in this group with wider band at 1244 cm^{-1} , while the other isomers 2-(methoxy)benzyl and 4-(methoxy)benzyl have sharper band in the same area as shown in Figure (37).



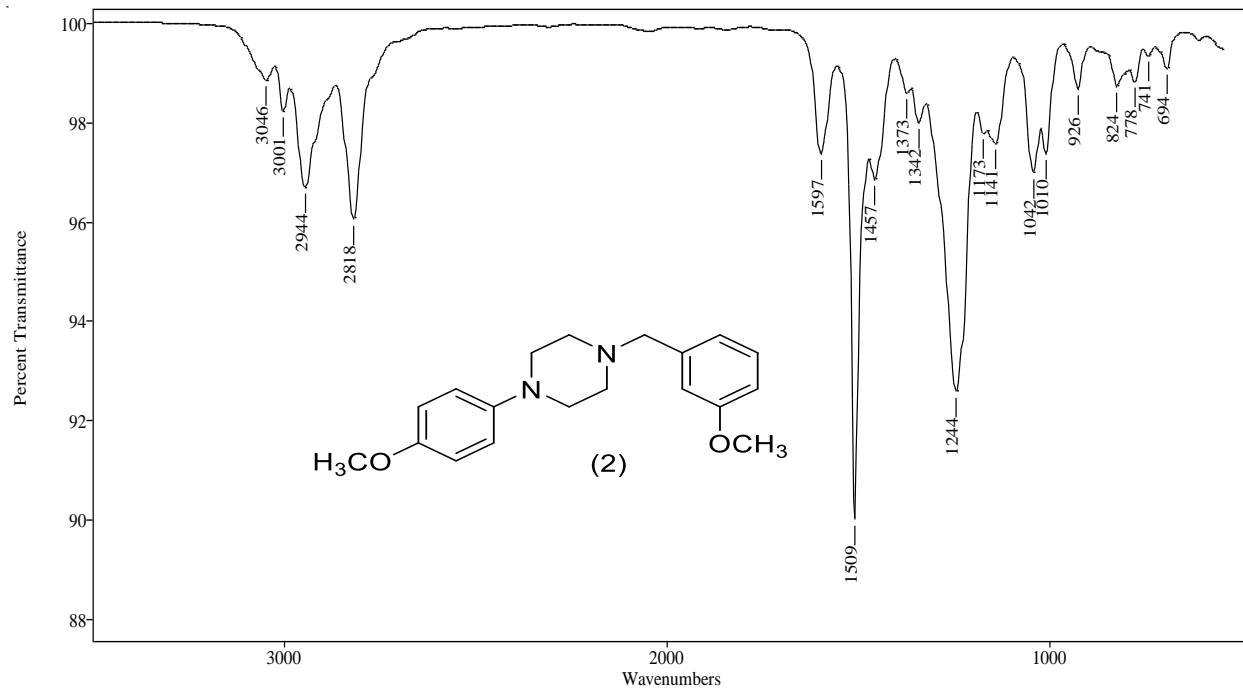
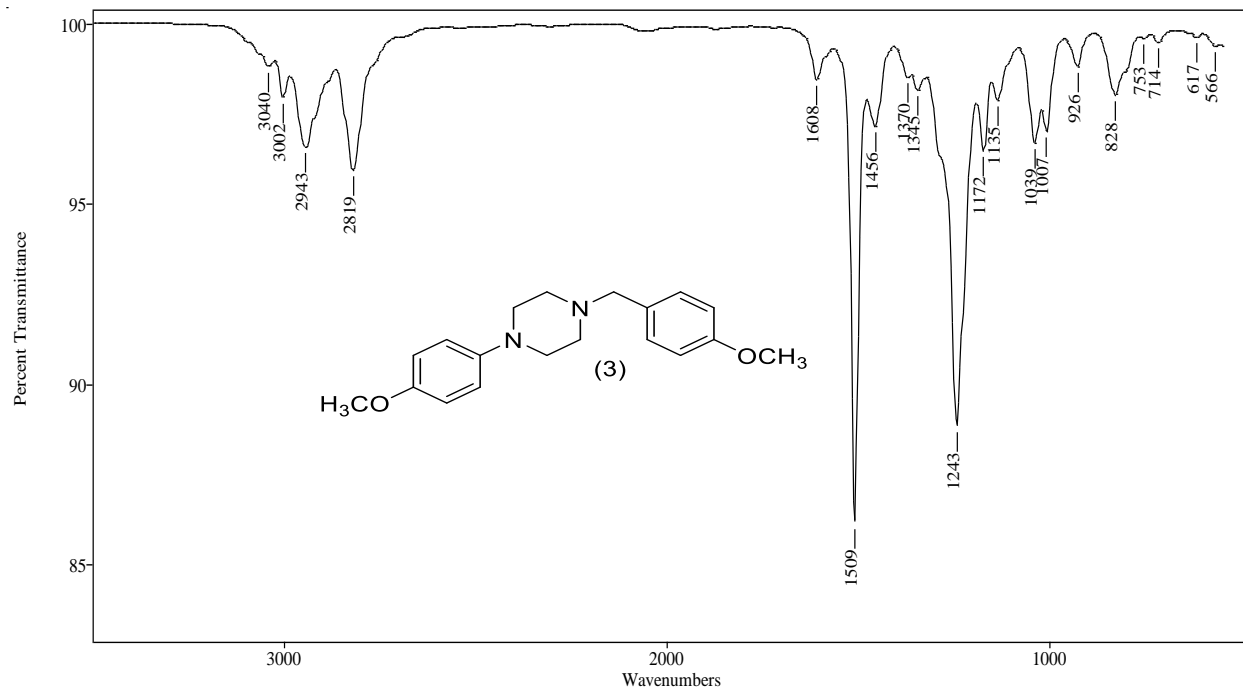


Figure 37. Vapor phase IR spectra of N-(methoxy) benzyl-4-methoxyphenylpiperazine (Group 9)

3.9.4. Conclusion

This group has similar mass spectra characteristic as the previous two groups of monomethoxybenzyl. The base peak ion for all three spectra is m/z 121, the product ion at m/z 91 is significantly more abundant for the 2-methoxybenzyl isomer and decreases in relative intensity for the 3-methoxybenzyl isomer and is much less significant for the 4-methoxybenzyl isomer. The (GC-IRD) result provides characteristic absorption bands that used to differentiate between the three regioisomers. The 3-(methoxy)benzyl has a unique band at 1597 cm^{-1} , this band is smaller in other two compounds. Also, 3-(methoxy)benzyl is the only isomer in this group with wider band at 1244 cm^{-1} , while the other isomers 2-(methoxy)benzyl and 4-(methoxy)benzyl have sharper band

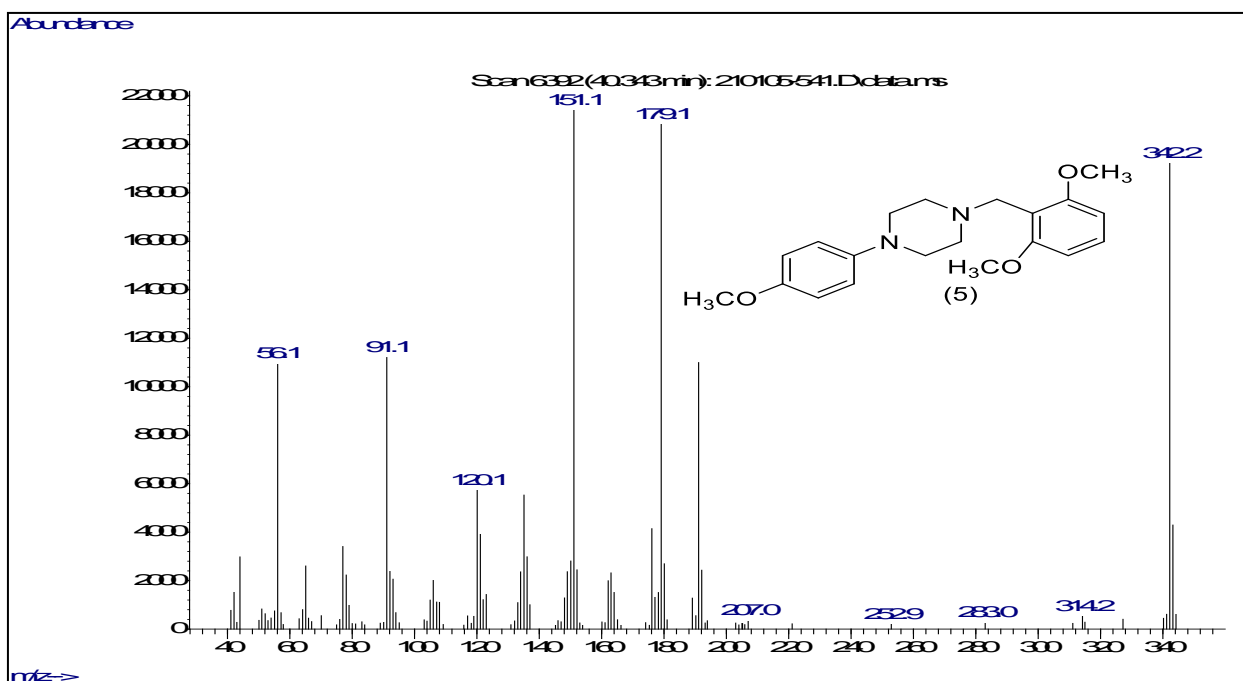
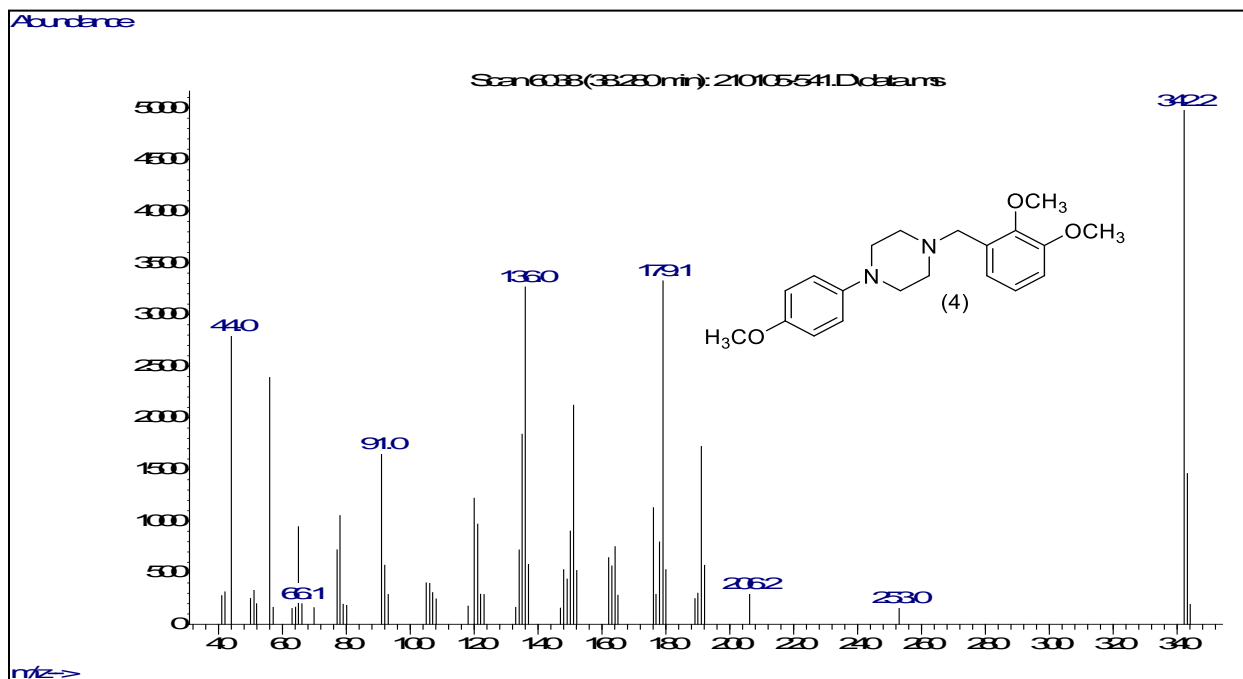
3.10. Analysis of 1-[N-(dimethoxybenzyl)-4-(4-(methoxyphenyl)piperazine (Group 10)

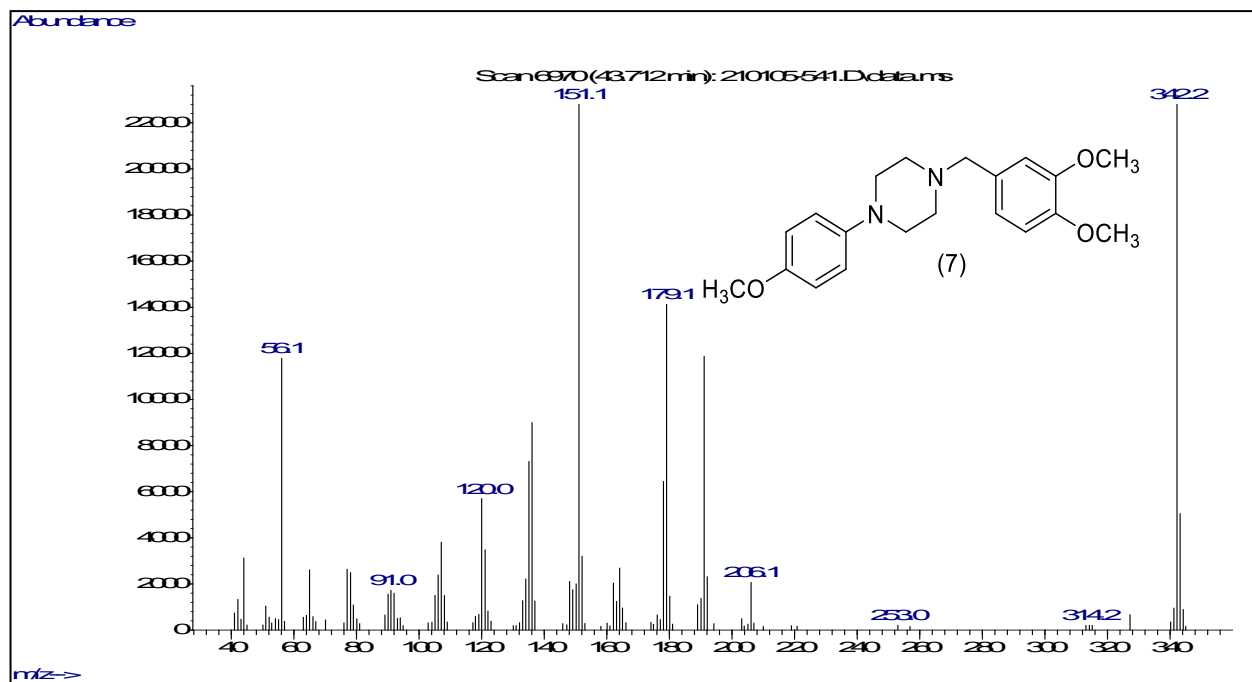
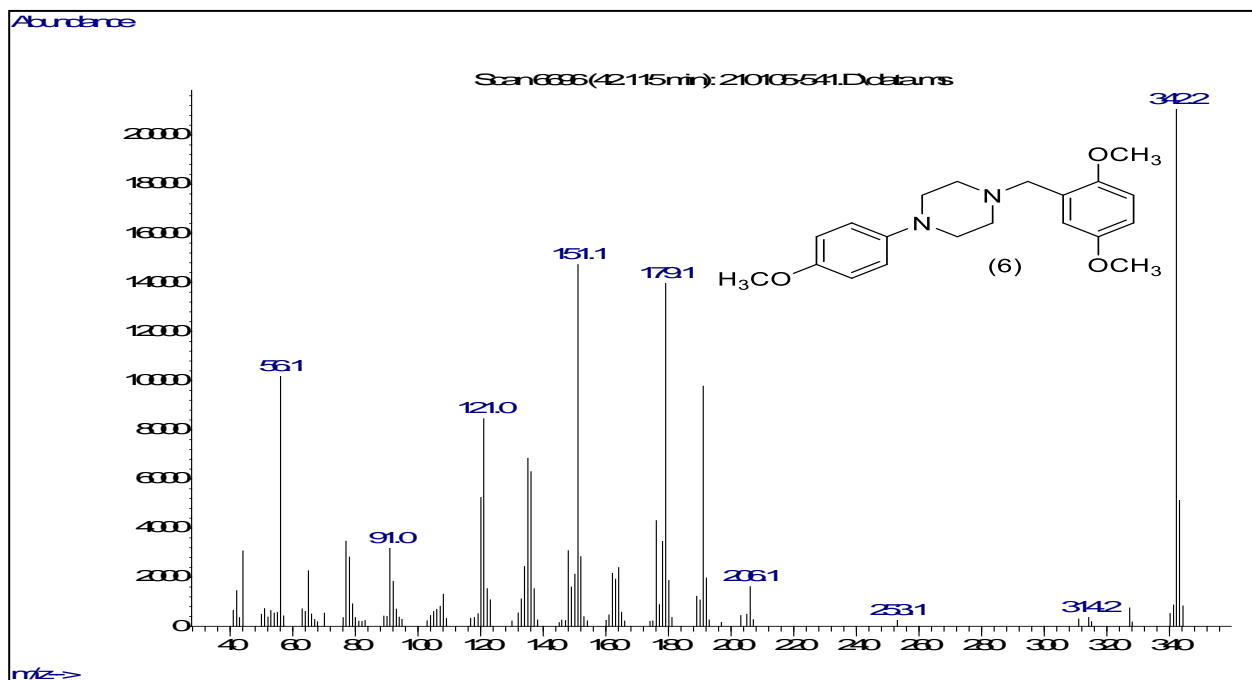
Six regioisomers of N-(dimethoxy) benzylpiperazines -4-methoxyphenyl have identical mass spectra with almost equivalent fragments. The only difference between these regioisomers is the position of dimethoxy substitution on the benzylic side. The mass spectra for these six compounds did not show characteristic ion fragment for specific identification, except for the 2,3-dimethoxy isomer at m/z 136 and the 3,5-dimethoxy isomer which shows a unique major fragment at m/z 152. Therefore, gas chromatographic separation coupled with infrared detection (GC-IRD) were used to provide direct confirmatory data for structural differentiation between the six regioisomers. The piperazines derivatives were resolved on a 30-meter capillary column containing an Rxi®-17Sil MS stationary phase.

3.10.1. Mass spectral studies

The EI mass spectra for these six regioisomers are available in Figure (38). Some of the major ions originating from the dimethoxybenzylpiperazine portion of the molecule show a 30 Da increase in mass based on the presence of the additional methoxy group compared to the monomethoxy benzyl containing ions. The proposed structures for the major fragment ions are summarized in Scheme (34). The major fragment at m/z 179 is the dimethoxybenzyl iminium-type radical cation which occurs via the equivalent process that produces the m/z 149 ion in the monomethoxybenzyl series. Additionally, the m/z 151 peak is the dimethoxybenzyl cation which can undergo the sequential rearrangement loss of formaldehyde producing the product ions at m/z 121 and m/z 91. The spectrum for the 2,3-dimethoxy isomer shows the m/z 136 which is unique to the 2,3-substitution pattern and represents the rearrangement of a methyl group from an aromatic ring methoxy group to the piperazine nitrogen (4-position) via a six-centered bond migration followed by elimination of the 1-[4-methoxyphenyl]-4-methylpiperazine and the m/z 136 oxymethoxybenzyl radical cation ($C_8H_8O_2$). The unique ion and base peak at m/z 152 allow the EI spectrum to differentiate the 3,5-dimethoxy isomer from the other five isomers in this series. This fragment at m/z 152 is the 3,5-dimethoxybenzyl radical cation and appears to be a structural uniqueness based on both aromatic rings substituted methoxy groups present in a *meta* relationship to the benzylic methylene group. The formation of this ion requires a hydrogen migration from the piperazine ring to the benzyl aromatic ring in order to form the m/z 152 radical cation. The dimethoxybenzyl cation at m/z 151 is the base peak for four of these six isomers, the 2,4-, 2,5-, 2,6-, and the 3,4-dimethoxy isomers. The radical cation at m/z 179 is essentially the base peak in the 2,3-isomer, but the m/z 179 also the co-base for 2,5- and 2,6 isomer sharing almost equal intensity with the m/z 151 fragment in this spectrum. The m/z 151 ion is the result of direct fragmentation initiated at the dimethoxybenzyl

aromatic ring. The EI-mass spectra for this group can clearly differentiate the 2,3- and 3,5-isomers from the other four isomers and from each other based on unique base peaks at m/z 179 and m/z 152, respectively as well as the additional confirmation for the 2,3-dimethoxybenzyl regioisomer provided by the significant m/z 136 ion.





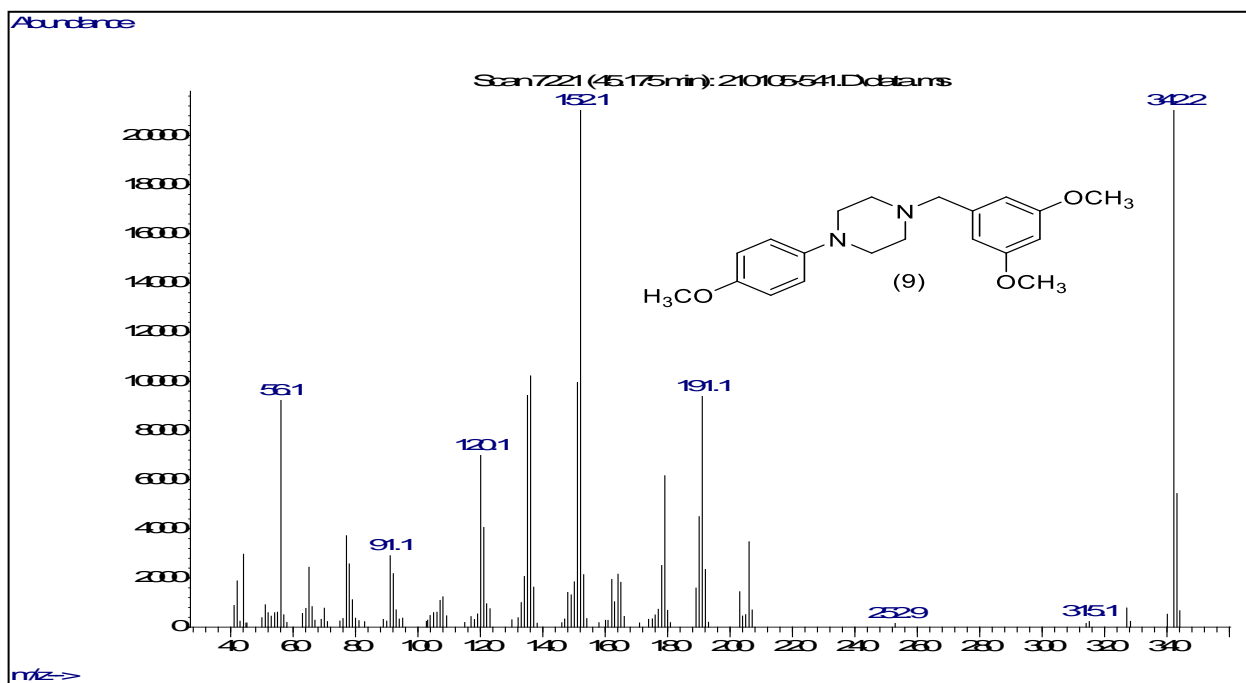
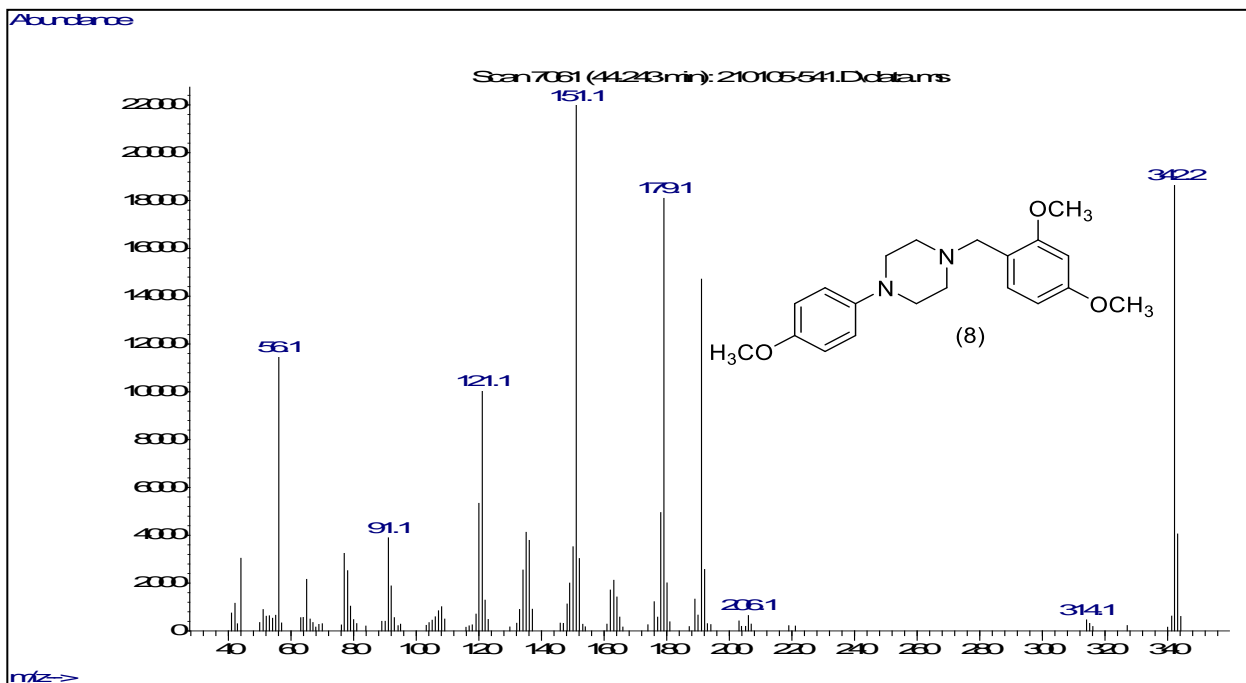
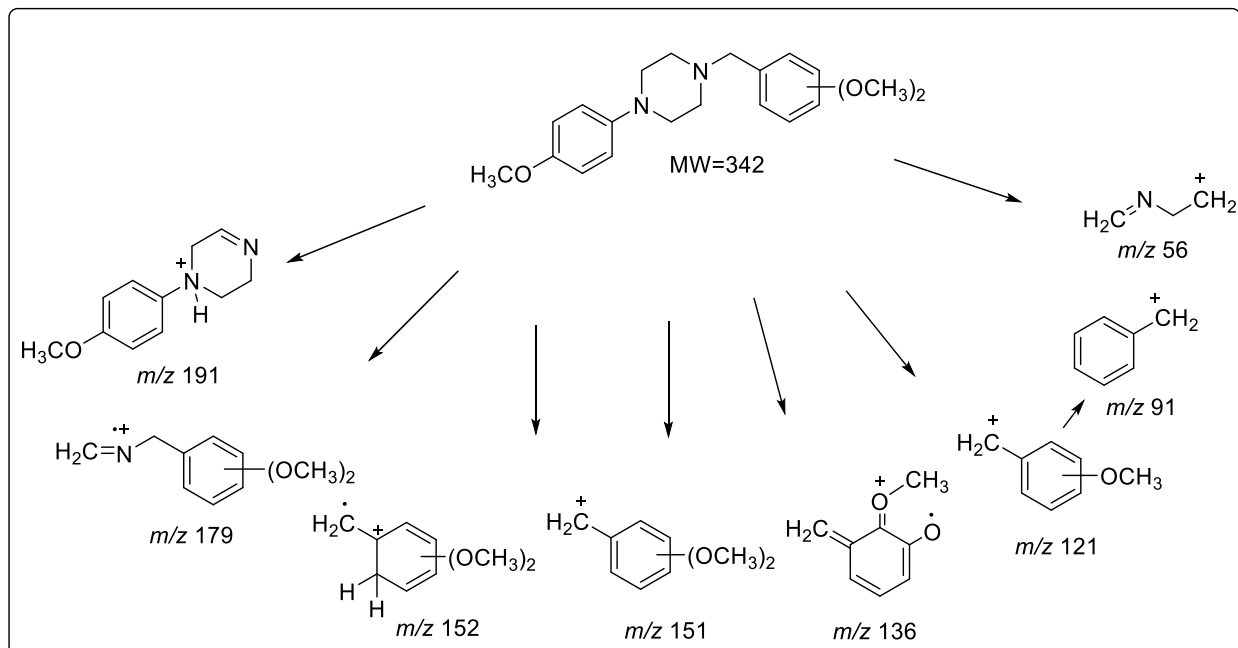


Figure 38. EI mass spectra of 1-(N- dimethoxybenzyl- 4- [4-methoxy phenyl piperazine) (Group 10)



Scheme 34. EI mass spectral fragmentation pattern of 1-(N-dimethoxybenzyl)-4-[4-methoxyphenyl]piperazine (Group 10)

3.10.2. Gas Chromatographic Separation

To differentiate the six regioisomers of this group, gas chromatographic separations were performed. The six compounds 1-(N-dimethoxybenzyl)-4-[4-methoxyphenyl]piperazine are differ in the dimethoxy substitution on the benzyl group. Gas chromatographic separation of the six compounds was carried out using a 30-meter capillary column coated with a 0.50 μm film of Rxi®-17Sil MS, a midpolarity phase; similar to 50% phenyl, 50% dimethyl polysiloxane. The compounds elute over approximately an 8-minutes window requiring a total run time of just over 58.0 minutes. The 2,3- dimethoxybenzyl isomer elutes first, followed by the 2,6- dimethoxybenzyl isomer, and last isomer elutes is the 3,5- dimethoxybenzyl isomer as shown in Figure (39).

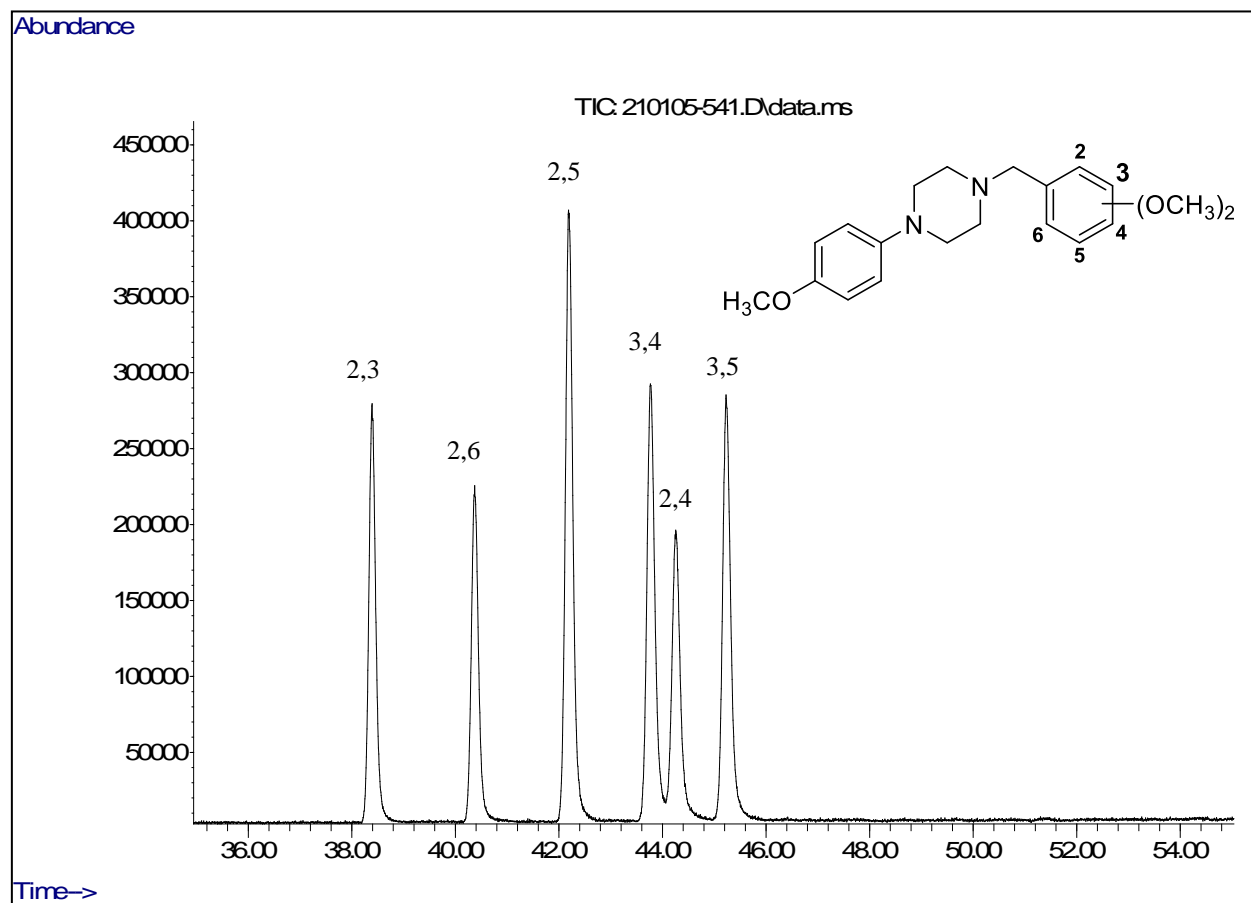
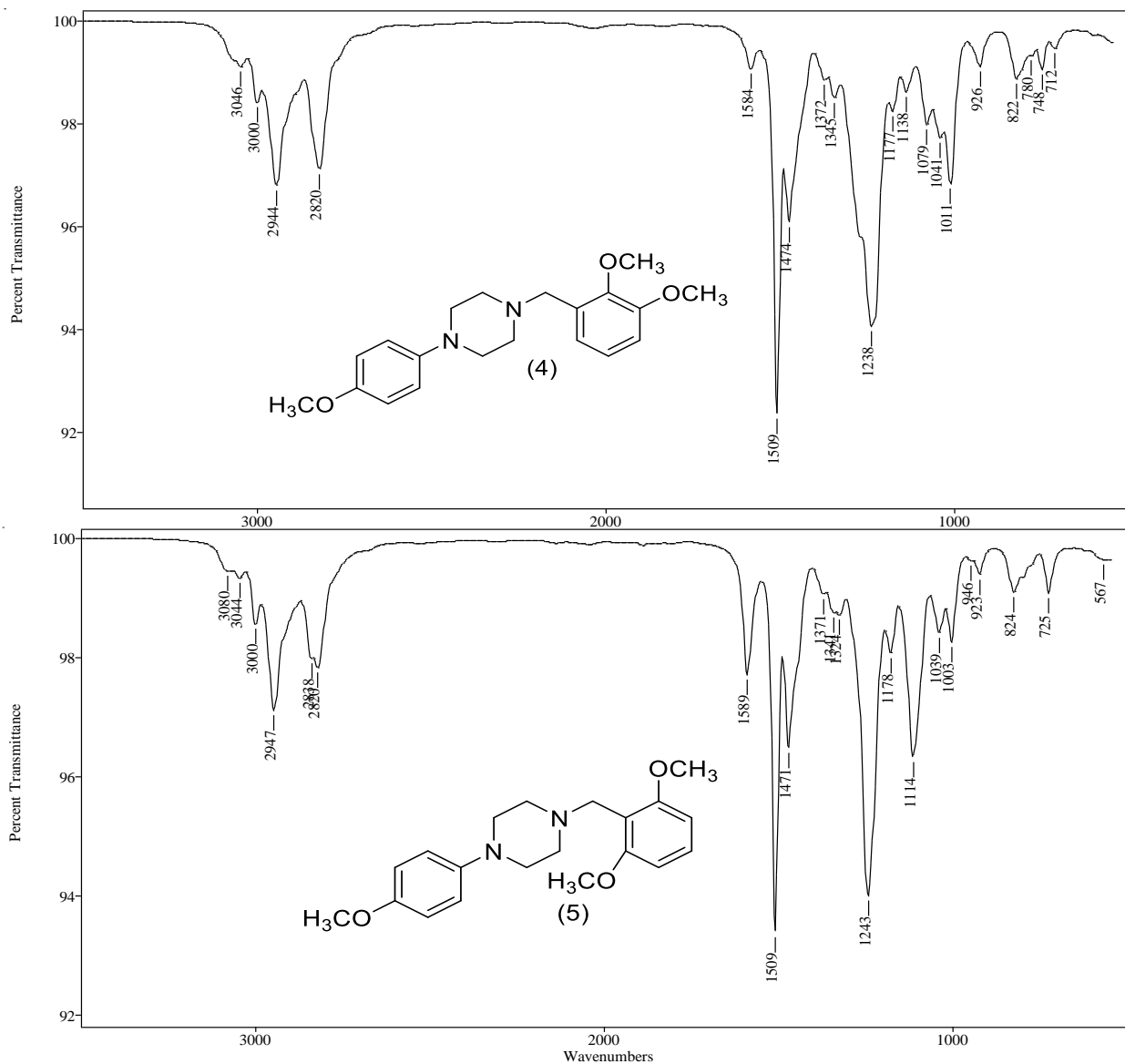


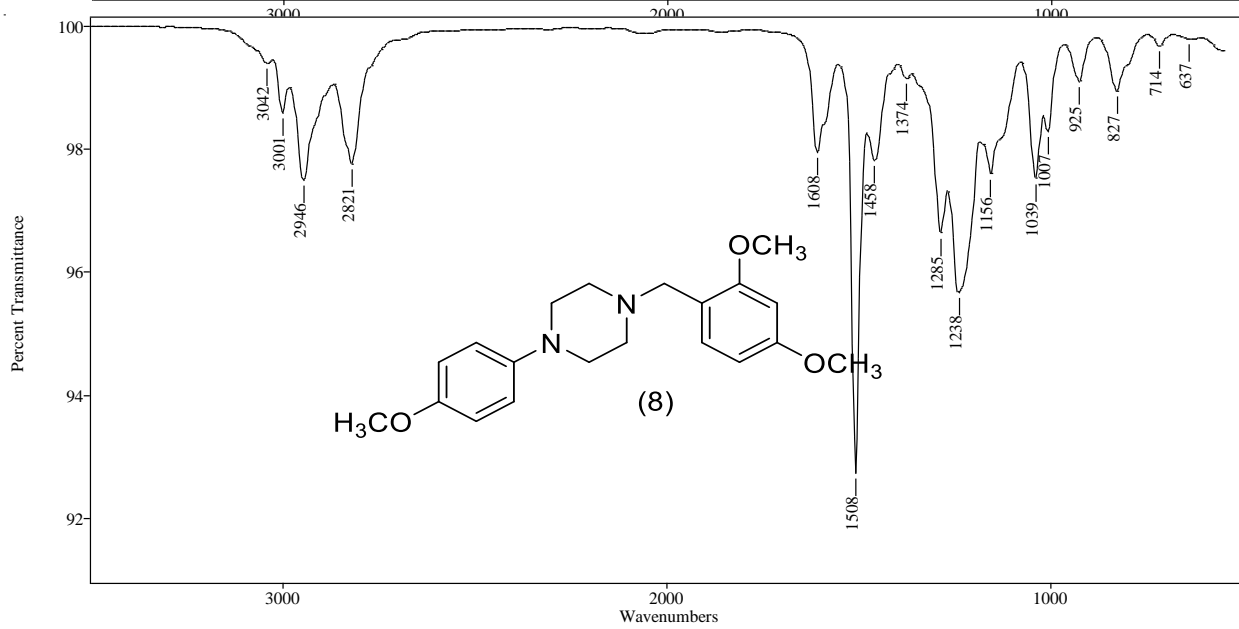
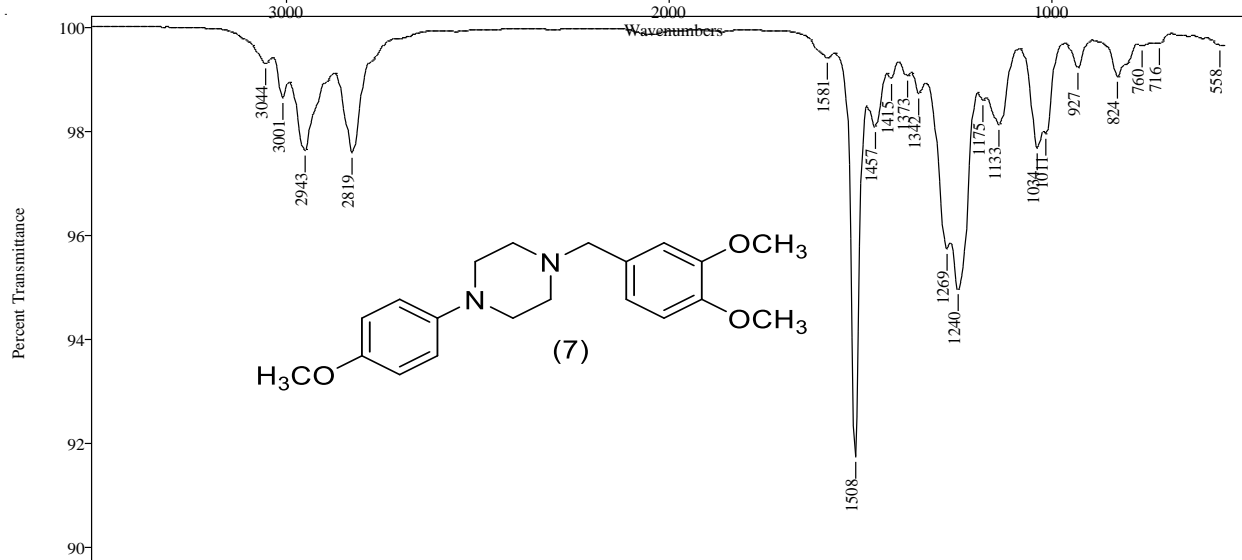
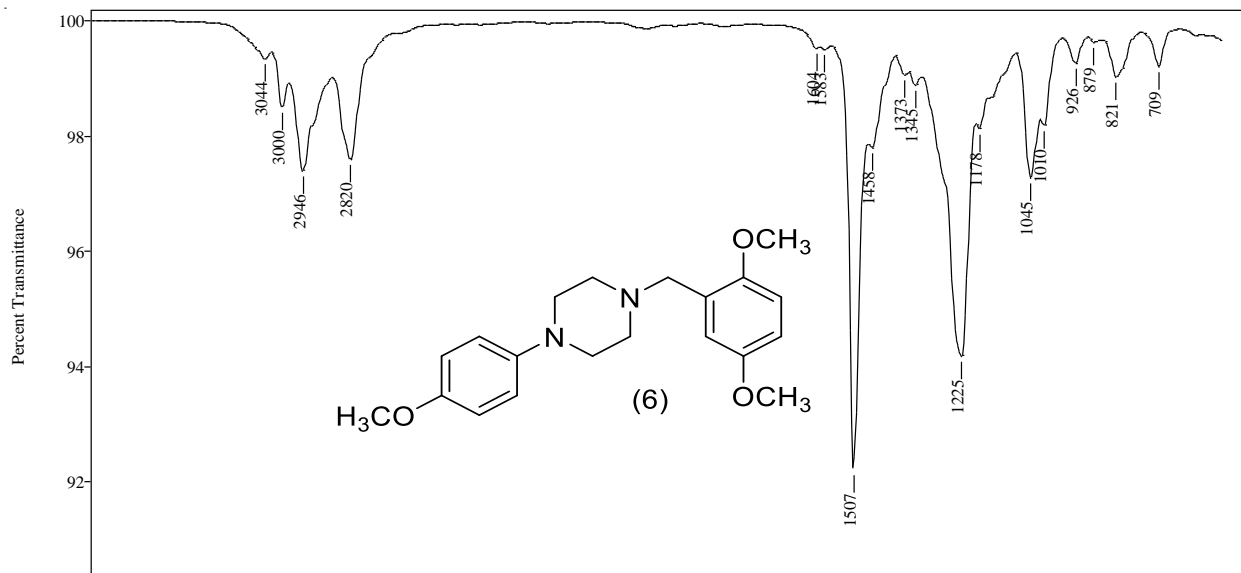
Figure 39. Gas chromatographic separation of 1-(N- dimethoxybenzyl- 4- [4-methoxy phenyl piperazine) (Group 10) using TP-7 program

3.10.3. Vapor-phase Infra-Red Spectrophotometry

Gas-chromatography coupled infrared detection (GC-IRD) was performed to differentiate between the six regioisomers of this group, Figure (40). All compounds display vapor phase IR spectrum with transmittance bands in the regions $580 - 1620 \text{ cm}^{-1}$ and $2810 - 3080 \text{ cm}^{-1}$. All six regioisomers have similar absorption bands in the region $2810 - 3080 \text{ cm}^{-1}$. The 2,3-dimethoxybenzyl isomer has broad absorption bands at 1238 cm^{-1} , and unique triple bands at $1011, 1041,$ and 1079 cm^{-1} . The 2,6- dimethoxybenzyl isomer has triple broad bands at $1156,$

1238, and 1285 cm^{-1} . The isomers 2,5- dimethoxybenzyl isomer and 2,4- dimethoxybenzyl isomer are sharing very tiny bands at 1581 cm^{-1} , but the 2,5- dimethoxybenzyl isomer differ by presence single broad band at 1225 cm^{-1} , while compound 2,4- dimethoxybenzyl isomer has double bands at 1240 and 1269 cm^{-1} . The 3,4- dimethoxybenzyl isomer is vary from all regioisomers in this group by presence two sharp bands at 1243 and 1509 cm^{-1} . The 3,5- dimethoxybenzyl isomer is the most characteristic compound in this group, it has doublet bands at 1153 and 1237 cm^{-1} , in addition to two sharp peaks at 1509 and 1598 cm^{-1} .





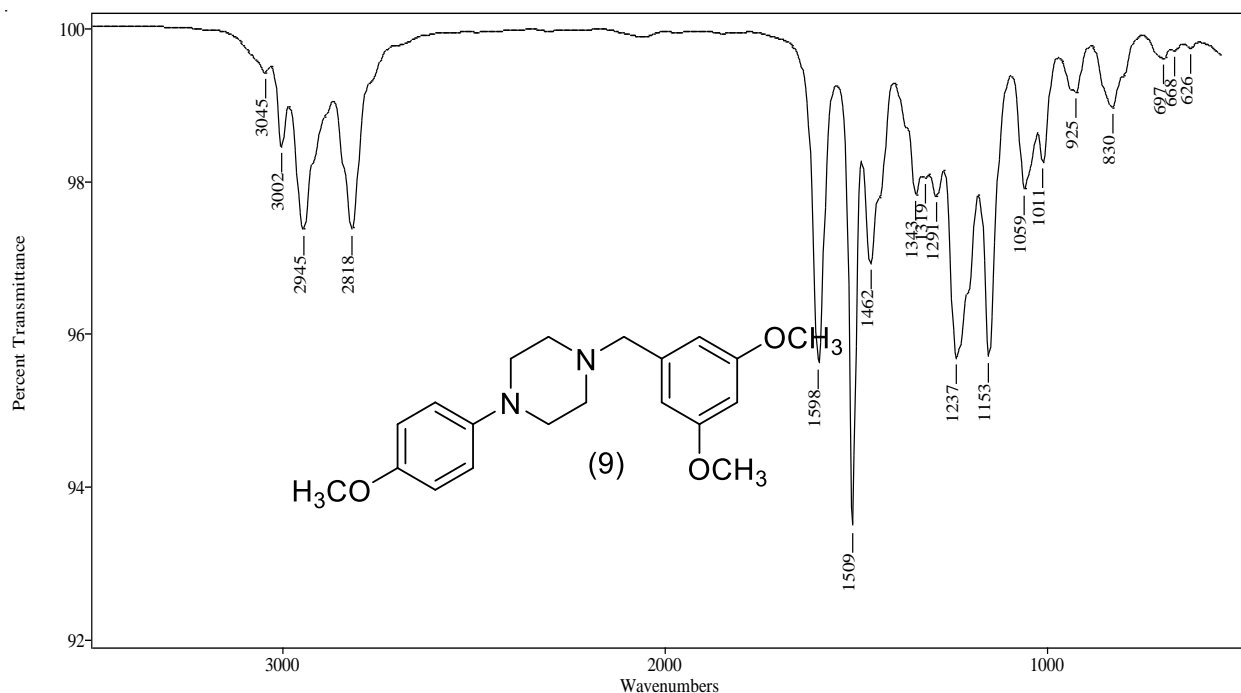


Figure 40. Vapor phase IR spectra of 1-(N-dimethoxybenzyl)-4-[4-methoxyphenyl]piperazine (Group 10)

3.10.4. Conclusions

The major EI-MS fragment ions occur via processes initiated by one of the two nitrogen atoms of the piperazine ring. The ion at m/z 191 observed in all nine spectra occurs from the loss of the substituted benzyl radical and the m/z 56 cation (C_3H_6N)⁺ is a characteristic piperazine ring fragment. The unique EI-MS fragments for the 2,3-dimethoxybenzyl- and 3,5-dimethoxybenzyl isomers at m/z 136 and m/z 152, respectively set apart these two compounds. The 2,3-dimethoxybenzyl isomer has broad absorption bands at 1238 cm^{-1} , and unique triple bands at 1011, 1041, and 1079 cm^{-1} . The 2,6-dimethoxybenzyl isomer has triple broad bands at 1156, 1238, and 1285 cm^{-1} . The isomers 2,5-dimethoxybenzyl isomer and 2,4-dimethoxybenzyl isomer are sharing very tiny bands at 1581 cm^{-1} , but the 2,5-dimethoxybenzyl isomer differ by presence single broad band at 1225 cm^{-1} , while compound 2,4-dimethoxybenzyl isomer has double bands

at 1240 and 1269 cm^{-1} . The 3,4- dimethoxybenzyl isomer is vary from all regioisomers in this group by presence two sharp bands at 1243 and 1509 cm^{-1} . The 3,5- dimethoxybenzyl isomer is the most characteristic compound in this group, it has doublet bands at 1153 and 1237 cm^{-1} , in addition to two sharp peaks at 1509 and 1598 cm^{-1} .

4. Materials and Methods of pharmacology

4.1. Chemicals and Reagents

MTT reagent Thiazolyl Blue Tetrazolium Bromide was obtained Tokyo Chemical Industry America. From Sigma Aldrich (St. Louis, MO), all the following chemicals were purchased: Phosphate buffer saline (PBS), Dimethylsulfoxide (DMSO), Nicotinamide adenine dinucleotide (NADH), 2', 7-dichlorofluoresceindiacetate (DCF-DA), Pyrogallol, Hydrogen Peroxide (H₂O₂), Phosphoric acid, o-phthalaldehyde (OPA), L-Glutathione reduced, Trichloroacetic acid, Thiobarbituric acid and Phenylmethanesulfonyl fluoride (PMSF). Fetal Bovine Serum (FBS), Dulbecco's Modified Eagle Medium (DMEM), Penicillin-Streptomycin Solution and Trypsin-EDTA solution were purchased from ATCC. Thermo Scientific Pierce 660 nm Protein Assay reagent kit was purchased (Pierce, Rockford, IL).

4.2. Rat dopaminergic neuron cells (N27)

To culture the neuronal cell line N27, the DMEM was prepared by adding Fetal Bovine Serum (10%) and Penicillin-Streptomycin Solution (1%) (Kovalevich and Langford 2013). The cytotoxicity (MTT) assay was performed by cultured the N27 cells in 75 cm² flasks at 37°C and 5% CO₂, after all the cells reached 80% confluency, they were detached by trypsinization. Then, the N27 cells were seeded in a 96 well plate at a density of 1 x 10⁵ cells/well, cells were used in 9-14 passages (Zheng et al. 2014).

4.3. Treatment design

To make 10mM stock solution, the compounds were dissolved in water according to molecular weight. All stock solutions were diluted to reach the appropriate concentrations to perform the experiments. Six different concentrations of 3-TFMPP, 3-TFMPPBz, MDBP, MDBzPP, BrDMP, and BrDMBzPP (1, 10, 100, 200, 500, 1000 μ M) were achieved by serial dilution in serum-enriched fresh culture medium to assess the neurotoxicity profile. To evaluate the neurotoxicity, N27 cells were exposed to different concentrations for 24, 48 hours, while to elucidate the mechanism of neurotoxicity of the novel piperazines derivatives, the N27 cells were exposed to 100 μ M and 1000 μ M of drug for 24 hours. Each experiment was done by using freshly prepared designer drugs solution.

4.4. Cytotoxicity Assay

To assess the neurotoxicity of piperazine compounds, the MTT assay was used as a quantitative measurement tool of the cell metabolic activity. This colorimetric assay works by reduction of the yellow-colored water-soluble tetrazole reagent, MTT (3-(4,5-dimethylthiazol-2-yl)-2,5-diphenyltetrazolium bromide) to an insoluble blue crystal formazan through succinate dehydrogenases. The insoluble crystals formazan are quantified calorimetrically at 570nm (Berridge, Herst, and Tan 2005; Mosmann 1983). After incubation with compounds for 24 and 48 hours, each well of cultured cells received 200 μ L of 12mM MTT solution accompanied with fresh culture medium. The MTT solution was incubated for 2 hours at 37°C, then evacuated the medium and 200 μ L of DMSO was placed to solubilize the formazan crystal and kept for 10 minutes. The absorbance was measured at 570 nm using a microtiter plate reader (Synergy HT, Bio-Tek

Instruments Inc., Winooski, VT, USA). Results were expressed graphically as % cell viability (Zhang et al. 2014).

4.5. Protein quantification

Protein quantification was accomplished using Thermo Scientific Pierce 660 nm Protein Assay reagent kit (Pierce, Rockford, IL). Bovine serum albumin (BSA) was used as a standard for protein measurement.

4.6. Quantifying Reactive Oxygen Species

The evaluation of reactive oxygen species formation was estimated spectrofluorometrically at excitation wavelength of 492 nm and emission wavelength of 527 nm, by measuring the transformation of non-fluorescent chloromethyl-DCF-DA (2', 7- 32 dichlorofluoresceindiacetate, DCF-DA) to fluorescent DCF. N27 cell homogenates were treated by piperazine solution compounds then incubated for with 0.05% w/v solution of DCFDA in ethanol (10 µl), and phosphate buffer (150 µl) at 37°C for 1 hour. The fluorescent product DCF was measured using BioTek Synergy HT plate reader (BioTek, VT, USA). Results were expressed as percentage change from the control (Dhanasekaran, Tharakan, and Manyam 2008).

4.7. Nitrite assay

Nitrite and nitrate are the final products of nitric oxide oxidation pathways and these inorganic compounds used as an expression of nitric oxide production. By using Griess reagent, NO₂ reacts

with sulfanilamide under acidic condition leading to the production of diazonium ions. The diazonium ion association with N-(1-naphthyl) ethylenediamine form 36 chromophoric azo product that can be measured spectrophotometrically at 545 nm (Giustarini et al. 2008).

4.8. Quantification of hydrogen peroxide

A hydrogen peroxide standard curve was obtained utilizing fluorimetric plate reader (BioTek Synergy HT plate reader, BioTek, VT, USA) at 335nm (excitation wavelength) and 390nm (emission wavelength). Hydrogen peroxide content in control and drugs treated cells supernatant was calculated from slope obtained from standard curve. Results were expressed as hydrogen peroxide uM/mg protein (Ahuja, Buabeid, Abdel-Rehman, et al. 2017).

4.9. Tyrosine hydroxylase (TH) activity

The rate limiting step enzyme in the biosynthesis of dopamine, norepinephrine and epinephrine is aromatic hydroxylation by tyrosine hydroxylase. The substrate, tyrosine was added to the control and drugs treated cells supernatant and incubated for 30 minutes result in the formation of levodopa by tyrosine hydroxylase present in the sample. Following the above reaction, sodium periodate was added to the solution. The formed L-dopa in the control and drugs treated cells supernatant reacts with sodium periodate to form dopaquinone. Dopaquinone was measured spectrophotometrically at 475nm (Vermeer et al. 2013).

4.10. Monoamine oxidase (MAO) activity

To assess the monoamine oxidase activity, we measured the amount of 4-hydroxyquinoline formed as a result of kynuramine oxidation fluorometrically (Morinan and Garratt 1985) was measured. MAO activity was calculated as 4-hydroxyquinoline formed/hour/mg protein (Albano, Muralikrishnan, and Ebadi 2002; Muralikrishnan and Mohanakumar 1998).

4.11. Quantification of NADH content

A standard curve for NADH was obtained using a spectrophotometric plate reader (BioTek Synergy HT plate reader, BioTek, VT, USA) and was measured at 340nm. NADH content was calculated from the slope obtained from the standard curve. The results were expressed as NADH μ M/mg protein (Ahuja, Buabeid, Abdel-Rahman, et al. 2017).

4.12. Glutathione Content

The reaction of GSH and 34 o-phthalaldehyde (OPT) reaction produces a fluorescence product that can be measured spectrofluorometrically (Cohn and Lyle 1966). We mixed the cell homogenates were mixed with 0.1 M phosphoric acid to induce the protein precipitate, followed by centrifuging the samples at 12000 RPM for 10 minutes. Next the supernatant was incubated with 0.1% OPT for 20 minutes at room temperature, then the fluorescence measured at an excitation wavelength of 340 nm and an emission wavelength of 420 nm. A GSH standard curve

was prepared from commercially acquired GSH. The GSH content was calculated as mmol of GSH/ μ g protein (Muralikrishnan and Mohanakumar 1998).

4.13. Mitochondrial Complex-I Activity

Complex-I (NADH dehydrogenase) is the major constituent of respiratory chain which catalyzes the oxidation of NADH to NAD⁺. NADH dehydrogenase activity on N27 cells was determined spectrophotometrically at 340 nm, by mixing the cell homogenate with phosphate buffered saline and NADH. NADH oxidation was measured by the decrease in absorbance at 340 nm for 3 minutes. A standard curve was composed of commercially obtained NADH (Ramsay et al. 1986).

4.14. Statistical Analysis

Data were reported as mean \pm SEM. Statistical analysis was accomplished using one-way analysis of variance (ANOVA) followed by Dunnet's multiple comparisons test ($p < 0.05$) was considered to be statistically significant. Statistical analysis was performed using Prism-V software (La Jolla, CA, USA).

5. Pharmacology results

5.1. Piperazine derivatives induced dose-dependent and time-dependent reduction of dopaminergic (N27) cell viability

Piperazine based designer drugs have been abused to exert stimulant effect which resembles the well-known drugs of abuse (amphetamine, MDMA) by interacting with monoaminergic neurotransmission. Many piperazine derivatives have been reported as neurotoxic agents that led to dopaminergic neuronal death. BZP, 3-TFMPP, MDBP, and BrDMBP are considered the main abused piperazines available on the black market. In this study, we compared the neurotoxicity of reported piperazine derivatives to novel piperazine derivatives. N27 dopaminergic cells were treated with different doses (1, 10, 100, 200, 500, 1000 μ M) of piperazine derivatives (3-TFMPP, 3-TFMPPBz, MDBP, MDBzTFMPP, BrDMBP, and BrDMBzTFMPP) for 24 and 48 hours. The well-known neurotoxic piperazine derivatives 3-TFMPP was used as a positive control (Majrashi et al. 2018a). The piperazine derivatives used in this study induced differential dose-dependent and time-dependent reduction of dopaminergic neuronal viability compared to control ($n=30$, $p<0.0001$), Figure (41), Figure (42), and Figure (43). Treatment of N27 with well-known drug of abuse, 3-TFMPP, for 24 and 48 hours exhibited dose-dependent decrease in dopaminergic neuronal viability (90% reduction with 500 μ M and 1000 μ M in 24 hrs, $p<0.0001$). While the novel piperazine derivatives 3-TFMPPBz showed more significant reduction in neuronal viability when treated with same dose of 200 μ M induced 75% reduction in 24 hrs, and almost 95% reduction with 500 μ M and 1000 μ M) Figure (41).

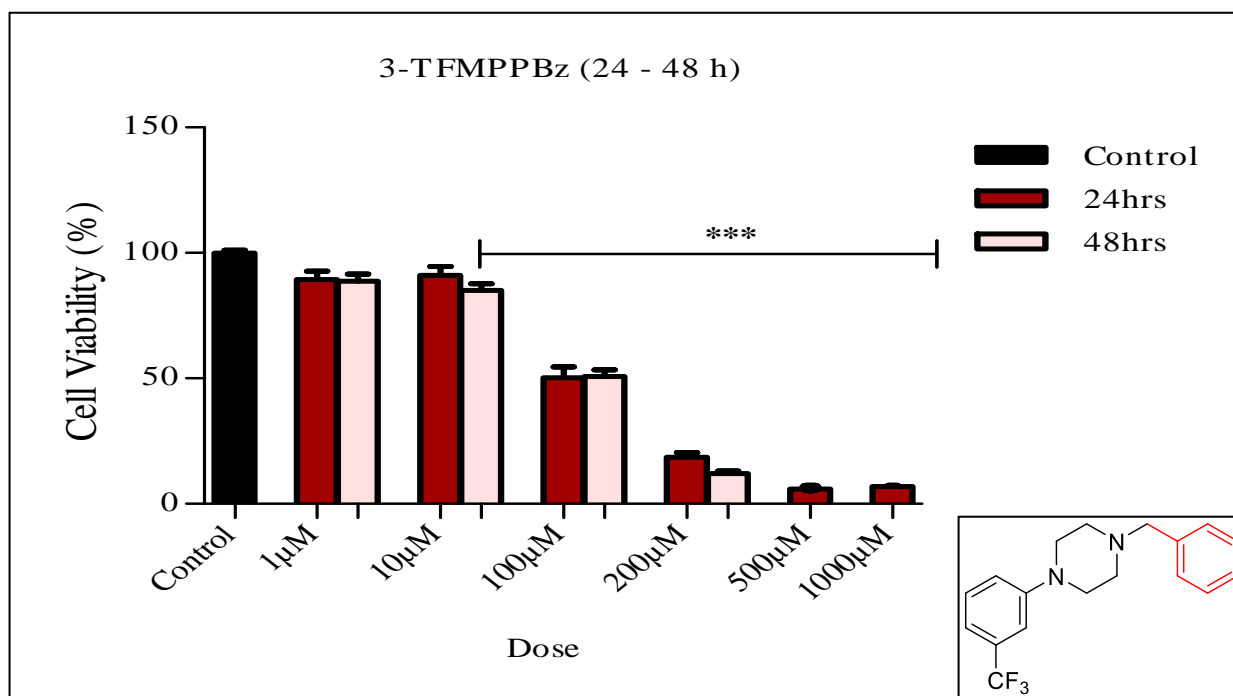
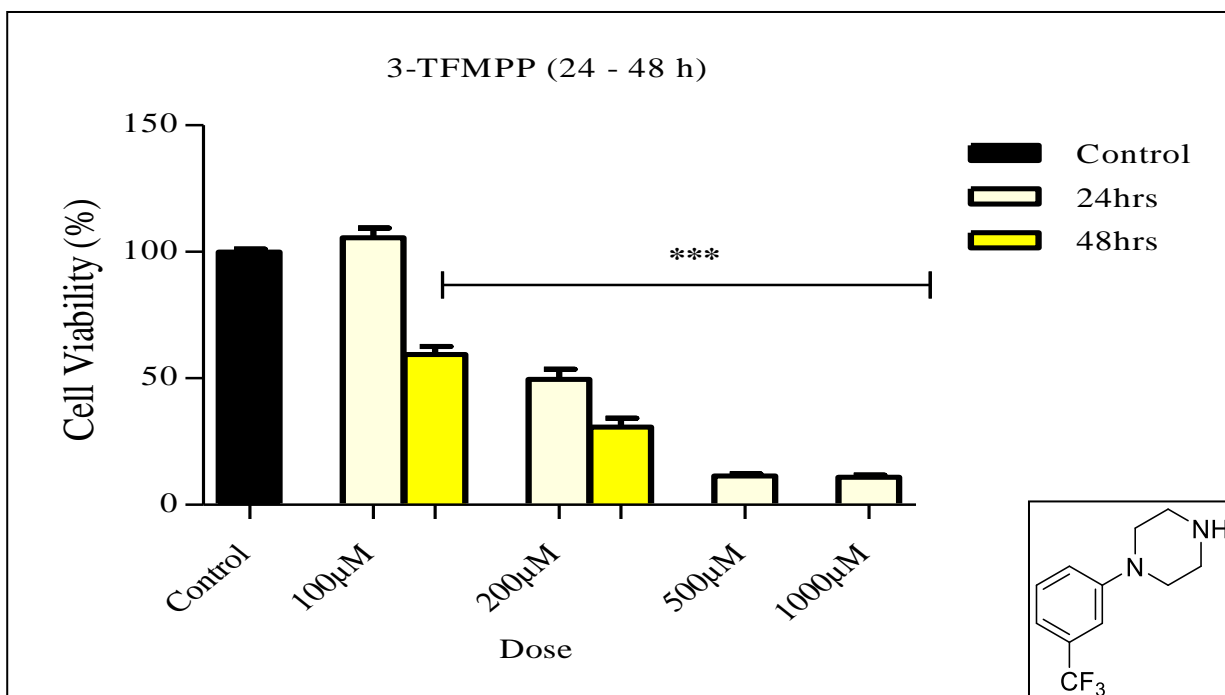
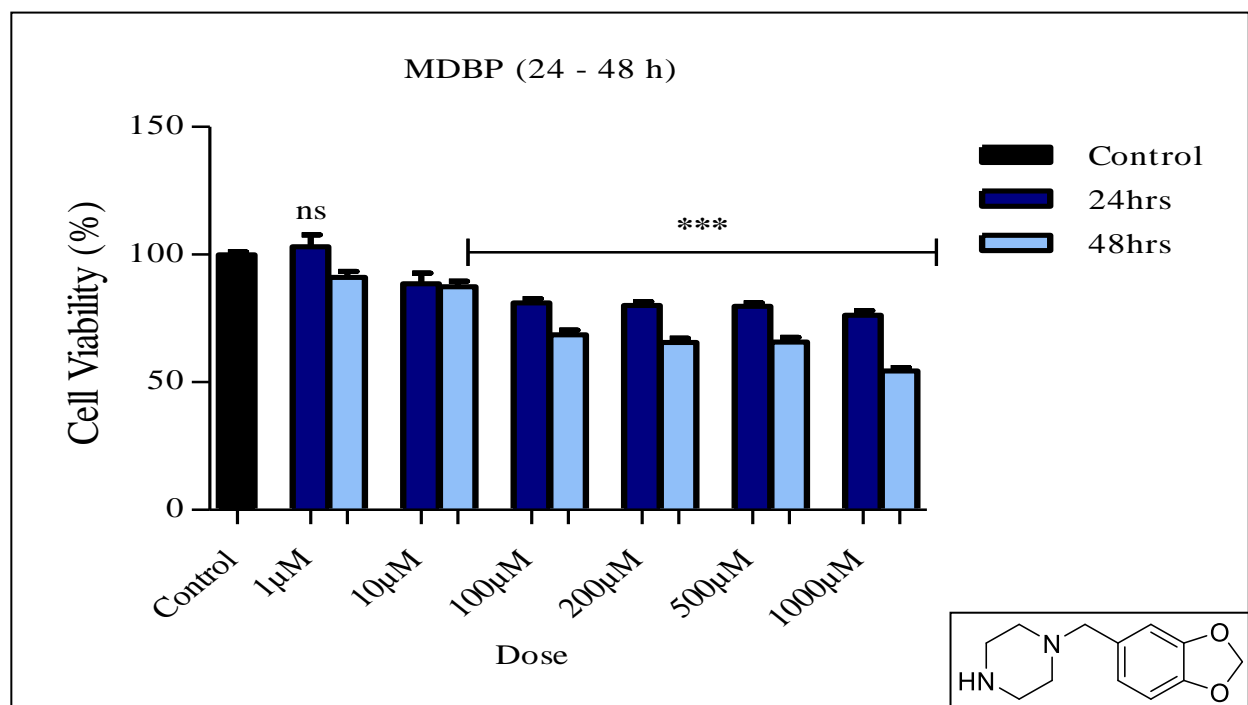


Figure 41. Effect of 3-TFMPP and 3-TFMPPBz on dopaminergic (N27) cells

Dopaminergic neuronal viability was evaluated through the MTT reduction assay. Results are expressed as percentage control \pm SEM. Statistical comparisons were made using one-way ANOVA/ Dunnet's multiple comparison tests. Note (*) indicates a statistically significant difference when compared to the control (***) $p < 0.001$, $n=30$)

The second set of compounds, MDBP and MDBzTFMPP demonstrated dose-dependent reduction in N27 dopaminergic neuronal viability at 24 and 48 hours. The reported drug of abuse MDBP (Arbo, Bastos, and Carmo 2012a) exhibited limited neurotoxicity (15% reduction in 24 hrs, 25% reduction in 48 hrs at 200 μ M, and 30% reduction at 500 μ M and 45% at 1000 μ M in 48 hrs). On the other hand, the novel piperazine derivatives MDBzTFMPP indicated higher and significant reduction in N27 dopaminergic neuronal cell viability when treated with same dose 75% reduction in 24 hrs, 80% reduction in 48 hrs, and almost 90% reduction with 500 μ M and 1000 μ M) Figure (42).



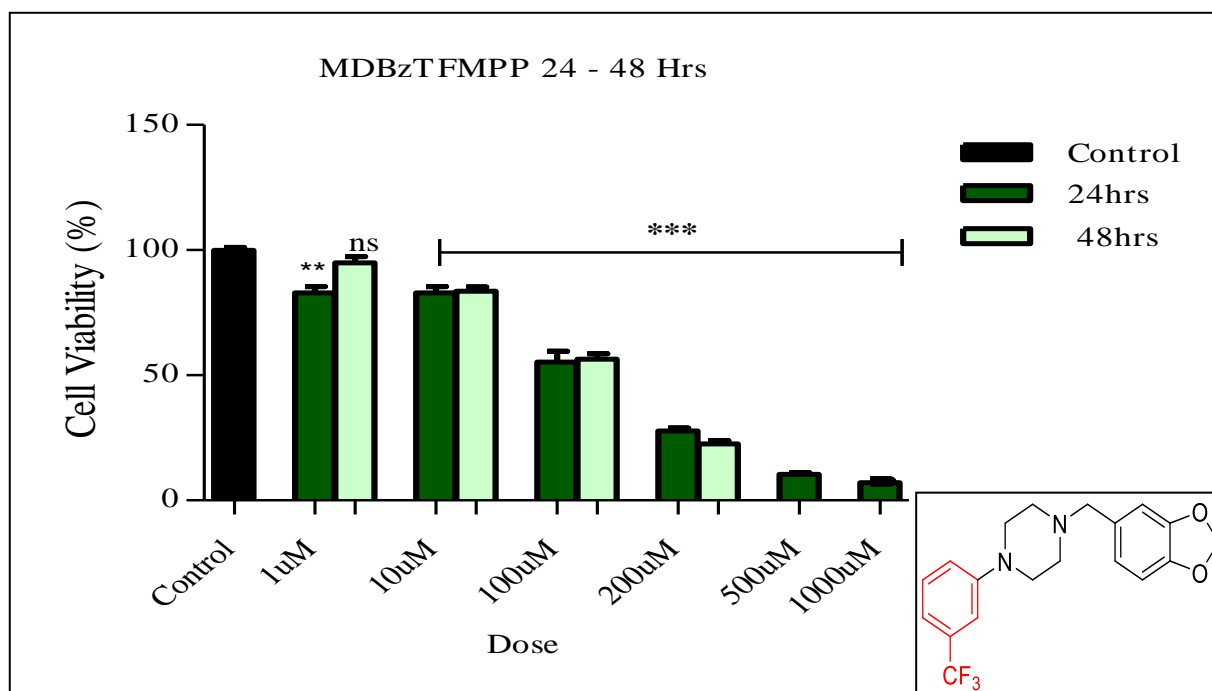


Figure 42. Effect of MDBP and MDBzTFMPP on dopaminergic (N27) cells

Dopaminergic neuronal viability was evaluated through the MTT reduction assay. Results are expressed as percentage control \pm SEM. Statistical comparisons were made using one-way ANOVA/ Dunnet's multiple comparison tests. Note (*) indicates a statistically significant difference when compared to the control (** $p < 0.01$, *** $p < 0.001$, $n=30$)

The third set of compounds, BrDMP and BrDMBzTFMPP also demonstrated dose-dependent significant decrease in dopaminergic neuronal viability. The reported drug of abuse BrDMP (Westphal et al. 2009) exhibited lower dopaminergic neurotoxicity (10% reduction in 24 hrs, 15% reduction in 48hrs at 200 μ M , but almost 85% reduction at 500 μ M and 90% at 1000 μ M in 48 hrs). Conversely, the novel piperazine derivatives BrDMBzTFMPP indicated higher and significant dopaminergic neurotoxicity, with 75% reduction in 24 hrs, 80% reduction in 48 hrs, and almost 90% reduction with 500 μ M and 1000 μ M) Figure (43).

To assess the neurotoxic mechanisms of reported drug of abuse 3,4-methylenedioxy benzyl piperazine (MDBP) and the novel MDBP derivative 3,4-methylenedioxybenzyl-3-trifluoromethylphenylpiperazine (MDBzTFMPPP) was evaluated. Among the six tested piperazine compounds, the MDBP exhibited the lowest neurotoxic effect on N27 dopaminergic neuronal cells. In contrast, the new derivative MDBzTFMPPP demonstrated a significantly higher neurotoxicity effect when compared to the parent compound MDBP. We evaluated the role of oxidative stress and mitochondrial dysfunction associated with the dopaminergic neurotoxicity induced by piperazine derivatives (MDBP and MDBzPP) after 24 hours of exposure. Based on the MTT assay, we choose two doses to investigate the neurotoxic dopaminergic mechanisms, the MDBP low dose at 100 μM (LD=100 μM) and the high dose at 1000 μM (HD=1000 μM). While the new derivative MDBzTFMPPP with low dose at 10 μM (LD=10 μM), and a high dose at 200 μM (HD= 200 μM).

5.2. MDBP and MDBzTFMPP generated ROS production

Generally, generation of ROS is connected to human illnesses such as neurodegenerative disorders atherosclerosis, and renal toxicity. The destruction of biological macromolecules such as DNA, protein and lipids occurs by oxidative stress that resulted from the generation of ROS. Antioxidants such as catalase, superoxide dismutase and glutathione can neutralize the harmful effects of ROS (Freeman and Crapo 1982). MDBP (HD) and MDBzTFMPP (LD and HD) significantly increased ROS generation in N27 dopaminergic neuronal cells as compared to the control ($n = 5$, $p < 0.0005$; Figure (44)).

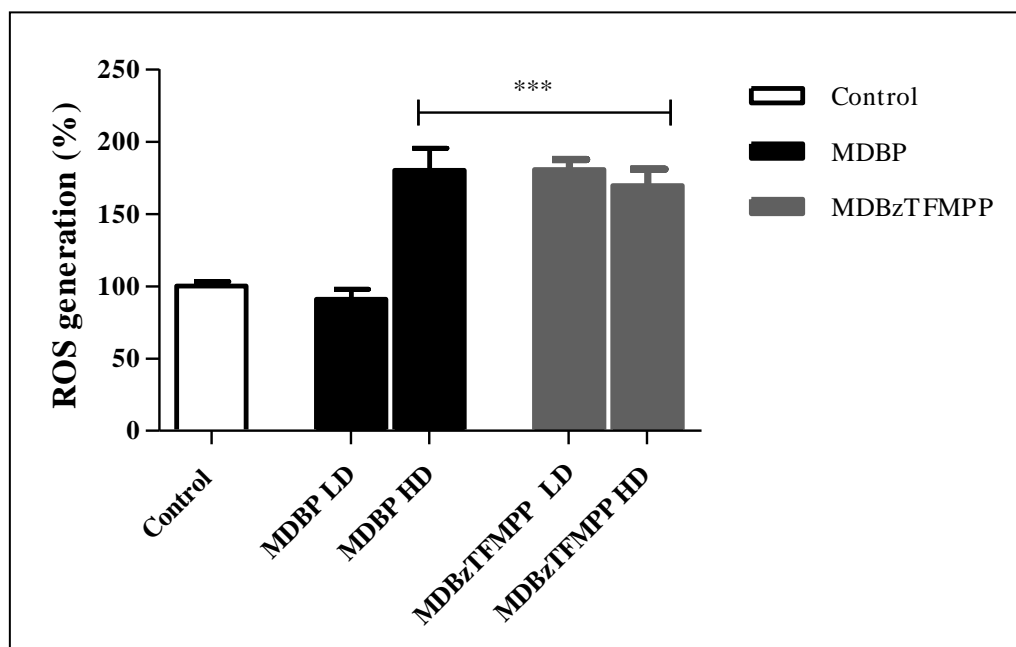


Figure 44. Effect of MDBP and MDBzTFMPP on ROS generation in N27 dopaminergic neuronal cells

MDBP and MDBzTFMPP induced oxidative stress by generating reactive oxygen species in N27 dopaminergic neuronal cells after 24 hours. The fluorescent product DCF was measured spectrofluorometrically. MDBP (HD) and MDBzTFMPP (both the doses) showed a significant increase in ROS generation (***p* < 0.001, *n*=5). Results are expressed as control ± SEM. Statistical comparisons were made using one-way ANOVA/Dunnet's multiple comparison tests.

5.3. MDBzTFMPP significantly increased the nitrite production

Many studies revealed that patient with Parkinson's disease have a high percent of nitric oxide production. This nitric oxide may lead to oxidative stress eventually causing dopaminergic neuronal damage (Qureshi et al. 1995). MDBzTFMPP (HD) significantly increased the nitrite production in N27 dopaminergic neuronal cells as compared to the control (***p* < 0.001, *n* = 5)

Figure (45).

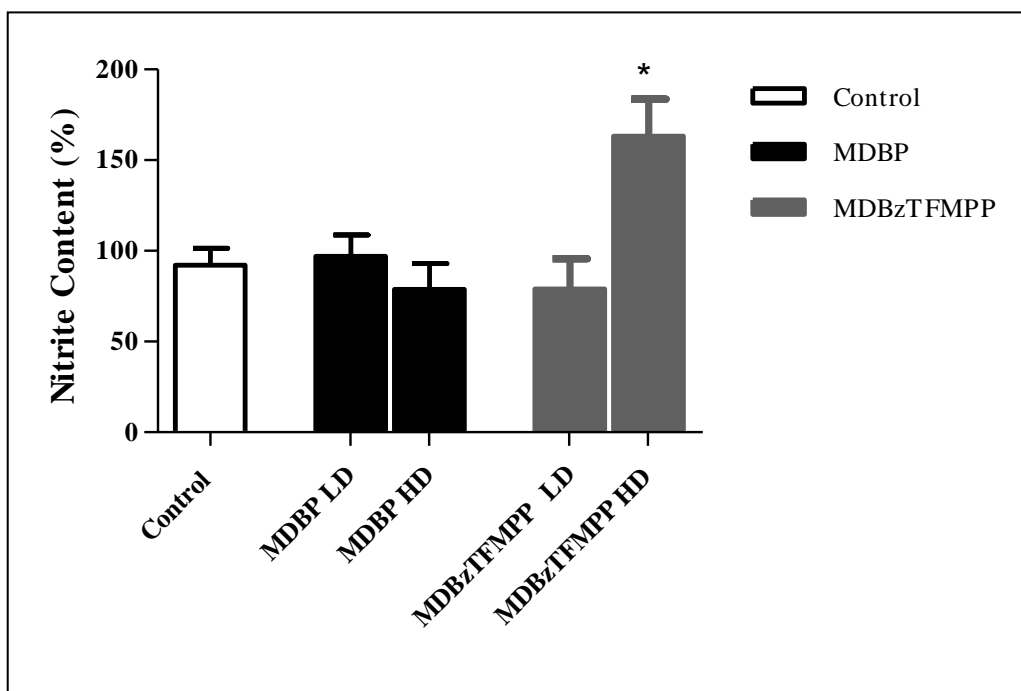


Figure 45. Effect of MDBP and MDBzTFMPP on Nitrite production in N27 neuronal cells

MDBzTFMPP significantly increase nitrite production in N27 dopaminergic neuronal cells after 24 hours (* $p < 0.05$, $n=5$). Nitrite production was determined spectrophotometrically at 540 nm. Results are expressed as control \pm SEM. Statistical comparisons were made using one-way ANOVA/Dunnet's multiple comparison tests

5.4. MDBP and MDBzTFMPP increased the production of H_2O_2

Oxidative stress results from an imbalance between the free radical scavengers and ROS, resulting in the release/production of more free radical species. The exposure of neurons to reactive / toxic free radical such as H_2O_2 leads to neurotoxicity and this mechanism is linked to many neurodegenerative diseases such as Alzheimer's disease and Parkinson's disease (Karuppagounder et al. 2014). MDBP (HD) and MDBzTFMPP (both the doses) significantly induced increases in H_2O_2 production in N27 dopaminergic neuronal cells as compared to the control ($n = 5$, $p < 0.0005$; Figure (46).

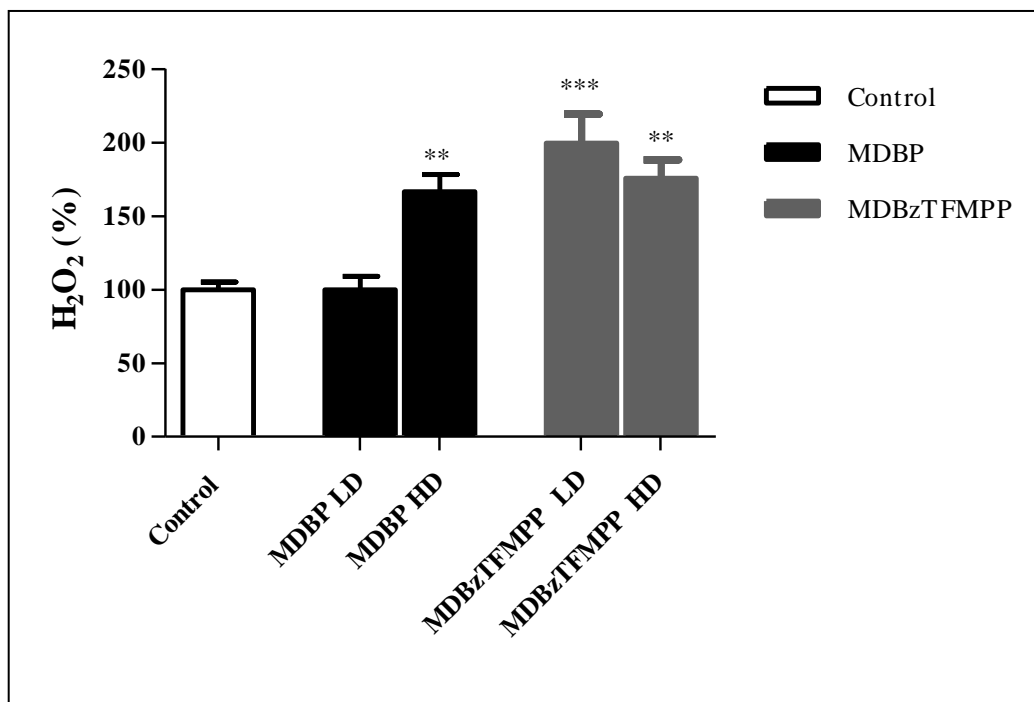


Figure 46. Effect of MDBP and MDBzTFMPP on H₂O₂ production in N7 neuronal cells

MDBP and MDBzTFMPP increase the production of H₂O₂ in N27 dopaminergic neuronal cells after 24 hours (**p < 0.01, ***p < 0.001, n=5). Results are expressed as control ± SEM. Statistical comparisons were made using one-way ANOVA/Dunnet's multiple comparison tests

5.5. MDBP significantly increased the GSH content

Glutathione is an antioxidant that scavenger the free radicals and protect cells from their harmful effect. MDBP (HD) significantly induced dose-dependent increase in GSH content in N27 dopaminergic neuronal cells as compared to the control (n=5, p< 0.0001); Figure (47).

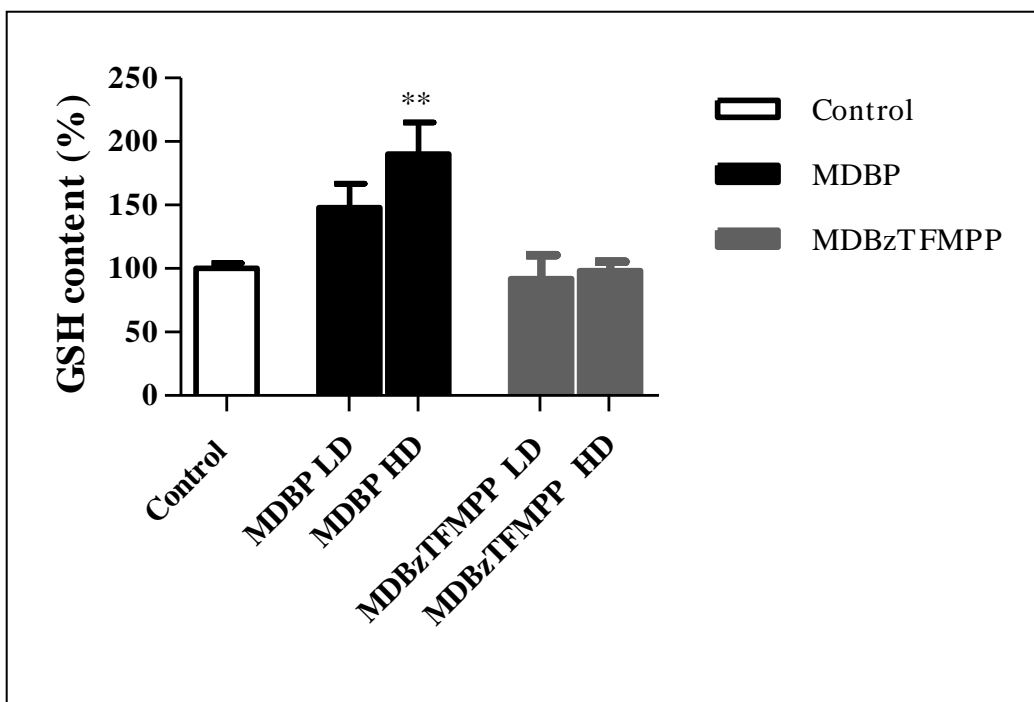


Figure 47. Effect of MDBP and MDBzTFMPP derivatives on GSH content in N27 neuronal cells

MDBP significantly induced dose-dependent increase GSH content in N27 dopaminergic neuronal cells after 24 hours (** $p < 0.01$, $n=5$). The condensation reaction between GSH and ophthalaldehyde (OPT) produce fluorescence at pH 8.0 that was measured spectrofluorometrically. Results are expressed as control \pm SEM. Statistical comparisons were made using one-way ANOVA/Dunnet's multiple comparison tests.

5.6. MDBP and MDBzTFMPP did not affect the Tyrosine Hydroxylase activity

The enzyme tyrosine hydroxylase modulates the biosynthesis pathways of catecholamines (dopamine, norepinephrine, and epinephrine). MDBP and MDBzPP did not affect the tyrosine hydroxylase activity Figure (48).

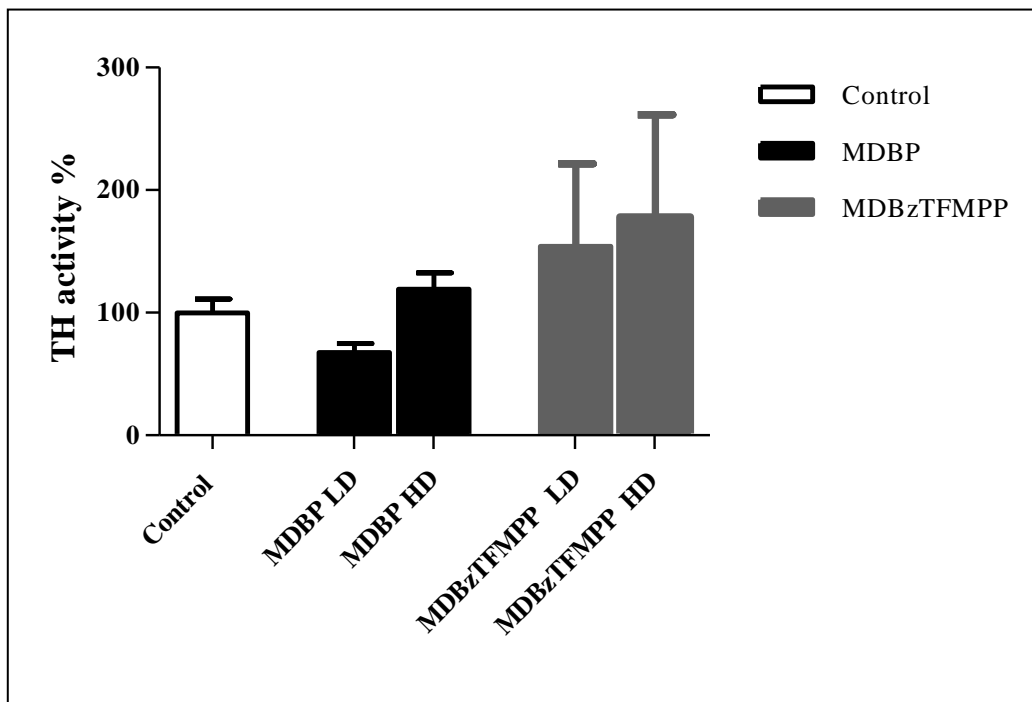


Figure 48. Effect of MDBP and MDBzTFMPP on the tyrosine hydroxylase TH activity in N27 neuronal cells

MDBP and MDBzTFMPP did not affect TH activity in N27 dopaminergic neuronal cells after 24 hours ($p \geq 0.05$, $n=5$). Results are expressed as control \pm SEM. Statistical comparisons were made using one-way ANOVA/Dunnett's multiple comparison tests.

5.7. MDBP and MDBzTFMPP decreased Monoamine oxidase (MAO) activity

Monoamine oxidase activity influences oxidative stress, apoptosis, glial activation, and the aggregated protein clearance. Furthermore, MAO activity has been connected to neurodegenerative diseases (Youdim and Lavie 1994), (Merad-Boudia et al. 1998). MDBP and MDBzTFMPP significantly decreased the MAO activity as compared to the control ($n = 5$, $p < 0.0005$; Figure (49)).

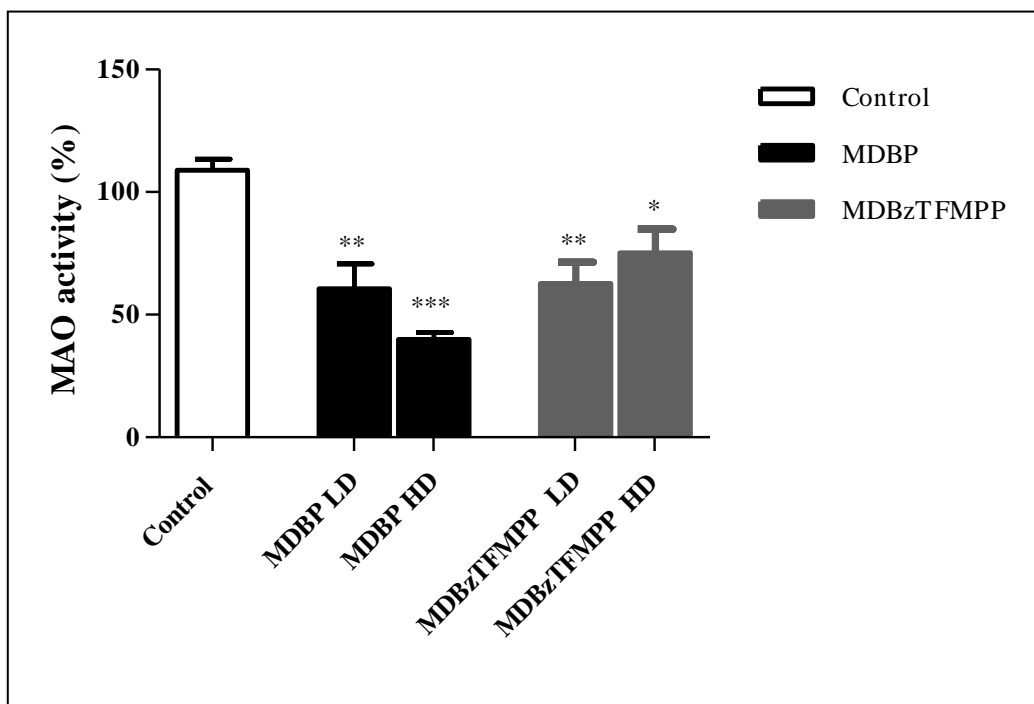


Figure 49. Effect of MDBP and MDBzTFMPP on mitochondrial monoamine oxidase (MAO) activity in N27 neuronal cells

MDBP (high dose) caused a significant decrease in MAO activity (* $p < .05$, ** $p < .01$, *** $p < 0.001$, $n=5$). Total MAO activity was determined fluorimetrically at 315 nm excitation / 380 nm emission. Results are expressed as control \pm SEM. Statistical comparisons were made using one-way ANOVA/Dunnet's multiple comparison tests

5.8. MDBzTFMPP significantly decreased the Mitochondrial Complex-I activity

Mitochondria are considered as a regulator of cell viability because respiration of mitochondrial is responsible for the production of energy (ATP). Many disorders such as Parkinson's disease, Alzheimer's disease and Huntington's disease have been associated with mitochondrial dysfunction and NADH depletion (Michael T Lin and Beal, 2006). MDBzTFMPP significantly induced dose-dependent decrease in the mitochondrial Complex I activity in N27 dopaminergic neuronal cells as compared to the control ($n = 5$, $p < 0.0005$), Figure (50.a). However, both the drugs had no effect on NADH content.

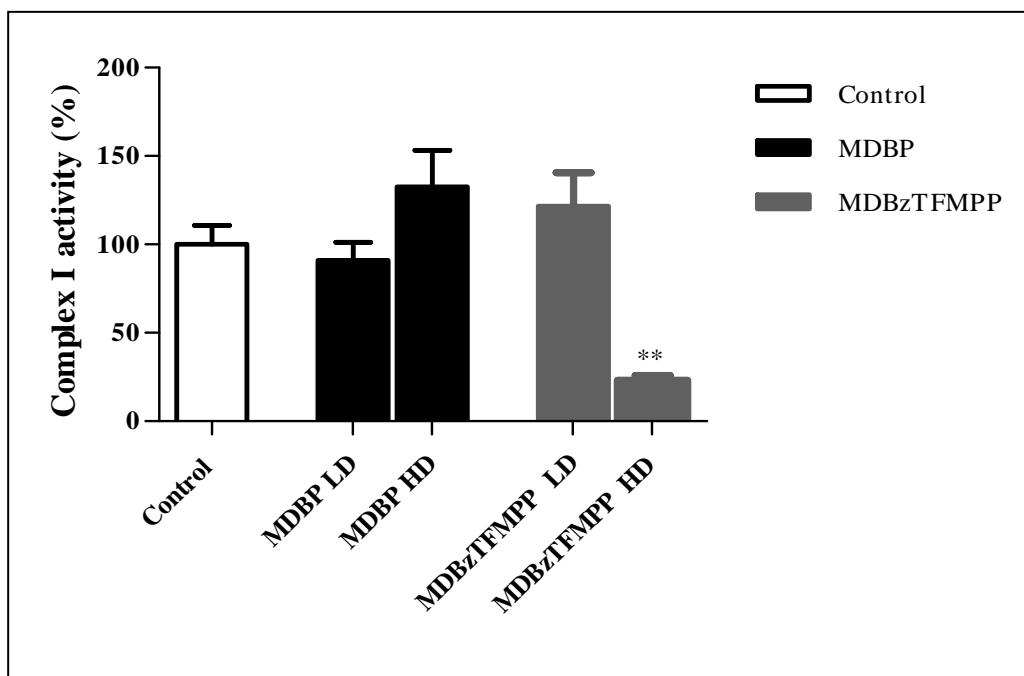


Figure 50.a. Effect of MDBP and MDBzTFMPP on Mitochondrial Complex-I activity in N27 neuronal cells

MDBzTFMPP significantly induced dose-dependent decrease in Complex I (** $p < 0.01$, $n=5$). Mitochondrial Complex-I activity was measured spectrophotometrically. Results are expressed as control \pm SEM. Statistical comparisons were made using one-way ANOVA/Dunnet's multiple comparison tests.

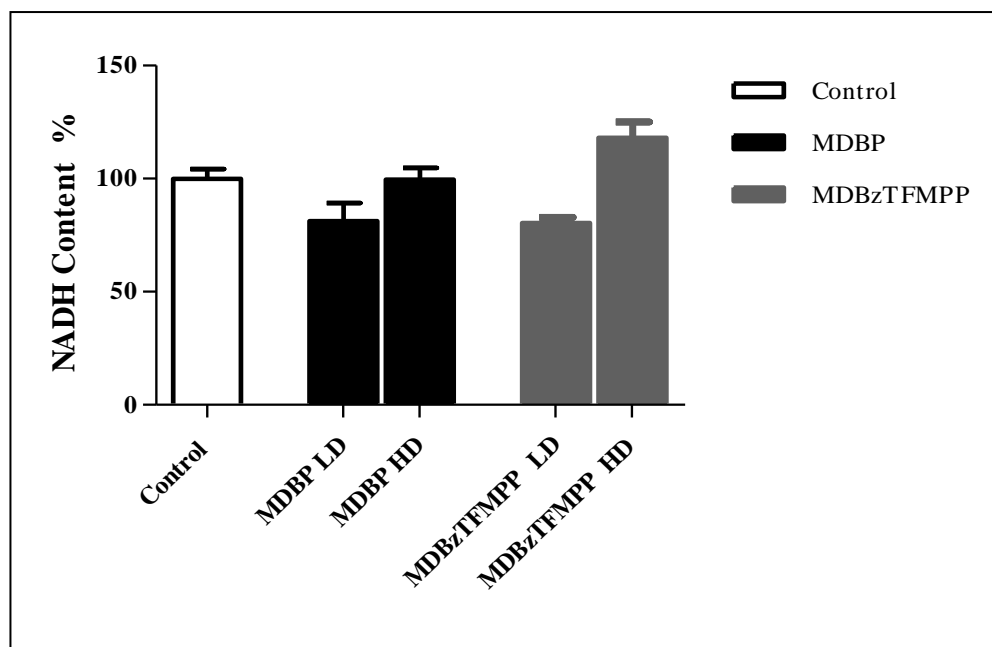


Figure 51.b. Effect of MDBP and MDBzTFMPP on NADH activity in N27 neuronal cells

MDBP and MDBzTFMPP did not affect NADH activity in N27 dopaminergic neuronal cells after 24 hours ($p \geq 0.05$, $n=5$). Results are expressed as control \pm SEM. Statistical comparisons were made using one-way ANOVA/Dunnet's multiple comparison tests.

6. Discussion of pharmacology studies

Novel piperazine designer drugs were synthesized, purified and their analytical profiles were characterized by GC-MS and IR in the current study. Furthermore, we have established the effects of the novel piperazine designer drugs on the dopaminergic neuronal cells. Likewise, the current study also investigated the mechanisms of actions of these substances related to their neuronal survival. In vitro simulations can be used as experimental and preliminary models prior to performing tasks with whole animals. Moreover, these in vitro models have numerous benefits, including the ability to focus on the precise target of interest in entirely regulated experimental conditions, allowing the research of specific neuronal mechanisms, being more time and cost-effective. Thus, the current work is one of the initial research studies investigating the comparative effect of novel piperazine derivatives. N27 dopaminergic neuronal cells are acceptable in vitro paradigm to establish the effect of the piperazine derivatives on dopaminergic neurotransmission. Dopamine (3,4-dihydroxyphenethylamine) is a monoamine and structurally a catecholamine and phenethylamine neurotransmitter derived from tyrosine. It exerts its effect by binding to the dopaminergic receptors, and the effect is controlled by the synthesizing enzymes (tyrosine hydroxylase, aromatic amino acid decarboxylase), release, reuptake (dopamine transporter), and metabolism by degrading enzyme (monoamine oxidase-b and catechol-O-methyl transferase). Neuronal viability is mainly affected by oxidative stress, apoptosis, inflammation, mitochondrial function, and excitotoxicity. Interestingly, the stimulants and/or psychoactive substances mainly exert their toxic effects by affecting the dopaminergic neurotransmission and inducing pro-oxidant, pro-inflammatory cytokines, pro-apoptotic effect while depleting ATP and increasing the glutamate content. These cellular actions result in excitotoxicity. We designed novel piperazine analogues based on the existing and known derivatives, TFMPP and BZP. Structural modification

of drugs has been shown to result in differential neurotoxicity on the dopaminergic neurons. The differential effects were attributed mainly due to the structural changes, receptor binding/affinity profile, as well as effects on the markers of oxidative stress, mitochondrial function, and apoptosis. Hence, in the future, more precise in vivo studies should be carried out to determine the pharmacokinetic and pharmacodynamic effects of these new psychoactive substances. These studies can assess and validate the potential toxic effects of these compounds and potential therapeutic agents containing these structures. If a new piperazine is found to be toxic, it will likely be withdrawn from the market and the public must be alerted and educated about the harmful effects of the drug. In this study, six piperazine compounds have been investigated for their effect on dopaminergic neuronal viability using N27 dopaminergic neuronal cells. The novel piperazine derivatives (3-TFMPPBz, MDBzTFMPP, and BrDMBzTFMPP) exhibited a more significant reduction in neuronal viability when compared with the parent compounds (3-TFMPP, MDBP, and BrDMBP). Furthermore, the mechanism of neurotoxicity for these piperazine derivatives has been investigated on two compounds, the MDBP and MDBzTFMPP, using various markers such as ROS, hydrogen peroxide, nitrite, glutathione and NADH content, and the activities of various enzymes such as mitochondrial Complex-I, monoamine oxidase, and tyrosine hydroxylase. The novel toxic MDBzTFMPP in this study has elevated the markers of oxidative stress (ROS, nitrite, and H₂O₂) but did not affect the glutathione content (antioxidant). The MDBzTFMPP significantly decreased the MAO activity and did not affect tyrosine hydroxylase activity. Moreover, the MDBzTFMPP significantly induced dose-dependent decrease in the mitochondrial Complex I activity but did not affect NADH content. 1-(3,4-methylenedioxybenzyl)-piperazine (MDBP), a piperazine designer drugs has been abused globally for the past few years. The current literature on MDBP reveals the techniques used for MDBP screening and quantification. Furthermore, effect

of MDBP on myocytes, hepatocytes, and *Caenorhabditis elegans* have been studied. However, there are very few *in silico*, *in vitro* and *in vivo* studies investigating the pharmacodynamic properties and dopaminergic neuropharmacological profile of MDBP. Hence, in this study, we investigated the pharmacodynamic properties and *in vitro* dopaminergic neuropharmacological effects of MDBP. By assessment of these markers the effect of MDBP on oxidative stress, mitochondrial function, and dopaminergic neurotransmission can be determined. In this study MDBP did not affect the dopaminergic neuronal viability and had no significant effect on tyrosine hydroxylase activity. Interestingly, MDBP was found to inhibit the activity of monoamine oxidase significantly. Similarly, MDBP had no deleterious effect on mitochondrial function. Due to the above effects, MDBP might have no or minimal dopaminergic neurotoxic effects. Thus, MDBP with additional valid *in vivo* studies might be a prospective prophylactic or therapeutic medication to treat various human and animal diseases.

7. Conclusion

Designer drugs represent a public health threat that has dramatically and continuously grown through the past two decades. The designer piperazine class is a part of this phenomenon of drug abuse with the potential of new derivatives belonging to this class introduced over the years. Historically BZP and 3-TFMPP are the most abused compounds among piperazine drug class with stimulant effects comparable to amphetamine and MDMA. In this study, we designed and synthesized many novel piperazine derivatives and regioisomers that contain the structural elements of both BZP and 3-TFMPP. These regioisomers have variable aromatic ring substitution patterns that resemble the common structural modifications in classical drugs of abuse. The majority of the novel piperazine isomers in this study share common electron ionization mass spectral fragment ions. However, we were able to differentiate piperazine isomers using the GC-MS. Additionally, the vapor phase infrared spectroscopy (GC-IRD) provided a fingerprint for direct identification for each isomer. Further, we also investigated the effect and mechanisms of a selected number of these drugs on the N27 dopaminergic neuronal cell viability. The markers studied were ROS, hydrogen peroxide, nitrite, glutathione, NADH content, the activities of mitochondrial Complex-I, monoamine oxidase and tyrosine hydroxylase. The novel piperazine derivatives exhibited differential dopaminergic neurotoxicity on the dopaminergic neurons due to oxidative stress and mitochondrial dysfunction.

8. Experimental

8.1. Materials

Most of the synthetic starting materials were purchased from Aldrich chemical company (Milwaukee, WI, USA). Piperazine, piperonal, benzaldehyde, sodium cyanoborohydride, sodium triacetoxyborohydride, d8-piperazine, 2-methoxybenzaldehyde, 3-methoxybenzaldehyde, 4-methoxybenzaldehyde, 2,3-dimethoxybenzaldehyde, 2,4-dimethoxybenzaldehyde, 2,5-dimethoxybenzaldehyde, 2,6-dimethoxybenzaldehyde, 3,4-dimethoxybenzaldehyde, 3,5-dimethoxybenzaldehyde, 2-methoxybenzaldehyde, 3-methoxybenzaldehyde, 4-methoxybenzaldehyde, 2-methoxybenzylbromide, 3-methoxybenzylbromide, 4-methoxybenzylbromide, 2,3-dimethoxybenzylbromide, 2,4-dimethoxybenzylbromide, 2,5-dimethoxybenzylbromide, 2,6-dimethoxybenzylbromide, 3,4-dimethoxybenzylbromide, 3,5-dimethoxybenzylbromide, 2-methoxy-5-methyl benzaldehyde, 2-Br, 4,5 dimethoxy benzaldehyde -, 3-Br, 4,5 dimethoxy benzaldehyde -, 4-Br, 2,5 dimethoxy benzaldehyde, 4-Br, 3,5- dimethoxy benzaldehyde, 5-Br, 2,3- dimethoxy benzaldehyde, 5-Br, 2,4- dimethoxy benzaldehyde, 6-Br, 2,3- dimethoxy benzaldehyde, 4-methoxyphenylpiperazine dihydrochloride was purchased Trans World Chemicals (Rockville, MD, USA). 3-methoxy-4-methyl benzoic acid methyl ester was purchased from TCI America (Portland, OR, USA). HPLC grade acetonitrile, methanol, toluene, tetrahydrofuran were purchased from Fisher Scientific, (Atlanta, GA, USA). Diethyl ether, 2-propanol, methylene chloride, carbon tetrachloride, benzene, tetrahydrofuran (THF) and chloroform were purchased from Fisher Scientific (Fair Lawn, N.J., USA). Organic solvents such as methanol (ACS grade), isopropanol (ACS grade), tetrahydrofuran (ACS grade), acetone (ACS grade), ethyl acetate (ACS grade), dichloromethane (ACS grade), petroleum ether (ACS grade)

were purchased from VWR (PA), tetrahydrofuran (anhydrous stabilized), benzene (ACS grade) from EMD Millipore (NJ).

8.2. Instruments

GC–MS System consisted of an Agilent Technologies (Santa Clara, CA) 7890A gas chromatograph and an Agilent 7683B auto injector coupled with a 5975C VL Agilent mass selective detector. The mass spectral scan rate was 2.86 scans/s. The GC was operated in splitless injection mode with a helium (ultra-high purity, grade 5, 99.999%) flow rate of 0.480 ml/minute and the column head pressure was 10 psi. The MS was operated in the electron ionization (EI) mode with an ionization voltage of 70 eV and a source temperature of 230 °C. The GC injector was maintained at 230, 150 or 250 °C and the transfer line at 280 °C. Samples were dissolved and diluted in high-performance liquid chromatography grade acetonitrile and introduced via the auto injector using an injection volume of 1- μ l.

GC–IR studies were carried out on a Hewlett-Packard 6890 Series gas chromatograph and a Hewlett-Packard 7683 series auto-injector coupled with an IRD-3 (Infrared detector Model-3) obtained from Analytical Solutions and Providers (ASAP), Covington, KY. The vapor phase infrared spectra were recorded in the range of 4000 to 550 cm^{-1} with a resolution of 16 cm^{-1} and a scan rate 1.50 scans/s. The GC injector was maintained at 250 °C and the transfer line A, the light pipe and the transfer line B temperatures were maintained at 250 °C. The GC was operated in the split injection mode (split ratio of 10:1) with a carrier gas helium (ultra-high purity, grade 5, 99.999%) flow rate of 2 ml/minute and the column head pressure was 2.62 psi.

All IR experiments were performed using the same parameters. The stationary phase used was a 30 m × 0.25 mm i.d. capillary column coated with 0.10 µm film of low polarity Crossbond® silarylene phase; similar to 5% phenyl, 95% dimethyl polysiloxane (Rxi®-5Sil MS) purchased from Restek Corporation (Bellefonte, PA). The temperature program consisted of an initial hold at 70 oC for 1.0 minute, ramped up to 250 oC at a rate of 25 oC/minute followed by a hold at 250 oC for 6.80 minutes. Samples were dissolved and diluted in high-performance liquid chromatography grade acetonitrile and introduced via the auto injector using an injection volume of 1-µl.

8.3. GC-Columns

Different capillary GC columns were evaluated throughout the course of this work. However, only columns showed best compromises between resolution and analysis time are illustrated in Table 2. All columns used were purchased from Restek Corporation (Bellefonte, PA) and have the same dimensions, 30 m x 0.25 mm i.d., and film depth (f.d.) of 0.10, 0.25 or 0.50 µm. Inlet pressure was converted according to the constant flow mode and the total flow was 60 ml/minute Table (3).

Column name	Composition	Length (m)	ID (mm)	Film thickness (μm)	Temperature ($^{\circ}\text{C}$)
Rxi [®] -17Sil MS	Midpolarity Crossbond [®] silarylene phase; similar to 50% phenyl, 50% dimethyl polysiloxane	30	0.25	0.25	360
Rtx [®] -5 MS	Crossbond [®] 5% diphenyl, 95% dimethyl polysiloxane	15	0.32	0.25	350
Rtx [®] -200	Crossbond [®] 100% trifluoropropylmethyl polysiloxane	30	0.25	.25	350

Table 3. List of columns used and their composition.

8.4. Temperature Programs

Different temperature programs were evaluated throughout the course of this work. However, only programs showing the best compromises between resolution and analysis time are illustrated in Table (4).

Temperature program name	Injector temperature $^{\circ}\text{C}$	Detector temperature $^{\circ}\text{C}$	Program setup
TP-1 (GC-MS) (System 1)	300	325	Initial hold of column temperature at 80 $^{\circ}\text{C}$ for 1.0 minute, ramped up to 300 $^{\circ}\text{C}$ at a rate of 30 $^{\circ}\text{C}/\text{minute}$ followed by a hold at 300 $^{\circ}\text{C}$ for 0.5 minutes, then ramped up to 340 $^{\circ}\text{C}$ at a rate of 5 $^{\circ}\text{C}/\text{minute}$ followed by a hold at 340 $^{\circ}\text{C}$ for 5.0 minutes

TP-2 (GC-MS) (System 1)	230	230	Initial hold of column temperature at 70 °C for 1.0 minute, then the temperature was ramped up to 260 °C at a rate of 5 °C/minute followed by a hold at 260 °C for 40.0 minutes
TP-3 (GC-MS) (System 1)	230	230	Initial hold of column temperature at 70 °C for 1.0 minute, ramped up to 245 °C at a rate of 70 °C/minute followed by a hold at 245 °C for 5.5 minutes, then ramped up to 300 °C at a rate of 5 °C/minute followed by a hold at 300 °C for 10.0 minutes
TP-4 (GC-MS) (System 1)	230	230	Initial hold of column temperature at 70 °C for 1.0 minute, then the temperature was ramped up to 260 °C at a rate of 15 °C/minute followed by a hold at 260 °C for 45.0 minutes
TP-5 (GC-MS) (System 1)	230	230	Initial hold of column temperature at 70 °C for 1.0 minute, then the temperature was ramped up to 260 °C at a rate of 3 °C/minute followed by a hold at 260 °C for 5.0 minutes
TP-6 (GC-MS) (System 1)	230	230	Initial hold of column temperature at 70 °C for 1.0 minute, then the temperature was ramped up to 300 °C at a rate of 5 °C/minute followed by a hold at 300 °C for 5.0 minutes
TP-7 (GC-MS) (System 1)	230	230	Initial hold of column temperature at 70 °C for 1.0 minute, ramped up to 245 °C at a rate of 30 °C/minute followed by a hold at 245 °C for 5.5 minutes, then ramped up to 300 °C at a rate of 1 °C/minute followed by a hold at 300 °C for 10.0 minutes
TP-8 (GC-IR)	250	250	Initial hold of column temperature at 70 °C for 1.0 minute, then was ramped up to 250 °C at rate of 25°C/minute followed by a hold at 250 °C for 6.80 minutes

Table 4. List of temperature programs used

8.5. Synthesis of Piperazine Regioisomers

8.5.1. Synthesis of 1-[N-(trifluoromethyl) phenyl]-4-benzylpiperazine

8.5.1.1. Synthesis of 1-[2-(trifluoromethyl) phenyl]-4-benzylpiperazine and 1-[4-(trifluoromethyl) phenyl]- 4-benzylpiperazine

A solution of either commercially available 2-trifluoromethyl phenyl piperazine (1.15g 5mM) or (1.15g 5mM) or 4-trifluoromethyl phenyl piperazine (1.15g 5mM) and benzaldehyde (0.53g 5mM) in 50 ml methanol was refluxed for two hours in a 100 ml round bottom flask. The reaction mixture was cooled to room temperature, then Sodium triacetoxyborohydride (2.12g, 10 mM) was then added and stirred overnight at room temperature. The reaction solution was then evaporated under reduced pressure at 60 °C to yield a white solid. This solid was suspended in 50 ml of 2 N HCl and extracted by 3X50 ml of benzene. The combined benzene extracts were evaporated under reduced pressure and the resulting in formation of a yellow precipitate. The acidic aqueous solution was then made alkaline to pH 12 by addition of sodium hydroxide pellets and extracted with 3X50 mL of dichloromethane. The combined DCM extracts were evaporated under reduced pressure using a rotary evaporator at 50 °C to yield oily product. The products obtained from both the benzene extracts and DCM extracts were dissolved in anhydrous diethyl ether, and hydrochloric acid gas was added to form the hydrochloride salt, then placed in the refrigerator for overnight. The product was isolated by gravity filtration and air dried to give white crystals. GC-MS analysed the products to confirm the consisted of desired product in the benzene extract. White crystals of 1-[2-(trifluoromethyl) phenyl]-4-benzylpiperazine (2.822g, 0.0088 mol), and 1-[4-(trifluoromethyl) phenyl]- 4-benzylpiperazine (2.84g, 0.0089 mol), MS, molecular weight 320, Table (5).

Compounds	Total yield	Crystallization solvent
2-TFMPPBz	2.2822 g	Ether
4-TFMPPBz	2.84 g	Ether

Table 5. Yields and crystallization solvents for the 1-[N-(trifluoromethyl) phenyl]-4-benzylpiperazine

8.5.1.2. Synthesis of 1-[3-(trifluoromethyl) phenyl]-4-benzylpiperazine

A solution of commercially available 3-trifluoromethyl phenylpiperazine (2.303 g, 10mM), benzyl bromide (1.711g, 10mM) and triethylamine (1.01g, 10mM) in dichloromethane 30ml was stirred in 100 ml round bottom flask overnight at room temperature. The reaction solution was then evaporated under reduced pressure at 60 °C to yield a white solid. This solid was suspended in 50 ml of 2 N HCl and extracted by 3X50 ml of benzene. The combined benzene extracts were evaporated under reduced pressure and the resulting in formation of a yellow precipitate. The acidic aqueous solution was then made alkaline to pH 12 by addition of sodium hydroxide pellets and extracted with 3X50 mL of dichloromethane. The combined DCM extracts were evaporated under reduced pressure using a rotary evaporator at 50 °C to yield oily product. The products obtained from both the benzene extracts and DCM extracts were dissolved in anhydrous diethyl ether, and hydrochloric acid gas was added to form the hydrochloride salt, then placed in the refrigerator for overnight. The product was isolated by gravity filtration and air dried to give white crystals. The products were analysed by GC-MS to confirm the consisted of desired product in the benzene extract. White crystals of 1-[3-(trifluoromethyl) phenyl]-4-benzylpiperazine (2.935 g, 0.0091 mol), MS, molecular weight 320, Table (6).

Compounds	Total yield	Crystallization solvent
3-TFMPPBz	2.935 g	Ether

Table 6. Table 3. Yields and Crystallization Solvents for the 1-[3-(trifluoromethyl) phenyl]-4-benzylpiperazine

8.5.2. Synthesis of 1-[2-(trifluoromethyl)benzyl]-, 1-[3-(trifluoromethyl)benzyl], and 1-[4-(trifluoromethyl)benzyl]-4-phenylpiperazine

A solution of either commercially available 2-trifluoromethylbenzaldehyde (3.48g 20mM) or 3-trifluoromethylbenzaldehyde (3.48g 20mM) or 4-trifluoromethylbenzaldehyde (3.48g 20mM) and phenyl piperazine (3.21g 20mM) in 50 ml methanol was refluxed for two hours in a 100 ml round bottom flask. The reaction mixture was cooled to room temperature, then Sodium cyanoborohydride (1.82g, 30 mM) was then added and the reaction mixture was stirred overnight at room temperature. The reaction solution was then evaporated under reduced pressure at 60 °C to yield a white solid. This solid was suspended in 50 ml of 2 N HCl and extracted by 3X50 ml of benzene. The combined benzene extracts were evaporated under reduced pressure and the resulting in formation of a white precipitate. The acidic aqueous solution was then made alkaline to pH 12 by addition of sodium hydroxide pellets and extracted with 3X50 mL of dichloromethane. The combined DCM extracts were evaporated under reduced pressure using a rotary evaporator at 50 °C to yield oily product. The products obtained from both the benzene extracts and DCM extracts were dissolved in anhydrous diethyl ether, and hydrochloric acid gas was added to form the hydrochloride salt, then placed in the refrigerator for overnight. The product was isolated by gravity filtration and air dried to give white crystals. GC-MS analyzed the products to confirm the consisted of desired product in the benzene extract. White crystals of 1-[2-(trifluoromethyl)

benzyl]-4-phenylpiperazine (2.254g, 0.007 mol), 1-[3-(trifluoromethyl) benzyl]-4-phenylpiperazine (2.94g, 0.0091 mol) and 1-[4-(trifluoromethyl) benzyl]-4-phenylpiperazine (2.714g, 0.0084 mol) were obtained by filtration, MS, molecular weight 320, Table (7).

Compounds	Total yield	Crystallization solvent
2-TFMBzPP	2.254 g	Ether
3-TFMBzPP	2.94 g	Ether
4-TFMBzPP	2.714 g	Ether

Table 7. Yields and Crystallization Solvents for 1-[N-(trifluoromethyl)benzyl]-4-phenylpiperazine

8.5.3. Synthesis of 1-[2-(methoxybenzyl)]-, 1-[3-(methoxybenzyl)]-, and 1-[4-(methoxybenzyl)]-4-[3-(trifluoromethyl)phenyl]piperazine

A solution of either commercially available 2-, 3-, or 4-methoxybenzylbromide 10mM (2g), 3-trifluoromethylphenylpiperazine monohydrochloride 10mM (2.66g), and triethylamine 10mM (1.01g) in dichloromethane 30ml was stirred in 100 ml round bottom flask overnight at room temperature. The reaction solution was then evaporated under reduced pressure at 60 °C to yield a white solid. This solid was suspended in 50 ml of 2 N HCl and extracted by 3X50 ml of benzene. The combined benzene extracts were evaporated under reduced pressure and the resulting in formation of a yellow precipitate. The acidic aqueous solution was then made alkaline to pH 12 by addition of sodium hydroxide pellets and extracted with 3X50 mL of dichloromethane. The combined DCM extracts were evaporated under reduced pressure using a rotary evaporator at 50 °C to yield oily product. The products obtained from both the benzene extracts and DCM extracts were dissolved in anhydrous diethyl ether, and hydrochloric acid gas was added to form the

hydrochloride salt, then placed in the refrigerator for overnight. The product was isolated by gravity filtration and air dried to give white crystals. The products were analysed by GC-MS to confirm the consisted of desired product in the benzene extract. Yellowish crystals of 1-[2-methoxybenzyl]-4-[3-(trifluoromethyl phenyl piperazine) (3.5g, 0.001 mol), white crystal of 1-[3- methoxybenzyl]-4-[3-(trifluoromethyl phenyl piperazine) (315mg, 0.0009 mol), and 1-[4-methoxybenzyl]-4-[3-(trifluoromethyl phenyl piperazine) (1.27g, 0.0036 mol), MS, molecular weight 350, Table (8).

Compounds	Total yield	Crystallization solvent
2-OMeBz-3-TFMPP	3.5 g	Ether
2-OMeBz-3-TFMPP	315 mg	Ether
2-OMeBz-3-TFMPP	1.27 g	Ether

Table 8. Yields and crystallization solvents for 1-[N-(methoxybenzyl)]-4-[3-(trifluoromethyl)phenyl]piperazine

8.5.4. Synthesis of 1-[N-(dimethoxybenzyl)]-4-[3-(trifluoromethyl)phenyl]piperazine

8.5.4.1. Synthesis of 1-[2,4-(dimethoxybenzyl)]-, 1-[2,6-(dimethoxybenzyl)]-, and 1-[3,4-(dimethoxybenzyl)]-4-[3-(trifluoromethyl)phenyl]piperazine

A solution of either commercially available 2,4-, 2,6-, or 3,4- dimethoxybenzaldehyde (1.66g, 10mM), 3-trifluoromethylphenylpiperazine monohydrochloride (2.66g, 10mM), and triethylamine (1.01g, 10mM) in 50 ml methanol was refluxed for two hours in a 100 ml round bottom flask. The reaction mixture was cooled to room temperature, then Sodium triacetoxyborohydride (4.22g,

10 mM) was then added and the reaction mixture was stirred overnight at room temperature. The reaction solution was then evaporated under reduced pressure at 60 °C to yield a white solid. This solid was suspended in 50 ml of 2 N HCl and extracted by 3X50 ml of benzene. The combined benzene extracts were evaporated under reduced pressure and the resulting in formation of a yellow precipitate. The acidic aqueous solution was then made alkaline to pH 12 by addition of sodium hydroxide pellets and extracted with 3X50 mL of dichloromethane. The combined DCM extracts were evaporated under reduced pressure using a rotary evaporator at 50 °C to yield oily product. The products obtained from both the benzene extracts and DCM extracts were dissolved in anhydrous diethyl ether, and hydrochloric acid gas was added to form the hydrochloride salt, then placed in the refrigerator for overnight. The product was isolated by gravity filtration and air dried to give white crystals. The products were analyzed by GC-MS to confirm the consisted of desired product in the benzene extract. white crystals of 1-[2,4-(dimethoxybenzyl)]-4-[3-(trifluoromethyl)phenyl]piperazine (175mg, 0.00046mol), 1-[2,6-(dimethoxybenzyl)]-4-[3-(trifluoromethyl)phenyl]piperazine (3.65g,0.0096 mol), and 1-[3,4-(dimethoxybenzyl)]-4-[3-(trifluoromethyl)phenyl]piperazine (2.25g, 0.0059 mol), MS, molecular weight 380, Table(9).

Compounds	Total yield	Crystallization solvent
2,4-DMBz-3-TFMPP	175 mg	Ether
2,6-DMBz-3-TFMPP	3.65 g	Ether
3,4-DMBz-3-TFMPP	2.25 g	Ether

Table 9. Yields and crystallization solvents for 1-[N-(dimethoxybenzyl)]-4-[3-(trifluoromethyl)phenyl]piperazine

8.5.4.2. Synthesis of 1-[2,3-(dimethoxybenzyl)]-, and 1-[2,5-(dimethoxybenzyl)]- 4-[3-(trifluoromethyl)phenyl]piperazine

A solution of either commercially available 2,3- or 2,5- dimethoxybenzyl chloride (1.86g, 10mM) 3-trifluoromethylphenylpiperazine monohydrochloride (2.66g, 10mM), and triethylamine (1.01g, 10mM) in dichloromethane 30ml was stirred in 100 ml round bottom flask overnight at room temperature. The reaction solution was then evaporated under reduced pressure at 60 °C to yield a white solid. This solid was suspended in 50 ml of 2 N HCl and extracted by 3X50 ml of benzene. The combined benzene extracts were evaporated under reduced pressure and the resulting in formation of a white precipitate. The acidic aqueous solution was then made alkaline to pH 12 by addition of sodium hydroxide pellets and extracted with 3X50 mL of dichloromethane. The combined DCM extracts were evaporated under reduced pressure using a rotary evaporator at 50 °C to yield oily product. The products obtained from both the benzene extracts and DCM extracts were dissolved in anhydrous diethyl ether, and hydrochloric acid gas was added to form the hydrochloride salt, then placed in the refrigerator for overnight. The product was isolated by gravity filtration and air dried to give white crystals. The products were analysed by GC-MS to confirm the consisted of desired product in the benzene extract. Yellowish crystals of 1-[2,3-dimethoxybenzyl]- 4-[3-(trifluoromethyl)phenyl]piperazine (2.28g, 0.006 mol) and white crystals of 1-[2,5- dimethoxybenzyl]- 4-[3-(trifluoromethyl)phenyl]piperazine (1.9g,0.005 mol), MS, molecular weight 380, Table (10).

Compounds	Total yield	Crystallization solvent
2,3-DMBz-3-TFMPP	2.28 g	Ether
2,5-DMBz-3-TFMPP	1.9 g	Ether

Table 10. Yields and crystallization solvents for 1-[N-(dimethoxybenzyl)]- 4-[3-(trifluoromethyl)phenyl]piperazine

8.5.4.3. Synthesis of 1-[3,5-(dimethoxybenzyl)]-4-[3-(trifluoromethyl phenyl piperazine)

A solution of either commercially available 3,5-dimethoxybenzylbromide (2.31g, 10mM), 3-trifluoromethylphenylpiperazine monohydrochloride (2.66g, 10mM), and triethylamine (1.01g, 10mM) in dichloromethane 30ml was stirred in 100 ml round bottom flask overnight at room temperature. The reaction solution was then evaporated under reduced pressure at 60 °C to yield a white solid. This solid was suspended in 50 ml of 2 N HCl and extracted by 3X50 ml of benzene. The combined benzene extracts were evaporated under reduced pressure and the resulting in formation of a white precipitate. The acidic aqueous solution was then made alkaline to pH 12 by addition of sodium hydroxide pellets and extracted with 3X50 mL of dichloromethane. The combined DCM extracts were evaporated under reduced pressure using a rotary evaporator at 50 °C to yield oily product. The products obtained from both the benzene extracts and DCM extracts were dissolved in anhydrous diethyl ether, and hydrochloric acid gas was added to form the hydrochloride salt, then placed in the refrigerator for overnight. The product was isolated by gravity filtration and air dried to give white crystals. The products were analyzed by GC-MS to confirm the consisted of desired product in the benzene extract. white crystals of 1-[3,5-dimethoxybenzyl]-4-[3-(trifluoromethyl phenyl piperazine) (2.85g, 0.0075 mol), MS, molecular weight 380, Table(11).

Compounds	Total yield	Crystallization solvent
3,5-DMBz-3-TFMPP	2.85 g	Ether

Table 11. Yields and crystallization solvents for 1-[3,5-(dimethoxybenzyl)]- 4-[3-(trifluoromethyl)phenyl]piperazine

8.5.5. Synthesis of Synthesis of 1-[2,3-(methylenedioxybenzyl)]-4-[3-(trifluoromethylphenyl) piperazine and 1-[3,4-(methylenedioxybenzyl)]-4-[3-(trifluoromethyl)phenyl]piperazine

A solution of either commercially available 2,3- or 3,4-methylenedioxybenzylaldehyde (1.5g, 10mM) 3-trifluoromethylphenylpiperazine monohydrochloride (2.66g, 10mM), and triethylamine (1.01g, 10mM) in 50 ml methanol was refluxed for two hours in a 100 ml round bottom flask. The reaction mixture was cooled to room temperature, then Sodium triacetoxyborohydride (3.17g, 15 mM) was then added and stirred overnight at room temperature. The reaction solution was then evaporated under reduced pressure at 60 °C to yield a white solid. This solid was suspended in 50 ml of 2 N HCl and extracted by 3X50 ml of benzene. The combined benzene extracts were evaporated under reduced pressure and the resulting in formation of a white precipitate. The acidic aqueous solution was then made alkaline to pH 12 by addition of sodium hydroxide pellets and extracted with 3X50 mL of dichloromethane. The combined DCM extracts were evaporated under reduced pressure using a rotary evaporator at 50 °C to yield oily product. The products obtained from both the benzene extracts and DCM extracts were dissolved in anhydrous diethyl ether, and hydrochloric acid gas was added to form the hydrochloride salt, then placed in the refrigerator for overnight. The product was isolated by gravity filtration and air dried to give white crystals. The products were analyzed by GC-MS to confirm the consisted of desired product in the benzene extract. White crystals of 1-[2,3-(methylenedioxybenzyl)]-4-[3-(trifluoromethylphenyl)piperazine (2.9g, 0.0079 mol) and 1-[3,4-(methylenedioxybenzyl)]-4-[3-(trifluoromethylphenyl)piperazine (3.14g, 0.0086 mol), MS, molecular weight 364, Table(12).

Compounds	Total yield	Crystallization solvent
2,3-MDBz-3-TFMPP	2.9 g	Ether
3,4-MDBz-3-TFMPP	3.14 g	Ether

Table 12. Yields and crystallization solvents for 1-[N-(methylenedioxybenzyl)]-4-[3-(trifluoromethyl)phenyl]piperazine

8.5.6. Synthesis of 1-[N-(bromo-dimethoxybenzyl)]- 4-[3-(trifluoromethyl)phenyl]piperazine

A solution of either commercially available 2Br-4,5-, 3Br-4,5-, 4Br-2,5-, 4Br-3,5-, 5Br-2,3-, 5Br-2,4-, 6Br-2,3-dimethoxybenzaldehyde (2.59g, 10mM), 3-trifluoromethylphenylpiperazine monohydrochloride (2.66g, 10mM), and triethylamine (1.01g, 10mM) in 50 ml methanol was refluxed for two hours in a 100 ml round bottom flask. The reaction mixture was cooled to room temperature, then Sodium triacetoxyborohydride (6.33g, 30 mM) was then added and stirred overnight at room temperature. The reaction solution was then evaporated under reduced pressure at 60 °C to yield a white solid. This solid was suspended in 50 ml of 2 N HCl and extracted by 3X50 ml of benzene. The combined benzene extracts were evaporated under reduced pressure and the resulting in formation of a white precipitate. The acidic aqueous solution was then made alkaline to pH 12 by addition of sodium hydroxide pellets and extracted with 3X50 mL of dichloromethane. The combined DCM extracts were evaporated under reduced pressure using a rotary evaporator at 50 °C to yield oily product. The products obtained from both the benzene extracts and DCM extracts were dissolved in anhydrous diethyl ether, and hydrochloric acid gas was added to form the hydrochloride salt, then placed in the refrigerator for overnight. The product

was isolated by gravity filtration and air dried to give white crystals. The products were analyzed by GC-MS to confirm the consisted of desired product in the benzene extract. White crystals of 1-[2-Bromo-4,5-(dimethoxybenzyl)-4-[3-(trifluoromethylphenyl)piperazine (840mg, 0.0018 mol), 1-[3-Bromo-4,5-(dimethoxybenzyl)-4-[3-(trifluoromethylphenyl)piperazine (3.3g, 0.0072 mol), 1-[4-Bromo-2,5-(dimethoxybenzyl)-4-[3-(trifluoromethylphenyl)piperazine (4.17g, 0.0091 mol), 1-[4-Bromo-3,5-(dimethoxybenzyl)-4-[3-(trifluoromethylphenyl)piperazine (47 mg, 0.0001 mol), 1-[5-Bromo-2,3-(dimethoxybenzyl)-4-[3-(trifluoromethylphenyl)piperazine (4.4g, 0.0096 mol), 1-[5-Bromo-2,4-(dimethoxybenzyl)-4-[3-(trifluoromethylphenyl)piperazine (4.61g, 0.01 mol), 1-[6-Bromo-2,3-(dimethoxybenzyl)-4-[3-(trifluoromethylphenyl)piperazine (43 mg, 0.0009 mol), MS, molecular weight 458, Table (13).

Compounds	Total yield	Crystallization solvent
2-Br-4,5DM-3-TFMPP	840 mg	Ether
3-Br-4,5DM-3-TFMPP	3.3 g	Ether
4-Br-2,5DM-3-TFMPP	4.17 g	Ether
4-Br-3,5DM-3-TFMPP	47 mg	Ether
5-Br-2,3DM-3-TFMPP	4.4 g	Ether
5-Br-2,4DM-3-TFMPP	4.61 g	Ether
6-Br-2,3DM-3-TFMPP	43 mg	Ether

Table 13. Yields and crystallization solvents for 1-[N-(bromo-dimethoxybenzyl)]- 4-[3-(trifluoromethyl) phenyl]piperazine

8.5.7. Synthesis of 1-(3-chlorophenyl)-4-[(N-methoxybenzyl)piperazine

A solution of either commercially available 2-, 3-, or 4-methoxybenzaldehyde (1.36g, 10mM), 3-chlorophenylpiperazine monohydrochloride (1.96g, 10mM) and triethylamine (1.01g, 10mM) in 50 ml methanol refluxed for two hours in a 100 ml round bottom flask . The reaction mixture was cooled to room temperature, then Sodium triacetoxyborohydride (3.17g, 15 mM) was then added and stirred overnight at room temperature. The reaction solution was then evaporated under reduced pressure at 60 °C to yield a white solid. This solid was suspended in 50 ml of 2 N HCl and extracted by 3X50 ml of benzene. The combined benzene extracts were evaporated under reduced pressure and the resulting in formation of a white precipitate. The acidic aqueous solution was then made alkaline to pH 12 by addition of sodium hydroxide pellets and extracted with 3X50 mL of dichloromethane. The combined DCM extracts were evaporated under reduced pressure using a rotary evaporator at 50 °C to yield oily product. The products obtained from both the benzene extracts and DCM extracts were dissolved in anhydrous diethyl ether, and hydrochloric acid gas was added to form the hydrochloride salt, then placed in the refrigerator for overnight. The product was isolated by gravity filtration and air dried to give white crystals. The products were analyzed by GC-MS to confirm the consisted of desired product in the benzene extract. White crystals of 1-[2-(methoxybenzyl)-4-[3-(chlorophenyl)piperazine (3.65g, 0.011 mol), brownish crystal of 1-[3-(methoxybenzyl)-4-[3-(chlorophenyl)piperazine (2.9 g, 0.0091 mol), and 1-[4-(methoxybenzyl)-4-[3-(chlorophenyl)piperazine (560 mg, 0.0017 mol), MS, molecular weight 316, Table (14).

Compounds	Total yield	Crystallization solvent
2-OMeBz-3-CIPP	3.65 g	Ether
3-OMeBz-3-CIPP	2.9 g	Ether
4-OMeBz-3-CIPP	560 mg	Ether

Table 14. Yields and crystallization solvents for 1-(3-chlorophenyl)-4-[(N-methoxybenzyl)piperazine

8.5.8. Synthesis of 1-(chlorophenyl)-4-[(N-(dimethoxybenzyl)piperazine

A solution of either commercially available 2,3-, 2,4-, 2,5-, 2,6-, 3,4-, or 3,5-dimethoxy benzaldehyde (1.66g, 10mM), 3-chlorophenylpiperazine monohydrochloride (1.96g, 10mM) and triethylamine (1.01g, 10mM) in 50 ml methanol was refluxed for two hours in a 100 ml round bottom flask. The reaction mixture was cooled to room temperature, then Sodium triacetoxyborohydride (3.17g, 15 mM) was then added and stirred overnight at room temperature. The reaction solution was then evaporated under reduced pressure at 60 °C to yield a white solid. This solid was suspended in 50 ml of 2 N HCl and extracted by 3X50 ml of benzene. The combined benzene extracts were evaporated under reduced pressure and the resulting in formation of a white precipitate. The acidic aqueous solution was then made alkaline to pH 12 by addition of sodium hydroxide pellets and extracted with 3X50 mL of dichloromethane. The combined DCM extracts were evaporated under reduced pressure using a rotary evaporator at 50 °C to yield oily product. The products obtained from both the benzene extracts and DCM extracts were dissolved in anhydrous diethyl ether, and hydrochloric acid gas was added to form the hydrochloride salt, then placed in the refrigerator for overnight. The product was isolated by gravity filtration and air dried

to give white crystals. The products were analyzed by GC-MS to confirm the consisted of desired product in the benzene extract, except for 2,4- and 3,4--(dimethoxybenzyl)-4-[3-(chlorophenyl)piperazine the product was in the DCM extract. Brownish crystals of 1-[2,3-(dimethoxybenzyl)-4-[3-(chlorophenyl)piperazine (1.3 g, 0.0037 mol), 1-[2,4-(dimethoxybenzyl)-4-[3-(chlorophenyl)piperazine (425 mg, 0.0012 mol), 1-[2,5-(dimethoxybenzyl)-4-[3-(chlorophenyl)piperazine (452 mg, 0.0013 mol), 1-[2,6-(dimethoxybenzyl)-4-[3-(chlorophenyl)piperazine (1.9 g, 0.0054 mol), 1-[3,4-(dimethoxybenzyl)-4-[3-(chlorophenyl)piperazine (170 mg, 0.00049 mol), and 1-[3,5-(dimethoxybenzyl)-4-[3-(chlorophenyl)piperazine (590 mg, 0.0017 mol), MS, molecular weight 346, Table(15). The 2,5- and 3,5--(dimethoxybenzyl)-4-[3-(chlorophenyl)piperazine were recrystallized with isopropanol.

Compounds	Total yield	Crystallization solvent
2,3-DMBz-3-CIPP	1.3 g	Ether
2,4-DMBz-3-CIPP	425 mg	Ether
2,5-DMBz-3-CIPP	452 mg	Ether/iPrOH
2,6-DMBz-3-CIPP	1.9 g	Ether
3,4-DMBz-3-CIPP	170 mg	Ether
3,5-DMBz-3-CIPP	590 mg	Ether/iPrOH

Table 15. Yields and crystallization solvents for 1-(chlorophenyl)-4-[(N-(dimethoxybenzyl)piperazine

8.5.9. Synthesis of 1-[N-(methoxybenzyl)]-4-[4-(methoxyphenyl)piperazine

8.5.9.1. Synthesis of 1-[2-(methoxybenzyl)-, and 1-[3-(methoxybenzyl)]-4-[4-(methoxyphenyl)piperazine

A solution of either commercially available 2-, or 3-methoxybenzaldehyde (136mg, 1mM), 4-methoxyphenylpiperazine dihydrochloride (265mg, 1mM), and triethylamine (200mg, 2mM) in 30 ml methanol was refluxed for two hours in a 100 ml round bottom flask. The reaction mixture was cooled to room temperature, then Sodium triacetoxyborohydride (633mg, 3mM) was then added and stirred overnight at room temperature. The reaction solution was then evaporated under reduced pressure at 60 °C to yield a white solid. This solid was suspended in 50 ml of 2 N HCl and extracted by 3X50 ml of benzene. The combined benzene extracts were evaporated under reduced pressure and the resulting in formation of a white precipitate. The acidic aqueous solution was then made alkaline to pH 12 by addition of sodium hydroxide pellets and extracted with 3X50 mL of dichloromethane. The combined DCM extracts were evaporated under reduced pressure using a rotary evaporator at 50 °C to yield oily product. The products obtained from both the benzene extracts and DCM extracts were dissolved in anhydrous diethyl ether, and hydrochloric acid gas was added to form the hydrochloride salt, then placed in the refrigerator for overnight. The product was isolated by gravity filtration and air dried to give white crystals. The products were analyzed by GC-MS to confirm the consisted of desired product in the dichloromethane extract. White crystals of 1-[2-(methoxybenzyl)]-4-[4-(methoxyphenyl)piperazine (66mg, 0.0002 mol), and 1-[3-(methoxybenzyl)]-4-[4-(methoxyphenyl)piperazine (34mg, 0.0001 mol), 4-methoxybenzyl 4-methoxy phenyl piperazine (37mg , 0.00011 mol), MS, molecular weight 312, Table (16).

Compounds	Total yield	Crystallization solvent
2-OMeBz-4-OMePP	66 mg	Ether
3-OMeBz-4-OMePP	34 mg	Ether

Table 16. Yields and crystallization solvents for 1-[N-(methoxybenzyl)-4-[4-(methoxyphenyl)piperazine

8.5.9.2. Synthesis of 1-[4-(methoxybenzyl)]-4-[4-(methoxyphenyl)piperazine

A solution of commercially available 4-methoxybenzaldehyde (136mg, 1mM), 4-methoxyphenyl piperazine dihydrochloride (265mg, 1mM), and triethylamine (200mg, 2mM) in 30 ml methanol was refluxed for two hours in a 100 ml round bottom flask. The reaction mixture was cooled to room temperature, then Sodium cyanoborohydride (186 mg, 3mM) was then added and the reaction mixture was stirred overnight at room temperature. The reaction solution was then evaporated under reduced pressure at 60 °C to yield a white solid. This solid was suspended in 50 ml of 2 N HCl and extracted by 3X50 ml of benzene. The combined benzene extracts were evaporated under reduced pressure and the resulting in formation of a white precipitate. The acidic aqueous solution was then made alkaline to pH 12 by addition of sodium hydroxide pellets and extracted with 3X50 mL of dichloromethane. The combined DCM extracts were evaporated under reduced pressure using a rotary evaporator at 50 °C to yield oily product. The products obtained from both the benzene extracts and DCM extracts were dissolved in anhydrous diethyl ether, and hydrochloric acid gas was added to form the hydrochloride salt, then placed in the refrigerator for overnight. The product was isolated by gravity filtration and air dried to give white crystals. The products were analysed by GC-MS to confirm the consisted of desired product in the

dichloromethane extract. White crystals of 4-methoxybenzyl 4-methoxy phenyl piperazine (37mg, 0.00011 mol), MS, molecular weight 312, table (17).

Compounds	Total yield	Crystallization solvent
4-OMeBz-4-OMePP	37 mg	Ether

Table 17. Yields and crystallization solvents for 1-[4-(methoxybenzyl)-4-[4-(methoxyphenyl)]piperazine

8.5.10. Synthesis of 1-[N-(dimethoxybenzyl)]-4-[4-(methoxyphenyl)]piperazine

8.5.10.1. Synthesis of 1-[2,3-(dimethoxybenzyl)-, 1-[2,5-(dimethoxybenzyl)-, and 1-[2,6-(dimethoxybenzyl)]-4-[4-(methoxyphenyl)]piperazine

A solution of either commercially available 2,3-, 2,5-, 2,6-dimethoxybenzaldehyde (166mg, 1mM), 4-methoxy phenyl piperazine dihydrochloride (265mg, 1mM), and triethylamine (200mg, 2mM) in 30 ml methanol was refluxed for two hours in a 100 ml round bottom flask. The reaction mixture was cooled to room temperature, then Sodium triacetoxyborohydride (633mg, 3mM) was then added and stirred overnight at room temperature. The reaction solution was then evaporated under reduced pressure at 60 °C to yield a white solid. This solid was suspended in 50 ml of 2 N HCl and extracted by 3X50 ml of benzene. The combined benzene extracts were evaporated under reduced pressure and the resulting in formation of a white precipitate. The acidic aqueous solution was then made alkaline to pH 12 by addition of sodium hydroxide pellets and extracted with 3X50 mL of dichloromethane. The combined DCM extracts were evaporated under reduced pressure using a rotary evaporator at 50 °C to yield oily product. The products obtained from both the

benzene extracts and DCM extracts were dissolved in anhydrous diethyl ether, and hydrochloric acid gas was added to form the hydrochloride salt, then placed in the refrigerator for overnight. The product was isolated by gravity filtration and air dried to give white crystals. The products were analyzed by GC-MS to confirm the consisted of desired product in the dichloromethane extract. White crystals of 1-[2,3-(dimethoxybenzyl)-4-[4-(methoxyphenyl)piperazine (17mg, 0.000047 mol), 1-[2,5-(dimethoxybenzyl)- 4-[4-(methoxyphenyl)piperazine (42mg, 0.0001 mol), 1-[2,6-(dimethoxybenzyl)-4-[4-(methoxyphenyl)piperazine (450mg, 0.001 mol), MS, molecular weight 342, Table(18). The 2,3- and 2,5-(dimethoxybenzyl)- 4-[4-(methoxyphenyl)piperazine were recrystallized with isopropanol.

Compounds	Total yield	Crystallization solvent
2,3-DMBz-4-OMePP	17 mg	Ether/iPrOH
2,5-DMBz-4-OMePP	42 mg	Ether/iPrOH
2,6-DMBz-4-OMePP	450mg	Ether

Table 18. Yields and crystallization solvents for 1-[N-(dimethoxybenzyl)-4-[4-(methoxyphenyl)piperazine

8.5.10.2. Synthesis 1-[2,4-(dimethoxybenzyl)-, 1-[3,4-(dimethoxybenzyl)-, and 1-[3,5-(dimethoxybenzyl)- 4-[4-(methoxyphenyl) piperazine

A solution of either commercially available 2,4-, 3,4-, or 3,5-dimethoxybenzaldehyde (166mg, 1mM), 4-methoxyphenylpiperazine dihydrochloride (265mg, 1mM), and triethylamine (200mg, 2mM) in 30 ml methanol was refluxed for two hours in a 100 ml round bottom flask. The reaction mixture was cooled to room temperature, then sodium cyanoborohydride (186 mg, 3mM) was then added and stirred overnight at room temperature. The reaction solution was then evaporated under

reduced pressure at 60 °C to yield a white solid. This solid was suspended in 50 ml of 2 N HCl and extracted by 3X50 ml of benzene. The combined benzene extracts were evaporated under reduced pressure and the resulting in formation of a white precipitate. The acidic aqueous solution was then made alkaline to pH 12 by addition of sodium hydroxide pellets and extracted with 3X50 mL of dichloromethane. The combined DCM extracts were evaporated under reduced pressure using a rotary evaporator at 50 °C to yield oily product. The products obtained from both the benzene extracts and DCM extracts were dissolved in anhydrous diethyl ether, and hydrochloric acid gas was added to form the hydrochloride salt, then placed in the refrigerator for overnight. The product was isolated by gravity filtration and air dried to give white crystals. The products were analyzed by GC-MS to confirm the consisted of desired product in the dichloromethane extract. White crystals of 1-[2,4-(dimethoxybenzyl)-4-[4-(methoxyphenyl)piperazine (398mg, 0.0011 mol), 1-[3,4-(dimethoxybenzyl)-4-[4-(methoxyphenyl)piperazine (107mg, 0.00031 mol), 1-[3,5-(dimethoxybenzyl)-4-[4-(methoxyphenyl)piperazine (530mg, 0.0015 mol), MS, molecular weight 342, Table (19).

Compounds	Total yield	Crystallization solvent
2,4-DMBz-4-OMePP	398mg	Ether
3,4-DMBz-4-OMePP	107mg	Ether
3,5-DMBz-4-OMePP	530mg	Ether

Table 19. Yields and crystallization solvents for 1-[N-(dimethoxybenzyl)-4-[4-(methoxyphenyl)piperazine

8.5.11. Synthesis of 3,4- methylenedioxybenzyl piperazine

A solution of commercially available 3,4-methylenedioxy benzyl aldehyde (1.5g, 10mM) and piperazine (1.72g, 20mM) in methanol was stirred for half an hour. Then sodium cyanoborohydride (1.86g, 30 mM) was added and the mixture was allowed to stir for half an hour. The reaction was quenched by adding ice/water mixture and stirring the mixture for 20 min followed by extracting the final product using dichloromethane (3x30 ml). The combined organic extract was dried with anhydrous magnesium sulfate, filtered and evaporated to yield yellow oil. The products are isolated by solvent extraction by flash pump chromatography 10:90 petroleum ether- DCM. The separated products were collected in test tubes with and purified by thin layer chromatography (TLC) using same solvent system. The required fractions of product were gathered and analysed by GC-MS for confirmation. The oil was dissolved in anhydrous diethyl ether, and hydrochloric acid gas was added to form the hydrochloride salt. White crystals of 3,4-methylenedioxybenzylpiperazine (590 mg, 0.012 mol) were obtained by filtration. MS, molecular weight 220, Table (20).

Compounds	Total yield	Crystallization solvent
MDBP	590 mg	Ether

Table 20. Yields and crystallization solvents for 3,4-methylenedioxybenzyl piperazine

8.5.12. Synthesis of 1-(4-Bromo-2,5-dimethoxybenzyl)piperazine

A solution of commercially available 4-Bromo-2,5-dimethoxybenzaldehyde (2.49g, 10mM) and piperazine (1.72g, 20mM) in methanol was stirred for half an hour. Then sodium

cyanoborohydride (1.86g, 30 mM) was added and the mixture was allowed to stir for half an hour. The reaction was quenched by adding ice/water mixture and stirring the mixture for 20 min followed by extracting the final product using dichloromethane (3x30 ml). The combined organic extract was dried with anhydrous magnesium sulfate, filtered and evaporated to yield yellow oil. The products are isolated by solvent extraction by flash pump chromatography 10:90 petroleum ether- DCM. The separated products were collected in test tubes with and purified by thin layer chromatography (TLC) using same solvent system. The required fractions of product were gathered and analyzed by GC-MS for confirmation. The oil was dissolved in anhydrous diethyl ether, and hydrochloric acid gas was added to form the hydrochloride salt. White crystals of 1-(4-Bromo-2,5-dimethoxybenzyl) piperazine (436 mg, 0.011 mol) were obtained by filtration. MS, molecular weight 315, Table (21).

Compounds	Total yield	Crystallization solvent
BrDMBP	436 mg	Ether

Table 21. Yields and crystallization solvents for 1-(4-Bromo-2,5-dimethoxybenzyl)piperazine

9. References

- Abdel-Hay, Karim M., Jack DeRuiter, and C. Randall Clark. 2013. "Gas Chromatography/Mass Spectrometry Analysis of the Six-Ring Regioisomeric Dimethoxybenzyl-N-Methylpiperazines (DMBMPs)." *Rapid Communications in Mass Spectrometry* 27 (22): 2551–58. <https://doi.org/10.1002/rcm.6716>.
- Abdel-Hay, Karim M., Jack DeRuiter, and C. Randall Clark. 2012. "Differentiation of Methylbenzylpiperazines (MBPs) and Benzoylpiperazine (BNZP) Using GC-MS and GC-IRD." *Drug Testing and Analysis* 4 (6): 441–48. <https://doi.org/10.1002/dta.383>.
- Ahuja, Manuj, Manal Buabeid, Engy Abdel-Rahman, Mohammed Majrashi, Kodeeswaran Parameshwaran, Rajesh Amin, Sindhu Ramesh, et al. 2017. "Immunological Alteration & Toxic Molecular Inductions Leading to Cognitive Impairment & Neurotoxicity in Transgenic Mouse Model of Alzheimer's Disease." *Life Sciences* 177 (May): 49–59. <https://doi.org/10.1016/j.lfs.2017.03.004>.
- Ahuja, Manuj, Manal Buabeid, Engy Abdel-Rehman, Mohammed Majrashi, Kodeeswaran Parameshwaran, Rajesh Amin, Sindhu Ramesh, et al. 2017. "Immunological Alteration & Toxic Molecular Inductions Leading to Cognitive Impairment & Neurotoxicity in Transgenic Mouse Model of Alzheimer's Disease." *Life Sciences*. <https://doi.org/10.1016/j.lfs.2017.03.004>.
- Albano, C B, D Muralikrishnan, and M Ebadi. 2002. "Distribution of Coenzyme Q Homologues in Brain." *Neurochemical Research* 27 (5): 359–68. <http://www.ncbi.nlm.nih.gov/pubmed/12064350>.
- Almalki, Ahmad J., C. Randall Clark, Younis Abiedalla, and Jack DeRuiter. 2020. "GC-MS Analysis of N-(Bromodimethoxybenzyl)-2-, 3-, and 4-Methoxyphenethylamines: Inverse Analogues of the Psychoactive 25B-NBOMe Drug." *Forensic Chemistry* 21 (December): 100277. <https://doi.org/10.1016/j.forc.2020.100277>.
- Almalki, Ahmad J., C. Randall Clark, and Jack DeRuiter. 2019. "GC-MS Analysis of Regioisomeric Substituted N-Benzyl-4-Bromo-2,5-Dimethoxyphenethylamines." *Forensic Chemistry* 14 (June): 100164. <https://doi.org/10.1016/j.forc.2019.100164>.
- Alver, Özgür, Cemal Parlak, and Mustafa Şenyel. 2007. "FT-IR and NMR Investigation of 1-Phenylpiperazine: A Combined Experimental and Theoretical Study." *Spectrochimica Acta - Part A: Molecular and Biomolecular Spectroscopy* 67 (3–4): 793–801. <https://doi.org/10.1016/j.saa.2006.08.035>.
- Arbo, M. D., M. L. Bastos, and H. F. Carmo. 2012a. "Piperazine Compounds as Drugs of Abuse." *Drug and Alcohol Dependence* 122 (3): 174–85. <https://doi.org/10.1016/j.drugalcdep.2011.10.007>.
- Arbo, M.D., M.L. Bastos, and H.F. Carmo. 2012b. "Piperazine Compounds as Drugs of Abuse." *Drug and Alcohol Dependence* 122 (3): 174–85. <https://doi.org/10.1016/J.DRUGALCDEP.2011.10.007>.
- Auerbach, S. B., J. J. Rutter, and P. J. Juliano. 1991. "Substituted Piperazine and Indole Compounds Increase

- Extracellular Serotonin in Rat Diencephalon as Determined by in Vivo Microdialysis.” *Neuropharmacology* 30 (4): 307–11. [https://doi.org/10.1016/0028-3908\(91\)90054-F](https://doi.org/10.1016/0028-3908(91)90054-F).
- Balakumar, Pitchai, Khin Maung-U, and Gowraganahalli Jagadeesh. 2016. “Prevalence and Prevention of Cardiovascular Disease and Diabetes Mellitus.” *Pharmacological Research*. Academic Press. <https://doi.org/10.1016/j.phrs.2016.09.040>.
- Bassetto, Marcella, Pieter Leyssen, Johan Neyts, Mark M. Yerukhimovich, David N. Frick, Matthew Courtney-Smith, and Andrea Brancale. 2017. “In Silico Identification, Design and Synthesis of Novel Piperazine-Based Antiviral Agents Targeting the Hepatitis C Virus Helicase.” *European Journal of Medicinal Chemistry* 125: 1115–31. <https://doi.org/10.1016/j.ejmech.2016.10.043>.
- BAUMANN, MICHAEL H., ROBERT D. CLARK, ALLISON G. BUDZYNSKI, JOHN S. PARTILLA, BRUCE E. BLOUGH, and RICHARD B. ROTHMAN. 2004. “Effects of ‘Legal X’ Piperazine Analogs on Dopamine and Serotonin Release in Rat Brain.” *Annals of the New York Academy of Sciences* 1025 (1): 189–97. <https://doi.org/10.1196/annals.1316.024>.
- Berridge, Michael V, Patries M Herst, and An S Tan. 2005. “Tetrazolium Dyes as Tools in Cell Biology: New Insights into Their Cellular Reduction.” *Biotechnology Annual Review* 11: 127–52. [https://doi.org/10.1016/S1387-2656\(05\)11004-7](https://doi.org/10.1016/S1387-2656(05)11004-7).
- Boer, Douwe De, Ingrid J. Bosman, El??d Hidv??gi, Carmo Manzoni, Andr??s A. Benk??, Louren??o J A L Dos Reys, and Robert A A Maes. 2001. “Piperazine-like Compounds: A New Group of Designer Drugs-of-Abuse on the European Market.” *Forensic Science International* 121 (1–2): 47–56. [https://doi.org/10.1016/S0379-0738\(01\)00452-2](https://doi.org/10.1016/S0379-0738(01)00452-2).
- Bossong, M. G., T. M. Brunt, J. P. Van Dijk, S. M. Rigter, J. Hoek, H. M.J. Goldschmidt, and R. J.M. Niesink. 2010. “MCPD: An Undesired Addition to the Ecstasy Market.” *Journal of Psychopharmacology* 24 (9): 1395–1401. <https://doi.org/10.1177/0269881109102541>.
- Braccio, Mario Di, Giancarlo Grossi, Maria Grazia Signorello, Giuliana Leoncini, Elena Cichero, Paola Fossa, Silvana Alfei, and Gianluca Damonte. 2013. “Synthesis, in Vitro Antiplatelet Activity and Molecular Modelling Studies of 10-Substituted 2-(1-Piperazinyl)Pyrimido[1,2-a]Benzimidazol-4(10H)-Ones.” *European Journal of Medicinal Chemistry* 62 (April): 564–78. <https://doi.org/10.1016/j.ejmech.2013.01.026>.
- Brito, Adriane F., Lorrane K.S. Moreira, Ricardo Menegatti, and Elson A. Costa. 2019. “Piperazine Derivatives with Central Pharmacological Activity Used as Therapeutic Tools.” *Fundamental and Clinical Pharmacology* 33 (1): 13–24. <https://doi.org/10.1111/fcp.12408>.
- Butler, Rachael A., and Janie L. Sheridan. 2007. “Highs and Lows: Patterns of Use, Positive and Negative Effects of Benzylpiperazine-Containing Party Pills (BZP-Party Pills) amongst Young People in New Zealand.” *Harm Reduction Journal* 4: 1–10. <https://doi.org/10.1186/1477-7517-4-18>.

- Campbell, H, W Cline, M Evans, J Lloyd, and A W Peck. 1973. "Comparison of the Effects of Dexamphetamine and 1-Benzylpiperazine in Former Addicts." *European Journal of Clinical Pharmacology* 6 (3): 170–76. <http://www.ncbi.nlm.nih.gov/pubmed/4586849>.
- Cappelli, Andrea, Germano Giuliani, Andrea Gallelli, Salvatore Valenti, Maurizio Anzini, Laura Mennuni, Francesco Makovec, Aroldo Cupello, and Salvatore Vomero. 2005. "Structure-Affinity Relationship Studies on Arylpiperazine Derivatives Related to Quipazine as Serotonin Transporter Ligands. Molecular Basis of the Selectivity SERT/5HT3 Receptor." *Bioorganic and Medicinal Chemistry* 13 (10): 3455–60. <https://doi.org/10.1016/j.bmc.2005.03.008>.
- Carroll, F Ivy, Anita H Lewin, S Wayne Mascarella, Herbert H Seltzman, and P Anantha Reddy. 2012. "Designer Drugs: A Medicinal Chemistry Perspective." *Annals of the New York Academy of Sciences* 1248 (February): 18–38. <https://doi.org/10.1111/j.1749-6632.2011.06199.x>.
- Che, Xiaoying, Chunquan Sheng, Wenya Wang, Yongbing Cao, Yulan Xu, Haitao Ji, Guoqiang Dong, Zhenyuan Miao, Jianzhong Yao, and Wannian Zhang. 2009. "New Azoles with Potent Antifungal Activity: Design, Synthesis and Molecular Docking." *European Journal of Medicinal Chemistry* 44 (10): 4218–26. <https://doi.org/10.1016/j.ejmech.2009.05.018>.
- Chetan, Bhadaliya, Mahesh Bunha, Monika Jagrat, Barij Nayan Sinha, Philipp Saiko, Geraldine Graser, Thomas Szekeres, et al. 2010. "Design, Synthesis and Anticancer Activity of Piperazine Hydroxamates and Their Histone Deacetylase (HDAC) Inhibitory Activity." *Bioorganic and Medicinal Chemistry Letters* 20 (13): 3906–10. <https://doi.org/10.1016/j.bmcl.2010.05.020>.
- Chilmonczyk, Zdzisław, Krzysztof J. Krajewski, and Jacek Cybulski. 2002. "Rigid Analogues of Buspirone and Gepirone, 5-HT1A Receptors Partial Agonists." *Farmaco* 57 (11): 917–23. [https://doi.org/10.1016/S0014-827X\(02\)01279-X](https://doi.org/10.1016/S0014-827X(02)01279-X).
- Cohen, Bruce M Z, and Rachael Butler. 2011. "BZP-Party Pills: A Review of Research on Benzylpiperazine as a Recreational Drug." *The International Journal on Drug Policy* 22 (2): 95–101. <https://doi.org/10.1016/j.drugpo.2010.12.002>.
- Cohn, V H, and J Lyle. 1966. "A Fluorometric Assay for Glutathione." *Analytical Biochemistry* 14 (3): 434–40. <http://www.ncbi.nlm.nih.gov/pubmed/5944947>.
- Davidson, J. Tyler, and Glen P. Jackson. 2019. "The Differentiation of 2,5-Dimethoxy-N-(N-Methoxybenzyl)Phenethylamine (NBOMe) Isomers Using GC Retention Indices and Multivariate Analysis of Ion Abundances in Electron Ionization Mass Spectra." *Forensic Chemistry* 14 (June): 100160. <https://doi.org/10.1016/j.forc.2019.100160>.
- Davies, S., D. M. Wood, G. Smith, J. Button, J. Ramsey, R. Archer, D. W. Holt, and P. I. Dargan. 2010. "Purchasing 'legal Highs' on the Internet-Is There Consistency in What You Get?" *Qjm* 103 (7): 489–93.

<https://doi.org/10.1093/qjmed/hcq056>.

- DeRuiter, Jack, Ashleigh Van Cleave, Audinei de Sousa Moura, Younis Abiedalla, and C. Randall Clark. 2017. "GC-MS and GC-IR Analysis of Disubstituted Piperazine Analogues of Benzylpiperazine and Trifluoromethylphenylpiperazine." *Journal of Pharmaceutical Sciences and Pharmacology* 3 (2): 133–45. <https://doi.org/10.1166/jpsp.2017.1085>.
- Dhanasekaran, Muralikrishnan, Binu Tharakan, and Bala V Manyam. 2008. "Antiparkinson Drug--Mucuna Pruriens Shows Antioxidant and Metal Chelating Activity." *Phytotherapy Research : PTR* 22 (1): 6–11. <https://doi.org/10.1002/ptr.2109>.
- Dickson, Amber J, Shawn P Vorce, Justin M Holler, and Timothy P Lyons. 2010. "Detection of 1-Benzylpiperazine, 1-(3-Trifluoromethylphenyl)-Piperazine, and 1-(3-Chlorophenyl)-Piperazine in 3,4-Methylenedioxymethamphetamine-Positive Urine Samples." *Journal of Analytical Toxicology* 34 (8): 464–69. <http://www.ncbi.nlm.nih.gov/pubmed/21819791>.
- Eriksson, Elias, Göran Engberg, Ola Bing, B.m., and Hans Nissbrandt. 1999. "Effects of MCPP on the Extracellular Concentrations of Serotonin and Dopamine in Rat Brain." *Neuropsychopharmacology* 20 (3): 287–96. [https://doi.org/10.1016/S0893-133X\(98\)00070-0](https://doi.org/10.1016/S0893-133X(98)00070-0).
- Fantegrossi, W E, G Winger, J H Woods, W L Woolverton, and A Coop. 2005. "Reinforcing and Discriminative Stimulus Effects of 1-Benzylpiperazine and Trifluoromethylphenylpiperazine in Rhesus Monkeys." *Drug and Alcohol Dependence* 77 (2): 161–68. <https://doi.org/10.1016/j.drugalcdep.2004.07.014>.
- Foroumadi, Alireza, Shahla Mansouri, Saeed Emami, Javad Mirzaei, Maedeh Sorkhi, Nosratollah Saeid-Adeli, and Abbas Shafiee. 2006. "Synthesis and Antibacterial Activity of Nitroaryl Thiadiazole-Levofloxacin Hybrids." *Archiv Der Pharmazie* 339 (11): 621–24. <https://doi.org/10.1002/ardp.200600108>.
- Freeman, B A, and J D Crapo. 1982. "Biology of Disease: Free Radicals and Tissue Injury." *Laboratory Investigation; a Journal of Technical Methods and Pathology* 47 (5): 412–26. <http://www.ncbi.nlm.nih.gov/pubmed/6290784>.
- Gaillard, G. Everett. 1955. "Clinical Evaluation of a New Antihistamine, Buclizine Hydrochloride (Vibazine)." *Journal of Allergy* 26 (4): 373–76. [https://doi.org/10.1016/0021-8707\(55\)90066-6](https://doi.org/10.1016/0021-8707(55)90066-6).
- Gaillard, Yvan P., Anne Claire Cuquel, Alexandra Boucher, Ludovic Romeuf, Fabien Bevalot, Jen Michel Prevosto, and Jean Marie Menard. 2013. "A Fatality Following Ingestion of the Designer Drug Meta-Chlorophenylpiperazine (MCPP) in an Asthmatic-HPLC-MS/MS Detection in Biofluids and Hair." *Journal of Forensic Sciences* 58 (1): 263–69. <https://doi.org/10.1111/j.1556-4029.2012.02254.x>.
- Gee, Paul, Mark Gilbert, Sandra Richardson, Grant Moore, Sharon Paterson, and Patrick Graham. 2008a. "Toxicity from the Recreational Use of 1-Benzylpiperazine." *Clinical Toxicology* 46 (9): 802–7. <https://doi.org/10.1080/15563650802307602>.

- . 2008b. “Toxicity from the Recreational Use of 1-Benzylpiperazine.” *Clinical Toxicology* 46 (9): 802–7. <https://doi.org/10.1080/15563650802307602>.
- Gee, Paul, Tom Jerram, and David Bowie. 2010. “Multiorgan Failure from 1-Benzylpiperazine Ingestion Legal High or Lethal High.” *Clinical Toxicology* 48 (3): 230–33. <https://doi.org/10.3109/15563651003592948>.
- Gijsman, H. J., A. F. Cohen, and J. M.A. Van Gerven. 2004. “The Application of the Principles of Clinical Drug Development to Pharmacological Challenge Tests of the Serotonergic System.” *Journal of Psychopharmacology* 18 (1): 7–13. <https://doi.org/10.1177/0269881104040205>.
- Giustarini, Daniela, Isabella Dalle-Donne, Roberto Colombo, Aldo Milzani, and Ranieri Rossi. 2008. “Is Ascorbate Able to Reduce Disulfide Bridges? A Cautionary Note.” *Nitric Oxide* 19 (3): 252–58. <https://doi.org/10.1016/j.niox.2008.07.003>.
- Groombridge, Christopher J. 1996. “NMR Spectroscopy in Forensic Science.” *Annual Reports on NMR Spectroscopy* 32 (C): 215–97. [https://doi.org/10.1016/S0066-4103\(08\)60080-0](https://doi.org/10.1016/S0066-4103(08)60080-0).
- Johnstone, Alice C, Rod A Lea, Katie A Brennan, Susan Schenk, Martin A Kennedy, and Paul S Fitzmaurice. 2007. “Benzylpiperazine: A Drug of Abuse?” *Journal of Psychopharmacology (Oxford, England)* 21 (8): 888–94. <https://doi.org/10.1177/0269881107077260>.
- Kálai, Tamás, Mahmood Khan, Mária Balog, Vijay Kumar Kutala, Periannan Kuppusamy, and Kálmán Hideg. 2006. “Structure-Activity Studies on the Protection of Trimetazidine Derivatives Modified with Nitroxides and Their Precursors from Myocardial Ischemia-Reperfusion Injury.” *Bioorganic and Medicinal Chemistry* 14 (16): 5510–16. <https://doi.org/10.1016/j.bmc.2006.04.040>.
- Karuppagounder, Senthilkumar S., Dwipayana Bhattacharya, Manuj Ahuja, Vishnu Suppiramaniam, Jack DeRuiter, Randall Clark, and Muralikrishnan Dhanasekaran. 2014. “Elucidating the Neurotoxic Effects of MDMA and Its Analogs.” *Life Sciences* 101 (1–2): 37–42. <https://doi.org/10.1016/j.lfs.2014.02.010>.
- Katz, D.P., J. Deruiter, D. Bhattacharya, M. Ahuja, S. Bhattacharya, C.R. Clark, V. Suppiramaniam, and M. Dhanasekaran. 2016a. “Benzylpiperazine: ‘A Messy Drug.’” *Drug and Alcohol Dependence* 164 (July): 1–7. <https://doi.org/10.1016/j.drugalcdep.2016.04.010>.
- Katz, D P, J Deruiter, D Bhattacharya, M Ahuja, S Bhattacharya, C R Clark, V Suppiramaniam, and M Dhanasekaran. 2016b. “Benzylpiperazine: ‘A Messy Drug.’” *Drug and Alcohol Dependence*, May. <https://doi.org/10.1016/j.drugalcdep.2016.04.010>.
- Khatri, Manisha, Santosh Kumar Rai, Sameena Alam, Anjana Vij, and Manisha Tiwari. 2009. “Synthesis and Pharmacological Evaluation of New Arylpiperazines N-{4-[4-(Aryl) Piperazine-1-YI]-Phenyl}-Amine Derivatives: Putative Role of 5-HT1A Receptors.” *Bioorganic and Medicinal Chemistry* 17 (5): 1890–97. <https://doi.org/10.1016/j.bmc.2009.01.043>.

- Kovalevich, Jane, and Dianne Langford. 2013. "Considerations for the Use of SH-SY5Y Neuroblastoma Cells in Neurobiology." *Methods in Molecular Biology (Clifton, N.J.)* 1078: 9–21. https://doi.org/10.1007/978-1-62703-640-5_2.
- Koves, Eva M. 1995. "Use of High-Performance Liquid Chromatography-Diode Array Detection in Forensic Toxicology." *Journal of Chromatography A* 692 (1–2): 103–19. [https://doi.org/10.1016/0021-9673\(94\)00840-6](https://doi.org/10.1016/0021-9673(94)00840-6).
- Kranenburg, Ruben F., Chris K. Lukken, Peter J. Schoenmakers, and Arian C. van Asten. 2021. "Spotting Isomer Mixtures in Forensic Illicit Drug Casework with GC–VUV Using Automated Coelution Detection and Spectral Deconvolution." *Journal of Chromatography B*, March, 122675. <https://doi.org/10.1016/j.jchromb.2021.122675>.
- Kubacka, Monika, Szczepan Mogilski, Barbara Filipek, and Henryk Marona. 2013. "Antiarrhythmic Properties of Some 1,4-Disubstituted Piperazine Derivatives with A1-Adrenoceptor Affinities." *European Journal of Pharmacology* 720 (1–3): 237–46. <https://doi.org/10.1016/j.ejphar.2013.10.021>.
- Kulig, Katarzyna, Jacek Sapa, Alicja Nowaczyk, Barbara Filipek, and Barbara Malawska. 2009. "Design, Synthesis and Pharmacological Evaluation of New 1-[3-(4-Arylpiperazin-1-Yl)-2-Hydroxy-Propyl]-3,3-Diphenylpyrrolidin-2-One Derivatives with Antiarrhythmic, Antihypertensive, and α -Adrenolytic Activity." *European Journal of Medicinal Chemistry* 44 (10): 3994–4003. <https://doi.org/10.1016/j.ejmech.2009.04.028>.
- Lin, Joanne C, Reem K Jan, HeeSeung Lee, Maree-Ann Jensen, Rob R Kydd, and Bruce R Russell. 2011. "Determining the Subjective and Physiological Effects of BZP Combined with TFMPP in Human Males." *Psychopharmacology* 214 (3): 761–68. <https://doi.org/10.1007/s00213-010-2081-7>.
- Lohray, Braj Bhushan, Vidya Bhushan Lohray, Brijesh Kumar Srivastava, Sunil Gupta, Manish Solanki, Purvi Pandya, and Prashant Kapadnis. 2006. "Novel 4-N-Substituted Aryl Pent-2-Ene-1,4-Dione Derivatives of Piperazinylloxazolidinones as Antibacterials." *Bioorganic and Medicinal Chemistry Letters* 16 (6): 1557–61. <https://doi.org/10.1016/j.bmcl.2005.12.025>.
- Luethi, Dino, and Matthias E. Liechti. 2020. "Designer Drugs: Mechanism of Action and Adverse Effects." *Archives of Toxicology*. Springer. <https://doi.org/10.1007/s00204-020-02693-7>.
- Maher, Hadir M, Tamer Awad, and C Randall Clark. 2009. "Differentiation of the Regioisomeric 2-, 3-, and 4-Trifluoromethylphenylpiperazines (TFMPP) by GC-IRD and GC-MS." *Forensic Science International* 188 (1–3): 31–39. <https://doi.org/10.1016/j.forsciint.2009.03.009>.
- Majrashi, Mohammed, Mohammed Almaghrabi, Maali Fadan, Ayaka Fujihashi, Wooseok Lee, Jack Deruiter, C. Randall Clark, and Muralikrishnan Dhanasekaran. 2018a. "Dopaminergic Neurotoxic Effects of 3-TFMPP Derivatives." *Life Sciences* 209 (April): 357–69. <https://doi.org/10.1016/j.lfs.2018.07.052>.
- . 2018b. "Dopaminergic Neurotoxic Effects of 3-TFMPP Derivatives." *Life Sciences* 209 (September): 357–

69. <https://doi.org/10.1016/j.lfs.2018.07.052>.
- . 2018c. “Dopaminergic Neurotoxic Effects of 3-TFMPP Derivatives.” *Life Sciences* 209 (September): 357–69. <https://doi.org/10.1016/j.lfs.2018.07.052>.
- Manley, Paul W., Francesca Blasco, Jürgen Mestan, and Reiner Aichholz. 2013. “The Kinetic Deuterium Isotope Effect as Applied to Metabolic Deactivation of Imatinib to the Des-Methyl Metabolite, CGP74588.” *Bioorganic and Medicinal Chemistry* 21 (11): 3231–39. <https://doi.org/10.1016/j.bmc.2013.03.038>.
- Martino, Maria Vittoria, Luca Guandalini, Lorenzo Di Cesare Mannelli, Marta Menicatti, Gianluca Bartolucci, Silvia Dei, Dina Manetti, Elisabetta Teodori, Carla Ghelardini, and Maria Novella Romanelli. 2017. “Piperazines as Nootropic Agents: New Derivatives of the Potent Cognition-Enhancer DM235 Carrying Hydrophilic Substituents.” *Bioorganic and Medicinal Chemistry* 25 (6): 1795–1803. <https://doi.org/10.1016/j.bmc.2017.02.019>.
- Merad-Boudia, M, A Nicole, D Santiard-Baron, C Saillé, and I Ceballos-Picot. 1998. “Mitochondrial Impairment as an Early Event in the Process of Apoptosis Induced by Glutathione Depletion in Neuronal Cells: Relevance to Parkinson’s Disease.” *Biochemical Pharmacology* 56 (5): 645–55. <http://www.ncbi.nlm.nih.gov/pubmed/9783733>.
- Monitoring Centre for Drugs, European, and Drug Addiction. n.d. “Keywords Precursors Amphetamine MDMA Methamphetamine Speed Meth Crystal Meth Ecstasy Synthetic Drugs BMK PMK P-2-P MDP-2-P EU Regulations Control Measures Pre-Precursors Designer Precursors Drug Precursor Developments in the European Union.”
- Monteiro, Márcia Sá, Maria de Lourdes Bastos, Paula Guedes de Pinho, and Márcia Carvalho. 2013. “Update on 1-Benzylpiperazine (BZP) Party Pills.” *Archives of Toxicology* 87 (6): 929–47. <https://doi.org/10.1007/s00204-013-1057-x>.
- Morinan, A, and H M Garratt. 1985. “An Improved Fluorimetric Assay for Brain Monoamine Oxidase.” *Journal of Pharmacological Methods* 13 (3): 213–23. <http://www.ncbi.nlm.nih.gov/pubmed/3923270>.
- Mosmann, T. 1983. “Rapid Colorimetric Assay for Cellular Growth and Survival: Application to Proliferation and Cytotoxicity Assays.” *Journal of Immunological Methods* 65 (1–2): 55–63. <http://www.ncbi.nlm.nih.gov/pubmed/6606682>.
- Muralikrishnan, D, and K P Mohanakumar. 1998. “Neuroprotection by Bromocriptine against 1-Methyl-4-Phenyl-1,2,3,6-Tetrahydropyridine-Induced Neurotoxicity in Mice.” *FASEB Journal : Official Publication of the Federation of American Societies for Experimental Biology* 12 (10): 905–12. <http://www.ncbi.nlm.nih.gov/pubmed/9657530>.
- Musselman, Megan E., and Jeremy P. Hampton. 2014. “‘not for Human Consumption’: A Review of Emerging Designer Drugs.” *Pharmacotherapy* 34 (7): 745–57. <https://doi.org/10.1002/phar.1424>.

- Nakamura, Yuji, Chie Sugita, Masaki Meguro, Shojiro Miyazaki, Kazuhiko Tamaki, Mizuki Takahashi, Yoko Nagai, et al. 2012. "Design and Optimization of Novel (2S,4S,5S)-5-Amino-6-(2,2-Dimethyl-5-Oxo-4-Phenylpiperazin-1-Yl)-4-Hydroxy-2-Isopropylhexanamides as Renin Inhibitors." *Bioorganic and Medicinal Chemistry Letters* 22 (14): 4561–66. <https://doi.org/10.1016/j.bmcl.2012.05.092>.
- Namera, Akira, Akihiro Nakamoto, Takeshi Saito, and Masataka Nagao. 2011. "Colorimetric Detection and Chromatographic Analyses of Designer Drugs in Biological Materials: A Comprehensive Review." *Forensic Toxicology*. Springer Tokyo. <https://doi.org/10.1007/s11419-010-0107-9>.
- Nikolova, I., and N. Danchev. 2008a. "Piperazine Based Substances of Abuse: A New Party Pills on Bulgarian Drug Market." *Biotechnology & Biotechnological Equipment* 22 (2): 652–55. <https://doi.org/10.1080/13102818.2008.10817529>.
- Nikolova, I, and N Danchev. 2008b. "Piperazine Based Substances of Abuse: A New Party Pills on Bulgarian Drug Market." *Biotechnology & Biotechnological Equipment* 22 (2): 652–55. <https://doi.org/10.1080/13102818.2008.10817529>.
- Peters, Frank T, Simone Schaefer, Roland F Staack, Thomas Kraemer, and Hans H Maurer. 2003. "Screening for and Validated Quantification of Amphetamines and of Amphetamine- and Piperazine-Derived Designer Drugs in Human Blood Plasma by Gas Chromatography/Mass Spectrometry." *Journal of Mass Spectrometry: JMS* 38 (6): 659–76. <https://doi.org/10.1002/jms.483>.
- Pettibone, D J, and M Williams. 1984. "Serotonin-Releasing Effects of Substituted Piperazines in Vitro." *Biochemical Pharmacology* 33 (9): 1531–35.
- Piplani, Poonam, and Chhanda Charan Danta. 2015. "Design and Synthesis of Newer Potential 4-(N-Acetylamino)Phenol Derived Piperazine Derivatives as Potential Cognition Enhancers." *Bioorganic Chemistry* 60 (May): 64–73. <https://doi.org/10.1016/j.bioorg.2015.04.004>.
- Pytko, Karolina, Elzbieta Zmudzka, Klaudia Lustyk, Anna Rapacz, Adrian Olczyk, Adam Galuszka, Anna Waszkielewicz, Henryk Marona, Jacek Sapa, and Filipek Barbara. 2016. "The Antidepressant- and Anxiolytic-like Activities of New Xanthone Derivative with Piperazine Moiety in Behavioral Tests in Mice." *Indian Journal of Pharmacology* 48 (3): 286–91. <https://doi.org/10.4103/0253-7613.182872>.
- Qureshi, G A, S Baig, I Bednar, P Södersten, G Forsberg, and A Siden. 1995. "Increased Cerebrospinal Fluid Concentration of Nitrite in Parkinson's Disease." *Neuroreport* 6 (12): 1642–44. <http://www.ncbi.nlm.nih.gov/pubmed/8527732>.
- Ramsay, R R, J Dadgar, A Trevor, and T P Singer. 1986. "Energy-Driven Uptake of N-Methyl-4-Phenylpyridine by Brain Mitochondria Mediates the Neurotoxicity of MPTP." *Life Sciences* 39 (7): 581–88. <http://www.ncbi.nlm.nih.gov/pubmed/3488484>.
- Romeiro, Luiz A.S., Marcos Da Silva Ferreira, Leandro L. Da Silva, Helena C. Castro, Ana L.P. Miranda, Cláudia

- L.M. Silva, François Noël, et al. 2011. "Discovery of LASSBio-772, a 1,3-Benzodioxole N-Phenylpiperazine Derivative with Potent Alpha 1A/D-Adrenergic Receptor Blocking Properties." *European Journal of Medicinal Chemistry* 46 (7): 3000–3012. <https://doi.org/10.1016/j.ejmech.2011.04.032>.
- Rosenbaum, Christopher D., Stephanie P. Carreiro, and Kavita M. Babu. 2012. "Here Today, Gone Tomorrow, and Back Again? A Review of Herbal Marijuana Alternatives (K2, Spice), Synthetic Cathinones (Bath Salts), Kratom, Salvia Divinorum, Methoxetamine, and Piperazines." *Journal of Medical Toxicology* 8 (1): 15–32. <https://doi.org/10.1007/s13181-011-0202-2>.
- Saeed, Makarem M., Nadia A. Khalil, Eman M. Ahmed, and Kholoud I. Eissa. 2012. "Synthesis and Anti-Inflammatory Activity of Novel Pyridazine and Pyridazinone Derivatives as Non-Ulcerogenic Agents." *Archives of Pharmacal Research* 35 (12): 2077–92. <https://doi.org/10.1007/s12272-012-1205-5>.
- Santos, A. D.C., L. M. Dutra, L. R.A. Menezes, M. F.C. Santos, and A. Barison. 2018. "Forensic NMR Spectroscopy: Just a Beginning of a Promising Partnership." *TrAC - Trends in Analytical Chemistry*. Elsevier B.V. <https://doi.org/10.1016/j.trac.2018.07.015>.
- Schep, Leo J., Robin J. Slaughter, J. Allister Vale, D. Michael G. Beasley, and Paul Gee. 2011. "The Clinical Toxicology of the Designer 'Party Pills' Benzylpiperazine and Trifluoromethylphenylpiperazine." *Clinical Toxicology* 49 (3): 131–41. <https://doi.org/10.3109/15563650.2011.572076>.
- Shaquiquzzaman, Mohammad, Garima Verma, Akranth Marella, Mymoona Akhter, Wasim Akhtar, Mohemmed Faraz Khan, Sharba Tasneem, and Mohammad Mumtaz Alam. 2015. "Piperazine Scaffold: A Remarkable Tool in Generation of Diverse Pharmacological Agents." *European Journal of Medicinal Chemistry* 102: 487–529. <https://doi.org/10.1016/j.ejmech.2015.07.026>.
- Sharma, Anjali, Sharad Wakode, Faizana Fayaz, Shaik Khasimbi, Faheem H. Pottoo, and Avneet Kaur. 2020. "An Overview of Piperazine Scaffold as Promising Nucleus for Different Therapeutic Targets." *Current Pharmaceutical Design* 26 (35): 4373–85. <https://doi.org/10.2174/1381612826666200417154810>.
- Sharma, Poornima, Anjali Sharma, Faizana Fayaz, Sharad Wakode, and Faheem H. Pottoo. 2020. "Biological Signatures of Alzheimer's Disease." *Current Topics in Medicinal Chemistry* 20 (9): 770–81. <https://doi.org/10.2174/1568026620666200228095553>.
- Simmler, Linda D, Anna Rickli, York Schramm, Marius C Hoener, and Matthias E Liechti. 2014. "Pharmacological Profiles of Aminoindanes, Piperazines, and Pipradrol Derivatives." *Biochemical Pharmacology* 88 (2): 237–44. <https://doi.org/10.1016/j.bcp.2014.01.024>.
- Singh, K., H.H. Siddiqui, P. Shakya, P. Bagga, A. Kumar, M. Khalis, M. Arif, and S. Alok. 2015. "Piperazine-A Biologically Active Scaffold." *International Journal of Pharmaceutical Sciences and Research* 6 (10): 4145–58. [https://doi.org/10.13040/IJPSR.0975-8232.6\(10\).4145-58](https://doi.org/10.13040/IJPSR.0975-8232.6(10).4145-58).
- Sleno, Lekha, Roland F. Staack, Emmanuel Varesio, and Gerard Hopfgartner. 2007. "Investigating the in Vitro

- Metabolism of Fipexide: Characterization of Reactive Metabolites Using Liquid Chromatography/Mass Spectrometry.” *Rapid Communications in Mass Spectrometry* 21 (14): 2301–11.
<https://doi.org/10.1002/rcm.3092>.
- Staack, Roland F., and Hans H. Maurer. 2004. “New Designer Drug 1-(3,4-Methylenedioxybenzyl) Piperazine(MDBP): Studies on Its Metabolism and Toxicological Detection in Rat Urine Using Gas Chromatography/Mass Spectrometry.” *Journal of Mass Spectrometry* 39 (3): 255–61.
<https://doi.org/10.1002/jms.556>.
- Staack, Roland F. 2007. “Piperazine Designer Drugs of Abuse.” *The Lancet* 369 (9571): 1411–13.
[https://doi.org/10.1016/S0140-6736\(07\)60646-1](https://doi.org/10.1016/S0140-6736(07)60646-1).
- Staack, Roland F, and Hans H Maurer. 2005. “Metabolism of Designer Drugs of Abuse.” *Current Drug Metabolism* 6 (3): 259–74. <http://www.ncbi.nlm.nih.gov/pubmed/15975043>.
- Staack, Roland F, Liane D Paul, Dietmar Springer, Thomas Kraemer, and Hans H Maurer. 2004. “Cytochrome P450 Dependent Metabolism of the New Designer Drug 1-(3-Trifluoromethylphenyl)Piperazine (TFMPP). In Vivo Studies in Wistar and Dark Agouti Rats as Well as in Vitro Studies in Human Liver Microsomes.” *Biochemical Pharmacology* 67 (2): 235–44.
- Sun, Miao Kun, Thomas J. Nelson, and Daniel L. Alkon. 2015. “Towards Universal Therapeutics for Memory Disorders.” *Trends in Pharmacological Sciences*. Elsevier Ltd. <https://doi.org/10.1016/j.tips.2015.04.004>.
- Sun, Qing Yan, Wan Nian Zhang, Jian Ming Xu, Yong Bing Cao, Qiu Ye Wu, Da Zhi Zhang, Chao Mei Liu, Shi Chong Yu, and Yuan Ying Jiang. 2007. “Synthesis and Evaluation of Novel 1-(1H-1,2,4-Triazol-1-Yl)-2-(2,4-Difluorophenyl)-3-[(4-Substitutedphenyl)-Piperazin-1-Yl]-Propan-2-Ols as Antifungal Agents.” *European Journal of Medicinal Chemistry* 42 (8): 1151–57. <https://doi.org/10.1016/j.ejmech.2006.11.003>.
- Sun, Wen Xue, Ya Jing Ji, Yun Wan, Hong Wei Han, Hong Yan Lin, Gui Hua Lu, Jin Liang Qi, Xiao Ming Wang, and Yong Hua Yang. 2017. “Design and Synthesis of Piperazine Acetate Podophyllotoxin Ester Derivatives Targeting Tubulin Depolymerization as New Anticancer Agents.” *Bioorganic and Medicinal Chemistry Letters* 27 (17): 4066–74. <https://doi.org/10.1016/j.bmcl.2017.07.047>.
- Tagat, Jayaram R., Stuart W. McCombie, Ruo W. Steensma, Sue Ing Lin, Dennis V. Nazareno, Bahige Baroudy, Nicole Vantuno, Serena Xu, and Jia Liu. 2001. “Piperazine-Based CCR5 Antagonists as HIV-1 Inhibitors. I: 2(S)-Methyl Piperazine as a Key Pharmacophore Element.” *Bioorganic and Medicinal Chemistry Letters* 11 (16): 2143–46. [https://doi.org/10.1016/S0960-894X\(01\)00381-X](https://doi.org/10.1016/S0960-894X(01)00381-X).
- Takahashi, Misako, Machiko Nagashima, Jin Suzuki, Takako Seto, Ichirou Yasuda, and Takemi Yoshida. 2009. “Creation and Application of Psychoactive Designer Drugs Data Library Using Liquid Chromatography with Photodiode Array Spectrophotometry Detector and Gas Chromatography-Mass Spectrometry.” *Talanta* 77 (4): 1245–72. <https://doi.org/10.1016/j.talanta.2008.07.062>.

- Takhi, Mohamed, C. Murugan, M. Munikumar, K. M. Bhaskarreddy, Gurpreet Singh, K. Sreenivas, M. Sitaramkumar, et al. 2006. "Synthesis and Antibacterial Activity of Novel Oxazolidinones Bearing N-Hydroxyacetamide Substituent." *Bioorganic and Medicinal Chemistry Letters* 16 (9): 2391–95. <https://doi.org/10.1016/j.bmcl.2006.01.109>.
- Tancer, Manuel E., and Chris Ellyn Johanson. 2001. "The Subjective Effects of MDMA and MCPP in Moderate MDMA Users." *Drug and Alcohol Dependence* 65 (1): 97–101. [https://doi.org/10.1016/S0376-8716\(01\)00146-6](https://doi.org/10.1016/S0376-8716(01)00146-6).
- Tennant, Thomas, Matthew C. Hulme, Thomas B.R. Robertson, Oliver B. Sutcliffe, and Ryan E. Mewis. 2020. "Benchmark NMR Analysis of Piperazine-Based Drugs Hyperpolarised by SABRE." *Magnetic Resonance in Chemistry* 58 (12): 1151–59. <https://doi.org/10.1002/mrc.4999>.
- Tsutsumi, Hiroe, Munehiro Katagi, Akihiro Miki, Noriaki Shima, Tooru Kamata, Mayumi Nishikawa, Kunio Nakajima, and Hitoshi Tsuchihashi. 2005a. "Development of Simultaneous Gas Chromatography-Mass Spectrometric and Liquid Chromatography-Electrospray Ionization Mass Spectrometric Determination Method for the New Designer Drugs, N-Benzylpiperazine (BZP), 1-(3-Trifluoromethylphenyl)Piperazine (TFMPP)." *Journal of Chromatography. B, Analytical Technologies in the Biomedical and Life Sciences* 819 (2): 315–22. <https://doi.org/10.1016/j.jchromb.2005.02.016>.
- . 2005b. "Development of Simultaneous Gas Chromatography-Mass Spectrometric and Liquid Chromatography-Electrospray Ionization Mass Spectrometric Determination Method for the New Designer Drugs, N-Benzylpiperazine (BZP), 1-(3-Trifluoromethylphenyl)Piperazine (TFMPP) and Their Main Metabolites in Urine." *Journal of Chromatography B: Analytical Technologies in the Biomedical and Life Sciences* 819 (2): 315–22. <https://doi.org/10.1016/j.jchromb.2005.02.016>.
- Upadhyaya, Ram Shankar, Sanjay Jain, Neelima Sinha, Nawal Kishore, Ramesh Chandra, and Sudershan K. Arora. 2004. "Synthesis of Novel Substituted Tetrazoles Having Antifungal Activity." *European Journal of Medicinal Chemistry* 39 (7): 579–92. <https://doi.org/10.1016/j.ejmech.2004.03.004>.
- Vermeer, Lydia M., Colin A. Higgins, David L. Roman, and Jonathan A. Doorn. 2013. "Real-Time Monitoring of Tyrosine Hydroxylase Activity Using a Plate Reader Assay." *Analytical Biochemistry* 432 (1): 11–15. <https://doi.org/10.1016/j.ab.2012.09.005>.
- Wang, Hongliang, Junhai Xiao, Dapeng Gao, Xian Zhang, Hui Yan, Zehui Gong, Tinmin Sun, and Song Li. 2011. "Pharmacophore-Based Design, Synthesis, and Biological Evaluation of Novel Chloro-Pyridazine Piperazines as Human Rhinovirus (HRV-3) Inhibitors." *Bioorganic and Medicinal Chemistry Letters* 21 (3): 1057–59. <https://doi.org/10.1016/j.bmcl.2010.12.001>.
- Welz, Anna, and Marcin Koba. 2020. "Piperazine Derivatives as Dangerous Abused Compounds." *Acta Pharmaceutica* 70 (4): 423–41. <https://doi.org/10.2478/acph-2020-0035>.

- Westphal, Folker, Thomas Junge, Ulrich Girreser, Stefan Stobbe, and Sylvia Brunet Pérez. 2009. "Structure Elucidation of a New Designer Benzylpiperazine: 4-Bromo-2,5-Dimethoxybenzylpiperazine." *Forensic Science International* 187 (1–3): 87–96. <https://doi.org/10.1016/j.forsciint.2009.03.003>.
- Wikström, Maria, Per Holmgren, and Johan Ahlner. 2004. "A2 (N-Benzylpiperazine) a New Drug of Abuse in Sweden." *Journal of Analytical Toxicology* 28 (1): 67–70. <https://doi.org/10.1093/jat/28.1.67>.
- Wilkins, C, M Girling, P Sweetsur, T Huckle, and J Huakau. 2006. "Legal Party Pill Use in New Zealand." *Centre for Social and Health Outcomes Research and Evaluation (SHORE)*, 1–62. <http://www.sleepwake.co.nz/massey/fms/Colleges/College of Humanities and Social Sciences/Shore/reports/Legal party pills in New Zealand report3.pdf>.
- Wilkins, Chris, Paul Sweetsur, and Melissa Girling. 2008. "Patterns of Benzylpiperazine/Trifluoromethylphenylpiperazine Party Pill Use and Adverse Effects in a Population Sample in New Zealand." *Drug and Alcohol Review* 27 (6): 633–39. <https://doi.org/10.1080/09595230801956140>.
- Wood, David M, Jenny Button, Satnam Lidder, John Ramsey, David W Holt, and Paul I Dargan. 2008. "Dissociative and Sympathomimetic Toxicity Associated with Recreational Use of 1-(3-Trifluoromethylphenyl) Piperazine (TFMPP) and 1-Benzylpiperazine (BZP)." *Journal of Medical Toxicology : Official Journal of the American College of Medical Toxicology* 4 (4): 254–57. <http://www.ncbi.nlm.nih.gov/pubmed/19031377>.
- "World Drug Report 2020." n.d. Accessed March 6, 2021. <https://wdr.unodc.org/wdr2020/index.html>.
- Xu, Yiming, Pengyun Liang, Haroon ur Rashid, Lichuan Wu, Peng Xie, Haodong Wang, Shuyan Zhang, Lisheng Wang, and Jun Jiang. 2019. "Design, Synthesis, and Biological Evaluation of Matrine Derivatives Possessing Piperazine Moiety as Antitumor Agents." *Medicinal Chemistry Research* 28 (10): 1618–27. <https://doi.org/10.1007/s00044-019-02398-2>.
- Yeap, Chan Wai, Chan Kee Bian, Ahmad Fahmi, and Lim Abdullah. 2010. "A Review on Benzylpiperazine and Trifluoromethylphenylpiperazine: Origins , Effects , Prevalence and Legal Status." *Health and the Environment Journal* 1 (2): 38–50.
- Youdim, M B, and L Lavie. 1994. "Selective MAO-A and B Inhibitors, Radical Scavengers and Nitric Oxide Synthase Inhibitors in Parkinson's Disease." *Life Sciences* 55 (25–26): 2077–82. <http://www.ncbi.nlm.nih.gov/pubmed/7527888>.
- Yu, Zhiyi, Guanying Shi, Qiu Sun, Hong Jin, Yun Teng, Ke Tao, Guoping Zhou, Wei Liu, Fang Wen, and Taiping Hou. 2009. "Design, Synthesis and in Vitro Antibacterial/Antifungal Evaluation of Novel 1-Ethyl-6-Fluoro-1,4-Dihydro-4-Oxo-7(1-Piperazinyl)Quinoline-3-Carboxylic Acid Derivatives." *European Journal of Medicinal Chemistry* 44 (11): 4726–33. <https://doi.org/10.1016/j.ejmech.2009.05.028>.
- Zhang, Mingjun, Jinmei Yang, Jing Shu, Changhong Fu, Shengnan Liu, Ge Xu, and Dechun Zhang. 2014.

“Cytotoxicity Induced by Nanobacteria and Nanohydroxyapatites in Human Choriocarcinoma Cells.”

Nanoscale Research Letters 9 (1): 616. <https://doi.org/10.1186/1556-276X-9-616>.

Zheng, Mengyuan, Manuj Ahuja, Dwipayana Bhattacharya, T Prabhakar Clement, Joel S Hayworth, and Muralikrishnan Dhanasekaran. 2014. “Evaluation of Differential Cytotoxic Effects of the Oil Spill Dispersant Corexit 9500.” *Life Sciences* 95: 108–17. <https://doi.org/10.1016/j.lfs.2013.12.010>.